# Design and Evaluation of a
# Knee-Extension-Assist

by

Alexander Noah Spring

A thesis
presented to the University of Waterloo
in fulfillment of the
thesis requirement for the degree of
Master of Applied Science
in
Systems Design Engineering

Waterloo, Ontario, Canada, 2010

## Author's Declaration

I hereby declare that I am the sole author of this thesis. This is a true copy of the thesis, including any required final revisions, as accepted by my examiners.

I understand that my thesis may be made electronically available to the public.

# Abstract

Quadriceps muscle weakness is a condition that can result from a wide variety of causes, from diseases like polio and multiple sclerosis to injuries of the head and spine. Individuals with weakened quadriceps often have difficulty supplying the knee-extension moments required during common mobility tasks. Existing powered orthoses that provide an assistive knee-extension moment are large and heavy, with power supplies that generally last less than two hours. A new device that provides a knee-extension-assist moment was designed to aid an individual with quadriceps muscle weakness to stand up from a seated position, sit from a standing position, and walk up and down an inclined surface. The knee-extension-assist (KEA) was designed as a modular component to be incorporated into existing knee-ankle-foot-orthoses (KAFO). The KEA consists of three springs that are compressed, as the knee is flexed under bodyweight, by cables that wrap around a sheave at the knee. The KEA returns the stored energy from knee flexion as an extension moment during knee extension. During swing or other non-weight bearing activities, the device is disengaged from the KAFO by decoupling the sheave from the KAFO knee joint, allowing free knee joint motion. A prototype was built and mechanically tested to determine KEA behaviour during loading and extension and to ensure proper KEA function. For biomechanical evaluation, able-bodied subjects used the prototype KEA while performing sit-to-stand, stand-to-sit, ramp ascent, and ramp descent tasks. The KEA facilitated sitting and standing, providing an average of 53 % of the required extension moment for the two participants, which allowed one participant to reduce quadriceps usage by 38 % and the other to perform sit-to-stand in a slower and more controlled manner that was not possible without the KEA. KEA use during ramp gait caused an overall increase in quadriceps activation by 76 %, on average, with use. Future efforts will be made to modify the design to improve functionality, especially for ramp gait, and to reduce device size and weight.

# Acknowledgements

There are a number of people I would like to thank who have helped make this work possible and to whom I am greatly indebted. First, a big thank you to my two supervisors, Dr. Jonathan Kofman and Dr. Edward Lemaire for providing me with this project and with the support and guidance I needed to complete it well. I also owe a huge thank you to Shawn Millar, the Ottawa Hospital Rehabilitation Centre gait lab technician, who put in a lot of time to help me with my research and teach me the ins and outs of biomechanical testing, and without whom I could not have completed my degree. The same to Tony Zandbelt, the Rehab Centre machinist, whose skills in the shop are unmatched. I would also like to thank the orthotists at the Rehab Centre, who took time out of their busy schedules to construct the orthosis for the biomechanical trials, as well as gave me insightful feedback and ideas on my design. Many thanks as well to my colleagues both at the University of Waterloo and at The Ottawa Hospital Rehabilitation Centre for their moral support and encouragement.

The biggest thank you of all would have to go to my family, who helped me learn the non-engineering lessons and skills that were required to complete this master's degree. They helped keep me grounded, well-balanced, and sane, as well as provided endless support, advice, and an ear that was always ready to listen.

I also would like to acknowledge the financial support provided to me by Natural Sciences and Engineering Research Council and the University of Waterloo, through the Alexander Graham Bell CGS M award and the President's Graduate Scholarship, respectively, which helped me avoid sharing the same fate as many a car company and investment bank over these past couple of years.

## Dedication

To my Mom and Dad, the world's most patient listeners and wisest advisers, this wouldn't have been possible without your endless support and guidance.

# Table of Contents

# List of Figures

# List of Tables

# Chapter 1. Introduction

Lower limb weakness affects millions of individuals around the world, limiting their mobility, and thus their independence and quality of life. Individuals whose impairments are associated with weakened quadriceps often have great difficulty providing the necessary knee extension moments for level-ground gait. Insufficient extension moments increase the risk of knee collapse while weight-bearing. In the United States alone, more than 1.5 million people use a full-leg or knee brace [1]. Typically, numbers for the Canadian population are approximately one tenth of those from the United States. Weakness in the lower limbs can have many causes: peripheral neurological diseases like poliomyelitis, post-polio syndrome, spina bifida, and poly neuropathy; muscular diseases such as muscular dystrophy and myasthenia gravis; central neurological diseases like multiple sclerosis, cerebral palsy, brain or spinal cord injury, and stroke [2]; and muscle atrophy and loss of strength due to old age. To provide stability to the leg during the weight-bearing or *stance phase* of gait, as well as other body-weight-bearing activities, a conventional knee-ankle-foot orthosis (KAFO) is often utilized. A KAFO is an assistive device that attaches to the user`s affected leg and locks the knee in full extension (Figure 1.1) [3].

Figure 1.1: Standard KAFO (from [3]).

KAFOs allow individuals to walk upright but do not fully restore able-bodied gait. Since the knee joint is restricted from flexing, attempting to swing the leg forward in the normal manner causes the foot to make contact with the ground. Therefore, the wearer must adopt an abnormal method of moving the affected limb forward, such as swinging the leg laterally outward while being swung forward, raising the ipsilateral hip to allow the braced leg to pass underneath unhindered, or vaulting up with the contralateral leg during the contralateral stance phase to provide the necessary clearance for the braced limb. These modifications result in increased energy expenditure during gait, and can lead to hip and back injuries [4].

In an attempt to overcome this limitation, a new generation of KAFO, called a stance control knee-ankle-foot orthosis (SCKAFO), has recently been developed to allow the knee to flex during swing phase while still providing support during stance phase [2, 5-10]. A SCKAFO can help to provide a more natural gait cycle and lower energy expenditure [4]. However, tasks that require high knee extension moments, such as standing up from seated, walking up inclines, stepping up onto curbs, and ascending stairs, are still difficult if not impossible for individual with weak quadriceps to perform without assistance. None of the existing KAFOs provide power to the knee to aid in performing these tasks.

If a sufficiently high extensor moment were provided by a new device to a KAFO`s unlocked knee joint, tasks requiring high knee-extension moments would become possible. A knee-extension-assist could provide greater mobility for individuals with quadriceps weakness who could not previously perform these tasks independently, and may permit a reduction in fatigue and risk of injury to those who perform these tasks with difficulty.

This thesis details the design, construction, and testing of a novel, modular, knee-extension-assist. The goal of the new assistive device is to provide an external extension moment to the human knee while the affected leg is weight-bearing for high knee-extension moment tasks; namely, sit-to-stand, stair ascent, and ramp ascent. Ideally, the device would have minimal weight and size, only be in operation when a knee-extension moment is needed, and not impede free knee flexion and extension. The new knee-extension-assist should assist the user without interfering with the function and detracting from the benefits of

2

the KAFO or SCKAFO, during level gait.

The research performed for this thesis entailed the full design, prototype construction, mechanical testing, and biomechanical functional evaluation of a knee-extension-assist (KEA). In a first design, an electro-mechanical approach was taken, focussing on assisting sit-to-stand and stair ascent. However, power sources and actively powered actuators would be too heavy for widespread use by individuals with quadriceps muscle weakness. In a second design, a passive approach, using springs to store and release energy as needed, was taken to power the knee-extension-assist while minimizing size and weight. A passive device requires a loading phase during knee flexion under bodyweight to supply an extension moment during knee extension. Stair ascent, which does not have flexion during stance, was eliminated from the device functional requirements. Ramp ascent, which does have knee flexion during stance, replaced stair ascent as a principal focus for device function. In addition, assistance for stand-to-sit and ramp descent, tasks that both have knee flexion during stance, were added. Detailed design, prototype construction, and mechanical testing were carried out on the second design. Finally, the KEA was attached to a KAFO and tested biomechanically to determine its functionality and effectiveness in providing assistance for sitting down from a standing position, standing up from a seated position, and ramp walking in ascent and descent.

Chapter 2 reviews the literature relevant to designing a KEA device: sit-to-stand, stair ascent, and ramp ascent biomechanics; relevant actuator technologies; and existing powered assistive devices. Following this, the rationale for creating this device, research objectives, design, development, and prototype fabrication processes are presented in Chapter 3. Chapter 4 presents mechanical testing while Chapter 5 presents the results and discusses the biomechanical trials. A discussion of results from the mechanical and biomechanical tests, as well as recommendations for future research is provided in Chapter 6. Research conclusions are given in Chapter 7.

# Chapter 2. Literature Review

In order to design a functional, novel extension-assist for a KAFO knee joint, background knowledge in a variety of fields is required. The following literature review begins with a review of sit-to-stand and stair ascent biomechanics, as they are common daily-living tasks that require high knee-extension moments and design specifications were initially based on these tasks. Ramp ascent is also briefly discussed since it was later included as an intended KEA function. Following the biomechanics review, a brief overview of relevant actuator technologies that could potentially be incorporated into the device is presented. The literature review finishes with an examination of existing powered mobility and joint extension-moment-assist devices currently available or in development.

## 2.1 Sit-to-Stand Movement

The sit-to-stand movement (STS) is a common every-day task that is essential for independent living. STS is a precursor to walking and many other daily activities [11-13]. However, STS is difficult for those with quadriceps muscle weakness due to the knee-extension moments required to straighten the leg and the need to move the body centre of mass (BCM) forward so that the BCM is within the base of support, to maintain balance [12, 14, 15]. A successful STS task involves upward movement of the body centre of mass from the seated position to one for standing, while maintaining balance [15].

### 2.1.1 Sit-To-Stand Conventions

STS is typically modeled as a two-dimensional, bilaterally symmetric movement [11, 16]. Since the body usually experiences the same kinematics and dynamics on both sides, STS is often examined in the sagittal plane, as shown in Figure 2.1.
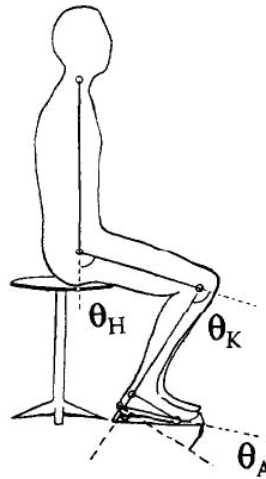
Figure 2.1: Sagittal plane view of joint angle definitions (from [15]). θH = hip angle, θK = knee angle, θA = ankle angle.

In this thesis, for hip and knee angles, joint flexion increases the joint angle, while joint extension, or straightening the limb, decreases the angle. Hip and knee angles are zero when the joint is straight. Ankle angle is between the foot and shank, with the angle set to zero for an actual angle of 90° [14, 15, 17, 18]. Plantarflexion, when the angle between shank and foot increases, is considered a positive rotation. Although these definitions are common, some studies report joint angles as being the angle from each segment to the horizontal [12, 16], while others may use the angle between the shank and the vertical as the ankle angle [19].

## 2.1.2  Sit-To-Stand Phases

Breaking down the STS task gives a better understanding of the sit-to-stand transfer biomechanics. Roebroeck [15] divided the STS motion into three phases, based on BCM motion (Figure 2.2):
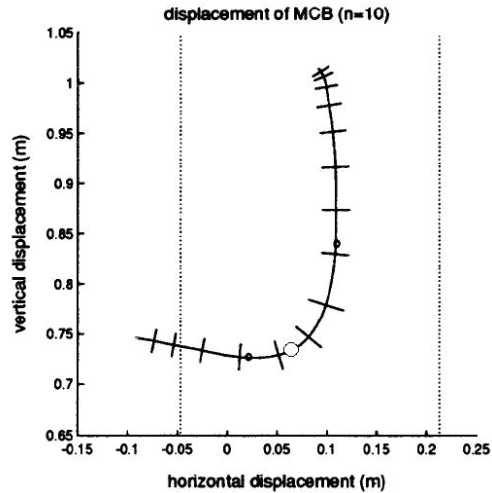
Figure 2.2: BCM Displacement over the full STS transfer (modified from [15]). Dashes on curve represent equal time steps. Solid dots delineate phases; open dot is instant of seat off. Origin is the ankle joint. Dotted lines indicate support base, i.e. foot length.

Phase 1 – Acceleration phase: In the first phase of STS, the BCM is accelerated horizontally solely through hip flexion, which rotates the trunk forwards. Phase 1 begins with the onset of trunk flexion and ends at the instant of maximal horizontal BCM velocity.

Phase 2 – Transition phase: BCM is decelerated horizontally and accelerated vertically. Momentum from trunk rotation is transferred to the legs, causing a positive thigh rotation through knee extension and slight negative ankle rotation. As a result, the BCM begins to accelerate vertically. Seat-off occurs early in this phase when the buttocks lift from the seat and the person becomes self-supported. Phase 2 begins at maximum BCM horizontal velocity and ends at maximum BCM vertical velocity.

Phase 3 – Deceleration phase: Vertical BCM deceleration occurs during this phase. Knee extension, hip extension, and ankle plantarflexion coordinate to raise the BCM while limiting its horizontal motion. By the end of Phase 3, the joints have been extended and the body is nearly vertical. Phase 3 begins at maximum BCM vertical velocity and ends at the completion of STS.

The transition phase (Phase 2) can be further broken down into three phases: horizontal trunk deceleration, the instant of momentum transfer to the legs causing seat-off, and the vertical BCM acceleration through hip and knee extension [20]. However, dividing the

6

transition phase into three separate phases assumes that there is no further trunk flexion after seat-off occurs, and this may not always be the case [11].

## 2.1.3 Body Centre of Mass and Base of Support

For successful STS, the BCM must be moved anteriorly via trunk flexion, as described in Phase 1, prior to being raised. When sitting upright, the weight of the subject is mainly borne by the seat and the BCM is therefore located behind the base of support provided by the feet. If there is not sufficient anterior motion before attempting to raise the BCM vertically, balance cannot be maintained because the line of action of the body weight through the BCM passes posterior to the heel [12]. For STS transfers longer than 1.5 s in duration, angular momentum from trunk rotation is small [18]. Therefore, for slower STS, the BCM must be brought within the base of support before vertical acceleration can occur. For faster rises, where trunk momentum plays a role in the STS motion, vertical BCM acceleration can begin before the BCM is brought within the base of support. However the BCM must be brought within the base of support as the trunk begins to decelerate for balance to be maintained [12].

## 2.1.4 Joint Moments

A range of STS joint moments have been reported in the literature. Even for healthy elderly individuals, the moments necessary for STS are much lower than the maximum moments the subjects can generate [12]. Net knee extension moments have been reported in the range of 0.3 to 1.4 Nm/kg (Table 2.1). Because the moments produced depend on how the motion is performed, there is disagreement as to whether the knee or the hip experiences the higher peak moment during STS [10, 12, 14-16, 18, 20].

Despite the hip and knee moment differences, general trends throughout STS motion are relatively consistent across studies. Peak joint moments occur very shortly after seat-off [11, 15]. Also, STS duration has little effect on the peak moments, although the slower the movement is performed, the longer the high moment values are sustained, which leads to higher muscular effort to complete the task [11].

7

Table 2.1: STS knee-joint moments [11, 13-18, 21]

| Study | Subjects* (female,male) | Knee Moment (Nm/kg) | Task Timing (s) |
|---|---|---|---|
| Sibella et al. (2003) | 40, 0 obese adults | 0.75 | self selected |
| | 3,7 adults | 0.38 | self selected |
| Shepherd, Gentile (1994) | 0,6 adults | 1.06 | self selected 1.2 - 2 |
| Roy et al. (2007) | 3,9 hemiparetic adults | 1.04 healthy side | na |
| | | 0.39 affected side | na |
| Roebroeck et al. (1994) | 6,4 adults | 0.88 | metronome 2.25 |
| Rodosky et al. (1989) | 5,5 young adults | 0.81 | na |
| Anan et al. (2008) | 13,1 elderly | .301-.439 | self selected 2.38 |
| Hughes et al. (1996) | 5,5 young adults | 1.41 | self selected |
| | 6,5 impaired elderly | 1.06 | self selected |
| Bahrami et al. (1999) | 3,7 adults | 0.88 | self selected 1.738 |

*healthy unless otherwise specified

## 2.2 Stair Ascent

Climbing stairs is another common activity that places a high demand on the lower limbs. While efforts have been made to make buildings more accessible to people with disabilities, there are still many instances in day-to-day life where ascending stairs is unavoidable. For someone with quadriceps muscle weakness, performing step-over-step stair ascent (SA) is not possible because a relatively large amount of knee extensor strength, compared to level gait, is needed [22, 23]. The step-by-step method, in which both feet are placed on the same step before ascending to the next, is often used as a replacement SA strategy. The non-affected leg is always used to raise the body up to the next stair while the affected leg merely provides support [24].

Normal SA involves reciprocal leg motion, in which the leading (stance) leg straightens, raising the body, while the trailing leg swings up to the next step. The weight of the individual is transferred to the previously swinging leg, which becomes the stance leg, while the newly unloaded leg becomes the trailing leg. This pattern, shown in Figure 2.3, repeats until all stairs have been mounted.

While the SA motion is not as accurately described by a two-dimensional analysis as STS, only sagittal plane kinematics and dynamics will be discussed, since the motions of SA mainly occur in the antero-posterior and vertical directions [25].

## 2.2.1 Stair Ascent Phases

The SA stride normally begins with the first foot contact and ends with the subsequent contact of the same foot two stairs above (100%) [25] (Figure 2.3). The average time taken to complete this cycle is approximately 1.4 to 1.45 s [26, 27]. There are two main phases of the SA cycle: stance phase, where the leg is weight bearing, and swing phase, which occurs when the leg is unloaded and swinging up to the next step [23]. Both can be broken down further according to the different objectives for the progression of movement [23, 25, 26, 27]. However, the subphases are not relevant to the KEA design, and are thus not presented here.

## 2.2.2 Centre of Mass and Centre of Pressure

Over the course of the SA cycle, the BCM moves vertically and horizontally. BCM is displaced anteriorly throughout the entire SA stride [25], and at no point is there substantial vertical BCM motion without concurrent forward BCM motion [23]. However, at the end of the stance phase, the BCM is displaced only anteriorly, with no vertical lift [25]. Sinusoidal lateral BCM movement occurs in the frontal plane, but the magnitude of this medio-lateral sway is small, approximately 4.4 cm at its maximum displacement from centre.

The centre of pressure (CP) during stair ascent remains within approximately 10 cm of the foot's metatarsal area. First contact with a stair occurs in the forefoot because the high knee flexion angle at contact orients the foot such that a high ankle dorsiflexion angle would



POSITION 1          POSITION 2          POSITION 3

Figure 2.3: Normal mode of stair ascent (from [24]).

9

be necessary to cause first contact with the heel [26]. The CP moves posteriorly after contact during weight acceptance on the foot at the start of the stance phase, due to contralateral ankle plantarflexion during the period of double leg support at the end of contralateral stance. This is followed by anterior CP movement when only one leg supports weight, until the next period with both legs supporting weight begins [25].

### 2.2.3 Joint Dynamics

Similarly to STS, larger joint moments are needed to successfully complete the SA cycle than to perform level gait, especially at the knee [22]. The maximum knee-extension moment is more than twice that involved in level walking [26]. However, the dynamics of ascending stairs is not as consistent as that of level walking [28] due to variation in SA strategies between subjects. In stair climbing, there is much variation in SA strategies between subjects, and even within subjects over the course of climbing a flight of stairs [22, 23]. Reported maximal knee extension moments vary widely in the literature (Table 2.2), from 0.51 Nm/kg [27], a similar moment to that of level walking [29], to 1.24 Nm/kg [30]. Commonly reported values are between 1.0 to 1.2 Nm/kg [24, 26, 29-31]. As an example of a strategy that may lead to a wide range of joint moment values, the subject rotates the trunk further over the support leg during SA, moving the BCM closer to the knee joint, thus reducing the knee moment and increasing the necessary hip moment [31]. This movement pattern may allow people with low knee extensor strength, but adequate hip strength, to ascent stairs unaided [23, 32].

There was also disagreement as to moments during the swing phase. McFayden and Winter [23] stated that successful swing is achieved through hip flexion paired with knee flexion in early swing, knee extension in mid swing, and another period of flexion late in the swing phase, with hip extension and foot dorsiflexion controlling foot placement at the very end of swing. Andriacchi et al. [22] stated that there is no muscle activity between mid swing and foot strike, while Reid et al. [24] wrote that there is zero moment at the knee for the entire swing phase, and that knee flexion occurs passively as a result of hip flexion.

Table 2.2: SA maximum knee joint moments for healthy individuals [22-24, 26, 27, 29-31, 33-36].

| Study | Subjects (female, male) | Knee Moment (Nm/kg) | Average Cadence* (step/min) |
|---|---|---|---|
| Costigan et al. (2002) | 20,15 young adults | 1.16 | 80.6 |
| Reid et al. (2007) | 8,9 adults | 0.96 | na |
| Salsich et al. (2001) | 5,5 adults | 1.11 | 85.85 |
| Riener et al. (2002) | 0,10 young adults | 1.15 | 85.1 |
| Protopapadaki et al. (2006) | 17,16 young adults | 0.51 | na |
| McFayden and Winter (1987) | 0,3 adults | 1.5 | na |
| Andriacchi et al. (1980) | 0,10 young adults | 0.76 | method not specified |
| Brechter and Powers (2001) | 5,5 adults | 1.16 | 142.1 |
| Reeves et al. (2008) | 8,5 elderly | 0.9 | 92 |
| Schmalz et al. (2006) | 20** young adults | 1.05 | na |
| Nadeau et al. (2003) | 5,6 adults | 0.98 | 93.6 |
| Spanjaard et al. (2008) | 0,10 young adults | 1.24 | metronome 88 |

*cadence self selected unless otherwise specified
**participant gender not specified

However, certain gait patterns are common to all SA strategies. Maximum knee extension moment is observed during knee extension at the beginning of single leg support [26, 29, 30]. As the knee extends, the BCM moves past the knee joint, causing the extension moment to decrease and eventually change to a slight flexion moment as the GRF passes anterior to the knee [22-24, 26, 27]. A maximum ankle plantarflexion moment occurs at the end of stance phase, just before knee extension begins for the contralateral leg [22, 23, 26, 27]. For all climbing strategies, stair ascent is a physically demanding task requiring high quadriceps strength to provide a high knee-extension moment.

## 2.3 Ramp Ascent

Walking up an inclined surface is another high-quadriceps-demand task in which knee flexion and extension occur while the leg is weight bearing (Figure 2.4) [37], and therefore is a third task that could be aided by a KEA. During incline walking, the foot contacts the ground with the knee at a slight flexion angle, dependant on the incline angle. In early stance, the knee angle increases by 10 to 15 degrees. The knee then extends, and knee angle decreases to approximately 10 degrees in late stance. The knee flexes again at the end of

stance, in preparation for swing, during which the foot is raised and moved anteriorly to be in position for the following stance phase.

Peak knee joint moment during ramp ascent is 0.64 Nm/kg for an 8.5° incline [37], considerably lower than for STS or SA. In addition, the knee joint moment is only an extension moment during the initial knee flexion and the first 15 degrees of the subsequent knee extension. Therefore, knee extension moments only occur in the first half of the stance phase (Figure 2.4). It would therefore be possible to provide an assistive extension moment only in the first half of stance, for the initial flexion and the following extension of approximately the same angle, since the knee joint moment becomes a flexion moment until the end of the stance phase. Because of the good match between task and device dynamics, providing an extension-assist for incline ascent was chosen to replace stair ascent as an objective for device function.
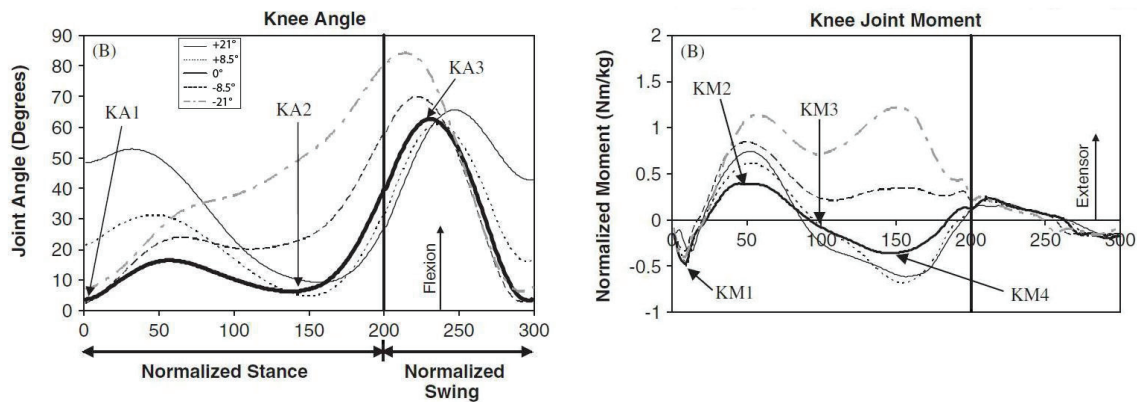


Figure 2.4: Knee joint angle and moment for incline walking (modified from [37]).

## 2.4 Relevant Technologies

Technologies that can provide the necessary extension moments for a KEA system were examined. In the field of active orthoses, active prostheses, and powered exoskeletons, actuators are used to apply moments to one or more device joints. A wide range of actuator technologies are available to provide power to anthropomorphic assistive devices, from traditional actuators like DC motors, to new, non-conventional actuators using technology that is in the development or testing phase [38-43]. The most common actuators in active

12

biomechanical devices are those conventionally used in robotics, DC motors, hydraulic actuators, and pneumatic actuators. New non-conventional actuators exploit special material properties of their components, such as a change in size, shape, or viscosity, to create a force or moment. For example, piezoelectrics, shape memory materials, contractile polymers, and electrorheological fluids.

Because assistive devices are worn by humans, actuators should be lightweight and small in size, unnoticeable when the assistive device is in use, and require a small and light power source, since entire device must be carried by the user. The actuator should provide a high torque while creating minimal noise or heat, have a fast and predictable response, and be easy to control.

The following sections briefly describe a number of actuator technologies, divided into conventional and non-conventional actuators.

## 2.4.1 Conventional Actuators

Conventional actuators utilize electromagnetic induction, where a current flows through a coil in the presence of a magnetic field to create an electromotive force (EMF) [44]. The actuator either uses the EMF directly, such as in a DC motor, or indirectly, using a DC motor to move a working fluid (i.e., hydraulics and pneumatics). However, other power sources, such as combustion engines, can also be used to power pneumatic or hydraulic actuators [45].

### 2.4.1.1 DC Motors

DC motors are a well known, reliable, and longstanding technology that are available in a wide range of sizes and ratings. For example, on the smaller end of the range, a 3 kg DC motor can provide approximately 4.4 Nm at 5000 rpm [46], whereas a 2g coreless micromotor can produce a 0.11 Nm moment at a speed of 13000 rpm [47].

To be suitable for active assistive devices, DC motors are often used in their smaller forms, to minimize device weight. The smallest DC motors are predominately coreless DC micromotors, in which the iron 'core' is removed from the rotor to reduce weight and inertial properties, and brushless DC micromotors, where the field magnets are located in the rotor

and the coil in the stator, eliminating the need for brushes and commutator. However, these small motors provide very low torques at high rotation rates, and therefore require a gearbox to obtain acceptable moments and operational speeds. Since conventional DC motors have relatively low power densities, large, heavy motors are necessary for applications where higher torques are needed, which would likely be too heavy for a person with a physical disability. DC motors are also noisy, which is undesirable since noise will draw attention to the assistive device or become irritating to the user [43].

A commonly used extension of the DC motor is the servomotor. This is a DC motor coupled with a reduction system to convert high motor speeds into high torques and a control system with a position sensor to monitor shaft rotation, allowing for precise positioning [43].

DC motors can also be used to create linear forces instead of torques through the use of a lead screw or ball screw. The motor turns a threaded shaft connected to an output via a non-rotating nut (lead screw) or ball bearing assembly (ball screw). The shaft rotation causes the nut or ball bearing assembly to move up or down, exerting a linear force on the attached output. Lead and ball screws greatly reduce DC motor's very high efficiency (Table 2.3). The efficiency losses for lead screws are mainly from friction between nut and shaft while, for the ball screw, the loss is mainly from the ball bearing assembly's relatively large weight [48].

Table 2.3: Efficiencies of DC motors with added components to convert rotational output to linear output [48]. $cP_{wt}$ is the corrected power to weight ratio, which takes into account the efficiency of each type of actuator.

| Actuator | Eff. | $P_{wt}$ (W/kg) | $cP_{wt}$ (W/kg) | Strength/Wt [KN/kg (kg f/kg)] |
|---|---|---|---|---|
| dc motor | 0.90 | 312 | 281 | — |
| + gearbox | 0.68 | 90 | 61 | — |
| + ballscrew | 0.81 | 150 | 122 | 1.2 (120) |
| + leadscrew | 0.27 | 150 | 41 | 1.2 (120) |
| Air muscle | 0.40 | 500–10k | 200–4k | 4.9–8.6 (500–875) |
| Human muscle | 0.45 | 500 | 225 | 6.4 (658) |

## 2.4.1.2 Hydraulic and Pneumatic Actuators

Hydraulic and pneumatic actuators use pumps to push a working fluid, usually oil or air, into a closed cylinder containing a piston connected to an output shaft. The fluid is pumped into one side of the cylinder, creating an internal pressure that forces the piston to move towards

the unpressurized end. As a result, the piston shaft exerts a linear pushing or pulling force on the connected component. Hydraulic actuators can provide larger forces than a similar pneumatic actuator. However, hydraulic actuators are normally quite heavy because they use oil as a working fluid, and are therefore normally used in devices that actively support their own weight, such as the BLEEX and Sarcos exoskeletons [49, 50], or are externally powered and/or supported [51].

To provide a joint moment, hydraulic and pneumatic actuators are often connected above and below the joint and offset from the joint centre, because they provide a linear force and thus require a moment arm through which to act. As a result, the moment created at the device joint is a function of joint angle, since the moment arm decreases as the joint extends (Figure 2.5). This actuator offset can make prevent the user from sitting or wearing the device under clothes [52, 53]. Traditional pneumatic cylinder actuators have been used in assistive devices by pulling on a link coupled to a joint, creating a moment about that joint [52]. While pneumatic cylinders have better power to weight ratios than electric actuators [52], a portable compressor or compressed air tank would be necessary to run the pneumatic cylinders in a wearable device. This would reduce the favorable power-to-weight ratio.
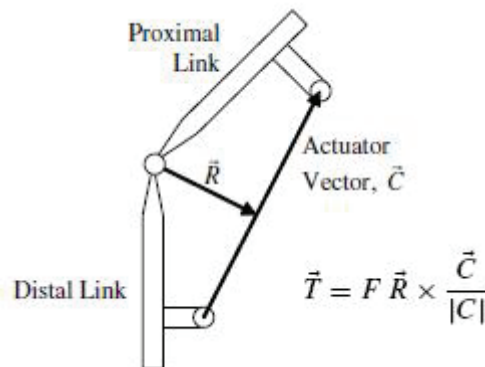


Figure 2.5: Torque provided by a hydraulic actuator (modified from [45]). F is the force applied by the hydraulic actuator.

## 2.4.2 Non-conventional Actuators

Non-conventional actuators typically exploit a component's special material properties, which can generate a force or moment. These special properties can be a change in size, shape, or viscosity as a response to an external stimulus. The materials can be metal alloys, piezoelectric materials, polymers, or fluids [39, 41, 43].

### 2.4.2.1 Non-Conventional Pneumatic Actuators

Non-conventional pneumatic actuators are extensively used in active orthoses, gait rehabilitation devices, and powered exoskeletons [52, 54-60]. The most commonly used is the pneumatic muscle actuator (PMA), or McKibben air muscle, a tubular rubber air bladder surrounded by a reinforcing braided mesh of flexible, though inelastic, fibres or wires [55]. Figure 2.6 shows a PMA and its makeup.

When a pneumatic muscle is pressurized, the rubber tube expands in volume. However, because the surrounding mesh cannot stretch, the tube can only expand radially. As a result, the mesh angle changes from approximately 5-10° to 40-45° to accommodate the increase in diameter (Figure 2.7), causing the length to shorten. Contraction upon pressurization can be used to apply a pulling force by attaching the actuator ends to device fixtures. McKibben air muscle can only produce contractile forces if it is in a stretched state when inactive [55, 61].



Figure 2.6: McKibben air muscle (a) in situ in an orthosis (adapted from [56]) and (b) detailing air muscle constitution (from [62]).

One attractive trait of pneumatic muscles is the lack of a catastrophic failure mode, especially for assistive devices. As a 'soft actuator', the user has a low risk of injury if an air

muscle fails, and thus PMAs are deemed safer than electrical or hydraulic actuators when providing similar forces [63]. PMAs are also compliant, allowing for use in non-linear configurations, such as following the shape of the body [54]. In addition, air muscles are relatively inexpensive compared to other actuator technologies [63].
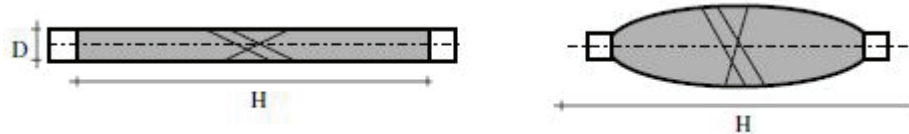


Figure 2.7: McKibben air muscle contraction showing the reduction in length and increase in fibre angle (adapted from [61]).

Pneumatic muscles are also popular because of the excellent power to weight, power to volume, and power to energy ratios. Repperger [64] reported that the 1 W/g pneumatic muscle power/weight ratio is five times greater than hydraulic or electric actuators and the 1 W/cc PMA power/volume ratio far exceeds standard hydraulic or electric-motor technologies [64]. As shown in Figure 2.8, McKibben air muscles can lift a 30 kg weight through a contraction of almost 20% its original length when pressurized to 0.45 MPa [55]. However, these favourable ratios do not take into account that the power supply and air pump must be carried by the wearer [52, 54-58, 60]. Once the weights of the power supply and pumps are added to the total actuator weight, pneumatic muscle measures of performance decrease considerably. Without including the batteries to power the system, which would be necessary
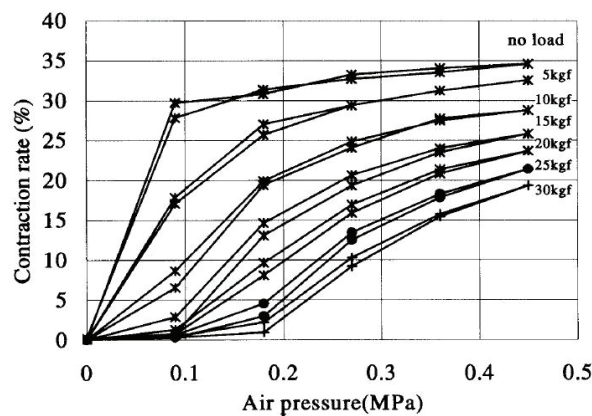


Figure 2.8: Contractile response of McKibben air muscles (from [55]).

17

for any portable actuator, the extra components of controllers, tanks, and compressors can weigh in excess of 4 kg [55].

Another problem with pneumatic muscle actuators is that they are less accurate and more difficult to control than DC motors, due to their non-linear response (Figure 2.8) [65]. As the bladder is pressurized, it expands radially and shortens longitudinally, producing a force that is proportional to the cross-sectional area of the bladder, a function of diameter squared:

$$\text{net force} = \text{pressure} * \Delta \text{ cross-sectional area} \qquad (2\text{-}1)$$

Furthermore, the cross-sectional area is not constant over the length of the air muscle. The PMA changes shape as the air muscle contracts, ballooning out more in the middle than at the ends as pressure increases. Also, actuator length is related to cross-sectional area by trigonometric functions, because the outer mesh dimensions, which define PMA length, are determined by the angles between the crossing fibres. These factors all contribute to a highly non-linear system that is difficult to control [63, 64].

As well as needing complex controls to use pneumatic air muscles effectively, PMAs have large energy losses caused by friction between the expanding rubber tube and the encasing fibre mesh. This friction causes heat and mechanical energy losses, causing hysteresis and shortening actuator life due to wear [62]. To mitigate this problem, pneumatic muscles have been created with the inextensible fibres arranged only longitudinally (Figure 2.9), essentially eliminating friction between the fibres and the rubber air bladder [62]. These air muscles are still non-linear, but hysteresis is reduced, service life is increased, and maximum force generated by the longitudinal pneumatic muscles is increased to approximately five times that of traditional McKibben muscles [61, 62]. However, since there is only longitudinal reinforcement, the actuator ruptures at much lower pressures than the traditional McKibben air muscle. While a McKibben air muscle can withstand pressures up to 0.8 MPa, the longitudinal air muscle can only withstand 0.2 MPa before the bladder fails. This results in lower maximum contraction ratios for the longitudinal air muscles [61, 62]. Saga and Saikawa [62] created a longitudinal air muscle using carbon fibre bundles that

18

can achieve similar contraction ratios at 0.2 MPA as McKibben muscles can at 0.6 MPa, but no force data for the actuator was presented.
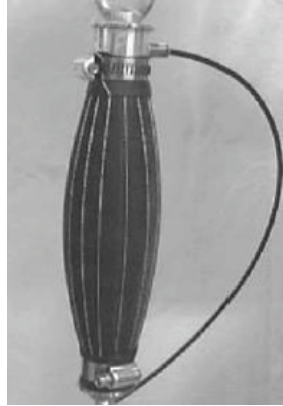


Figure 2.9: Longitudinal fibre pneumatic muscle actuator (from[62]).

A novel rotational pneumatic actuator was created by Yamamoto et al. [59] using pressure cuffs from sphygmomanometers separated from each other by aluminum plates (Figure 2.10). As the cuffs are inflated, they press apart on the plates, causing a moment about the joint to which the actuator is connected. However, this actuator is extremely big and bulky, and is therefore unsuitable for a small, discrete, and light full-leg orthosis.
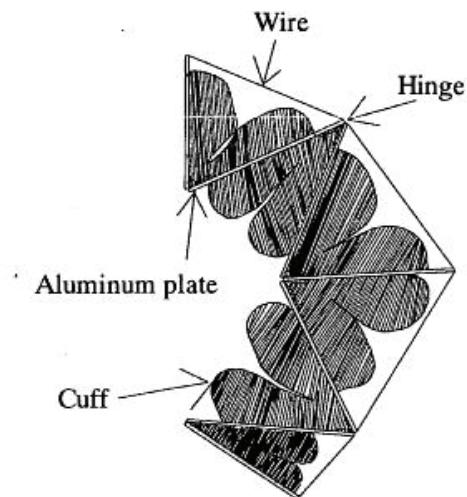


Figure 2.10: Rotational pneumatic actuator for the knee joint (from [59]).

## 2.4.2.2 Shape Memory Alloys

A shape memory alloy (SMA) is a metal alloy that undergoes deformations upon heating and cooling. If the metal is heated above a characteristic transition temperature, the internal atomic structure of the alloy transforms from martensite to austenite. Upon transition, the SMA attempts to revert to the configuration the material had when last in the austenitic phase. If there is resistance to this change in shape, the SMA can exert high forces to complete the transition [66, 67]. Upon cooling, the SMA transitions back to martensite. Once below the transition temperature, the specimen retains its austenitic shape until deformed by an external force. This deformation in easily accomplished since the SMA has a very low martensitic yield stress [66].

A number of SMAs have been discovered to date. However, nickel-titanium based alloys, commonly known as Nitinol alloys, are the most practical because they can undergo large amounts of strain upon transition relative to other SMAs [42], have good corrosion resistance, and have good electrical and mechanical properties [43, 66]. These materials can be used as actuators by attaching strained SMA wire to a load and passing an electric current through the wire. The current causes resistive heating and elevates the temperature of the material. Once passed the austenite transition temperature, the wire will contract and pull on the load. When the current stops, the wire cools naturally, and can be restrained with a small external load.

SMAs have very good strength-to-weight ratios and high strength-to-area ratios [43]. A 0.05 mm diameter Nitinol wire can lift over 7.25 kg. SMAs are light, extremely strong, and function silently. However, SMAs require temperatures between 55 and 100 °C to operate, have low cycle rates (they can only cycle as fast as the wire can cool), have high hysteresis, have a short service life, and can only achieve a 5% recovery strain, necessitating long lengths of wire to produce a large range of motion [43, 66].

## 2.4.2.3 Piezoelectric Actuators

Piezoelectric actuators use piezoelectric materials to create mechanical movement from electric fields [43]. In a piezoelectric material, an electric dipole is generated when the

material is strained. The opposite is also true, in that when a piezoelectric material is exposed to a voltage, the charged specimen strains and undergoes a mechanical displacement, which can be used to create piezoelectric motors. Due to the high forces from the piezoelectric effect, piezoelectric motors have a high power density and can thus be of small size and weight while still providing a high output torque [43]. There are two types of piezoelectric motors: rotary and ultrasonic.

Rotary piezoelectric motors (Figure 2.11) are similar to DC motors in that they are composed of a stator and a rotor. The stator is fabricated from a piezoelectric material, and is thus the active component, while the rotor is passive. When a voltage is applied to the contacts, the piezoelectric stator undergoes a strain and pushes on the rotor, which then rotates due to the large amount of friction generated between the two components. When the applied voltage is removed, the stator unstrains, but remains in contact with the rotor, though at a lower force and thus with a smaller amount of friction, preventing the rotor from rotating backwards. While able to provide large torques with small motor sizes, this actuator does not provide constant output motion because the stator return stroke occurs while still in contact with the rotor. Rotary piezoelectric motors are difficult to build and relatively expensive. [43]

For traveling wave ultrasonic motors, a propagating wave is generated in an elastic piezoelectric stator ring, causing particles on the ring surface to follow an elliptical path. Inside the ring is the rotor, which is turned by direct contact with the stator, through which the wave is traveling [40]. Figure 2.12 presents a schematic diagram outlining this process.
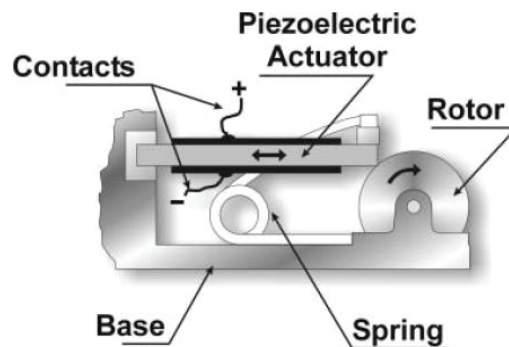


Figure 2.11: Rotary piezoelectric motor (from [43]).
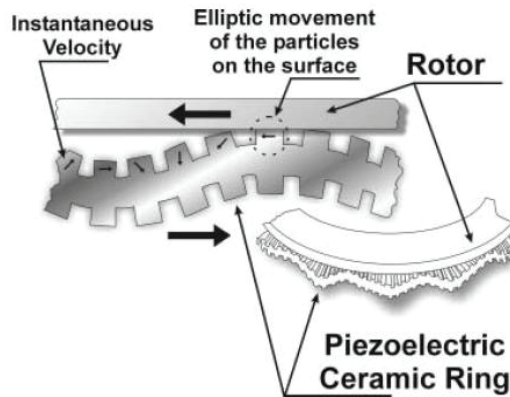
Figure 2.9: Stator and rotor of a traveling wave ultrasonic motor (from [43]).

Ultrasonic motors have a very high power density, and are able to provide high output torques at low rotational speeds, reducing the size of or eliminating the need for a transmission. These motors function silently, a very desirable trait for an actuator used in prostheses and orthoses, and do not create magnetic fields as do conventional DC motors. Ultrasonic motors have a fast response time due to low rotor inertia and are therefore easily controlled. When unpowered, torque and position are maintained, although ultrasonic motors are not back-driveable. [40, 43]

There are a number of disadvantages to ultrasonic motors. In order to create the propagation wave in the stator ring, a high frequency power supply is needed. Efficiencies of ultrasonic motors are lower than those of DC motors, and lifespans are shorter due to wear from contact between the stator and rotor rings. Heat generated could cause discomfort as well, due to close proximity of the motor to the skin for assistive devices. As with rotary piezoelectric motors, ultrasonic motors are also quite expensive. [40, 43]

### 2.4.2.4 Dielectric Elastomers

While still in the early development and testing phase, dielectric elastomers (DE) have been suggested for use as artificial muscles in robotics and wearable devices [41]. DEs can undergo large deformations, and have high energy densities, good efficiencies, and fast response times [68]. They are also silent, and have mechanical properties similar to natural muscle [41]. DEs function on the principle that like charges repel and opposites attract.

22

Flexible electrodes are attached to either side of a soft elastomer, and opposite charges are applied. This causes the two electrodes to be attracted to each other, compressing the elastomer in between. In order to conserve volume, the elastomer expands in the perpendicular directions. Repulsion of like charges within each flexible electrode serves to further increase area in the perpendicular directions [41]. When the power supply is turned off and the electrodes are short-circuited, the DE returns to its original shape [68].

There are a number of dielectric elastomer configurations for actuators. The most promising for linear actuation has the DE rolled into a cylinder and exerting an elongation force along its axis [41]. Use of this configuration for artificial muscles requires a compression spring inside the DE cylinder. While activated, the DE keeps the spring in an elongated state. The spring applies the contractile force when the DE is switched off [68]. This leads to a counter-intuitive and possibly inefficient actuator, because the 'relaxed' muscle state occurs when the DE is active. Even though they are lightweight, rolled DEs do no generate much force. Each 25 cm long roll provides only 15 N of force [68], necessitating a large number of DE rolls to create an actuator that can provide the high moments required for a powered leg orthosis. Due in large part to fatigue and contamination during fabrication, DEs also have a short and widely variable lifespan. DEs are vulnerable to numerous failure modes and are difficult to control due to their viscoelastic properties like creep, stress relaxation, and hysteresis [41]. Due to these and other issues, DEs are currently unsuitable for use in biomechanical devices.

## 2.4.2.5 Contractile Polymer Gel

Contractile polymer gels (CPG) undergo a change in volume in response to an external stimulus. CPG can be thermally, chemically, or electrically controlled, depending on the polymer gel used. The gels are light, and do not require large amounts for actuation, allowing CPG actuators to be small and compact [43]. However, the best properties are achieved when using a chemically activated system, in which the gel is immersed in a solution whose pH is altered to control contraction and expansion. This method creates hazardous waste in the form of salts, which must be dealt with, and necessitates a complicated delivery system for

the acidic and basic components that cause actuation [69]. CPGs are characterized by slow response times, from seconds to days for full activation [69, 70]. Stresses upwards of 1MPa, similar to that of natural muscle, can be generated with CPGs but they demonstrate very low power output per unit volume [69], low cycle frequencies, and high cost [43].

### 2.4.2.6 Electrorheological and Magnetorheological Fluids

Electrorheological (ERF) and magnetorheological (MRF) fluids consist of particles dispersed in an insulating fluid. These fluids can drastically change their viscosities or yield stresses when exposed to electric or magnetic fields, respectively. They have very fast response times and can create large, controllable resistive moments [39]. However, they are only able to resist motion, and thus are not suitable when active moments are needed.

## 2.5 Existing Devices

Much research has been done since the 1960s in the field of active orthoses, active prostheses, and powered exoskeletons, with similar difficulties and problems occurring in all fields [50]. Issues of non-portability [2, 52], large sizes and weights [71, 72], and heavy or fixed power supplies [52, 53, 73] are in the forefront of challenges that researchers are trying to overcome. This is especially true for the field of active orthoses. Active prostheses have the advantage over orthoses that they replace a body part and can replace the lost weight and bulk with powerful actuators and sufficient batteries [74]. Most exoskeletons support their own weight at all times, and therefore carry the heavy actuators and power supply necessary to run them [59, 73, 75-77]. Active orthoses, however, provide assistance by attaching to an existing limb, adding bulk and weight to a body part that does not function properly. As a result, active orthoses are often used in a clinical setting for gait training in a lab or on a treadmill, where a separate structure supports the device and body and a fixed power supply can be used. [53, 54, 60, 78]. However, this makes these orthoses non-portable, and thus unsuitable as a daily-use portable KAFO.

At times, there can be a blurring of lines between the categories of assistive technologies, especially between active orthoses and powered exoskeletons. In general, for

active orthoses, moments are applied to the device joints to cause or assist the user's motion, using a power source external to the human body [39, 50]. In the case of powered exoskeletons, the joint moments are often supplied by a powered actuator, according to the intended motion, to enhance moments generated by the user [50].

The following section is a review of powered assistive devices, including prostheses, exoskeletons, and orthoses. Included in the scope of powered orthoses are non-portable orthoses for rehabilitation and gait retraining. These large, heavy, and often fixed devices are not intended for daily use, but many use technologies that are potentially relevant to the design of a portable orthosis.

## 2.5.1 Active Prostheses

Several lower-limb prosthetic devices that use active components are available on the market. However, the majority use passive components controlled by small actuators to provide a variable resistive knee moment, but do not generate an extensor moment. This allows for a more natural level gait for the amputee, and easier navigation down inclines, down stairs, and across uneven ground [79, 80]. These devices weigh approximately one to two kilograms [80, 81] and can have a battery capacity of 45 hours [79], since the active components can have low power requirements (ex., open and close valves on hydraulic or pneumatic dampers). However, these devices do not assist the user in stair ascent or sit-to-stand tasks. The Otto Bock C-Leg, Freedom Innovations Plié MPC knee, and DAW Industries Self Learning Knee (SLK) [79, 82, 83] are prostheses that use actively controlled, passive hydraulic or pneumatic dampers to provide variable resistive knee moments.

The Ossur RHEO KNEE [84] uses magnetorheological fluid to generate resistive moments. Because the active component draws power to apply a charge to the MRF, to create resistive moments, the power requirement is again low but must be active at all times to maintain joint movement resistance. The RHEO KNEE cannot generate extension moments, as with hydraulic and pneumatic active prostheses.

The Power Knee (Figure 2.13), by Victhom Human Bionics, is an externally powered prosthetic leg that actively provides a moment to extend the knee, as opposed to only resisting knee flexion. In the initial version, data gathered from sensors strapped to the sound foot and ankle were sent wirelessly to the prosthesis to help determine the type of movement that should be provided. The current version uses embedded sensors in the device to provide movement classification data. The Power Knee can actively perform level gait up to 7 km/h, gait down and up inclines, stair descent and ascent, as well as sit-to-stand and stand-to-sit tasks. DC motors powered by 42V batteries are used to generate moments at the device knee joint, with a battery life of up to 6 hours continual use [74, 85, 86]. The prosthesis weighs 4.7 kg, and can support a 60 - 90 kg user. The sensors on the sound leg add another 90 g. However, the Power Knee does have certain limitations. Because Bluetooth technology is used in the system, the wearer should avoid utilizing the Power Knee while in close proximity to microwaves, cellular telephones, and wireless phones in operation, or any other Wi-Fi or Bluetooth device; which is something difficult to do in today's world. The device should not be used in bad weather, since the prosthesis is not allowed to come into contact with water. Furthermore, in order to ensure that the prosthesis performs the correct task at the correct times, the user must perform specific movements at the initiation of a new type of motion. For example, to ascend stairs, the user must come to a complete stop at the base of the stairs and begin ascending with the natural leg, exaggerating the height to which the



Figure 2.13: Victhom Power Knee (from [74]).

sound leg is lifted before striking the step with the forefoot. After the final stair, the user must either stop and stand on the sound leg, or strike the ground with the heel of the sound leg to transition back to normal gait [85].

## 2.5.2 Powered Exoskeletons

Powered exoskeletons are developed to augment an individual's load carrying abilities or provide powered assistance for locomotion. A lower extremity exoskeleton, BLEEX (Figure 2.14), allows greater load carriage through the use of a backpack attached to the device frame [45]. A full body exoskeleton, HAL-5 (Figure 2.15), allows the wearer to carry a larger load in their arms [87]. Locomotor assist devices lessen the demands placed on the leg muscles to aid people living with disabilities and reduce fatigue in workers who spend their time standing and squatting [75, 77]. Examples include HAL-3 (Figure 2.16) and Honda's walking assist device with bodyweight support system (Figure 2.17). However, because exoskeletons are bipedal, they have the advantage of supporting their own weight at all times; therefore, these designs may not be suitable for unilateral orthotic devices that are worn by the user. However, some insight can be gleaned on how the unilateral knee-extensor muscle-weakness problem can be solved.



Figure 2.14: The Berkeley Lower Extremity Exoskeleton, BLEEX (modified from [73]).

Figure 2.15: Full body exoskeleton, Hybrid Assistive Limb 5, HAL-5 (from [87]).

Figure 2.16: Hybrid Assistive
Limb 3, HAL-3 (from [87]).



Figure 2.17: Honda's walking assist device
with bodyweight support system (from [77]).

### 2.5.2.1 BLEEX

The Berkeley Lower Extremity Exoskeleton, BLEEX (Figure 2.14), is a lower-limb exoskeleton designed to aid the user in carrying heavy loads through the use of an attached backpack. BLEEX can support an extra 34 kg beyond what the user can naturally carry [45]. The exoskeleton consists of two externally powered robotic legs that attach to the legs of the operator, a power supply system located in a backpack attached to the device, and a central controller, also located in the backpack [49].

BLEEX is controlled using ground reaction force, acceleration, position, and orientation measurements taken from the exoskeleton. This information is used to determine exoskeleton motion such that the user feels minimal force from the device [45, 88]. The BLEEX system uses linear hydraulic actuators to provide moments to the device joints because hydraulic actuators have high power-to-weight ratios and a high degree of controllability [88]. Bidirectional hydraulic actuators were used on all joints because both active flexion and extension must be provided for tasks other than level walking [45]. During unloaded level walking with the BLEEX, the hydraulic actuators consume 1.1-1.3 kW of power. For comparison, the human body uses 165 W of power during level gait, giving a 14 % efficiency to the hydraulic actuation system [45, 88]. The total power output necessary to run the hydraulics and electrical control system safely is approximately 2.5 kW. Because a large

28

amount of power is required to run the system and BLEEX must be re-fuelable in the field, a special gasoline combustion power unit is used . Gasoline has a high energy to weight ratio [49] and is widely available. Additional stores of gasoline are also easy to carry. However, the power unit creates fumes and makes BLEEX a very noisy device. The BLEEX is therefore not suitable for use as a mobility aid. Furthermore, BLEEX is designed to transmit normal bodyweight loads to the wearer to give a natural feel [49], and would therefore not provide support to an individual who lacks the strength for normal load bearing.

## 2.5.2.2 Sarcos' Wearable Energetically Autonomous Robot

Sarcos Research Corporation also developed a lower body exoskeleton that uses a backpack for load carrying. Sarcos is also developing a full body exoskeleton, although it is still powered and controlled externally [89]. The lower body exoskeleton supports heavy loads, upwards of 84 kg [90]. Like BLEEX, Sarcos' exoskeleton uses hydraulic actuation. However, rotational hydraulic actuators, located at the device joints, provide the joint moments [50]. Ground reaction force is measured through sensors on a stiff metal plate, attached to the base of the foot [50]. As a result, the metatarsal joints in the foot cannot flex, which may result in unnatural and uncomfortable gait.

## 2.5.2.3 HAL

The Hybrid Assistive Limb 5 clinical type, also referred to as the HAL-5 Type-C (Figure 2.18), is another lower extremity exoskeleton. Instead of load carrying, this device is intended to assist the elderly and people with lower-limb disabilities by supplying part of the necessary joint moments for level walking, SA, or STS [91]. Hal-5 Type-C uses position, force, and acceleration sensors to determine what movement is desired and then supplies up to 60 Nm directly to the device joints using DC motors with harmonic drive transmissions [75, 87]. However, the motors are somewhat bulky and, while smaller than those on the previous generation device, HAL-3, the motors could impede arm swing during walking and prevent a comfortable and natural gait pattern. A computer controlling the device and a battery pack power supply are strapped to the user's waist [87], as seen in Figure 2.18. In the full body counterpart (HAL-5), a device meant for load carrying, the battery provides more

29

than 160 min of use per charge. Total system weight is 15 kg [87], which is self-supported by the exoskeleton [91]. For HAL-5, optimal device calibration for a given operator takes two months [50], which is inconvenient for would-be users since this would mean many trips to the clinic and a long period of unsteady gait before the user could benefit fully from the system.
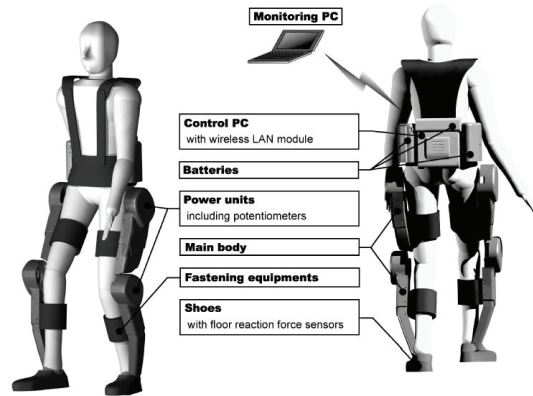


Figure 2.18: Controller and power supply placement for the HAL-5 Type-C (from [87]).

## 2.5.2.4 Honda Walking Assist Devices

Honda has developed two walk assist devices. The Stride Management Assist can only be used by people still capable of walking unaided. This first walk assist device straps around the waist and thighs of the user, and enhances hip flexion to increase stride length and augment walking speed. This device uses flat brushless DC motors, weighs 2.8 kg, and uses a 22V lithium ion battery to provide upwards of 2 hr usage time before a recharge is necessary [92]. The Stride Management Assist is not suitable for individuals with low quadriceps strength, since no knee moment support is provided and the user would therefore be in danger of collapse.

The Bodyweight Support System (Figure 2.19) is designed for people who are able to walk on their own [93] but require more support than the Honda Stride Management Assist. To use the Bodyweight Support System, the user wears shoes attached to the device and straddles a seat that carries a portion of their weight. This walk assist device weighs 6.5 kg,

30

and is driven by two DC motors powered by lithium ion batteries with a charge life of two hours [93]. The Bodyweight Support System is designed to provide an increasing assistive moment with increasing knee joint flexion angle [77]. In other words, when the user crouches or climbs stairs, a larger percentage of bodyweight is supported by the device than when the user performs level gait. However, the amount of aid would not be sufficient for people with quadriceps weakness. The device can reduce muscle activity by up to 23% during squatting and 19% during stair ascent [77]. Because the amount of support decreases with decreasing knee flexion angle, the assistive knee moment during level walking would be low, since level gait occurs with nearly straight legs, making the Bodyweight Support System more suited to fatigue reduction in labourers than as a mobility aid for individuals with quadriceps weakness. Another problem with the device is that because the design involves the use of a seat between the legs, it is not possible to sit while using the device.



Figure 2.19: Honda's walking assist device with bodyweight support system (from [77]).

## 2.5.2.5 Nurse Assisting Exoskeleton

Yamamoto et al. [59] developed a full body exoskeleton to assist nurses in handling and lifting patients (Figure 2.20). The 13.4 kg device was designed with all components posterior to the user, to not interfere with contact between the nurse and patient. The exoskeleton uses pressure cuffs to create rotary pneumatic actuators. As the cuffs are inflated, they push against one another and cause joint rotation as a result of actuator geometry [59]. Each cuff

in each actuator is inflated by its own micro air pump, all of which are powered by two nickel-cadmium batteries. The suit can support approximately half the weight of a patient, or 30 kg [94]. Muscle hardness sensors, strapped to the operator's arms and legs, are used to determine the desired motions for device control. Design deficiencies include: the air supply system did not function properly, with the leg actuators not receiving sufficient pressures; the shoulders are unpowered; and it is difficult to turn or kneel while wearing the suit [94]. Also, the suit is entirely behind the user and is quite bulky, and thus the user would be unable to sit. This also makes the exoskeleton inconvenient for use because the user might lose awareness of the extent of equipment and accidentally strike people or obstacles with the device.
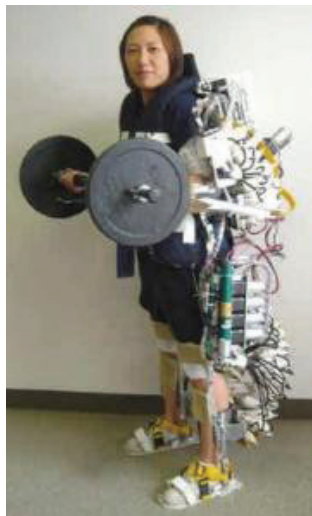


Figure 2.20: Full body exoskeleton for assisting nurses in lifting and maneuvering patients (from [50]).

### 2.5.3 Active Orthoses

Designing portable powered orthoses presents a large challenge to engineers due to restrictions on size and weight of the orthosis and power supply, since everything must be supported by the wearer instead of supported by the device, as with exoskeletons. Many powered orthoses were designed for clinical rehabilitation settings. In this setting, the orthoses do not need to be mobile or portable and can therefore be powered and supported by separate, fixed systems. However, many use the same technologies and design ideas that were considered for use in portable orthoses. The following section will be divided based on

the type of actuator used in the device: electric motors, pneumatic air muscles, pneumatic or hydraulic cylinders, and others.

### 2.5.3.1 Active Orthoses Using Electric Motors

One of the most common uses of electric motors in orthoses is in a lead screw or ball screw actuator [78, 95-97]. These actuators provide a linear force but can be attached to span a joint, thus providing a joint moment [53, 96, 97]. The motor can also be a part of a series elastic actuator (SEA), quite common in ankle-foot orthoses [78, 95, 98].

The Active Leg Exoskeleton (ALEX), a unilateral, non-portable, gait retraining orthosi that, uses lead screw actuators spanning the hip and knee to generate joint moments [96]. Because ALEX is a gait retraining device, its control scheme is based on assisting the patient as needed. The device only provides joint moments when the patient deviates from normal gait. This is achieved by resisting incorrect and assisting desired movements [99]. Device weight is externally supported and power comes from an outside source. Because the device is not very portable, ALEX can only be practically used on a treadmill (Figure 2.21).

Because a high transmission ratio was chosen, the lead screw actuators used by ALEX cannot be back-driven. However, back-drivability is important, especially in a gait retraining device, because back-drivability of a motor allows the user to generate the leg movement, if
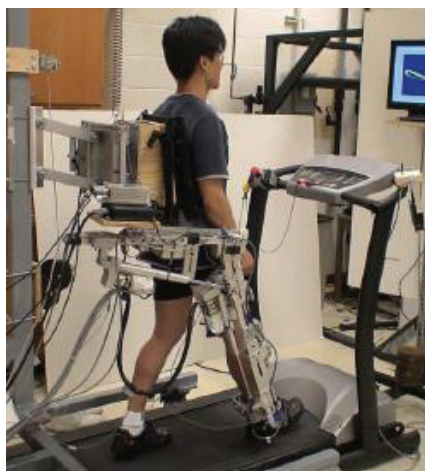


Figure 2.21: The Active Leg Exoskeleton in use. Actuators are DC motors with lead screws (from [99]).

they are able to provide the necessary joint moments, without much resistance from the orthosis. In order to obtain device 'back-drivability', the research group had to use complex compensation methods involving friction models and load cells on the lead screws. This level of complexity is undesirable, and avoidable if a lead screw design that allows for back-drivability is chosen.

Lokomat, another powered rehabilitation orthosis, meant for use on a treadmill by stroke victims or spinal-cord injury patients, is similar to ALEX. However, Lokomat is bilateral, and the weight of both the orthosis and the user are externally supported. Joint moments are supplied by four externally powered linear actuators, one at each hip and knee joint [100].

Ohta et al. [97] designed a motorized reciprocating gait orthosis (RGO) for paraplegics. The design used two 0.8 kg ball screw actuators (Figure 2.22) to provide a moment to each knee while performing level gait. With a stroke length of 150 mm, the actuator was able to permit a maximum flexion angle of 70°. Each actuator was powered by 12 nickel metal hydride batteries, which would last for approximately one hour of continuous use. However, the knee actuators only provided flexion and extension moments while the leg was in the swing phase of gait, resulting in very little load on the motors, and allowing for smaller and weaker motors to be used. This design would therefore not be capable of powering the stance leg during mobility tasks without increasing actuator size.
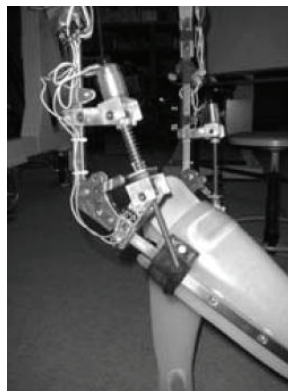


Figure 2.22: Ball screw actuator spanning the RGO knee joint (from [97]).

The device closest to satisfying the design objectives of this thesis, the Roboknee, by Yobotics (Figure 2.23) is a portable, unilateral, leg orthosis that provides a sufficient moment to power knee extension during walking, stair climbing, and deep knee bends. Roboknee uses a ball screw and compression springs to create a series elastic actuator (Figure 2.24), weighing 1.13 kg, which attaches to the user's thigh and calf. Actuator stroke is 30.5 cm and can provide a continuous force of 565 N and a maximum force of 1330 N [53]. The springs give some compliance to the actuator, resulting in more comfortable and less jarring knee motion [53]. Roboknee uses GRF (force sensors in the shoe) and knee angle and velocity (linear encoder that determines actuator stroke length), to determine what the desired motion is, and adjusts the SEA length accordingly [53].



Figure 2.23: The Roboknee, by Yobotics. (Modified from [53]).



(a)                                        (b)
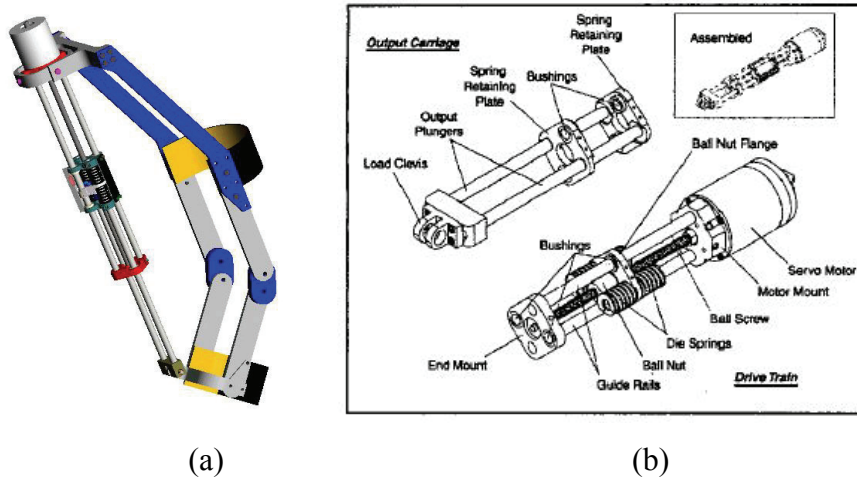
Figure 2.24: The ball screw series elastic actuator (a) in the device and (b) actuator design (Modified from [53]).

In order to be fully portable, the user must carry a backpack containing the computer control system and 4 kg of nickel metal hydride batteries. Even with 4 kg of batteries, the device can only be used for 30-60 min between charges [53] since the device is always active, even during level walking. This is insufficient for an orthosis, as an assistive device should provide a full day of support without the need for a recharge. The device also restricts the user from running. Sitting while wearing the Roboknee is not possible because the actuator spans from thigh to calf. In addition, the device is difficult to don and doff [53], increasing the likelihood of rejection by the user. This device has also only been tested on healthy individuals [101] so the benefit to those with weakened quadriceps is unclear.

Series elastic actuators are also used to create so-called robotic tendons. These often span the ankle joint of an ankle-foot orthoses (AFO) to correct for dropfoot, a motor deficiency condition that causes the foot to slap down when the heel makes contact with the ground and causes the toes to drag on the ground while the leg swings forward [78]. SEAs can also cushion the impact of heel-strike and provide plantarflexion assistance when the leg pushes off [95]. Robotic tendon SEAs use a lead screw to control the level of compression or extension of a spring to which a non-rotating nut is attached (Figure 2.25). The nut controls the spring force, and thus the moment provided to the joint.
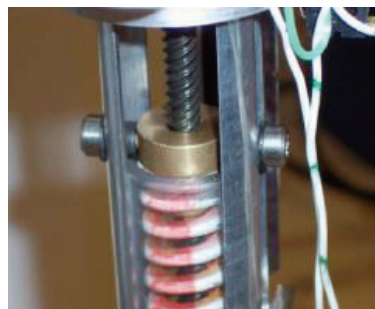


Figure 2.25: Lead screw and spring components of a robotic tendon SEA (from [48]).

Blaya and Herr [78] used a SEA in their AFO (Figure 2.26) to prevent dropfoot foot motion by controlling the length of a compression spring in the actuator throughout the gait cycle to produce varying dorsiflexion moments. The actuator, attached posterior to the leg, is initially extended for heel strike in order to provide a resistive moment to stop the foot from

36

slapping the ground upon heel impact. The joint moment is then removed to not impede plantarflexion during pushoff. This is achieved through actuator shortening, which allows the compression spring to elongate and return to its resting length. Finally, the SEA lengthens again, causing the foot to dorsiflex, so that the foot does not drag during swing. This method provides an active assistive moment only during swing.
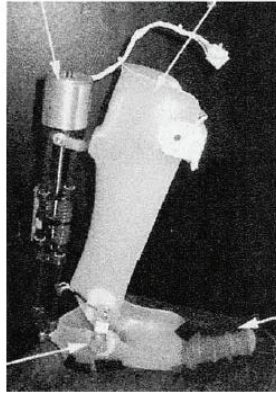


Figure 2.26: Series elastic actuator in an ankle-foot orthosis (modified from [78]).

Another AFO was designed by Oymagil and collagues using a 0.95 kg robotic tendon to provide a resistive moment at heel strike, similarly to Blaya and Herr, but also to provide an active plantarflexion moment to aid in push-off at the end of stance [95]. This is achieved by first extending a spring, through SEA shortening and natural ankle dorsiflexion that occurs between foot flat and the late stance phase of gait. The spring then releases its stored energy to provide a plantarflexion moment during push-off, producing positive work (Figure 2.27). The robotic tendon design provides all necessary resistive and propelling power for normal level walking [95]. However, this design relies on resistance from bodyweight to extend the spring to provide the moment about the joint. The design would therefore not be suitable for stair ascent, where there is no period of flexion while the affected limb is load-bearing before the extension moment is required. Both this AFO and that of Blaya and Herr are powered by a fixed source and, at this stage of development, are not portable devices [78, 95].
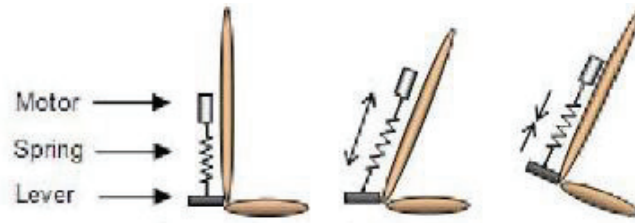
Figure 2.27: Schematic of robotic tendon SEA action to provide plantarflexion moment (from [95]).

The ABLE system [102] is a powered lower-body orthosis, wheeled foot platform, and telescoping crutch system for individuals with total lower body paralysis. The system does not allow for level gait, but instead uses platforms with motorized rollers attached to the feet to provide upright mobility to the user. During straight-line motion, the orthosis joints are locked with knee fully extended and crutches are used for balance. Turning is possible, but time consuming and complicated. Employing the telescoping crutches for additional lift, the powered orthosis enables the wearer to perform STS and SA, as well as ramp ascent, ramp descent, stand to sit, and stair descent, although the last two are performed with great difficulty. The components are powered by DC motors. The crutches use a ball screw design for linear actuation, while the orthosis joints and foot platforms use non-backdrivable worm gears. The complete system weighs 17 kg. This device is portable if a backpack containing a power supply is worn, but no information is given about use times or about the power supply itself. The device is meant for individuals with total lower body paralysis, to be used in lieu of a wheelchair.

Kong and Jeon [103] have designed a portable, bilateral lower-limb orthosis for the elderly (Figure 2.28). Instead of designing the device that bears the active component weight, the motors, controllers, and batteries were placed in a walker that drives on motorized castors in front of the orthosis user. The walker provides additional support to the patient, and allows for the orthosis itself to weigh under 3 kg. Cables and pulleys transmit torque from the four motors in the walker to the hip and knee joints (Figure 2.29), assisting in level gait and possibly ascent and descent for low grade inclines. The orthosis also aids in stand-to-sit and sit-to-stand, with the walker handle lowering and raising via pneumatic actuators during

38

these two tasks based on knee joint angle. The system uses potentiometers at the joints and air bladder pressure sensors located in the shoes and strapped tightly to the thighs to determine user intent through GRF and thigh muscle contraction. Because a cable and pulley system transmits power from the motors to the orthosis, the walker must remain a fixed distance from the user [50]. Also, the walker, which drives itself, could potentially lead the user at a pace that they are uncomfortable with or unable to keep up with at a given time. The walker also makes the system unsuitable for uneven surfaces, stairs, or the outdoors.



Figure 2.28: Portable bilateral walking assist orthosis for the elderly (from [103]).
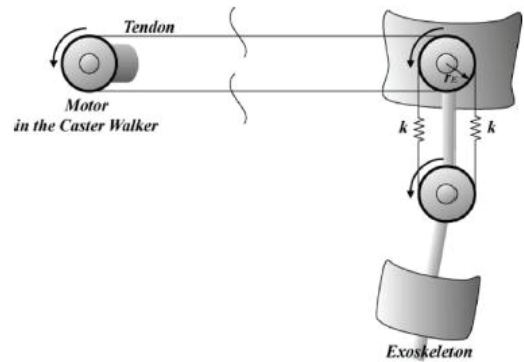
Figure 2.29: Transmission of torque from castor motor to orthosis (from [103]).

The Lower-extremity Powered Exoskeleton (LOPES) is another gait rehabilitation orthosis for use on a treadmill. The LOPES guides the legs through correct level walking gait cycles while providing the minimum necessary assistance [104]. Since LOPES is designed for rehabilitation-clinics, the driving motors are located external to the device. This device controls the movement of both legs, providing degrees of freedom for knee and hip flexion and hip abduction. External servomotors are attached to Bowden cables, where an inner wire moves within an outer tube. The motor pulls the inner wire, which is wrapped around a special actuator disc (Figure 2.30). The joint flexes or extends when the wire pulls on the actuator disc, depending on which side of the Bowden cable is retracted by the servomotor. Because the DC motors do not need to be on the orthosis, larger and stronger motors can be used for better output torques and control. The device delivered joint moments from 25 to 60

Nm, and a power up to 250 W [104]. However, a portable system based on LOPES may not be feasible since smaller motors may not be sufficient to overcome the large power losses from the friction between the wire and the actuator disc [104].



Figure 2.30: Bowden cable actuator for the LOPES rehabilitation orthosis (from [104]).

Ruthenberg et al. [71] designed the Powered Gait Orthosis (PGO) as an experimental device to determine the forces between a powered orthosis and its wearer during use. The device has one degree of freedom for each leg, since knee and hip joint movement is controlled by a single mechanism. One 13.2 V DC motor powers each leg through a complex 8-bar linkage (Figure 2.31). The hip joint is rotated by a four-bar crank-rocker, links 1-4, where link 1 is fixed to the torso and is thus the ground link. The knee is controlled by a cam-follower mechanism. Link 2, which is directly driven by the motor input and rotates the hip, also causes link 8 to turn, driving the knee through the proper angles for once cycle of gait. Through this mechanism, one complete crank revolution (link 2) produces one full cycle of gait for that leg. However, due to the linkage mechanism used to drive joint motion, only one mode of gait is possible, making other tasks like SA, STS, navigating around or over obstacles, or walking on uneven or inclined ground impossible. The orthosis is also extremely heavy, weighing 26.75 kg, although the authors stated that the next generation PGO will be approximately 10 kg. The control circuitry and battery pack can be fastened to the back of the orthosis corset, making the device portable. However, the PGO would be an impractical device for everyday use, due to the high weight and restricted joint motion.

40
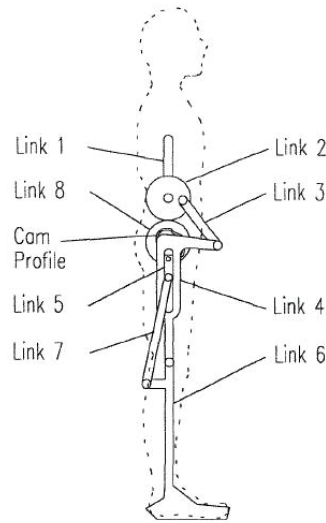
Figure 2.31: The Powered Gait Orthosis controlling hips and knees through 8-bar linkage (from [71]).

## 2.5.3.2 Active Orthoses Using Pneumatic Air Muscles

Pneumatic muscle actuators (PMAs) are popular for use in orthoses due to their high strength and light weight. However, achieving portability and low device weight is difficult because they require compressors or tanks to provide an ongoing pressurized air source. As a result, PMAs are often used in non-portable rehabilitation devices. Because orthosis designs using PMAs are often similar, only a few representative orthoses will be detailed in this section.

Researchers at the University of Michigan [54, 56, 60] have designed a number of ankle-foot and knee-ankle-foot orthoses using McKibben air muscles as actuators. All devices are meant for use in rehabilitation of individuals who have suffered neurological injuries, as well as experimental investigation into neuromechanical lower limb control during walking. All PMAs in these orthoses are powered by an external air source at pressures up to 6.2 bar. The simplest design (Figure 2.32) consists of a 1.3-1.7 kg AFO, using one PMA, or two in parallel, to provide powered plantarflexion [60]. A foot switch was placed inside the shoe at the forefoot to determine when air should be supplied to the PMA. One PMA could provide 1700 N when activated at its maximum length. The force dropped to zero when activated at 71% of its max length. In order to obtain sufficient plantarflexion moment, a moment arm of 10 cm was used, providing 57% of the total plantarflexion moment. The authors determined

41

that there were no significant differences in function between the AFO with one and with two PMA, because patients tended to walk with more plantarflexion when using the two-PMA AFO, leading to activation of the actuators at lower lengths, resulting in a lower contractile force, similar to the single-PMA AFO [60].



(a)                              (b)
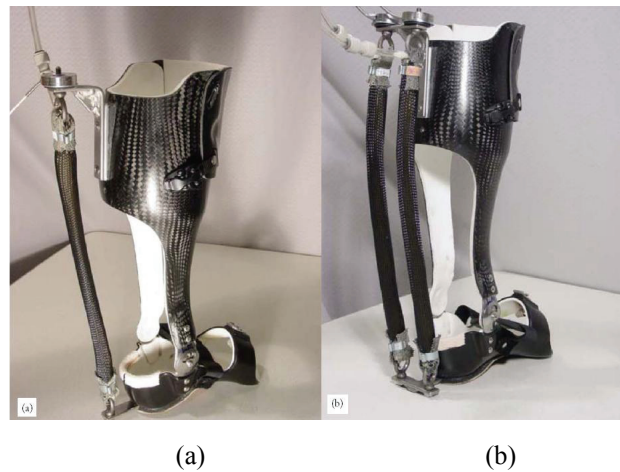
Figure 2.32: AFO for plantarflexion assist using (a) one and (b) two McKibben PMA (from [60]).

An improvement on this design used an AFO and two PMAs in an antagonistic pair (Figure 2.33a), to provide both powered plantarflexion and powered dorsiflexion [54]. The complete AFO weighed 1.7 kg. Instead of using footswitches, the PMAs were controlled through electromyography (EMG), with activation strength proportional to level of muscle contraction. The device was able to supply 36% of the peak plantarflexion moment and 123% of the peak dorsiflexion moment observed when a healthy individual walked in the AFO without the use of the PMAs. Besides being non-portable, this design also has the limitation of being somewhat bulky, and would be difficult to wear underneath clothing.

The device in Figure 2.33a was elaborated upon and converted into a full KAFO [56]. The KAFO (Figure 2.33b) can generate extension and flexion moments at the knee in addition to the plantarflexion and dorsiflexion moments at the ankle. However, the device was not tested, and so its performance and limitations are unknown. It is possible to see from Figure 2.33b that the KAFO is somewhat bulky and, as with the previous device, would likely not fit under clothing.
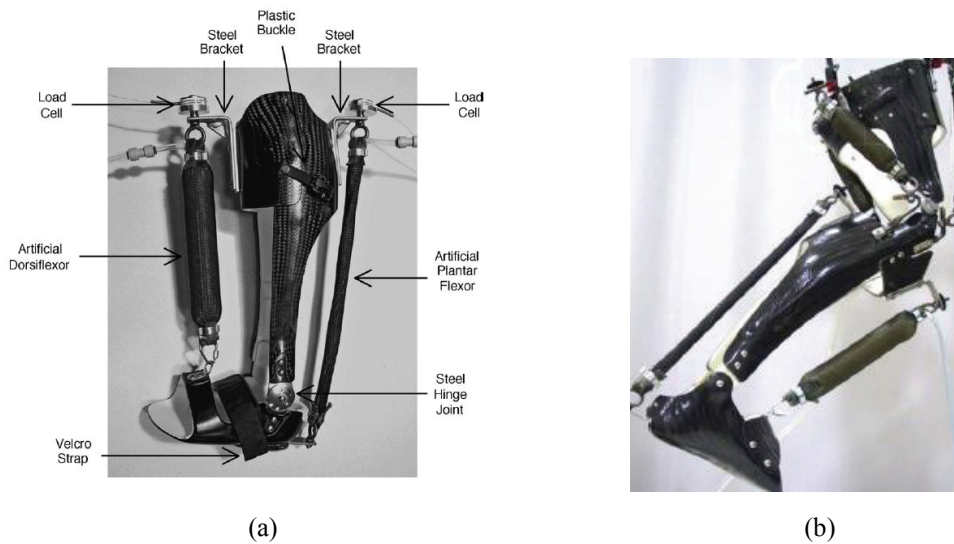
Figure 2.33: (a) AFO with antagonistic PMA pair to provide plantar and dorsiflexion torque (from [54]).
(b) The PMA actuated KAFO provides antagonistic moments about the knee and ankle (from [56]).

Costa and Caldwell have designed a full, bilateral, lower body orthosis to augment joint forces and assist in walking rehabilitation training for stroke and brain or spinal-cord injury patients [58]. Using PMAs to provide the joint moments, the orthosis can supply flexion-extension and abduction-adduction moments at the hips and flexion-extension moments at the knees and ankles (Figure 2.34). The system weight is 12 kg, including electronics but excluding external power and air supply. Experimental results showed that orthosis performance was not at an acceptable level.



Figure 2.34: Ten degree-of-freedom lower-body orthosis. Actuated by antagonistic PMA pairs (from [58]).

43

## 2.5.3.3 Active Orthoses Using Other Actuation Methods

In addition to PMAs, pneumatic cylinders can also be used for joint actuation. Belforte et al. [52] designed an active, bilateral, complete lower body orthosis for paraplegic individuals, with the goal of providing the support and joint moments needed to walk upright. The device was intended to be portable, for this design iteration, the orthosis was externally powered. The orthosis used two different pneumatic cylinder setups to power the joints. At the knee, a double end cylinder attached to a chain was used to create knee motion. The chain drove a sprocket at the knee joint, such that the linear motion of the pneumatic cylinder rod created a knee rotation (Figure 2.35a). At the hip, a pneumatic cylinder spanned the joint (Figure 2.35b). Moments above normal for gait were supplied to the knee to prevent collapse, with mechanical stops added to avoid joint hyperextension, which would injure the user. Since a large range of motion and high moments are required at the knee, having an actuator span the joint becomes impractical since attachment points must be far enough away from the joint centre to provide an adequate moment. This does not allow the orthosis to be worn under clothing and makes sitting difficult. For this reason, the chain-driven knee actuator was designed. However, placing the pneumatic cylinder distally on the leg greatly increases the leg's inertia. This is unfavorable in a unilateral orthosis or a device that would be passive and free swinging.



(a)  (b)
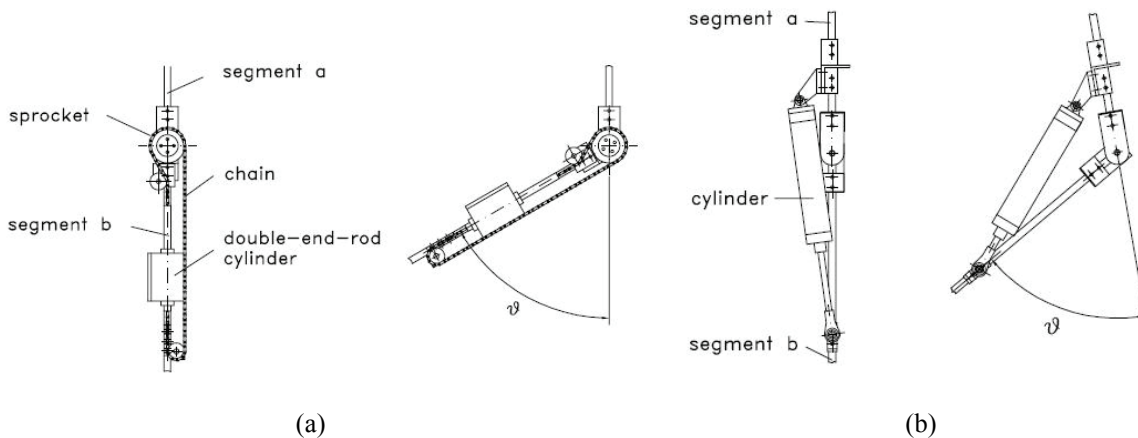
Figure 2.35: (a) The chain driven knee actuation system using a double-ended pneumatic cylinder and (b) the hip actuation system using a bi-directional pneumatic cylinder to span the joint (from [52]).

44

Saito et al. [51] designed a powered lower-limb orthosis for rehabilitation of paraplegic and hemiplegic patients, using hydraulic cylinders for actuation [51]. The four bilateral hydraulic actuators each span two joints, either hip and knee or knee and ankle (Figure 2.36), to mimic the biarticular muscles found in the legs in an attempt to create an orthosis motion that more closely resembles natural gait. As a result, when one actuator is active, both ends either extend or retract and control the movement of two joints. Saito stated that biarticular actuators also lead to control scheme simplification and weight savings due to the lower number of actuators. The total orthosis weight is 7 kg, not including the hydraulic pump and power supply that were both external to the device. Each actuator provides a standalone force of 390 N but higher applied forces and segment velocities could be achieved by combining multiple cylinders. However, due to the biarticular nature of the actuators, the two cylinders controlling the knees and ankles had to be placed on the inner shank. This forces the user to walk with splayed legs and introduces the danger of tripping if the inner actuators accidentally make contact. This is especially dangerous because orthosis users would likely lack the ability to recover from a stumble.



Figure 2.36: Biarticular hydraulic actuator placement (from [51]).

Active orthoses have also been designed to use the residual muscle strength of the wearer to power the orthosis [105, 106]. In functional electrical stimulation (FES), the thigh muscles are stimulated by an electrical current to cause muscle contraction and leg extension. This technique is normally employed during the swing phase of gait, and is intended for individuals who still have quadriceps strength but are unable to control contraction themselves, such as people with spinal cord injuries. However, FES is not suitable for generating the power needed for STS, SA, or ascending inclines, since individuals with weakened quadriceps muscles do not have the strength necessary for these movements. In addition, FES leads to rapid muscle fatigue and is unable to precisely control joint moments, making muscle stimulation a less favorable option.

While no information was found on shape memory alloys being used in lower limb orthoic devices, there has been research into SMA use in artificial hands. Bunhoo et al. [38] used SMA wires to create antagonistic actuators for flexion-extension and adduction-abduction of the fingers. However, the wires showed low actuation strains and forces, and were suggested as being better suited to a prosthetic hand for children. Because of these limitations, and those described in the earlier section, SMA actuation is not viable for a knee-ankle-foot orthosis knee-extension-assist.

# Chapter 3. Knee-Extension-Assist Design and Development

## 3.1 Rationale

Considering the diverse range of pathologies that can cause lower-extremity weakness [2] and the mobility difficulties from quadriceps weakness [18, 21, 32], there is a need for simple, inexpensive, effective leg orthoses to assist with high knee extension moment tasks. An orthosis that aids sitting, standing, climbing stairs, and walking on ramps would reduce reliance on others for assistance, ease the burden placed on family members or care-givers, and enable the orthosis user to lead a more independent lifestyle.

Traditional and stance control KAFOs have improved the ability of those with weakened quadriceps to perform level walking by providing lower limb support. Traditional KAFOs help people stand upright and walk while supporting their bodyweight on their affected limb. SCKAFOs give the wearer free knee motion during the swing phase of level walking, allowing the user to walk more naturally. However, these devices are unable to help the user complete common tasks that require a high level of quadriceps strength while the knee extends or flexes.

This research provides an assistive knee-extension moment to help individuals with weakened quadriceps to independently perform high knee-extension moment tasks; such as, STS, stand-to-sit, SA, and ramp walking.

As outlined in the previous chapter, a number of assistive devices can provide additional power to the knee to aid a user in completing tasks that require a higher knee moment than they are capable of generating unaided. These devices use a wide range of actuator technologies and power sources to provide external moments to a joint. Since these devices require external sources of power and large actuators, which are usually bulky and heavy, many are designed to be non-portable [51, 52, 54]. These devices therefore do not solve the problem of increasing mobility by providing an assistive knee moment, since their use is restricted to a fixed area, often a rehabilitation or gait training clinic. Other portable devices are often large and heavy bilateral exoskeletons, intended to augment the abilities of healthy

individuals [45, 59, 75, 90]. Because they are bilateral, these exoskeletons can support their own large weight and that of their heavy power supply. A portable, powered, unilateral orthosis has been previously designed [53], but, among other shortcomings, this device has a heavy power supply, with a limited battery life, whose weight must be supported directly by the orthosis user.

A small and light device that could provide an extension moment to the knee without being cumbersome would allow greater mobility for an individual with weakened knee extensor muscles. Being able to perform the previously difficult or impossible tasks of STS, ramp ascent, and SA greatly increases confidence, independence, and quality of life for individuals with a mobility disability.

## 3.2 Objectives

The goals of this research were to design, develop, and test a portable and fully wearable extension-assist device that provides a knee-extension moment to a KAFO (including SCKAFO) to aid the wearer in successfully performing high quadriceps demand tasks. The thesis objectives were to:

1. Design a modular component to be attached to a KAFO capable of providing an extension moment that would assist in sit-to-stand and stand-to-sit, incline ascent and descent, and stair ascent without impedance to knee motion during the swing phase of gait. The component size and weight should be minimal. Cost should be kept low. (Detailed design criteria are given in Section 3.3).

2. Manufacture a functional prototype of the KEA.

3. Carry out mechanical tests on the KEA to determine device performance.

4. Perform biomechanical testing of the new KEA on a KAFO worn by healthy individuals to determine device effectiveness in assisting the target tasks.

## 3.3 Design Criteria

Based on the review of orthotic-devices and relevant-technology literature and through discussions with rehabilitation professionals, the functional and structural requirements of a KEA device were determined. A quality function deployment (QFD) chart [107] (Table 3.1) lists and weights the importance (from 0 – least, to 10 – most) of the design requirements as determined by the user, the orthotist, and from the manufacturing perspective. The centre of the QFD chart shows the relationship between design requirements and quantitative performance and the engineering parameters that can be controlled in the design process. The strength of this relationship, determined by the investigator, is denoted by the letters a, b, c. The bottom of the chart provides the engineering parameters of existing devices. The ability of these devices to satisfy the design requirements is shown on the right. Target specifications (chart bottom) were determined for an ideal extension-assist device. The chart also provides insight into where other devices fail to fulfill the design criteria.

### 3.3.1 Functional Requirements

The ideal powered KEA would provide 100% of the required knee moment for sit-to-stand, ramp gait, and stair ascent. This corresponds to a maximum required knee moment of 126 Nm (mean + 1 standard deviation) [30], for a 90 kg individual. Since the device should be a modular component attached to a KAFO, total device weight should be below the maximum permissible weight of a commercial KAFO.

Table 3.1: Quality Function Deployment

Legend:
- 0 - Design doesn't meet requirement at all
- 1 - Design slightly meets requirement
- 2 - Design somewhat meets requirement
- 3 - Design mostly meets requirement
- 4 - Design completely meets requirement
- na - information not available
- x - does not apply

- a - weak relationship
- b - medium relationship
- c - strong relationship

\* - estimated from available data

**Engineering Parameters**

| Design Requirements | user | orthotist | manufacturer | max torque provided directly by motor (Nm) | max toque provided through energy storage (Nm) | max resistive torque during swing (Nm) | max user weight (kg) | max device weight (kg) | max device thickness (mm) | max device length (mm) | max device width (mm) | min distance from hip to device COM (cm) | max reaction time to activation (s) | max time for 90 deg knee extension (s) | max number of moving components | max total number of parts | min cycles to failure (cycles) | max peak device noise (dB) | min time between recharges (hr) | min time between servicings (months) | max price ($) | Traditional KAFO | Yakimovich SCKAFO | Honda Walking Assist Device | HAL-5 Type-C | RoboKnee |
|---|---|---|---|---|---|---|---|---|---|---|---|---|---|---|---|---|---|---|---|---|---|---|---|---|---|---|
| **Functional Performance** | | | | | | | | | | | | | | | | | | | | | | | | | | |
| provides high knee extension torque | 8 | 4 | | c | c | | | | | | a | | | a | | | | | | | b | 0 | 0 | 1 | 4 | 4 |
| stores energy during swing | | | | b | c | c | | b | | | a | | | | | | a | | | a | | 0 | 0 | 3 | 0 | 0 |
| low impedance to swing | 8 | 5 | | | | c | a | a | | | a | a | c | | | | | | | | | 0 | 4 | 4 | 2 | 1 |
| fast reaction time | | | | a | a | a | | | | | | | c | a | b | | | | a | | a | x | x | 4 | 3 | 1 |
| quick knee extension | | | | c | c | | b | b | a | a | a | | b | c | b | | | | | | a | x | x | 4 | 3 | 2 |
| low energy consumption | | | | b | b | | b | a | | | | | | b | b | | | | c | | | 4 | 4 | 2 | 2 | 1 |
| long fatigue life | | | | a | a | | a | | | | | | | | a | a | c | a | | a | | 4 | 1 | na | na | na |
| **Human Factors** | | | | | | | | | | | | | | | | | | | | | | | | | | |
| low weight | 10 | 4 | | b | b | | b | c | a | a | a | | a | a | a | b | | | | | a | 4 | 3 | 2 | 1 | 1 |
| low size | 10 | 4 | | b | b | | a | b | a | a | a | | | a | a | b | | | | | a | 4 | 3 | 0 | 0 | 0 |
| concealable under clothes | 3 | 5 | | | | | | | c | c | c | a | | | a | a | | | | | | 4 | 4 | 0 | 0 | 0 |
| provides natural movement | 3 | | | c | c | | a | b | c | b | c | b | a | c | a | | | | | | | 0 | 3 | 4 | 3 | 2 |
| automatically functions when needed | 5 | | | | | | | | | | | | a | | a | | | | | | | 0 | 2 | 4 | 3 | 3 |
| low noise | 6 | | | | | | | | | | | | | | a | a | | c | | | | 4 | 4 | na | 2 | 1 |
| low additional inertia on leg | | | | a | a | | b | b | | | | c | | | | | | | | | | 2 | 2 | 2 | 2 | 1 |
| easy to don/doff | 3 | 6 | | | | | | a | b | b | b | | | | a | a | | | | | | 2 | 2 | 4 | 1 | 0 |
| comfortable during extension assist | 6 | | | a | a | c | a | | b | b | b | | a | b | | | c | a | | c | | x | x | na | na | na |
| **Production** | | | | | | | | | | | | | | | | | | | | | | | | | | |
| low cost | 8 | 8 | | | | | a | a | | | | a | a | | a | a | a | | | | c | 4 | 3 | 1 | 0 | 2 |
| low device complexity | | 5 | 9 | | | a | | | | | | | a | | c | c | a | | | | b | 4 | 3 | 0 | 0 | 2 |
| low part complexity / easy to machining | | | 10 | | | | a | a | | | | | | | c | b | | a | | | c | 4 | 3 | 0 | 0 | 1 |
| simple / inexpensive / infrequent repairs | | 8 | | | | | a | | b | b | b | | a | b | c | c | b | | | c | | 4 | 2 | 1 | 1 | 2 |
| **Interface with Orthosis** | | | | | | | | | | | | | | | | | | | | | | | | | | |
| simple integration into KAFO | | 10 | | | | | a | a | a | b | b | | | | a | a | | | | | | x | 4 | x | x | x |
| compatable with multiple KAFOs | | 9 | | | | | a | a | b | b | b | | | | a | a | | | | | | x | x | x | x | x |
| | | | | | | | | | | | | | | | | | | | | | | | | | | |
| Traditional KAFO | | | | 0 | 0 | ? | 120 | 0.9 | | | | | 0 | x | 0 | 4 | | | x | x | c | | | | | |
| Ottawalk SCKAFO | | | | 0 | 0 | a | 90 | 2.3 | 16.5 | 208 | 59 | | x | x | 3 | 24 | 66 | | x | | b | | | | | |
| Honda Walking Assist Device | | | | <30\* | 0 | | >97\* | 6.5 | | | | | | | >6\* | | | a | 2 | | c | | | | | |
| HAL-5 Type-C | | | | >60\* | 0 | | >65\* | 15 | | | | | 0 | | >6\* | | | | 5 | | 1700 / month | | | | | |
| RoboKnee | | | | 200\* | 0 | | >125\* | 7\* | | | | | 0 | b | >2\* | | b | | 0.5 | c | | | | | | |
| Target | | | | 70 | 70 | 0 | 90 | 2.3 | 50 | 200 | 70 | | 0.1 | 3 | 4 | <20 | 10^6 | | 10 | 12 | 5000 | | | | | |

The ideal device would allow an individual with weak quadriceps to perform STS, ramp gait, and stair ascent tasks comfortably at near-normal speeds. The device would quickly sense when a knee-extension moment is required and automatically provide the appropriate extension moment to the knee. When extension-assist is not required, the device would be inactive, and provide no impedance to an individual's movements (i.e. during the swing phase of gait, knee extension and flexion would be unhindered). If the device were to impede any portion of the gait cycle, the increase in effort required would likely negate the benefits gained from the extension-assist, and the probability of device rejection would be high. The device would also run quietly, function for a full day (at least 14 hours) before a power supply recharge is needed, and be no more difficult to don and doff than a KAFO.

### 3.3.2 Structural Requirements

The device structural requirements dictate how well the functional requirements can be fulfilled. Size and weight are of utmost concern in orthosis design. Cosmetics are an extremely important issue for orthosis users. If a device is overly bulky, looks awkward, or causes the user to move unnaturally, people may reject the device, regardless of the benefits. Therefore, the ideal device would have minimal size, with power supply and electronics concealed. Minimal size is especially important medio-laterally, to reduce the risk of collision with external objects, the user's own arms laterally, and the contralateral limb medially. Bulkiness has been stated as a major reason for rejecting full-leg orthoses [108], and it is unlikely that excessive bulkiness would be permitted for a brace equipped with an extension-assist. Because there have not been studies that examine orthosis user tolerance to increased size, target dimensions were based on the technical information available on existing powered exoskeletons and the opinions of orthotics technicians and experts. Target dimensions of 50 mm thickness medio-laterally, 70 mm width anterio-posteriorly, and 200 mm length were chosen as being reasonable values.

Since orthoses add weight to an individual's already weak limb, only a very small device weight is permitted. Additional weight, and the increased rotational moment-of-inertia on a swinging limb caused by this weight, would increase the effort required to walk [109], which

the individual would already have difficulty performing. Although no studies on orthosis user tolerance to device weight were found, conversations with orthotists and experts in the field revealed that 2.3 kg (5 lbs) is thought to be the upper limit of what orthosis users are willing to don. Therefore, the ideal device should weigh less than 2.3 kg, with the mass concentrated as proximally on the leg as possible to minimize added moment-of-inertia to the limb.

Though minimizing size and weight are important, the device must also resist mechanical failure under the application of a 126 Nm knee-extension moment, the maximum required moment. The KEA must also withstand a large number of cycles without requiring servicing. Through an informal study conducted on one healthy individual over 10 days, the average number of stair ascent cycles per leg and sit-to-stand motions performed daily was 91, with a maximum of 136. Therefore, to last a 10 year lifetime without requiring replacement of components, the ideal device would be designed to perform approximately 300,000 cycles (91 cycles/day x 365 days x 10 years) without failing due to fatigue. However, yearly maintenance is often performed on KAFOs, and so the KEA should be able to perform approximately 30,000 cycles before it requires servicing. To increase device versatility, the KEA would ideally be a modular component that could be incorporated into an existing KAFO or SCKAFO.

### 3.3.3 Control Requirements

A control system is necessary to operate the actuator and to engage or disengage the actuator from the knee joint when extension-assist or zero joint impedance is required, respectively. The control system should use parameters from an individual's motion or involved forces to determine the required response, either measured on the device or body. Unnatural movements should not be required for proper device functioning. Chairs, stairs of varying sizes, and ramps of various grades must be able to be used. The best options for control parameters are knee angle and ground reaction force, since starting knee angles for the weight-bearing portions of STS, incline walking, and SA are much higher than for level walking and are fairly predictable [14, 17, 26]. Ankle and hip angles, and foot, shank, thigh and trunk accelerations are other measurable parameters, but these are either not unique to

STS, SA, and ramp walking, or the parameters can diverge from predictable values depending on the person's condition. For example, an individual with weak plantarflexors or dorsiflexors may require an orthosis with a rigid ankle joint and an elderly individual who walks in a stooped position would have a permanently flexed trunk.

A purely mechanical sensing system, such as an air bladder underfoot, could be used to realize a low-cost, simple, and lightweight control system. An electro-mechanical sensing system could also be used to achieve a greater level of actuator and device engagement system control. An electro-mechanical system could use pressure sensors, goniometers, and accelerometers, in addition to mechanical sensors.

### 3.3.4 Summary of Important Design Criteria

Table 3.2 lists the important design criteria outlined in the above sections for the design of an ideal knee-extension-assist device.

Table 3.2: Key Design Criteria

| Design Criteria | Target Value |
|---|---|
| Maximum weight | 2.3 kg (5 lbs) |
| Maximum thickness (medio-lateral) | 50 mm |
| Maximum width | 70 mm |
| Maximum length | 200 mm |
| Maximum extension moment | 126 Nm |
| Resistive knee joint moment during swing or device inactivity | 0 Nm |
| Maximum user weight | 90 kg |
| Power consumption | 14 hours between recharging |
| Time between servicing | 1 year |

### 3.4 Electro-Mechanical Device Design

The initial KEA design consisted of an electro-mechanically powered system to generate the extension moment. The design focused on providing full assistance for knee extension tasks, principally STS and SA, since these two tasks required the highest knee extension moments. Ramp ascent assistance would have been a secondary benefit of this design. Stand-to-sit and ramp descent tasks were not included in the functional requirements for the initial design. The following section outlines the initial design process.

### 3.4.1 Design Concept Generation

In order to generate a wide variety of design ideas, a function-concept map of device functions and actuators was created. A more detailed morphology table listed specific mechanisms that could perform the device functions. A large number of conceptual designs were created; each incorporating different actuators, mechanical linkages, or methods of delivering the supplied moment to the knee. Specific STS, SA, and ramp ascent events and measurable parameters that could be used to trigger and control the device were also determined in this conceptual design process.

The eight most promising conceptual designs were refined and compared in a decision matrix, which examines how well each device would satisfy the design requirements relative to the other designs. The result is a ranking of the conceptual designs in terms of ability to satisfy user needs. See Appendix A for the decision matrix and a brief description of the design concepts under comparison.

Using the decision matrix, the best conceptual design consisted of a single DC motor that would apply the extension-assist moment directly to the knee joint when required and then load a spring while the device was inactive, so that the stored spring energy could later augment the extension moment that is provided directly to the knee by the motor.

### 3.4.2 Design Concept Refinement

Once the best conceptual design was chosen, a final design refinement process was carried out to examine different options for the motor, spring type and placement, and method of torque transmission from the motor to the spring and knee joint. The optimal device configuration (Figure 3.1) was a set of bevel gears at the knee, driven by a DC motor attached to the upper support upright of the KAFO. The smaller bevel gear (pinion), attached to the motor output shaft, would drive the larger bevel gear, which would rotate about the orthosis knee joint pin.  The large bevel gear would selectively engage the pin, and thus the knee joint, through the use of a dog clutch on the knee joint pin. The clutch would be pneumatically actuated through the application of pressure on an air bladder underneath the user's foot. A torsion spring that could be loaded through 90 deg would encircle the hub of

54

the larger bevel gear, with one arm attached to the gear, and the other to the upper support upright.
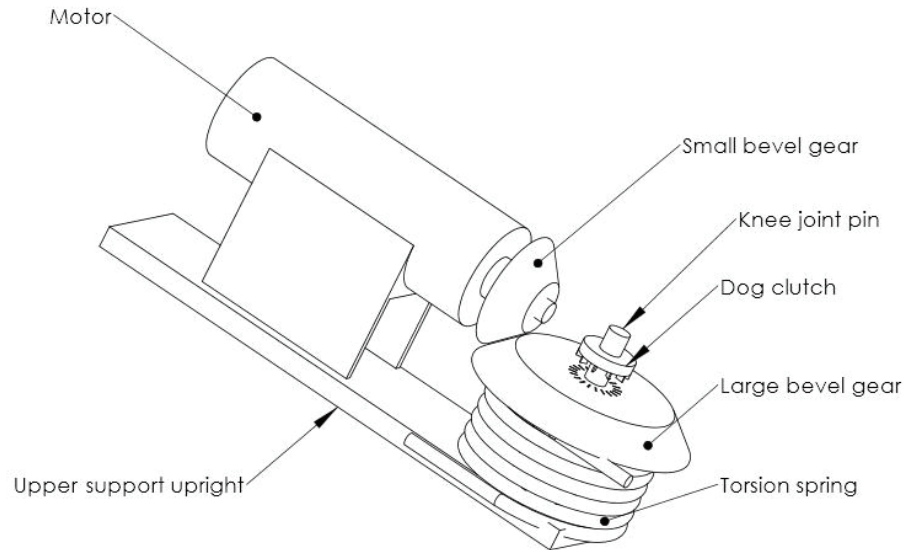


Figure 3.1: Powered device conceptual design sketch. Note: Not all parts shown.

With the dog clutch engaged, the larger gear would be coupled to the knee joint and the motor would drive knee extension directly (direct drive). With the clutch disengaged, the larger bevel gear would be free to rotate about the knee joint pin without impeding free knee joint motion, and the motor would load the spring by rotating in the opposite direction from that which drives knee extension. Because the clutch would only activate through pressure applied to the bladder underfoot, the spring could be loaded by the motor whenever the foot would not be load bearing, such as during the swing phase of stair climbing and incline ascent or while seated. When the leg would be load bearing, the motor would directly drive knee extension while the torsion spring would unload. The spring unloading would add to the extension moment provided by the motor, because the direction of unloading would be the same as that of knee extension. With the additional moment provided by the torsion spring, a smaller motor than one that could provide the entire required knee moment could be used. This design would allow use of space to be kept to a minimum. The bevel gears also allow for the largest dimension to be in the direction with the lowest constraint on size, proximo-distally along the thigh.

Device control would be achieved through a force sensing resistor (FSR) underneath the air bladder and a rotary encoder at the orthosis knee joint. Since tasks requiring an extension moment are characterized by a knee angle at foot contact much larger than that of level walking [15, 26], the device could be switched on any time the braced leg becomes load bearing with a knee angle greater than a pre-set starting angle, such as first contact with a stair, leg loading at initiation of STS, or the first stride of ramp ascent. The device would remain active throughout the task until weight acceptance on the braced leg would occur below the starting knee angle, for example the first stride on level ground after reaching the top stair or after completing STS. Extension moment activation during stance would cease upon weight acceptance at the smaller knee angle. In this way, the device would only function when needed for knee extension tasks and would be inactive at all other times. This would allow the orthosis to function passively, because it would have functioned without the KEA when extension assist was not necessary. With the device inactive when a knee moment is not required, power would not be supplied while using the orthosis, thus saving power as compared with other active orthoses and powered exoskeletons. The rotary encoder would also provide a signal to a controller that corresponds to the torsion spring angle. Matching the spring loading angle with the knee angle would ensure that there would be no residual moment from the spring acting on the gear at full knee extension. If there were to be residual moments applied to the gear, friction would make dog clutch disengagement difficult.

### 3.4.3 Detailed Design

With the conceptual design finalized, a more in-depth design was undertaken to determine the required motor specifications, spring stiffness, and part sizes necessary to meet the extension moment requirement. Spring sizing was performed first because the maximum moment a torsion spring within the size restrictions could provide would determine the motor requirements.

Spring sizing was carried out using torsion spring moment and fatigue equations [110] and finite life cycles-to-failure estimation calculations [110, 111]. The torsion spring moment *M* is given by:

$$M = k'\theta' \tag{3-1}$$

where $\theta'$ is the angular deflection of the spring in number of turns, and $k'$ is the spring rate:

$$k' = \frac{d^4 E}{10.8 D N_a} \quad, \tag{3-2}$$

in Nmm/turn. $E$ is the elastic modulus of the wire, $d$ is the wire diameter, $D$ is the mean coil diameter, and $N_a$ is the number of active coils in the spring:

$$N_a = N_b + \frac{l_1 + l_2}{3\pi D} \quad. \tag{3-3}$$

$N_b$ is the number of body turns or coils and $l_1$ and $l_2$ are the lengths of the two spring arms. The torsion-spring fatigue factor of safety $n_f$ for infinite-life was found using:

$$n_f = \frac{S_a}{\sigma_a} \quad, \tag{3-4}$$

where $S_a$ and $\sigma_a$ are the amplitude components of the spring fatigue strength and stress in the spring, respectively as follows:

$$S_a = \frac{r^2 S_{ut}^2}{2S_e} \left[ -1 + \sqrt{1 + \left(\frac{2S_e}{r S_{ut}}\right)^2} \right] \tag{3-5}$$

$$\sigma_a = K_i \frac{32 M_a}{\pi d^3} \quad, \tag{3-6}$$

where

$$S_e = \frac{S_r/2}{1 - \left(\frac{S_r/2}{S_{ut}}\right)^2} \tag{3-7}$$

$$K_i = \frac{4C^2 - C - 1}{4C(C-1)} \tag{3-8}$$

$S_{ut}$ is the ultimate tensile strength of the wire, $r = M_a / M_m$ is the slope of the load line where $M_a$ and $M_m$ are the amplitude and midrange components of the spring moment, respectively, with $M_a = M_m = M/2$ for a torsion spring which loads and fully unloads. $S_e$ is the endurance limit, and $S_r$ is the fatigue strength for helical torsion springs as determined by Associated Spring. $K_i$ is the inner-fiber stress correction factor and $C = D/d$ is the spring index.

The number of cycles-to-failure was determined using the following equations:

$$N = \left(\frac{\sigma_R}{a}\right)^{1/b} \tag{3-9}$$

$$\sigma_R = \frac{\sigma_a S_{ut}}{S_{ut} - \sigma_m} \tag{3-10}$$

$$a = \frac{(f S_{ut})^2}{S_e} \tag{3-11}$$

$$b = -\frac{1}{3}\log\left(\frac{f S_{ut}}{S_e}\right) \tag{3-12}$$

$$f = \frac{\sigma_F'}{S_{ut}}(2 \times 10^3)^b \tag{3-13}$$

$$\sigma_F' = 345 + S_{ut} \tag{3-14}$$

$$b = -\frac{\log(\sigma_F'/S_e)}{\log(2N_e)}, \tag{3-15}$$

where $N$ is the number of cycles to failure for the spring and $\sigma_R$ is the equivalent fully-reversed stress for combined loading cases with a midrange and amplitude stress, $\sigma_m$ and $\sigma_a$, respectively. $a$ and $b$ are constants determined from the Stress-Life (S-N) diagram based on $S_{ut}$ and $S_e$ of the material, and $f$ is the fraction of $S_{ut}$ that is equivalent to the fatigue stress at the start of the high-cycle fatigue range. $\sigma_F'$ is the true stress corresponding to fracture in one stress reversal, $b$ is the slope of the elastic-strain line in the Strain-Life ($\varepsilon$-$N$) graph, and $N_e$ is the number of cycles taken to reach the endurance limit of the material.

From the above equations, the maximum moment that could be applied in a quarter turn to a torsion spring with dimensions close to the design size requirements was 34 Nm. Such a spring would have a 6.6 mm wire diameter, an 83 mm outer coil diameter, a 28 mm coil height, and a mass of 0.2 kg. Using Equations (3-4) to (3-8), the Gerber fatigue criterion infinite-life factor of safety was calculated to be 0.82. Because of this low factor of safety for infinite life, the finite number of cycles to failure was calculated using Equations (3-9) to (3-15). The number of cycles to failure was approximately $2 \times 10^4$ cycles. The expected number of cycles per year was approximately $3 \times 10^4$, which would require the spring to be replaced every six to eight months. A spring was sourced (Appendix B) that best matched these characteristics, but fatigue tests would be required to determine the actual life of the spring.

With the spring providing 34 Nm of the 126 Nm extension moment design target, the maximum moment the motor would have to provide during direct drive would be 92 Nm. The use of 3:1 reduction ratio bevel gears would reduce the torque requirement to 31 Nm. The worst-case duty cycle that the motor would have to undergo would be during stair ascent for a 90 kg individual. The motor would first provide a constant 11.3 Nm moment for 1 s to load the spring. It would then provide 31 Nm, linearly reducing to 0 Nm in 2 s as the knee extends. The cycle (Figure 3.2) would repeat, without rest, half as many times as the number of stairs climbed (the sound leg of a unilateral orthosis user would be used for half the stairs).

The smallest motor that suited the output torque requirement was the Maxon RSF-14B Mini Series, 24 V brushless DC motor with a Harmonic Drive 100:1 reduction ratio gear head. Its maximum output torque with the gear head was 28 Nm at a max speed of 60 rpm, which, when reduced by the bevel gears, would result in 84 Nm at a max speed of 120 deg/s; less than the moment requirement, but deemed close enough to be sufficient. The motor and gear head weighed 0.8 kg, had a maximum diameter of 50 mm, and a total length of 168 mm.

A single-axis Galil CDS-3310 controller and drive was recommended by the motor supplier to control and drive the motor, as well as receive, process, and utilize data from the rotary encoder at the knee and the FSR under the foot. The Galil controller and drive was 13.1 cm x 20.9 cm x 1.9 cm (5.15 in x 8.25 in x 0.75 in) in size, and weighed 0.78 kg. It would be placed in a pouch worn around the user's waist, along with the battery pack.

To change the moment axis from the motor to the knee joint, a set of bevel gears was required. Commercially available bevel gears of different sizes and reduction ratios were
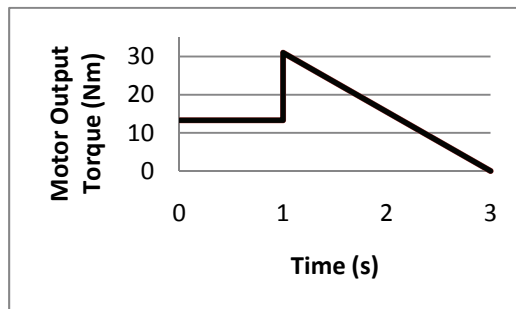


Figure 3.2: Theoretical worst-case duty cycle for the DC motor.

59

examined for size, weight, and moment requirements. However, no gear was sufficiently small and had enough strength to meet all requirements. Therefore, the moment requirement was sacrificed in order to not overly increase size and weight, a slightly more important design parameter, as shown in the QFD chart (Table 3.1). A 3:1 reduction ratio provided the best tradeoff between size and moment requirements. The closest match was a 38 mm/114 mm (1.5 in/4.5 in) pinion/gear set of steel bevel gears from Boston Gear. This set was able to transmit 67 Nm through the gear teeth to the knee joint, plus the 34 Nm from the spring through the gear hub for a total of 101 Nm, which was 80% of the total design target moment 126 Nm. The weight of the two gears was 0.89 kg (1.95 lbs). Using gears one size smaller, it would only be possible to transmit 21 Nm through the teeth to the knee joint, well below the 92 Nm required from the motor. Gears one size larger weighed 2.98 kg (6.55 lbs). Both of these gear sizes (one size smaller, and one size larger) resulted in unacceptable parameters for at least one key design requirement.

At this stage of the in-depth design, a design review was performed. The combined weight of the spring, motor, controller, and bevel gears (2.49 kg) was too great, especially since there would be significant additional weight due to the battery pack, mounting brackets, and the dog-clutch for engaging and disengaging the bevel gears with the KAFO knee joint. The size, though to a lesser extent, was also deemed too great. The large bevel gear situated at the knee was 114 mm in diameter and the assembly would be at least 70 mm wide medio-laterally, due to the size of the bevel gears and motor. With current technologies and without adding other means of handling the device weight, the electro-mechanical approach would result in a unilateral knee-extension device that was not likely to be used by individuals with weakened quadriceps. Therefore, instead of continuing the development of the motor and spring hybrid powered device, the design was altered to use only passive power. Energy would be stored in passive elements such as springs by loading under the user's own body weight and the energy could then be released to provide the extension-assist moment.

**3.5 Spring Powered Device – Preliminary Design**

Because of the importance of low device size and weight to an orthosis user, a new spring-powered device was designed with passive components that were lighter and smaller than the electro-mechanical components of the motor-powered extension-assist design.

**3.5.1 Revision of Objectives and Design Criteria**

The passively powered knee-extension-assist was designed for high-knee-moment tasks using only springs for actuation. Since the user's bodyweight is a suitable way to load springs without introducing an active power source, knee flexion under body weight could store enough energy in the springs to provide a useful joint moment upon release of the spring strain energy. Knee flexion during stand-to-sit occurs naturally. For STS, energy can be stored in the springs as the knees flex and released when the individual is ready to stand up. Extension-assist for STS would therefore remain as a primary objective of the device.

For stair ascent, it would be difficult to implement the STS design since knee flexion during stair ascent occurs only while the leg is in swing. A ground reaction force acting on the foot would be needed to provide the knee-flexion moment to load the springs. In swing, energy can only be generated through the force of gravity acting on the shank and the muscular force of the hamstrings, which flex the knee upon contraction. These forces would not be sufficient to generate a knee flexion moment to load the springs such that, upon energy release, meaningful extension assistance could be provided for SA. Therefore, stair ascent was omitted as a target task.

Without SA extension-assist, assistance for incline ascent became a more important functional feature of the passive design, since incline ascent would become the means of moving between levels, such as on a ramp into a building. As was explained in Section 2.3, during incline walking, knee flexion and extension occur while the leg is weight bearing (Figure 2.4), making incline walking a task that can potentially be aided by the passive KEA. The kinematics and kinetics of incline gait suit those of a passive device well, since the springs would load as initial knee flexion occurs, and fully unload once the knee has extended. The required moment then switches to a flexion moment, as described in Section

61

2.3. The device would thus provide the extension moment only when required, dropping to zero at the appropriate time in the gait cycle. Because of the good match between task and device dynamics, providing an extension-assist for incline ascent was chosen as a target task.

Since the passive design would require the springs to be loaded during knee flexion, the KEA would also be capable of providing an extension moment to resist knee flexion. As a result, the passive KEA would be able to assist stand-to-sit and ramp descent, two tasks that require a knee-extension moment to resist knee flexion. Therefore, assistance for stand-to-sit and ramp descent were added as secondary device function objectives.

Size and weight requirements for the device were also re-examined. The 50 mm medio-lateral thickness was considered too great, since it would be difficult to wear a device under clothes. Therefore, 20 mm was recommended as a target thickness. Maximum weight remained at 2.3 kg, but the device should ideally be less than 0.7 kg (1.5 lbs).

To keep the size and weight within the target specifications, the knee-extension moment requirement was also lowered. Using the torsion spring sourced for the motorized device as an indicator of spring capabilities, the new design requirement for extension-assist was set to 50% of the STS knee joint moment for a 90 kg individual, plus one standard deviation. Based on the highest STS knee-extension moment found in the literature, 1.41 Nm/kg [18], this corresponds to approximately 39 Nm.

The device would still be designed as a modular component for installation onto a custom KAFO or SCKAFO by a certified orthotist.

### 3.5.2 Design Concept Generation and Refinement

Several designs were investigated for the extension assist to provide the extension torque from energy stored in passive components. An initial examination into spring suitability was conducted on compression, extension, torsion, elastic rubber, and flat springs, to determine the maximum extension moment achievable while remaining within the device size restrictions. Through proprietary spring modeling software used by the spring manufacturing company (Advanced Spring Design) and available spring specifications, it was determined

that compression springs would provide the most appropriate stiffness-to-size ratio, and therefore be capable of generating the largest knee-joint moment while complying with the size restrictions of 20 mm width mediolaterally, 200 mm length, and 70 mm width anteroposteriorly in the sagittal plane. The most promising design concept used 8088 N/m spring-constant compression springs in parallel.

The final passive KEA design houses the springs mid-way up the thigh and compresses the springs during knee flexion while the braced limb is weight bearing. The KEA converts the linear spring force to a moment about the knee by providing a moment arm for the spring force to act on. In STS mode, the springs can be locked in a compressed state to prevent unwanted knee extension while the user is seated. By changing from STS mode to ramp mode, the springs can be allowed to compress and extend to provide a moment during incline walking. The KEA can also decouple from the KAFO knee joint to eliminate device impedance on the knee during swing, or while the braced leg is otherwise unloaded.

## 3.6 Spring Powered Device – In-Depth Design

### 3.6.1 Device Structure

The KEA (Figure 3.3) derives its extension-assist from three compression springs in parallel, housed in a rectangular aluminum case fastened to the lateral side of the upper KAFO upright. The springs are oriented longitudinally along the thigh. The distal ends of the springs press against the distal end of the case. The proximal ends of the springs are housed in the trough of a U-shaped beam that is free to slide proximally and distally inside the case. The springs are in a slightly preloaded state when the device is at full extension because the length of the spring case is shorter than the free length of the springs. The U-beam is attached to two steel proximal cables that run between the three springs and out of the case through holes in its distal end. The distal ends of the proximal cables (2.4 mm, 3/32 in. diameter) are attached to the distal cable (3.2 mm, 1/8 in. diameter) via a cable connector.

The distal cable is attached to the knee disk, located at the knee joint. The knee disk

rotates on a bearing around a pin set in the knee disk support, attached to the lateral side of the lower KAFO upright. The knee disk can be locked in place by extending the sliding lock into the knee disk notch (Figure 3.4). Retracting the sliding lock allows the knee disk to spin freely. The sliding lock is moved by a pneumatic actuator secured to the KAFO upright and is held by the two square sliding lock supports fastened to the knee disk support. The actuator is activated by applying bodyweight to an air-bladder underfoot

When the knee disk is locked in place and the knee is flexed, the U-beam is pulled distally via the cables and the springs are compressed. When the knee is extended, the springs extend and apply a force on the U-beam to move it proximally. The spring force is transmitted to the knee disk via the cables and causes the extension-assist moment to be applied to the knee joint. When the knee disk is able to spin freely, the cables do not pull on the U-beam, and thus the knee is able to rotate without impedance. Details of device function are provided in Section 3.6.3.

A spring locking mechanism is included to resist proximal U-beam movement, preventing unwanted spring extension, and to apply the extension-assist moment only when desired. The locking mechanism (Figure 3.5) consists of a round rod with multiple ratchet notches cut into one side and one long notch cut into the opposite side. The rod passes through slots in the proximal case end, distal case end, and U-beam, and through the middle of the centre spring. The rod is prevented from sliding axially by a nut on the threaded end of the rod, on the outside of the distal case end. The notches in the rod, either the ratchet notches or the single long notch, depending on the rod orientation about its longitudinal axis, engage with the edge of the slot in the U-beam to prevent proximal U-beam movement. The slots in the U-beam and case ends permit enough lateral locking rod travel to disengage the notch from the U-beam. U-beam disengagement occurs when extension-assist is desired or when the U-beam moves distally to the next ratchet notch during spring compression. The locking rod is biased to notch engagement by the locking rod spring pin and locking rod spring (Figure 3.5).
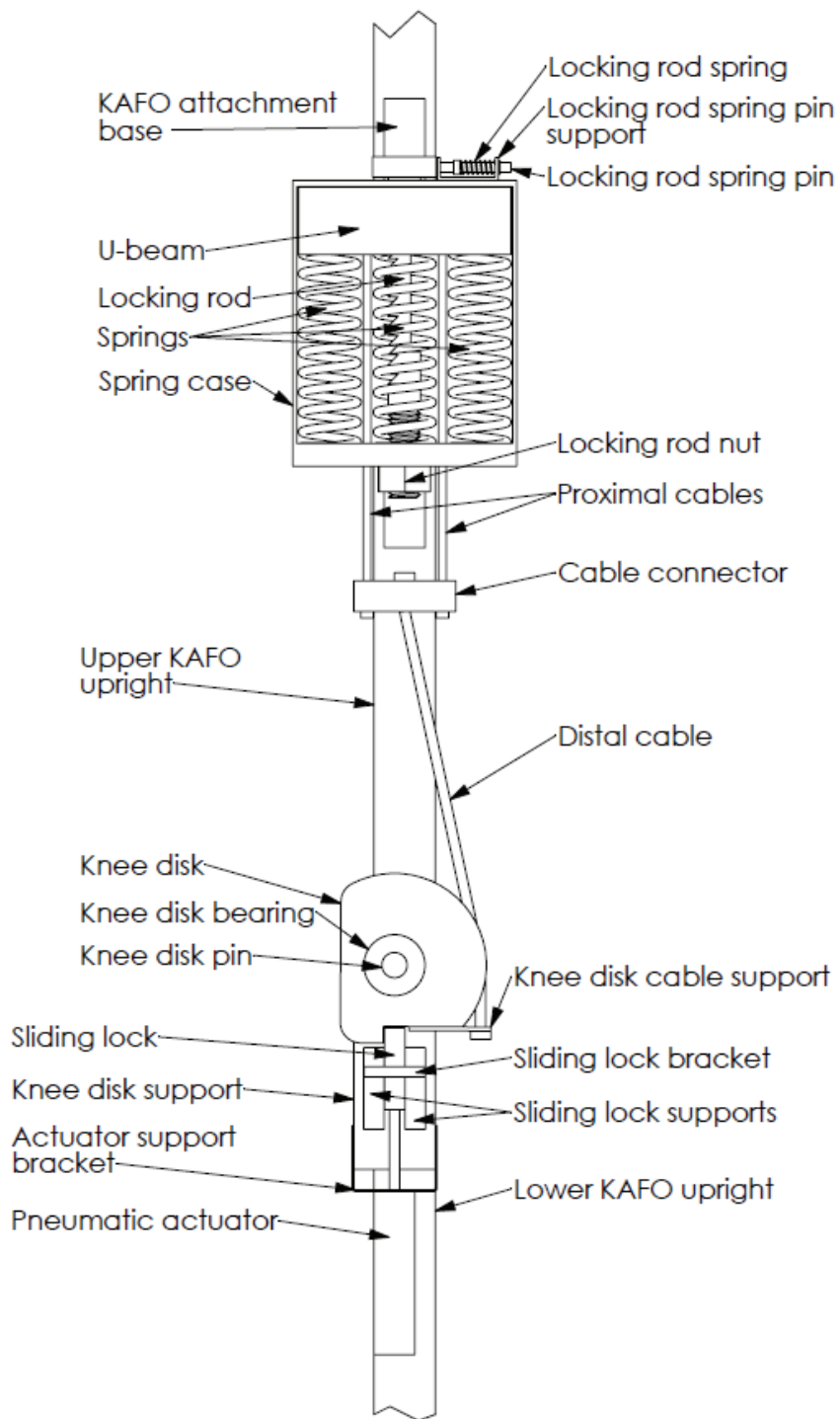
Figure 3.3: Lateral (sagittal plane) view of the knee-extension-assist. Spring case cover and air bladder are not shown.
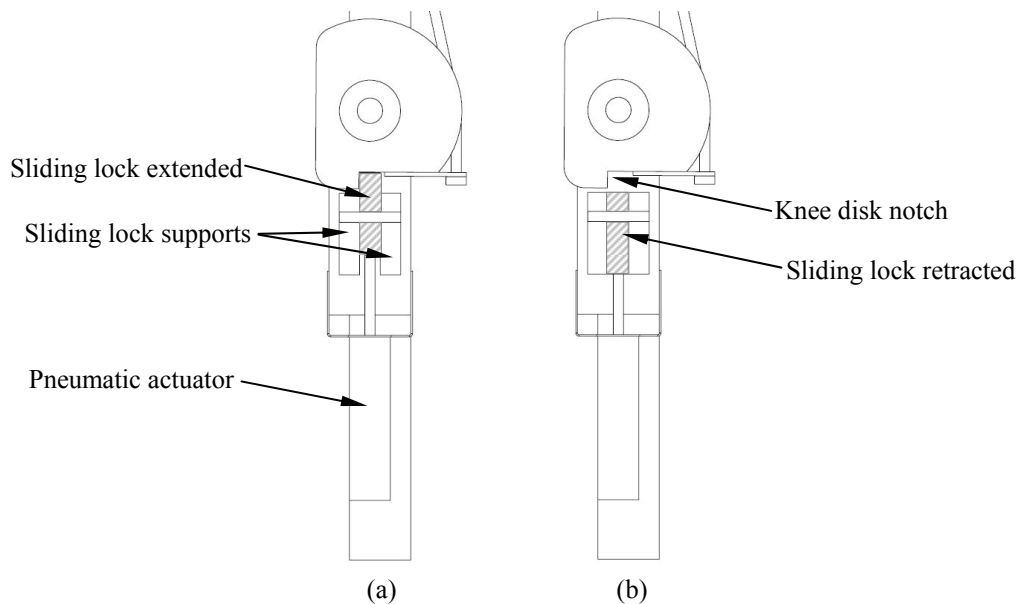
Figure 3.4: Knee disk assembly showing the sliding lock (a) engaged and (b) disengaged from the knee disk notch.

The overall dimensions for the spring case assembly, the device component that attaches to the upper orthosis support upright, were 106 mm in length, 69.5 mm in width (anterioposterior), and 26.7 mm in thickness (mediolateral) (Figure 3.6). The knee disk assembly (the device component that attaches to the lower orthosis support upright) was 149.7 mm long, 46.8 mm wide, and 19 mm thick (Figure 3.6). The thickness of the spring case assembly was slightly above the target thickness but was deemed within acceptable limits. Although the total length of the device was greater than the target specification, the two assemblies were each well below the target length of 200 mm. Since the two assemblies were located at different positions along the leg, the device length was deemed acceptable.
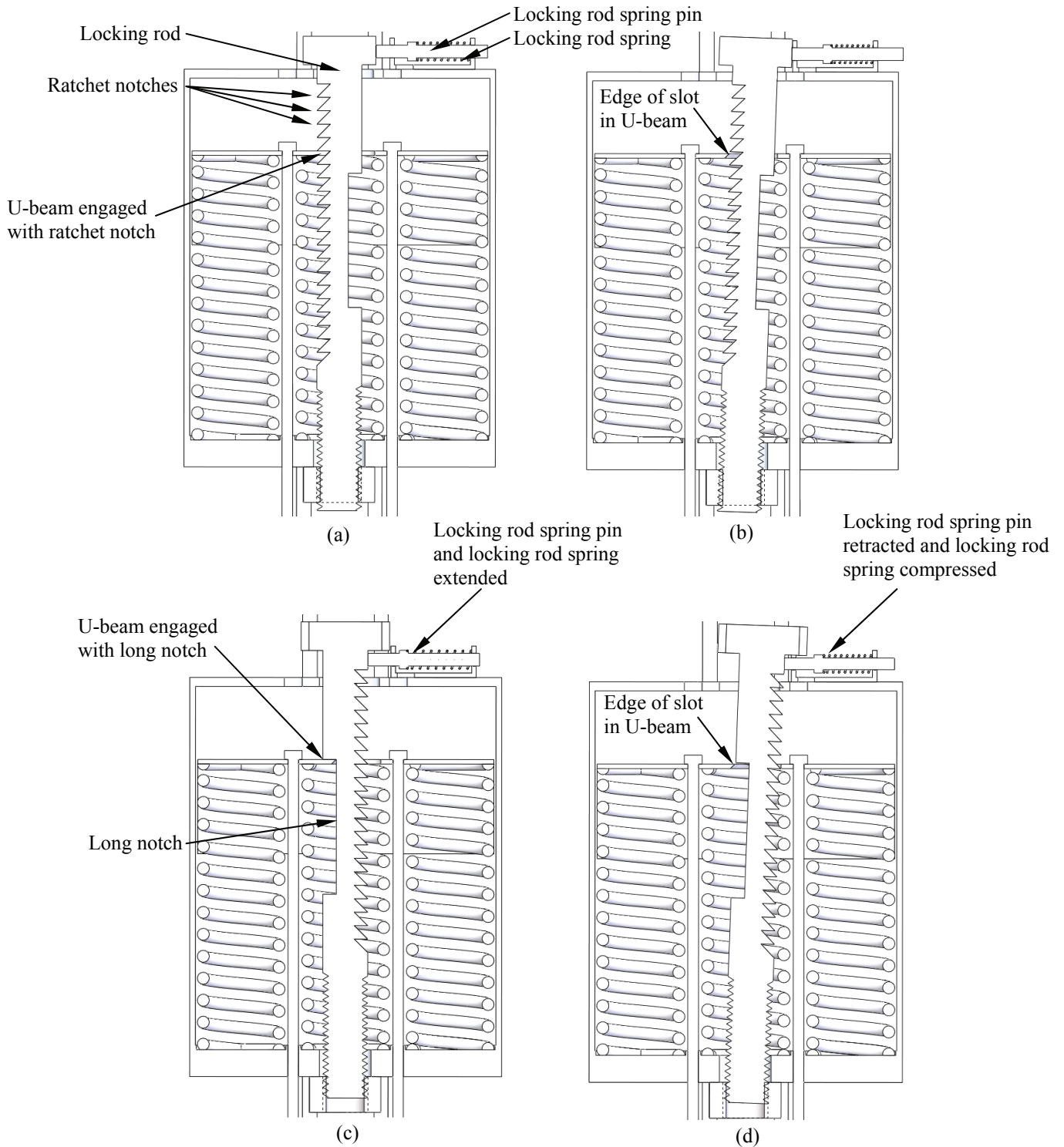
Figure 3.5: Cross-section of the spring case assembly showing the locking rod (a) engaged with a ratchet notch for STS, (b) disengaged from ratchet notch, (c) engaged with the long notch for ramp walking, and (d) disengaged from the long notch.
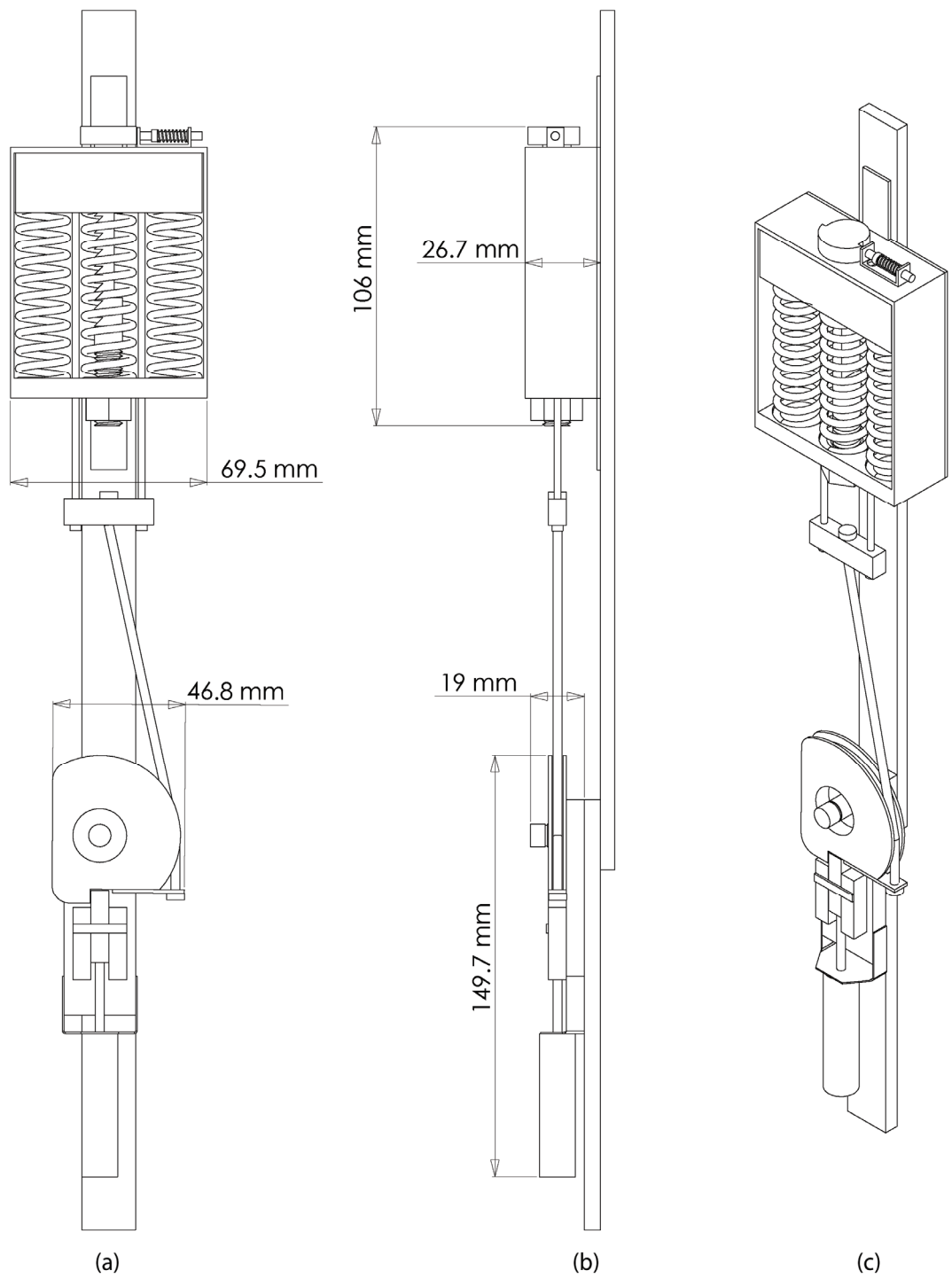
Figure 3.6: (a) Lateral (sagittal) plane (b) frontal plane and (c) isometric views of the KEA.

### 3.6.2 Device Performance

Early in the in-depth design phase, commercially available compression springs suitable to the application were sourced. With the spring specifications, device performance was calculated and optimized to provide a high extension-assist moment while attempting to keep the device size under the design criteria. Linear spring forces that would produce STS extension moments for a given knee disk radius and user weight were calculated (Appendix C). The equation:

$$F = M_p/R \qquad\qquad (3\text{-}16)$$

was used to determine the required spring force, F, from the moment corresponding to a given percent assist, Mp, and disk radius, R. The calculated spring forces, along with the maximum spring compression at 90° rotation (Appendix C), were compared to the springs sourced. A maximum spring force of 500 N could be achieved from one spring in 90° of knee flexion using a 2.5 cm radius knee disk (providing 4 cm of spring compression); a 10 cm long, 2.7 mm wire diameter spring (Appendix D); and an initial spring compression of 2 cm. Since the spring's outer diameter is less than 2 cm, three springs could be used in parallel to produce 1500 N of force and still remain within the size constraints. With the 2.5 cm knee disk, 37.5 Nm could be provided, 47.3% of the 79.2 Nm required knee-joint extension moment for STS for a 90 kg individual. This maximum moment was very close to the design requirement of 50%. In the ramp walking mode, the maximum stance knee angle is approximately 30°. The resulting spring compression would provide 36.5 % of the 57.6 Nm moment required for a 90 kg individual (Appendix C). Table 3.3 shows the percent of required knee-extension moment provided by the KEA to assist users of varying weights in performing STS and ramp ascent.

Table 3.3: Percent of required knee-extension moment provided by the KEA to users of different weights

| User Weight (kg) | STS (%) | Ramp Ascent (%) |
|:---:|:---:|:---:|
| 50 | 85 | 66 |
| 60 | 71 | 55 |
| 70 | 61 | 47 |
| 80 | 53 | 41 |
| 90 | 47 | 37 |

### 3.6.3 Device Function

The passively-powered KEA was designed to address two difficult tasks for people with quadriceps muscle weakness: sit-to-stand, where the individual rises from a seated position into a fully upright standing position and ramp ascent, where an individual walks up an inclined surface. The devices should also assist, or at least permit, stand-to-sit and ramp descent. To select between stand-to-sit/STS and ramp walking modes, the user should manually rotate the locking rod 180°, to align the correct locking rod notch type, either the multiple ratchet notches for stand-to-sit/STS or the single long notch for ramp walking, with the edge of the slot in the U-beam, with which the notches engage (Figure 3.5). To prevent the user from misaligning the locking rod during mode selection, the locking rod head has stops (Figure 3.7) to prevent rod over-rotation and provide haptic feedback that the correct amount of rotation has been reached.

The following sections explain how the KEA was designed to function for STS and ramp walking assistance, respectively. Figure 3.8 illustrates the forces and moments acting on the device during use.
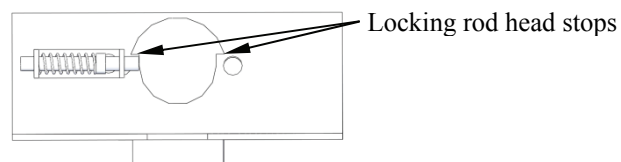


Figure 3.7: Proximal end view of the spring case assembly.

70
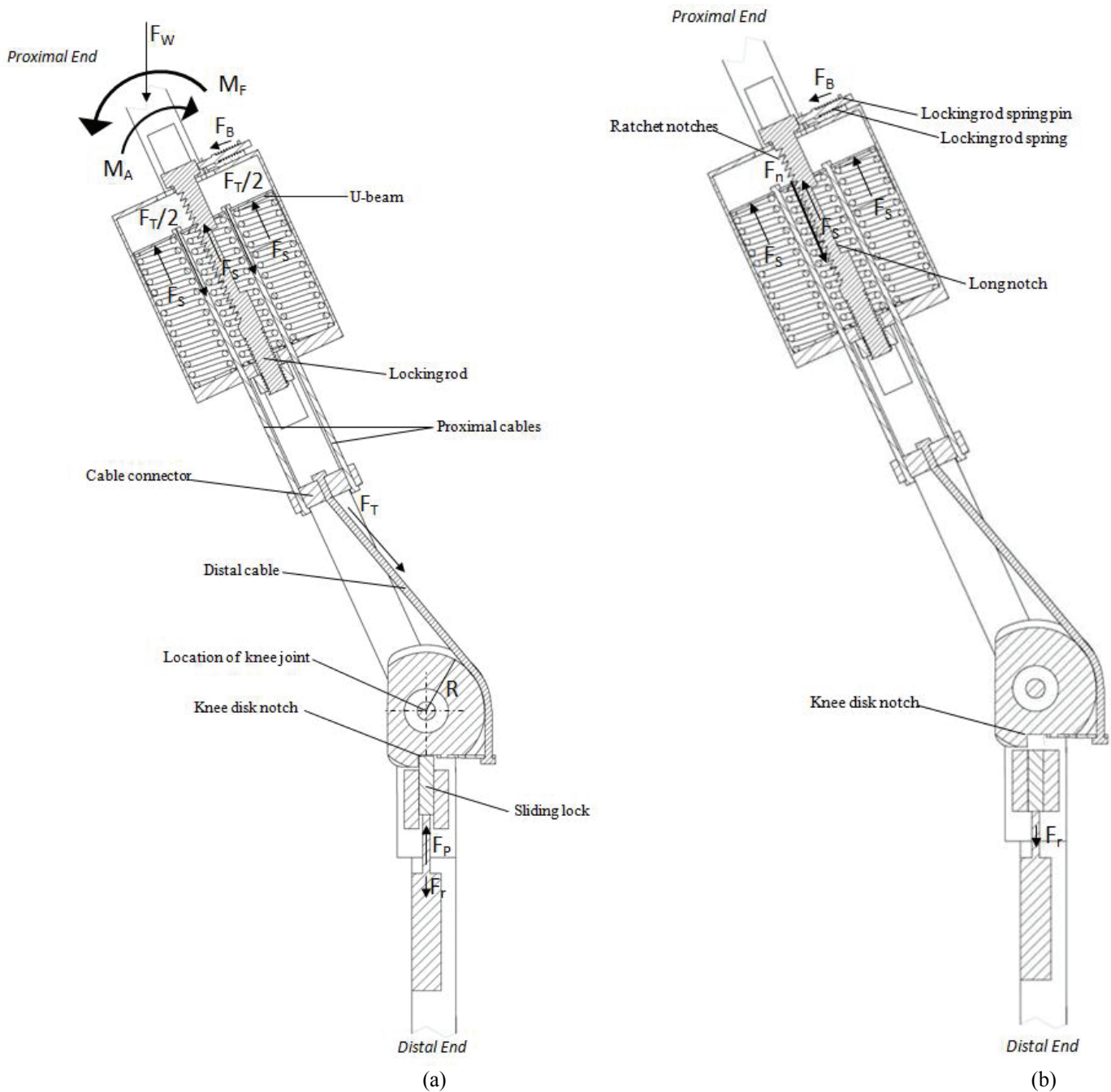
Figure 3.8: Forces and moments acting on the device when (a) springs are loaded or unloaded and (b) when springs are locked in place. Forces and moments are the same for STS and ramp walking. During ramp walking, the locking rod is rotated 180° from position shown such that the long notch faces the edge of the U-beam slot and engages with the U-beam. (The diagrams are not free-body diagrams).

71

## 3.6.3.1 Sit-to-Stand Mode

### 3.6.3.1.1 Sit-to-Stand Mode Overview

The KEA uses the wearer's own body weight as the force to compress the springs and thus store energy. To provide the assistive knee-joint moment during sit-to-stand, the springs must be pre-loaded prior to the user being in the seated position. As a result, there are two parts to the STS extension-assist: a pre-loading phase during which the springs are loaded under the bodyweight as they complete stand-to-sit and an extension phase, during which the energy stored in the springs is returned as an assistive knee-joint moment.

### 3.6.3.1.2 Loading Phase

Once positioned in front of the seat in which the user will sit, and with the locking rod rotated such that the ratchet notches face the edge of the slot in the U-beam (Figure 3.5a), as described above, the user is ready to begin the loading phase. With the legs fully extended, the user stands with weight distributed evenly on both feet. The user's weight, $F_W$, on the air bladder underneath the foot of the braced leg generates the linear pneumatic actuator force, $F_P$ (Figure 3.8a). The actuator force pushes the sliding lock upwards into the knee disk notch, to prevent knee disk rotation. With the knee disk locked in place, a knee-flexion moment, $M_F$, generates tension in the distal cable, $F_T$, at a moment arm equal to the knee disk radius, $R$, since the distal cable wraps around the disk. The tensile force in the distal cable is transmitted to the proximal cables via the cable connector. The proximal cables, in turn, transmit $F_T$ to the U-beam, and therefore to the springs. The result is that a flexion moment, $M_F$, applies a compressive force to the three springs $F_T = -3F_S$. The force $3F_S$ from the three springs, therefore, acts through the cables at a moment arm of $R$ to generate the knee-extension-assist moment, $M_A = F_T R$, that opposes the knee flexion moment, $M_F$, and provides resistance to knee flexion during the loading phase.

The knee flexion moment, $M_F$, is generated when the force $F_W$ due to user body weight moves posterior to the knee joint. $M_F$ increases as knee angle increases, because the distance between the knee joint and the body-weight force vector $F_W$, i.e. the moment arm at which $F_W$ acts, grows with increasing knee angle. Whenever the knee flexion moment, $M_F$,

generates a tensile force, $F_T$, that exceeds the total spring force (of all springs) exerted at that knee angle, $3F_S$, the knee flexes, the U-beam travels distally inside the spring case, and the springs compress. Spring compression results in an increase in the spring extension force, $F_S$, to maintain $F_T = -3F_S$. Therefore, as knee flexion occurs, the extension force from the springs, $3F_S$, increases, and consequently, the extension-assist moment provided by the KEA, $M_A$, increases. Therefore, the lower the seat that the user sits on, the greater the knee flexion angle reached, and thus the greater the extension-assist moment that can be released by the device upon standing.

When the user becomes seated, body weight, $F_W$, is transferred from the legs to the seat, and causes $M_F$ to drop to zero (Figure 3.8b). With $M_F = 0$, the springs would be free to extend from their compressed state. However, to store in the springs the energy added through the compression introduced during stand-to-sit, the U-beam is prevented from moving proximally while the user is seated by the ratchet notches in the locking rod. The locking rod spring biases the rod to notch engagement by applying a force $F_B$ to the locking rod spring pin that pushes against the head of the locking rod. Therefore, during distal U-beam movement during knee flexion, the edge of the slot in the U-beam automatically engages with each subsequent notch in the locking rod as the edge of the U-beam slot aligns with each notch. When $M_F$ drops to zero, the spring force causes the U-beam to move proximally (extending the knee) until further proximal movement is prevented by the force $F_n$ exerted by the flat face of the last notch with which the U-beam engaged. In this way, energy is kept stored in the springs until the user is ready to perform sit-to-stand. The resistive force from the notch, $F_n$, prevents the U-beam from moving and the springs from extending, and thus eliminates cable tension, $F_T$. With cable tension $F_T = 0$, the extension-assist moment $M_A = F_T R = 0$, and the device provides no moment to the knee joint. Transfer of body weight to the seat removes the pressure from the air bladder, and the pneumatic actuator force $F_P$ disappears. With $F_P = 0$, the small pneumatic actuator return-spring force, $F_r$, pulls the sliding lock away from the knee disk, and thus allows the knee disk to rotate freely. As a result, while seated, the user is free to extend and flex their knee as desired without

73

impedance from the device and without the device losing the energy that was stored during stand-to-sit.

At the end of the loading phase, the springs are compressed and locked in position, the user is fully supported by the seat, and the braced knee joint is free to extend and flex without impedance to the knee joint from the KEA.

### 3.6.3.1.3 Extension Phase

To begin the extension phase of STS extension-assist (Figure 3.8a), the user's centre of mass must first be brought forward, such that a portion of their body weight is supported by the feet. Forward CM movement can be achieved by anterior trunk displacement through hip flexion. The portion of bodyweight acting through the affected leg on the air bladder returns $F_P$ and thus returns the sliding lock into the knee disk notch. The knee disk is maintained in the proper position to reengage with the sliding lock because the cables have a slight resistance to bending that holds the knee disk in place whenever the knee flexes and extends freely. Once the sliding lock is engaged with the knee disk notch, the knee disk is prevented from rotating about its pin and the KEA is thus coupled to the orthosis knee joint. When a portion of body weight is supported by the user, a portion of force $F_W$ from body weight is applied to the device and generates a small knee-joint flexion moment, $M_F$. Since the knee disk is not able to rotate freely, tension $F_T$ is reintroduced into the cables. The cables, in turn, apply $F_T$ to the U-beam in the distal direction, and thus remove a portion of the spring force, $3F_S$, from the notch face and thus reduce the force between the locking rod notch face and the U-beam, $F_n$. The tension generated in the cables also begins to apply the knee-extension moment, $M_A$. In order to maintain the extension moment during knee extension, the user, with partial body weight still borne by the feet, manually disengages the locking-rod notch from the edge of the slot in the U-beam (Figure 3.5b). Disengagement is accomplished by pulling the proximal end of the locking rod in the anterior direction; i.e. in the direction opposing the locking rod spring force $F_B$. Disengagement of the locking rod from the U-beam eliminates $F_n$, and thus permits proximal U-beam motion and spring extension. With the notch disengaged and $F_n = 0$, the full force from the springs, $3F_S$, is applied to the cables

74

via the U-beam. The full spring force applied to the cables generates the maximal cable tension, $F_T$, which acts at the moment arm $R$ of the knee-disk radius, to generate the full extension-assist moment $M_A$ that will aid the user during STS.

With the assistive knee-extension moment applied by the KEA, the user can begin to rise. However, the springs provide less than the full required knee joint moment for STS, and consequently, the user must provide the remainder of the required extension moment. The additional required moment can be generated through additional knee-joint moment from quadriceps contraction in the unaffected leg, and the affected leg, if possible. If the additional moment quadriceps contraction is insufficient, the user can also lower the required knee joint moment for STS by rising with an increased hip angle. An increased hip angle (an increase in hip flexion) moves the centre of mass closer to the knee joints, and thus decreases the moment arm at which body weight acts about the knee. A smaller moment arm reduces the knee flexion moment that must be opposed, and thus reduces the knee-joint moment required for STS. Increased hip flexion does, however, increase the hip-extension moment required for successful STS completion. If the user is unable to provide the increased hip extension moment through an increase in muscle activation of the hip extensors, the hip-extension moment could be augmented by pressing the hands into the thighs.

As the user rises and the knee angle decreases, the springs extend and return the stored energy in the form of a linearly decreasing assistive knee joint moment, $M_A$, that closely resembles the required knee joint moment. At the end of STS, the user is standing fully upright and the springs are at their maximum allowable elongation, restricted from elongating further by the spring case. The tension $F_T$ in the cables drops to zero, and the device provides no moment to the knee, $M_A = 0$, as desired. If bodyweight is subsequently removed from the braced leg, the pressure on the air bladder is removed, the pneumatic actuator force $F_P$ is eliminated, the sliding lock retracts from the knee disk notch due to the return spring force, $F_r$, and free knee motion is permitted.

Throughout the STS motion, the user must maintain manual disengagement of the locking rod to oppose $F_B$, since the locking rod spring pin continually applies $F_B$ to bias the

locking rod to notch engagement. Continual manual disengagement ensures that the U-beam does not reengage with a more proximal notch during STS. Reengagement would stop further spring elongation and eliminate the assistive extension moment. The locking rod can be held in the unlocked position with the hand placed on the thigh to allow the device user to simultaneously apply a force on the thigh to increase the hip extension moment and thus aid STS, as described above.

### 3.6.3.2 Ramp Mode

**3.6.3.2.1.1 Ramp Mode Overview**

Passively providing a useful knee extension-assist moment for ramp ascent using only bodyweight to load the springs is a more challenging problem than for STS. In STS, knee flexion often occurs from a 0° to 90° knee angle during the loading phase when the springs are compressed. In ramp ascent, the relatively short loading phase, approximately the first quarter of the ramp-ascent gait-cycle stance phase, involves only 10 to 15 degrees of knee flexion during which the springs can be compressed. In order to store enough energy in the springs to provide a useful extension-assist moment during ramp ascent, a high spring force is required during the limited stance-phase knee flexion and extension. Exaggeration of knee flexion at the start of stance phase in a 'bounce' type movement may also be necessary, to increase the spring compression through increased knee flexion. The extra knee flexion would increase the extension-assist moment that could be provided. For ramp descent, the KEA would provide an extension moment to resist knee flexion and thereby assist the leg in supporting body weight. The KEA would allow the knee to flex, but not collapse, during stance, and permit the unaffected leg to swing forward in preparation for its next stance phase. KEA ramp mode involves an initial preloading phase to achieve the high spring force required, followed by cyclical stance and swing phases, and finally an unloading phase to remove the preload. These phases are explained in more detail in the following sections.

**3.6.3.2.2 Preloading Phase**

The preloading phase is used to begin both ramp ascent and descent. With the user at either the top or bottom of the incline, KEA ramp mode (for both ascent and descent) commences

with manual rotation of the locking rod to the ramp walk position, with the single long notch of the locking rod facing the edge of the slot in the U-beam (Figure 3.5c), as described at the start of Section 3.6.3. The user stands with both legs evenly supporting body weight. The weight borne by the braced limb is transmitted to the air bladder under the foot of the braced leg. The applied weight creates pressure in the air bladder that generates the pneumatic actuator force, $F_P$. The pneumatic actuator force pushes the sliding lock into the notch in the knee disk (Figure 3.4), and thereby couples the knee disk to the knee joint.

Before ramp ascent and descent begin, the user must apply a preload to raise the force needed to compress the springs during early stance phase, and thus the energy stored in the springs and the extension-moment provided to the user in mid-stance knee extension. To generate the preload, the user flexes their knees while standing to generate tension $F_T$ in the cables and compresses the springs, as during the loading phase of STS mode. Once a knee flexion angle that corresponds to the desired spring preload force is reached, the slot in the U-beam engages with the long notch of the locking rod (Figure 3.5). The proximal face of the long notch prevents the U-beam from moving proximally, and thus prevents the springs from elongating when the knee angle decreases below the angle at which engagement between the notch and U-beam occurred. As a result, the device provides zero knee-joint moment between the knee angle at which the preload was set and full knee extension. Unimpeded knee flexion for foot placement on the ramp is thus permitted. The distal face of the long notch is 4 cm distal to the proximal face, and therefore the U-beam is not constrained from moving distally (Figure 3.5c). The knee flexion beyond the preload knee angle that occurs during the slight knee flexion of early stance in ramp ascent and during the knee flexion of ramp descent (Figure 2.4) thus compresses the springs beyond the preload length and creates the tension $F_T$ in the proximal and distal cables that generates the extension-assist moment, $M_A$, required during ramp walking.

The knee angle at which the preload occurs can be changed by adjusting the proximal-distal position of the notch using a nut on the distal end of the locking rod. The notch position for ramp ascent should be set such that the flexion angle at which the preload occurs corresponds to the starting knee angle of the ramp ascent gait cycle, when the heel comes

into contact with the ramp. The initial setting would be for standard access ramps, and it would be at the user's discretion to change it for other inclines. If desired, for ramp descent, the notch location could also be adjusted to correspond to the starting knee angle for ramp descent. A change of notch location also changes the amount of preload force. A higher notch engagement knee angle corresponds to a higher preload force, and thus energy stored, for an equivalent amount of knee flexion during ramp ascent. Since a higher notch-engagement knee-angle would be used for a steeper incline, the KEA provides more assistance the greater the incline.

### 3.6.3.2.3 Ramp Ascent Stance Phase

With the preloading phase completed, the KEA provides zero knee-joint impedance and thus permits free knee motion between full extension and the starting knee angle at ramp-ascent heel strike. With the KEA preload knee angle ideally set to the natural ramp-ascent starting knee flexion angle, the ramp-ascent gait cycle can therefore commence stance phase with the foot placed in a natural position. As slight knee flexion begins at the start of ramp-ascent stance, the body weight, $F_W$, that loads the braced leg, compresses the springs beyond the preload length to generate the knee extension moment, $M_A$. During flexion, the extension moment resists knee flexion and protects against leg collapse at the knee. Knee flexion ends by the start of the second quarter of stance. Knee extension follows flexion, and the springs return the energy stored during flexion as an assistive knee-extension moment that helps the user raise their body up and over their planted foot. Similarly to STS, the springs do not provide 100% of the required knee extension moment for ramp ascent, and the user must produce the remainder of the required moment. The additional moment can be provided by using a handrail or by generating a muscle moment from the affected quadriceps, if possible. Alternatively, an additional hip extension moment can be generated through increased hip extensor muscle activity or by using the hands to push on the thigh. A 'bounce' type movement could also be performed whereby the user would allow the affected knee to flex beyond the normal angle for ramp ascent, and then push off quickly with the unaffected leg at the end of its stance phase that precedes the bounce. The return of the additional energy

stored in the springs, combined with the push from the unaffected leg, may provide the user with the moment needed to extend the knee.

By 50% of stance, the knee is extended back to the preload angle and the springs are returned to the preload length. Between the preload angle and full extension, the KEA does not provide an assistive moment to extend the knee. An extension moment is not required from the KEA in the second half of ramp-ascent stance, since a knee flexion moment is normally generated by the leg in able-bodied ramp gait, as described in Section 3.5.1.

### 3.6.3.2.4 Ramp Descent Stance Phase

Similarly to ramp ascent, ramp-descent stance phase begins with weight acceptance on the affected limb. In early stance, the knee angle surpasses the preload angle, and the KEA provides the extension-assist moment, $M_A$, to resist knee flexion. For normal ramp descent, knee flexion occurs until nearly the end of stance, and thus spring compression and knee flexion resistance continues until late stance-phase. By late stance phase, though, the center of mass of the user has moved in front of the knee joint. The anterior CM movement causes the moment arm at which the body weight force vector $F_W$ acts, to reduce to zero and then increase in front of the knee. The change in moment arm would cause the flexion moment from body weight, $M_F$, to decrease below that of the assistive moment, $M_A$, generated by the total spring force, $3F_S$. As a result, the springs would extend back to the preload length and the knee would extend aided by the extension moment.

### 3.6.3.2.5 Swing Phase

As the braced leg begins swing phase, bodyweight is removed from the affected leg. As a result, pressure is removed from the air bladder under the affected foot, and the sliding lock retracts from the knee disk notch (Figure 3.4). With the sliding lock retracted, the knee disk can rotate freely about the knee disk pin. When knee flexion occurs in early swing to permit the foot to clear the ground as it swings forward, the cables pull on the knee disk. However, because the knee disk is not coupled to the orthosis joint, the knee disk rotates around the knee disk pin, and thus prevents tension from being generated in the cables. Free knee joint

motion is thus possible during swing. Once swing-phase knee-flexion is complete, knee extension occurs to bring the foot into position to accept body weight at the start of the next stance phase. As the knee extends back to the preload angle, the intrinsic stiffness of the wire cables allows the cables to return the knee disk to its preload angle position. At the preload angle position, the knee disk can be locked by the sliding lock when weight is accepted by the braced leg at the start of the next stance phase.

### 3.6.3.2.6 Unloading Phase

Once the end of the ramp or incline is reached, the user must remove the preload. The user stands with body weight borne evenly by both legs. The knees are flexed slightly under bodyweight to generate tension $F_T$ in the cables. The cable tension reduces the force $F_n$ between the locking rod notch and the U-beam, and thus reduces friction between the two components to allow for easier manual disengagement of the locking rod from the U-beam. The cable tension also prevents sudden extension of the compressed springs when the locking rod is disengaged. Sudden spring extension could potentially put the user off-balance or cause discomfort. With the knees flexed slightly, the proximal end of the locking rod is manually pulled in the anterior direction, to separate the edge of the U-beam slot from the notch (Figure 3.5d). The knees are then extended to return the U-beam to the proximal end of the spring case and the springs to the maximum permitted extension allowed by the casing. Once the springs are at maximum permitted extension, no tension exists in the proximal and distal cables, and thus no extension-assist moment is provided by the KEA to the knee.

### 3.6.4 Structural Analysis

Once the springs were sourced and knee disk size determined, as described in Section 3.6.2, the forces and moments that would act on the device were known, and therefore the stresses the device would be subjected to during use could be determined. Static and dynamic stress analyses under maximum loading conditions of 1500 N at 90° of knee flexion were carried out in order to determine the optimal size and material for each component. The following section describes the methods used to determine the size, material, and maximum stresses for each device component.

### 3.6.4.1 Static Stress Analysis

A static stress analysis was carried out to calculate the magnitude of the static stresses experienced by the device components under maximal spring loading. Component dimensions and materials were adjusted during the analysis process to obtain acceptable stress levels and maintain low device size and weight.

### 3.6.4.1.1 Bending, Tensile, and Shear Stresses

Bending stresses under peak loading conditions were calculated for all components subjected to a bending moment using the standard flexure formula for beams in bending [110]:

$$\sigma_b = \frac{Mc}{I}, \tag{3-17}$$

where $M$ is the max moment applied to the beam, $c$ is the perpendicular distance from the neutral axis to the farthest point from the neutral axis on which $M$ acts, and $I$ is the moment of inertia of the cross-sectional area computed about the neutral axis with component features that reduce cross-sectional area, such as notches and holes, taken into account.

To correct for stress concentrations, the stresses calculated for components with features such as holes or cuts were then multiplied by a static stress concentration factor, $K_t$. Static stress concentration factor values were based on component geometry and type of stress concentration feature [110].

To calculate the moment of inertia, $I$, for the complex U-beam shape, the cross-sectional area was broken down into three rectangles. Equation (3-18) [112] was used to determine the location of the neutral axis for the U-beam. Equation (3-19) was then used to determine the overall moment of inertia from the sum of $I$ for each of the three rectangles, with the distance from the neutral axis accounted for.

$$\bar{y}_U = \frac{\sum_{n=1}^{3} \bar{y}_{rn} A_n}{\sum_{n=1}^{3} A_n} \tag{3-18}$$

$$I = \sum_{n=1}^{3} (\bar{I}_n + A_n d_n{}^2), \tag{3-19}$$

where $\bar{y}_U$ is the distance to the neutral axis from a chosen edge, $\bar{y}_r$ is the location of the neutral axis from that chosen edge, and $A$ is the area of each component rectangle. $\bar{I}$ is the

81

moment of inertia for the component rectangle, and $d$ is the distance from the centroid of the component rectangle to the neutral axis.

To determine maximum moments applied to KEA components, the graphical method for the creation of shear, $V$, and moment, $M$, diagrams for a beam under a load $w$, was used [112]. Change in shear and moment as a function of distance along the beam, $x$, is given by:

$$\Delta V = - \int w(x)dx \qquad (3\text{-}20)$$

$$\Delta M = \int V(x)dx . \qquad (3\text{-}21)$$

Assessment of bending stresses was important for the U-beam, the distal end of the spring case, the KAFO attachment base, the notches in the locking rod, the cable connector, and the knee disk support, because of the large applied bending moments. The static bending stresses and the corresponding static factors of safety are listed in Table 3.4.

Table 3.4: Maximum bending stresses at important locations and corresponding static factors of safety.

| Component | Bending Stress (MPa) | Static Factor of Safety |
|---|---|---|
| U-beam | 229 | 4.7 |
| Distal spring case end | 166 | 3.0 |
| KAFO attachment base | 404 | 2.6 |
| Locking rod notch | 490 | 2.2 |
| Cable connector | 372 | 2.9 |
| Knee disk support | 468 | 2.3 |

Shear, $\tau$, and tensile stress, $\sigma$, were calculated using the standard stress equations [110]:

$$\tau = \frac{F_s}{A_s} \quad , \quad \sigma = \frac{F_t}{A_t}, \qquad (3\text{-}22)$$

where $F$ is the applied force and $A$ is the cross-sectional area of the member. The subscript $s$ applies to members loaded in shear, and $t$ to members loaded in tension or compression.

Tensile and shear stresses were typically much lower than bending stresses. Shear stresses were highest at the locking rod notches, the edge of the slot in the U-beam where the locking rod notches engage, the sliding lock, and the knee disk notch. Table 3.5 outlines the results of the shear stress calculations.

Table 3.5: Shear stress analysis results at important locations

| Component | Shear Stress (MPa) | Static Factor of Safety |
|---|---|---|
| Locking rod notches | 164 | 6.5 |
| Edge of U-beam slot | 135 | 7.9 |
| Sliding lock | 60 | 18 |
| Knee disk notch | 72 | 7.0 |

Tensile stresses were only significant for the locking rod and the proximal and distal cables. Maximum tensile stress in the locking rod occurred at the thinnest sections, where the single long notch and the ratchet notches both reduced the locking rod diameter by 3 mm. The maximum stress was 113 MPa, for a factor of safety of 9.5. Tensile stresses on the cables were not directly calculated. Commercially available cables are rated for a certain breaking load, and it is recommended that a factor of safety of approximately 5 is used when determining a working load. Cable size was therefore chosen based on the rated breaking strength provided by the manufacturers. A load of 1500 N on the thicker distal cable and on the two, thinner proximal cables resulted in factors of safety of 4.5 and 5.5 respectively.

3.6.4.1.2 Pin and Fastener Stresses

Bending, shear, and bearing stresses, $\sigma_{bd}$, $\tau$, and $\sigma_{br}$, respectively, for the knee disk pin, and rupture stresses, $\sigma_r$, for connected members, were calculated using the equations [110]:

$$\sigma_{bd} = \frac{(Ft/2)c}{I} \tag{3-23}$$

$$\tau = \frac{F}{A_p} \tag{3-24}$$

$$\sigma_{br} = \frac{F}{td} \tag{3-25}$$

$$\sigma_r = \frac{F}{A_m}, \tag{3-26}$$

where $F$ is the force applied to the pin and $t$ is the total thickness of parts connected by the pin (grip). $I$ and $c$ are moment of inertia and distance to the neutral axis, as described for Equation (3-17). $A_p$ is the cross-sectional area of the pin, $t$ is the thickness of the thinnest connected member, $d$ is the pin diameter, and $A_m$ is the net cross-sectional area of the

thinnest connected member, with the holes required for the pin taken into account.

Fasteners used to secure the upper and lower device assemblies to the KAFO uprights created shear joints. Therefore, only shear, bearing, and rupture stress calculations were necessary [110]. Table 3.6 shows the stresses calculated and the corresponding factors of safety. All values were deemed acceptable.

Table 3.6: Knee disk pin and fastener stresses and factors of safety (n). All stresses ($\sigma_{bd}$, $\tau$, $\sigma_{br}$, and $\sigma_r$) are in MPa, while factors of safety ($n_{bd}$, $n_\tau$, $n_{br}$, and $n_r$) are dimensionless.

| Component | $\sigma_{bd}$ | $n_{bd}$ | $\tau$ | $n_\tau$ | $\sigma_{br}$ | $n_{br}$ | $\sigma_r$ | $n_r$ |
|---|---|---|---|---|---|---|---|---|
| Knee disk pin | 239 | 4.5 | 60 | 17.9 | 125 | 8.6 | 18.6 | 57.5 |
| KAFO attachment base screws | -- | -- | 60 | 16.3 | 98 | 10.9 | 23 | 47.3 |
| Proximal knee disk support screw | -- | -- | 249 | 3.9 | 123 | 8.7 | 23 | 46.5 |
| Distal knee disk support screw | -- | -- | 85 | 11.5 | 84 | 12.8 | 16 | 68.4 |

### 3.6.4.2 Dynamic Stress Analysis

Determination of dynamic stresses of the various components was also required, because the device would be loaded cyclically during use.

Each loading cycle could potentially load device components from an unstressed state up to the maximum stress calculated in the static analysis. Therefore, for the dynamic analysis, the minimum and maximum stresses applied to a given component, $\sigma_{min}$ and $\sigma_{max}$, were taken as zero and the maximum calculated static stress for that component, respectively. Based on these minimum and maximum stresses, nominal midrange and amplitude components of the cyclical stress, $\sigma_{m0}$ and $\sigma_{a0}$, respectively, [110] were determined:

$$\sigma_{m0} = \frac{\sigma_{max}+\sigma_{min}}{2} \ , \ \ \sigma_{a0} = \left|\frac{\sigma_{max}-\sigma_{min}}{2}\right| \qquad (3\text{-}27)$$

Nominal midrange and amplitude stresses were then corrected for stress concentrations due to features such as holes and notches. Some materials are not fully sensitive to the presence of these features and so the static stress concentration factor, $K_t$, was reduced to the fatigue stress concentration factor, $K_f$. The fatigue stress concentration factor is calculated based on $K_t$ and the notch sensitivity of the material, $q$, according to Equation (3-28). $K_f$ is then used to determine the maximum midrange and amplitude stress components, $\sigma_m$ and $\sigma_a$, respectively,

applied to the device component, following Equation (3-29) [110].

$$K_f = 1 + q(K_t - 1) \qquad (3\text{-}28)$$

$$\sigma_m = K_f \sigma_{m0} \quad , \quad \sigma_a = K_f \sigma_{a0} \qquad (3\text{-}29)$$

The maximum midrange and amplitude stress components were used to determine the fatigue factor of safety for infinite life, $n_f$. The fatigue failure criterion used to determine $n_f$ was the ASME-elliptic criterion [110], given by:

$$\left(\frac{\sigma_a}{S_e}\right)^2 + \left(\frac{\sigma_m}{S_y}\right)^2 = \frac{1}{n_f^2} , \qquad (3\text{-}30)$$

where $S_e$ and $S_y$ are the material modified endurance limit and yield strength, respectively.

Since the KEA operates in close contact with a person, components were designed to achieve a factor of safety for infinite life of at least two, even though the number of cycles the KEA would undergo in its life was projected to be approximately $3.0 \times 10^5$ cycles, as stated in Section 3.3.2. In cases where the factor of safety was close to two, the number of cycles to failure, $N$, of the component was calculated to ensure that fatigue life was sufficient to withstand at least twice the number of projected cycles. The method of calculation was the same as that used for fatigue life of the torsion spring, described in Section 3.4.3 (Eq.s (3-9) to (3-15)). Table 3.7 presents a summary of the infinite-life fatigue factors of safety, $n_f$, for the highly stressed components and the number of cycles to failure for components with a factor of safety of 2.5 or less.

Table 3.7: Infinite-life factor of safety for highly stressed components and cycles to failure where appropriate.

| Component | Infinite-life factor of safety ($n_f$) | Cycles to failure ($N$) |
|---|---|---|
| U-beam | 3.4 | -- |
| Distal spring case end | 2.5 | $28.2 \times 10^6$ |
| KAFO attachment base | 2.2 | $3.5 \times 10^9$ |
| Locking rod notch | 2.3 | $12.3 \times 10^9$ |
| Edge of U-beam hole | 2.2 | $3.5 \times 10^9$ |
| Cable connector | 3.6 | -- |
| Knee disk pin | 3.7 | -- |
| Knee disk notch | 4.2 | -- |
| Knee disk support | 2.8 | -- |
| Proximal knee disk support screw | 2.8 | -- |

### 3.6.5 Component Details

The following section presents the function, structure, and material of each KEA component (Figure 3.3). A partial exploded view of the KEA, in which the spring case assembly components can be more easily viewed, can be found in Appendix E.

### 3.6.5.1 Springs

The springs act as the 'passive actuator' of the device. Upon compression during knee flexion under body weight, the springs store energy. The stored energy is released when the springs extend during weight-bearing knee extension of the braced leg, at a time chosen by the user. Three springs are used in parallel, and are compressed a maximum of 6 cm. An initial compression is applied to the springs such that when the springs are fully extended within the spring case, the springs are still compressed by 2 cm from their free length. When the device is in use, a maximum additional compression of 4 cm can be applied. Maximum compression corresponds to a total 1500 N spring force from the three springs, which provides an extension-assist of 47 % for STS for a 90 kg individual, as described previously.

Each spring, made from round music wire, has an outer diameter of 19.6 mm, a wire diameter of 2.6 mm, a resting length of 102 mm, and a closed length of 39.6 mm, and weighs 35 g. The manufacturer-predicted fatigue life for the springs is 100,000 cycles. The life of the KEA was estimated at 30,000 cycles per year for 10 years (Section 3.3.2). Therefore, spring replacement should occur yearly when the KAFO is brought in for servicing, to achieve a spring-life factor of safety greater than two.

### 3.6.5.2 Spring Case and KAFO Attachment Base

The spring case houses the springs and holds the distal ends of the springs in place. The spring case is machined from a single 7075-T651 aluminum plate and has shallow circular recesses in the distal end into which the springs fit. To secure the spring case to the KAFO uprights, the KAFO attachment base, cut from 0.05 in. 17-4 precipitation hardened (PH) stainless steel sheet, is fastened to the underside of the spring case by four UNC 4-40, SAE grade 8 screws. The KAFO attachment base is fastened to the KAFO upright through the tabs

protruding from the ends of the base by four UNC 10-32, SAE grade 8 screws (Appendix E).

### 3.6.5.3 U-Beam

The U-beam fits around the proximal ends of the springs. The springs sit in the trough of the 'U' shape and the legs of the 'U' extend above and below the springs. The U-beam is not fixed to the device, and can therefore move both proximally and distally within the spring case. The U-beam has three main functions: to act as a moving surface that can compress the three springs in unison, to provide a location for proximal cable attachment so that the cable tension force can be transmitted to the springs, and to engage with the notches of the locking rod to prevent undesired spring extension. A slot in the middle of the U-beam with one end rounded and one end straight (Figure 3.9) allows the locking rod to pass through. The straight edge of the slot engages with the locking rod notches and is chamfered to 45° to allow for full engagement with the 45° ratchet notches.
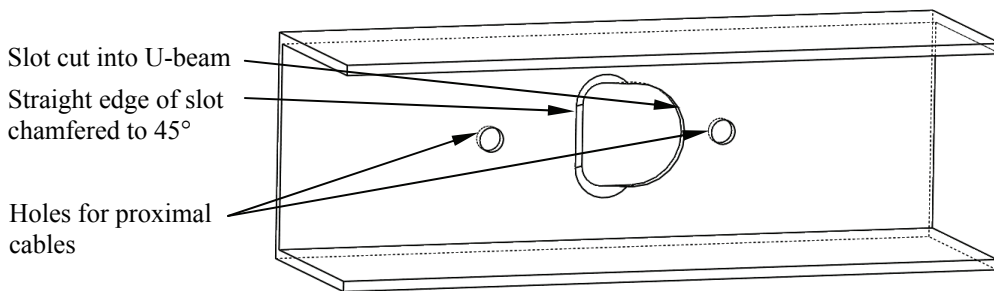


Figure 3.9: An isolated view of the U-beam showing the holes for cable attachment, the slot for the locking rod, and the chamfered straight edge of the slot

The shape of the U-beam was chosen because of its ability to resist bending with minimal material, and thus with minimal component size and weight. 17-4 PH stainless steel was used. Wall thickness of 1.3 mm and segment lengths of 20 mm were sufficient to withstand the applied forces. The 'U' shape also constrains the proximal ends of the springs to help prevent the springs from shifting perpendicular to their axis during KEA use.

### 3.6.5.4 Locking Rod

The locking rod locks the U-beam in place when knee flexion stops to prevent unwanted spring extension. On one side of the rod are the multiple, 45° ratchet notches that create the

ratcheting locking mechanism for STS. Notch width is 3 mm, which causes the notches to engage with the U-beam at every 6.75° of knee flexion. On the opposite side of the locking rod is the single, square, long notch, used to maintain the ramp walk preload. All notches are 3 mm deep in the 10 mm diameter, 17-4 PH stainless steel locking rod. A nut on the threaded distal end of the locking rod prevents the locking rod from moving proximally when the springs are locked in a compressed state. The proximal head on the locking rod prevents the rod from moving distally. When spring extension is desired, the locking rod head is manually moved anteriorly, as described in Section 3.6.3, to disengage the notch from the U-beam and allow the springs to extend.

### 3.6.5.5 Locking Rod Spring, Spring Pin, and Spring Pin Support

The mechanism that automatically engages the locking rod notches with the edge of the slot in the U-beam consists of a small compression spring, a stepped pin, and a support to hold the pin and spring in place (Figures 3.3, 3.5, and 3.8). The locking rod spring pushes the locking rod spring pin into the locking rod to bias the rod to the locked position. The locking rod spring and spring pin allow sufficient lateral displacement of the locking rod to disengage a notch from the U-beam when the locking rod is moved anteriorly.

The locking rod spring pin and locking rod spring pin support were designed around the springs found in common 'click-top' pens, because of the pen spring availability and suitability to the task. Because of the low forces acting on the subassembly, the locking rod spring pin and locking rod spring pin support are lightweight and inexpensive 6061 aluminum.

### 3.6.5.6 Proximal Cables, Distal Cable and Cable Connector

Two sets of cables transmit the force between the springs and the knee joint (Figure 3.3). The two proximal cables attach to the U-beam, pass between the three springs, and exit the spring case through holes in the distal case end. The proximal cables also prevent the springs from moving laterally, which would result in the entanglement of one spring in another. The distal ends of the proximal cables attach to the two outer holes of the cable connector. The distal

cable runs from the middle hole of the cable connector, around the knee disk, to the knee disk cable support. During weight-bearing knee flexion, the distal cable wraps around the knee disk and moves the U-beam distally, to compress the springs via the cable connector and proximal cables.

The proximal cables are 3/32 in. diameter, 7 x 19 strand, stainless steel aircraft cables. The distal cable is a 1/8 in. diameter, 19 x 7 strand, stainless steel aircraft cable. The 19 x 7 wire strand configuration increases cable flexibility but slightly decreases the cable strength relative to the 7 x 19 strand equivalent. The added flexibility is desired since the distal cable must wrap around the knee disk. Cables are secured to other components by end stops, small cylinders of aluminum or copper compressed onto the ends of the cables, to prevent the cables from pulling through holes when under tension. The cable connector is made from a rectangular piece of 17-4 PH stainless steel.

### 3.6.5.7 Knee Disk, Knee-Disk Bearing, and Knee-Disk Cable Support

The knee disk transforms the linear spring force into a knee-joint moment by providing a moment arm with which the spring force can act (Figure 3.8). To achieve a linear moment response that follows the natural linear decrease of the knee moment for STS, the segment of the disk around which the cable wraps is circular, with a 25 mm radius. The disk has a groove cut into the edge to guide the cable as it wraps around the disk, as described in section 3.6.2, to prevent the cable from slipping off the disk edge. The knee disk rotates freely about the knee joint pin on a bearing (KG 698Z), and therefore a mechanism is required to couple the knee disk to the orthosis joint. The mechanism that locks the knee disk into place fits into a notch cut into the bottom of the knee disk. The knee disk notch is rectangular, but is extended to the anterior end of the disk. To facilitate ease of locking, the notch has a 5° tolerance on the knee angle position for locking, and thus allows the knee disk to be coupled to the KAFO for any knee angle within the range of 0° to 5°. The posterior side of the knee disk, which does not bear high stresses or support the cable, was cut away to reduce knee-disk size and weight.

The notch also allows the knee-disk cable support to be fastened easily to the knee disk because it provides a flat surface on which to secure the flat cable support. The hole of the knee-disk cable support, through which the distal cable passes, is aligned with the knee disk such that when the cables are under tension, the distal cable pulls perpendicularly to the knee disk cable support, and thus avoids introducing a sharp bend in the cable at the attachment point that would generate higher local stresses in the cable.

The knee disk is made of 7075-T651 aluminum. To produce a small and thin knee disk cable support, 2.54 mm thick 17-4 PH stainless steel sheet was used.

### 3.6.5.8 Sliding Lock, Sliding-Lock Supports and Sliding-Lock Bracket

The function of the sliding lock subassembly (Figures 3.3 and 3.4) is to prevent the knee disk from rotating about the knee disk pin and therefore temporarily fix the knee disk to the lower upright. Any moment applied to the knee disk with then be transmitted to the lower orthosis upright, and will thus generate a knee extension moment, the primary function of the device. When the sliding lock is engaged with the knee disk notch, the lower and upper assemblies are coupled. With the two assemblies coupled, the springs can be compressed and extended with knee flexion and extension, respectively. Three identical 5 mm square rods make up the sliding lock and its supports. The sliding lock is prevented from moving laterally by the two sliding lock supports and outwards, away from the body, by the thin sliding lock bracket that is secured to the two sliding lock supports using stainless steel screws. The sliding lock can therefore only move proximally and distally.

The sliding lock and sliding lock supports were fabricated from 17-4 PH stainless steel. The sliding lock supports are fastened to the knee disk support using UNC 4-40, SAE grade 8 screws. A small tapped hole in the distal end of sliding lock is used to link the sliding lock with the piston of the pneumatic actuator that controls the position of the sliding lock. The sliding lock bracket does not experience significant loads and is therefore made from light, inexpensive, 6061 aluminum sheet.

### 3.6.5.9 Knee-Disk Support and Knee-Disk Pin

The knee disk support (Figure 3.3) has two main functions. Primarily, it provides a base for the components of the knee disk assembly for fastening to the lower KAFO upright. Because of the high bending moments in the knee disk support due to the applied loads to the lower assembly by the cables, the knee disk support is made from 17-4 PH stainless steel. The fasteners are also larger in diameter than the others used; UNC 10-32, SAE grade 8 high strength screws.

The knee-disk pin, press fit into a hole in the knee disk support, resists the loads from the knee disk, while permitting knee-disk rotation when the knee disk is unlocked. The pin, made of 17-4 PH stainless steel, is fit with a circlip to prohibit the knee disk bearing from moving axially along the pin.

### 3.6.5.10 Pneumatic Actuator, Actuator Support Bracket, and Air Bladder

A single-action pneumatic actuator (Bimba 3/8" air cylinder) with return spring is used to control the sliding lock position. When the orthosis is load bearing, the plunger extends to move the sliding lock proximally into the notch in the knee disk and thus lock the knee disk in place. When the orthosis is unloaded, the actuator retracts the sliding lock distally away from the knee-disk notch to allow the knee disk to rotate about the knee disk pin.

The actuator is powered by a custom-made, heat-sealed plastic air bladder placed under the foot of the braced leg, and is connected to the actuator by nylon series 32-4 mm high pressure tubing. The pressure on the air bladder from body weight generates an actuator force that overcomes the actuator return-spring force and engages the sliding lock with the notch in the knee disk. When pressure is removed from the air bladder, the return spring force created during piston extension retracts the piston and sliding lock.

The actuator support bracket secures the pneumatic actuator to the knee disk support. More importantly, the bracket maintains alignment between the pneumatic actuator and the sliding lock. Slight misalignments between the lines of action of the actuator and the sliding lock inhibit smooth piston extension when pressure is applied to the air bladder. The actuator

support bracket does not experience large loads and was therefore fabricated from 18 Ga. 6061 aluminum sheet.

### 3.6.6 Failure Mode Analysis

A failure mode analysis was performed on the KEA design (Appendix F). The analysis indicated which device components would lead to the most severe consequences in the event of failure. The results showed that failure of the fasteners used to secure the device to the KAFO and failure of the spring locking mechanism, either from locking rod notch failure, U-beam failure, or poor engagement between notch and U-beam, could result in the most serious failure modes, with the possibility of user injury. Considerations for the development and testing of the KEA that arose from the analysis are as follows:

1. All fasteners bearing high loads should be high strength, UNC grade 8 or metric class 12.9 fasteners, to achieve low stresses while maintaining low fastener size and weight. Extra fasteners were used to provide redundancy. Conservative fastener use would not greatly affect the overall size and weight of the device.

2. Locking rod notches and the edge of the slot in the U-beam that engages with the notches should be designed for a very high number of cycles to failure (Table 3.7).

3. If necessary, the wall thickness of the area around the slot in the U-beam can be reinforced to 3 mm and still fit inside the locking-rod ratchet-notches.

4. If poor notch engagement occurs during testing, a stiffer locking rod spring should be used.

5. Should the end stops slip during testing, stainless steel end stops, which provide a gripping strength greater than the breaking strength of the cable to which the stop is secured, are available as an alternative to aluminum and copper. However, stainless steel end stops are larger and heavier than the aluminum or copper counterpart and the equipment required for installation is costly. Accordingly, stainless steel stops would only be used if necessary.

## 3.7 Prototype Development

After completion of the design phase, a prototype was constructed and mounted onto KAFO uprights for mechanical and biomechanical testing (Figure 3.10). Additional prototype photos are provided in Appendix G.



Hex bolt locking rod

Brass plate

Spring beam (mostly hidden)

Spring case assembled from separate pieces for sides, bottom, and ends.

Aluminum strips to secure springs
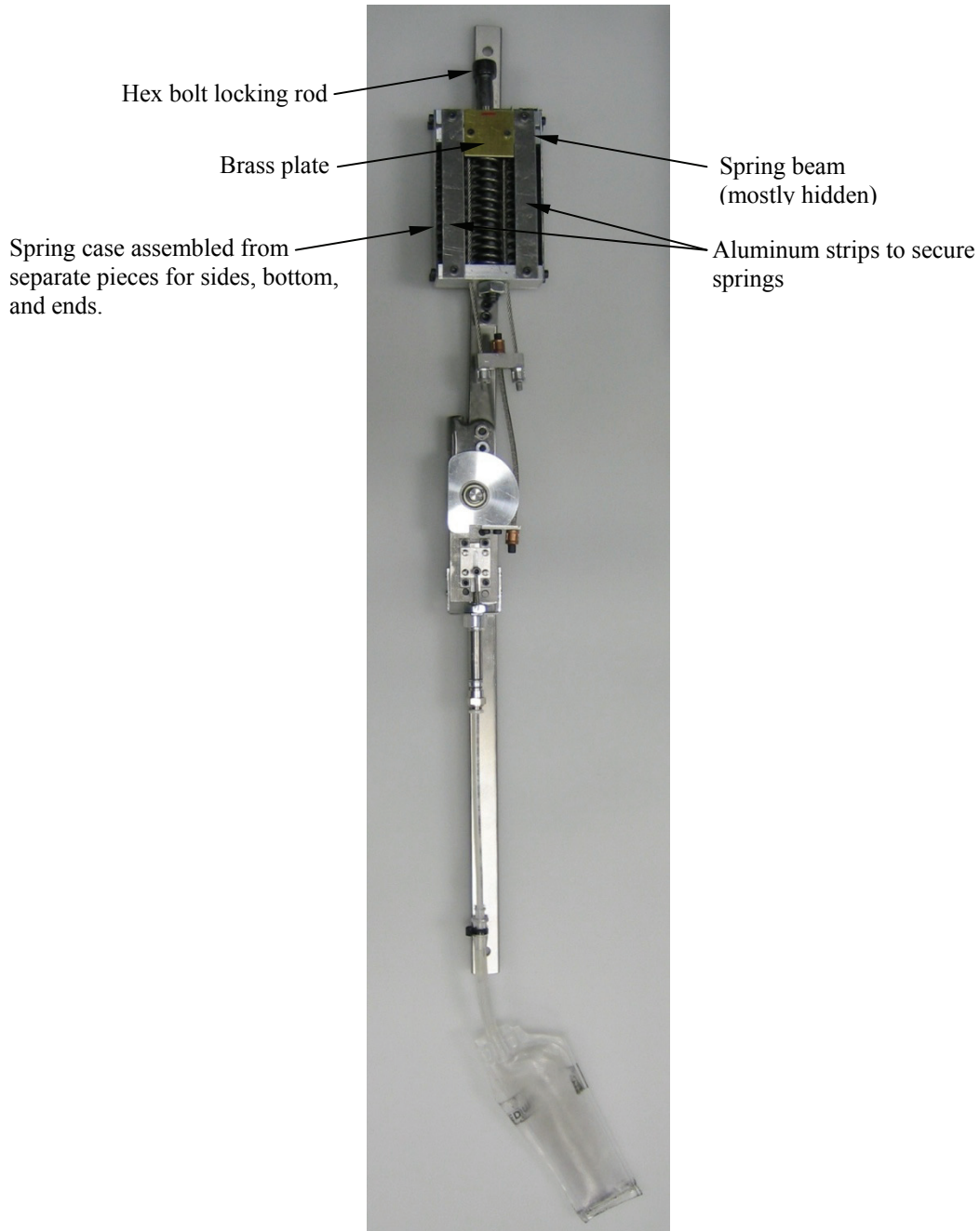
Figure 3.10: KEA device prototype.

93

### 3.7.1 Design Modifications for Prototype Development

To facilitate prototype construction and minimize cost, a number of modifications were made to the KEA design. For safety, all modifications were designed more conservatively than the original component through the use of stronger materials or increased dimensions.

To avoid machining out a large block of aluminum for the spring case, the case was assembled from several separate pieces (Figure 3.10). Case sides and bottom were made from 0.05 in. thick 17-4 PH stainless steel sheet and were fastened to the proximal and distal case ends. The case ends were cut from 3/8 in. thick 7075-T651 aluminum bar. The KAFO attachment base was made from three sheets of 0.05 in. thick 17-4 PH stainless steel. The first sheet was also the spring case bottom. To permit visual examination of the functioning of the device during use, the case cover was replaced by only two strips of 6061 aluminum (Figure 3.10) secured above the two outer springs to safeguard against spring buckling; the inner spring was prevented from buckling by the locking rod. Fasteners were all high strength class 12.9 M3 screws.

17-4 PH stainless steel sheet requires intermediate heat treatments in order to be bent without losing mechanical integrity. However, heat treatment equipment was not available where the prototype was made. To avoid the need for heat treatment, the U-beam was replaced by an aluminum bar with a backing of 17-4 PH stainless steel (Figure 3.10). The aluminum provides the required resistance to bending while the stainless steel backing engages with the locking rod notches. The modified U-beam will be called the spring beam from this point on.

For the locking rod, a class 12.9 M10 hex cap bolt was used instead of 17-4 PH stainless steel (Figure 3.10). Class 12.9 bolts have a higher yield stress than 17-4 PH stainless steel, and come threaded on one end and with a head on the other. The head was not machined to include the stops for the locking rod spring pin. Instead, a mark was placed on the locking rod head to provide a visual cue for proper alignment.

The dimensions of the cable connector, knee disk support, sliding lock, and sliding lock supports were all increased so all pieces could be cut from the same 17-4 PH bar without

requiring subsequent machining to reduce sizes to the original design specifications.

A single-action Bimba 3/8" diameter pneumatic actuator was available from a previous device. The available actuator was modified with a return spring fashioned from an extension spring attached to the actuator support bracket and the sliding lock.

Following initial testing where spring beam rotation occurred within the spring casing, a 30 mm x 30 mm x 1.5 mm brass plate (Figure 3.10) was fastened to the spring beam to slide between the two aluminum strips covering the outer springs. The brass plate acted as a linear bearing and stopped spring beam rotation when the springs were compressed and locked.

### 3.7.2 Prototype Size and Weight

The prototype weighed 0.668 kg (1.47 lb), meeting the 0.68 kg design requirement for weight. The spring case assembly measured 158 mm long, due to the length of the locking rod. The spring case measured 111 mm long. The majority of the additional prototype spring case length was caused by the increased thickness of the spring beam and proximal end of the spring case. Little width and thickness were added to the spring case assembly from modifications for the prototype. The width was 70 mm and the medio-lateral thickness was 27 mm, very close to the values of the original design, 69 mm and 25 mm, respectively. The knee disk assembly was 167 mm long, 48 mm wide, and 20 mm thick. The extra length was a result of the pneumatic actuator quick-connect fitting that permitted easy connection of the air bladder. The quick connect fitting was not included in the original design and would be excluded in the final design.

### 3.7.3 Prototype Cost

Prototype fabrication took place at the Ottawa Hospital Rehabilitation Centre machine shop, at a total estimated cost of at $3114. The major expense was the cost of the skilled labour. Fabrication took an estimated total of 37.5 hours at a cost of $80 per hour, totaling $3000. Materials used in fabrication cost an estimated total of $114. A bill of materials can be found in Appendix H. For future one-off prototypes, fabrication cost could be reduced to $1427 by outsourcing the machining.

## Chapter 4. Mechanical Evaluation

Mechanical evaluation of the KEA prototype was conducted to determine the extension-assist moment provided, as well as to ensure proper device function before testing the KEA on human participants. The prototype was mounted on ¾ in. x 3/16 in., ¼ hard 304-2B stainless steel KAFO uprights (Becker Orthotics), the strongest available KAFO uprights, in preparation for mechanical testing. The uprights were connected by a single axis rear-offset knee joint, which is an orthosis knee joint with the joint centre slightly posterior to the centerline of the uprights.

Tests were conducted using a tensile testing machine (Instron 4482 universal tester). First, the distal cable was detached from the knee disk, the entire knee disk assembly along with the lower KAFO upright was removed, and the upper KAFO upright with the spring case assembly attached was mounted in the Instron. The tensile testing machine was then used to pull the distal cable, to measure the spring force exerted during spring compression. The KEA and KAFO uprights were then reassembled, and the uprights were mounted onto the tensile testing machine. The tensile testing machine was then used to flex and extend the joint with the KEA providing the extension-assist moment, to measure the amount of force resisted during joint flexion and supplied during joint extension, in order to determine the moments provided by the device during use.

The testing machine was controlled via a computer running Instron 9 Series software. Data was sampled at the maximum measuring frequency of the testing machine, 20 Hz. Due to intrinsic error in the testing machine, four consecutive data points were missed approximately every 10 s.

### 4.1 Spring Response Tests

To empirically test the response of the springs, the spring case assembly was mounted in the tensile testing machine and the distal cable was pulled to compress the springs.

### 4.1.1 Purpose

Although the specifications for the springs purchased were supplied by the manufacturer, the actual response of the system would likely differ from that stated by the manufacturer due to variance in the spring constants among the different springs, as well at the presence of some undesired motion in the system due to cable lengthening and shifting of components upon loading, and friction. To determine the actual response of the spring case assembly as a whole, the springs were compressed *in situ*.

### 4.1.2 Procedure

For the spring response test, the lower KAFO support upright and the knee disk assembly were detached from the upper KAFO support upright and spring case assembly. The upper KAFO upright was secured to the tensile testing machine and the distal cable was held from below by a serrated grip clamp (Figure 4.1). The test consisted of raising the tensile testing machine crosshead (tensile testing machine extension) which raises the spring case while the distal cable is held by the fixed lower grip. This generates tension in the cables and pulls on the spring beam (Appendix G), thereby compressing the springs.

A low clamping force was used such that the load was transmitted to the cable through the end stop, and not through a large clamping force on the cable. The locking rod was removed from the device so that, upon return of the tensile testing machine crosshead to its original position, the springs would elongate without locking. The tensile testing machine crosshead was raised at 300 mm/minute, after a number of prior trials at varying extension rates revealed that there was no difference in measured spring response with changing crosshead speed. At the starting position for the test, there was no slack, but minimal tension, in the cables. Each trial was set to end after an extension of 40 mm, the amount of spring compression that would occur in 90° of knee flexion. The forces exerted over the functional range of the KEA could thus be measured. Ten trials were performed and the mean and standard deviation of the spring extension force exerted on the tensile testing machine via the proximal and distal cables were calculated.
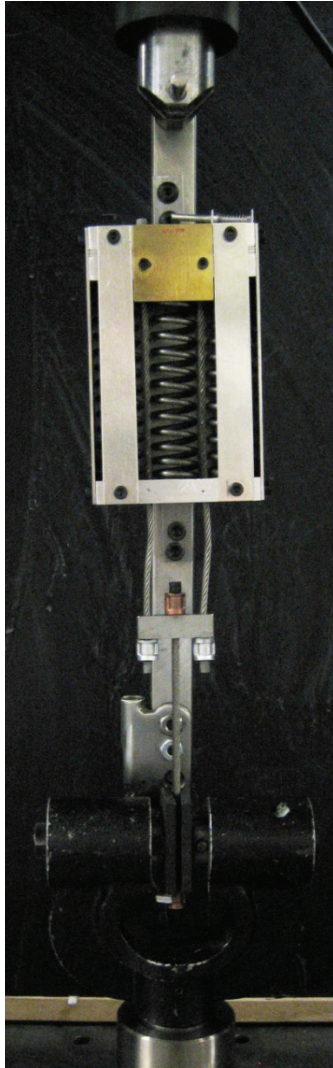
Figure 4.1: Photograph of the spring-response test setup.

### 4.1.3 Results

The results from the ten trials are presented in Figure 4.2. The force response increased linearly with spring compression starting from an initial preload force of 331 N. The force curve had very little variation across trials. Average standard deviation across the trials was 4.2 N, and only 2.8 N if the force curve before the preload was reached is ignored. In all trials, the crosshead traveled 2 mm before the 331 N preload was reached. In the first 2 mm of the first trial, there was adjustment and alignment of components within the system and stretch of the wire cables as the force exerted by the tensile testing machine increased to 331

N. For the remaining nine trials, there was no further adjustment or alignment of components. Instead, the 1 mm of slack in the cables produced from the system adjustments in the first trial was taken up with no measurable force, followed by 1 mm of cable stretch as the force from the tensile testing machine increased the cable tension to the spring preload force. Once cable tension exceeded the preload, the springs began to compress. The generated spring force was lower than the manufacturer specifications for a given spring compression. The average measured preload of 331 N was 69 % of the 480 N theoretical preload that should have existed in the springs at full extension within the spring case. The average spring rate was calculated from the linear portion of the ten trials, and was found to be 8405 N/m, slightly higher than the 8088 N/m rate specified by the manufacturer. Even with the elevated spring rate, at 42 mm of tensile testing machine extension (reached with 2 mm of tensile testing machine overshoot) which corresponded to 40 mm of actual spring compression, the spring force was 1334.6 ± 2.7 N, or 89% of the rated 1500 N.

Although the force response from the springs was lower than expected, at 40 mm of spring compression the springs were not quite fully compressed, as was expected from the manufacturer specifications, indicating that higher forces could potentially be reached at further compression.
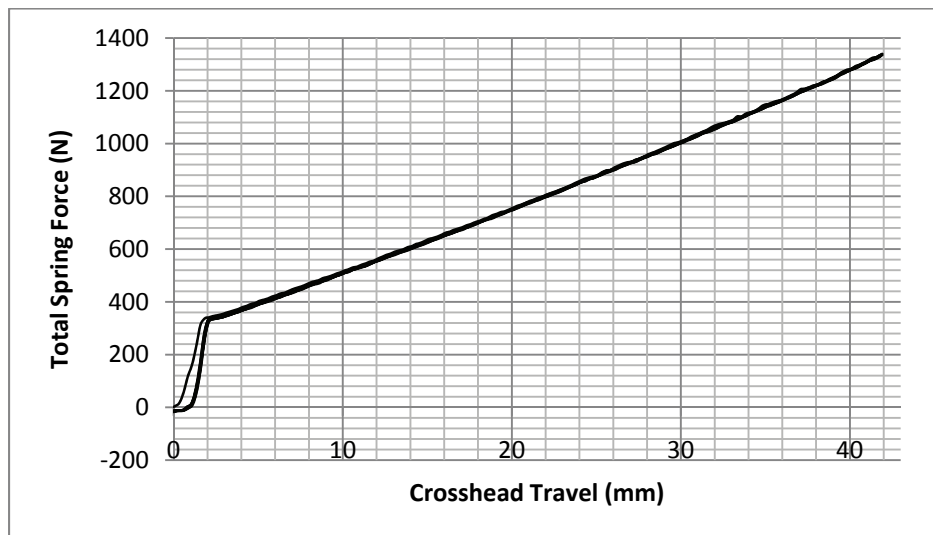


Figure 4.2: Spring response results for ten mechanical testing trials. Note that although the test was set to stop at 40 mm extension, 1-2 mm of system overshoot occurred in each trial. The ten curves drawn have the same line thickness. The lines appears thicker due to line overlap.

## 4.1.4 High Load Spring Response Test

In the initial mechanical test, the springs did not reach their closed length after 40 mm of compression. It was therefore possible to achieve higher return forces using the same springs with additional spring compression. A second test of five trials was carried out using the same setup as described above, but with the trials set to end when 1500 N was reached, instead of at a specified extension. Results would indicate if it was possible to attain the desired 1500 N spring force before reaching the closed length (full compression) of the springs, and at what amount of system extension.

### 4.1.4.1 Results

Results from the high load spring response test are shown in Figure 4.3. A linear response after an initial loading phase to reach the spring preload and low variability (average standard deviation of 7.2 N) again characterized the system response. The spring force reached 1500 N at 46.6 mm of extension, 4.6 mm greater than expected. The slight upturn at the end of each curve (Figure 4.3) represents the beginning of the rapid increase in force seen when a spring reaches its closed length, since the spring cannot compress any further. This test indicated that the maximum total return force obtainable from the three springs was approximately 1500 N, as indicated by the manufacturer, but at a compression that exceeded the specifications.
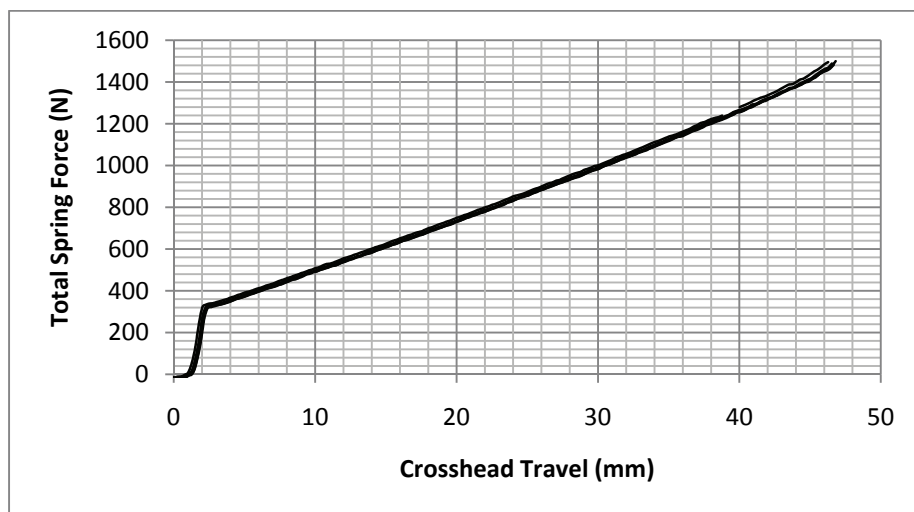


Figure 4.3: High load spring response test results for the five trials.

100

## 4.2 KEA Loading Response Test

For the second stage of testing, the KEA and KAFO uprights were reassembled and mounted onto the tensile testing machine (Figure 4.4). The setup used permitted linear testing machine compression to be converted into a flexion moment applied to the KAFO joint. The linear compressive force required from the tensile testing machine to flex the joint could then be used to calculate the extension moment provided by the KEA to the joint during loading.
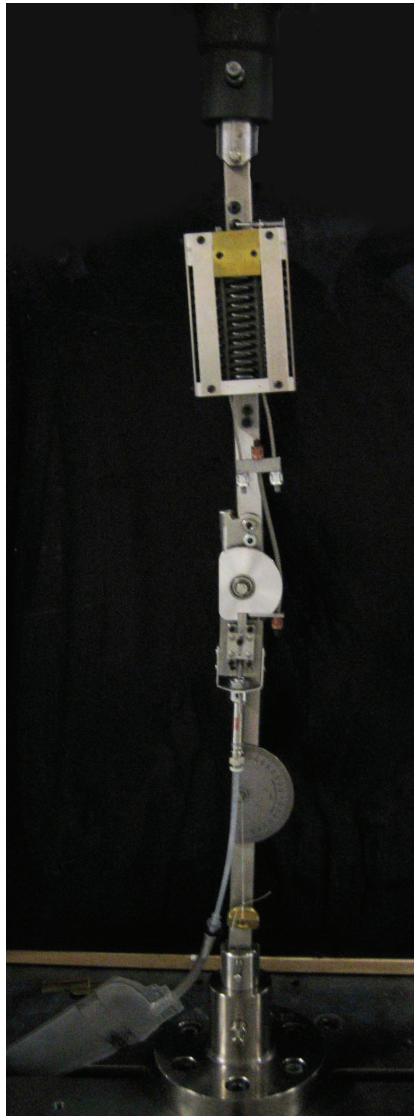


Figure 4.4: Photograph of the test setup used for the KEA loading response test.

### 4.2.1 Purpose

The loading response test was conducted to determine the actual resistive joint moment provided by the KEA during knee joint flexion for comparison to the theoretical values. The test would also reveal whether the device loaded properly, and if there were design flaws that needed to be addressed with respect to spring loading during flexion.

### 4.2.2 Procedure

The KEA and the KAFO uprights were mounted into the tensile testing machine with a starting position as shown in Figure 4.4. Custom machined steel clevises were used to secure the ends of the uprights to the tensile testing machine mounts while allowing rotation about an axis parallel to the joint axis. A protractor with a plumb line hanging from its centre was adhered to the lower KAFO upright to indicate joint angle. The locking rod was removed from the KEA to allow the springs to return to full extension as the tensile testing machine crosshead returned to its starting position after each trial. For convenience, the pneumatic actuator return spring was also removed so that between tests the sliding lock would remain engaged with the knee disk, and thus the actuator would not have to be activated before each trial through manual application of pressure to the air bladder.

Before each trial commenced, the tensile testing machine crosshead was positioned such that there was slight flexion of the KAFO joint. The initial flexion was to ensure that the joint would not remain locked in full extension, which would cause the uprights to buckle upon loading. The initial flexion angle corresponded to the angle at which the cables were taut, but not under tension. The angle was measured as being 5° using the protractor. To determine the end point of the test, the crosshead was lowered under manual control until a joint flexion angle of 90° was reached. The crosshead travel required to reach 90° was then input into the tensile testing machine control software as the compression to be applied during the test.

The joint was then flexed to 90° ten times. For each trial, the compressive force applied by the crosshead to the KAFO uprights during compression was measured and recorded by the tensile testing machine software. Each trial ended with the joint at 90° (Figure 4.5). When each trial ended, the tensile testing machine crosshead returned to the starting position. The crosshead speed was kept at 300 mm/min, as prior tests on the entire KEA at varying speeds had again shown that device response was independent of crosshead speed. The resistive moment to flexion supplied by the KEA during loading was calculated from trial results. Instantaneous moment arms and knee angles were calculated using the measured starting angle and the crosshead travel at a given time. The moment arm was then multiplied by the compressive force exerted by the tensile testing machine to determine the resistive moment at the corresponding joint angle.
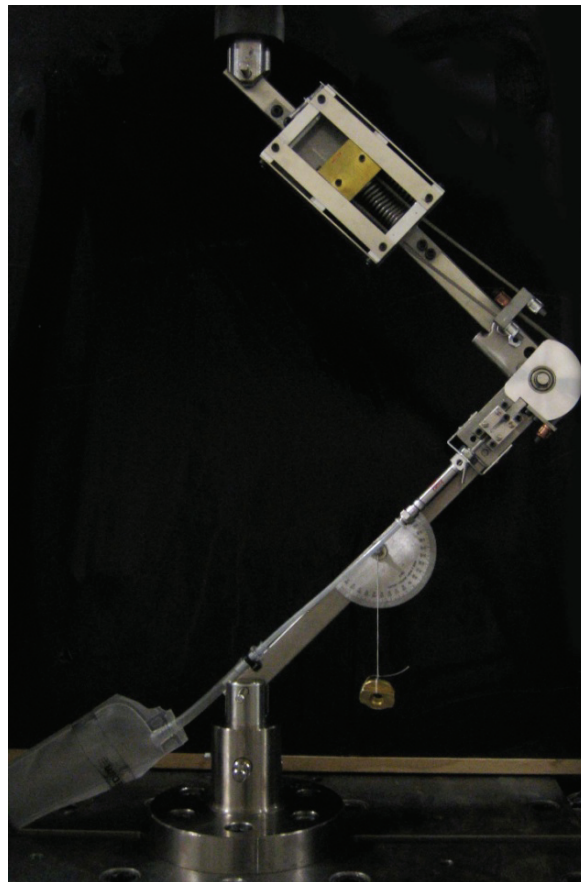


Figure 4.5: Photograph of the KEA at the completion of a KEA loading response test trial. Trials were complete when a 90° joint angle was reached, as shown.

### 4.2.3 Results

The force-displacement results from the KEA loading response test are shown in Figure 4.6. At the beginning of each trial, there was a sharp peak in the force exerted by the tensile testing machine of approximately 1230 N. The spike in applied force occurred when the joint angle was low, and thus the moment arm that the force acted on was very small. Force was expected to increase with little displacement at the start of the test until a joint moment large enough to overcome the initial spring preload was reached. Once the initial spring preload was reached, it would be expected that the rate of increase of the force provided by the tensile testing machine would drop and the moment arm would begin to increase. This is because the moment arm is an exponential function of KAFO compression (Figure 4.7), and therefore the moment arm would increase faster at the start of the trial than during the later stages. As a result, early on in the trial, the force required from the tensile testing machine to flex the joint would drop, as the moment arm increased faster than the increase of spring force, according to:

$$F_S \, R = F_T \, d \hspace{4cm} \text{(4-1)}$$

where $F_S$ is the force from the springs, R is the knee disk radius, $F_T$ is the force from the tensile testing machine, and d is the moment arm.

The drop in force from the tensile testing machine spike would appear in the applied force curve. Once the rate of increase of moment arm more closely resembled the rate of increase of spring force, the measured loading response would be expected to flatten out, and this was observed during the tests. However, this explanation does not explain the high 1230 N value of the spike observed, since, based on the preload measured in the spring response tests, the force required to generate a moment that could overcome the preload at the initial knee angle should have been 419 N. The peak observed was approximately three times that magnitude. What likely occurred was that the initial knee angle was not set at a sufficiently large value, and this therefore caused much of the tensile testing machine force at the beginning of each trial to be transmitted through the KAFO uprights to the joint. At 1.3 mm compression, which corresponded to a 9.2° joint angle, the applied force peaked, and then decreased

rapidly for the next 6 mm (Figure 4.6), to levels closer to expected values. The force required to flex the joint reduced to below 250 N for the last three-quarters of each trial, and leveled off by the end of the trials at 208.1 ± 2.1 N, on average (Figure 4.6). As was the case with the previous tests, the KEA response exhibited low variability across the ten trials, with the exception of during the spike in force. Ignoring the force measurements from 1 mm of compression on either side of the force peak, where there was an average standard deviation of 46.7 N, average standard deviation for the ten trials was 2.0 N.
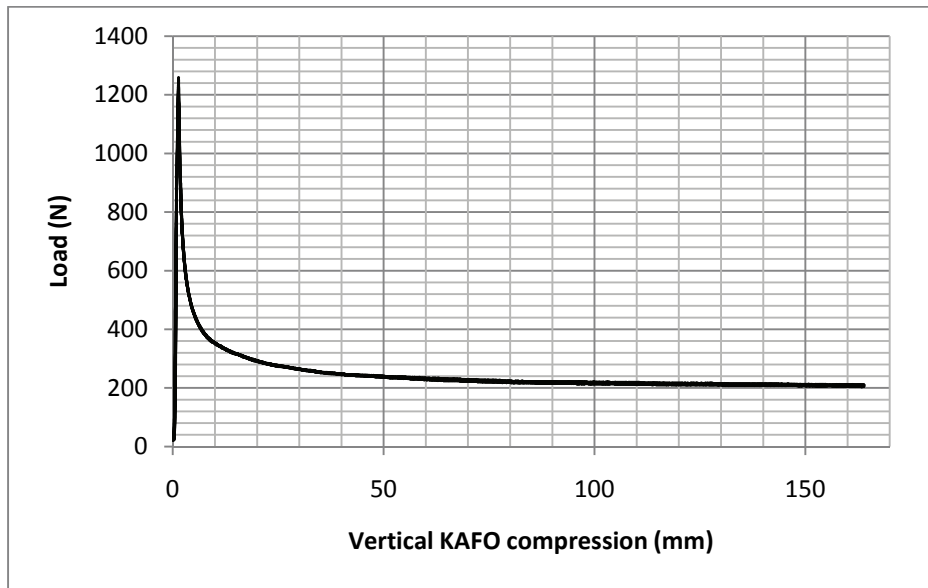


Figure 4.6: Force-displacement results from ten trials of 90° KAFO joint flexion.
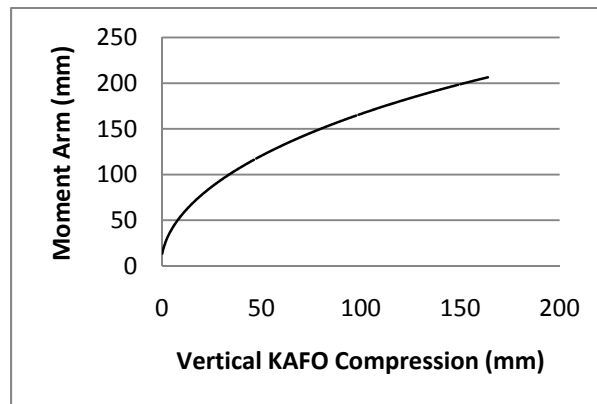


Figure 4.7: Moment arm increase as a function of vertical KAFO compression during loading.

The load-displacement measurements were then used to calculate joint moments and angles (Figure 4.8) to determine the moment supplied by the KEA during spring loading. The spike in force observed in the force-displacement data resulted in a spike in joint moment at a low knee angle. The moment peaked to 28.9 ± 1.0 Nm at the 9.2° knee angle and then decreased. Afterwards, the moment increased linearly until the end of the trial, as expected. The final extension moment provided was 42.9 ± 0.46 Nm at 87° of joint flexion, 5.4 Nm larger than the theoretical maximum moment provided by the KEA and 8 % more than the design requirement target value. The discrepancy between calculated and observed moments was most likely due to friction between the proximal cables and the holes in the distal spring case end through which they passed. From visual inspection of the KEA during the trials, the springs appeared to compress properly, the spring beam moved smoothly through the spring case, and the distal cable wrapped easily around the knee disk. All of this indicated that there were no major problems associated with loading the device.
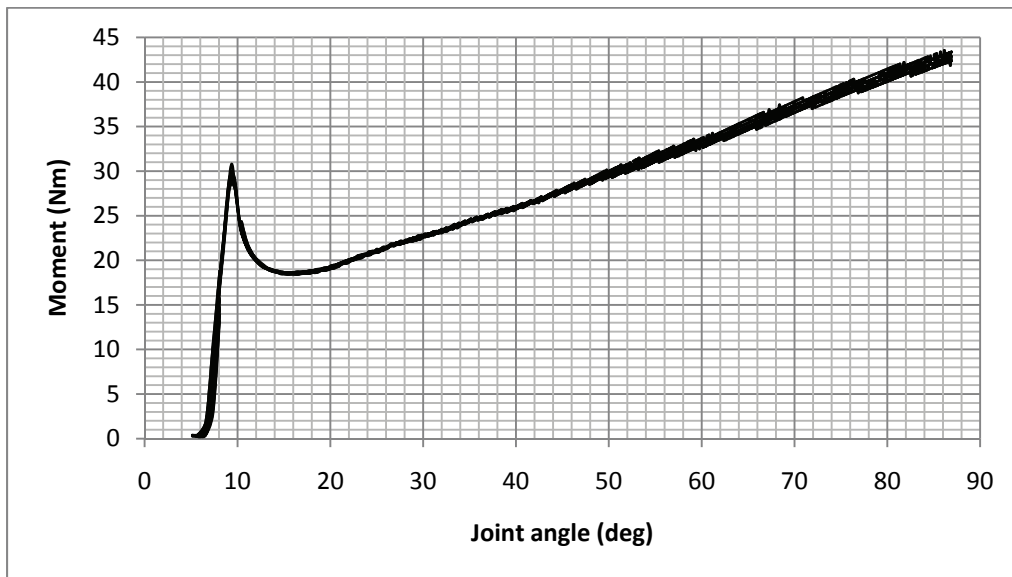


Figure 4.8: Extension moment provided by the KEA during loading, as a function of joint angle.

## 4.3 KEA Extension-Assist Response Test

The KEA extension-assist response test was performed to determine the assistive extension moment provided by the KEA during extension. The test measured the vertical force exerted by the KAFO uprights on the tensile testing machine during joint extension. The results were used to calculate the extension-assist moment provided by the KEA.

### 4.3.1 Purpose

The purpose of the test was to determine the actual extension-assist moment provided by the device during joint extension for comparison with the theoretical value. The test would also uncover any problems that may exist with KEA function during extension.

### 4.3.2 Procedure

The test procedure followed the loading response test procedure (Section 4.2) closely, but in reverse. The device remained installed in the tensile testing machine as shown in Figure 4.4. The crosshead was manually controlled and lowered until a 90° joint angle had been reached. This position (Figure 4.5) was the starting point of the extension-assist response test. The tensile testing machine extension to occur during the test was set at 5 mm less than the crosshead travel that was required to reach a 90° joint angle. The 5 mm reduction was to ensure that the tensile testing machine did not extend beyond full joint extension due to system overshoot and damage the KEA.

From the initial position, the tensile testing machine underwent the prescribed extension at 300 mm/min. The force exerted by the KAFO uprights on the mounts, caused by the KEA extension-assist moment, was measured. The empirical extension-assist moment was then calculated from the force-displacement measurements, as was performed for the loading response test. The process was repeated for ten trials.

### 4.3.3 Results

The force-displacement curves obtained during the ten extension-assist response trials are shown below in Figure 4.9. The curves contain characteristics similar to those obtained during the loading response test: a flat, approximately constant component, and a component

with a sharp rise in force near full joint extension. However, the extension-assist response exhibited a large decrease in force at the start of each trial, before the flat component began. The drop in force averaged 77.5 N, with the initial force equal to the force observed at the end of the loading response test trials. Since the extension-assist response trials began in the same position that the loading response trials finished, the drop in force was most likely a result of the same friction that caused the higher flexion-resistance moment in the loading test, as described in Section 4.2.3; i.e. during joint extension, the friction between the proximal cables and the distal spring case end opposes the spring extension force, reducing the extension moment provided.

The rise in force at the end of the trial was small in comparison to that observed during the previous test. The extension-assist response test ended before the peak in force was reached, but the peak would most likely have been much lower in magnitude, since the large spike in the loading response test was caused mainly by loading downward directly through the KAFO uprights and joint, and was thus a phenomenon that would only be observed during loading. In the extension test, what was observed was the expected peak due to the high rate of moment arm change at low joint angles, as was explained in Section 4.2.3.
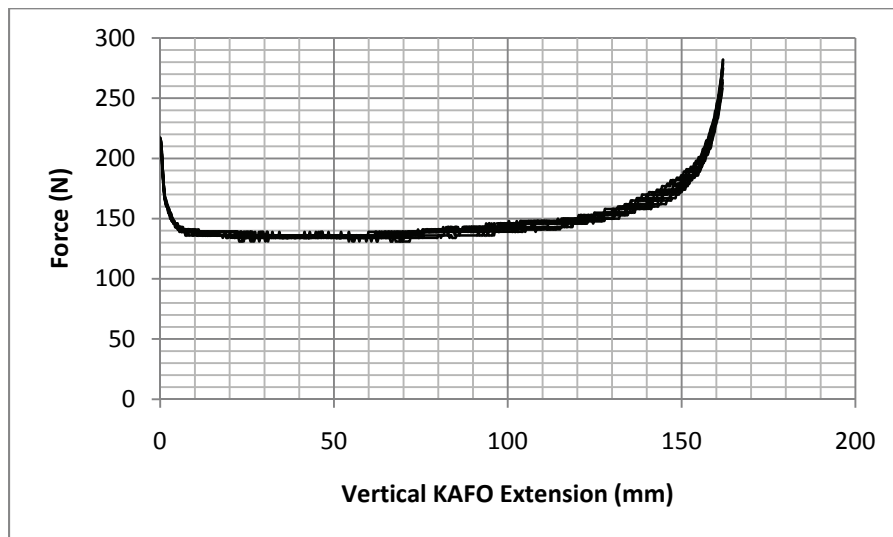


Figure 4.9: Force-displacement results from extension-assist response trials.

108

The results of the test were used to calculate the extension-assist moment supplied by the KEA during joint extension (Figure 4.10). It can be seen that the drop in force due to friction caused an initial drop of 16.4 Nm, and reduced the moment to 28.4 Nm, 76 % of the theoretical device performance and a 36% extension-assist for a 90 kg individual. The shape of the moment-angle curve was as expected, with a linear decrease through the full range of joint extension; the small rise in force that commenced at the end of the trial (Figure 4.9) was not large enough to cause a spike in extension-assist moment.
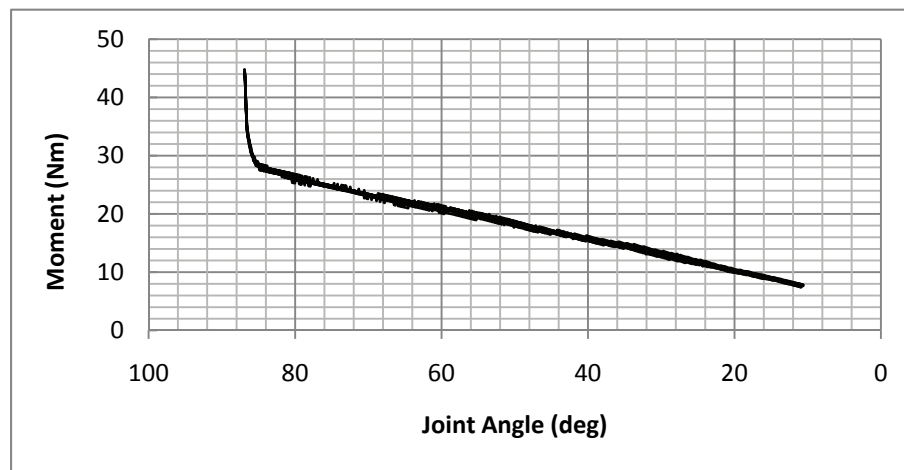


Figure 4.10: Extension-assist moment provided by the KEA during joint extension.

## 4.4 KEA Function Tests

For the KEA function tests, the locking rod and pneumatic actuator return spring were reinstalled, and the KEA was tested as a whole to ensure that it was safe to use.

### 4.4.1 Purpose

The purpose of this series of tests was to observe the function of the device as a whole, as it would be used when worn by an individual. The function of the locking rod, locking rod spring pin and locking rod spring, the sliding lock, pneumatic actuator, actuator return spring, and air bladder were tested. Although force response data were gathered automatically by the tensile testing machine during certain portions of the test, the test was mainly qualitative, since the purpose was to observe whether the KEA functioned properly as a system. The

compression and return of the springs through joint flexion and extension, respectively, had already been tested in the previous tests. The main goal of the KEA function tests was to determine whether the locking rod successfully held the spring beam in place while the springs were compressed, and whether the sliding lock successfully engaged with, and disengaged from, the knee-disk notch at the desired times.

### 4.4.2 Procedure

The function tests were performed using the same setup as the loading response and extension-assist response tests (Figures 4.4 and 4.5), but with the locking rod and actuator return spring reinstalled. The entire procedure resulted in twelve flexion-extension cycles. The twelve cycles mimicked three cycles of KEA STS mode use, since one full STS mode cycle (stand-to-sit and sit-to-stand) would involve four parts. For a full STS cycle, the user: 1) loads the device during stand-to-sit; 2) is free to extend the leg when seated, while the spring beam is locked in place; 3) returns the leg to the flexed position and places a portion of body weight on the braced leg to reengaged the knee disk; and 4) manually disengages the locking rod during STS to obtain the extension-assist from the KEA.

To simulate stand-to-sit (1), with the KEA in the same starting position as in the loading response test (Figure 4.4), i.e. with the KEA slightly flexed to remove slack from the cables, the air bladder was manually compressed to engage the sliding lock with the knee disk. The KEA was then flexed to 90°. To simulate free extension (2), the KEA was automatically returned by the mechanical testing machine to the starting position with the spring beam locked in place by the locking rod and the knee disk disengaged (Figure 4.11). To simulate return to the flexed position (3) in preparation for STS, the protocol for (1) was recommenced, and the KEA was flexed again to 90° with the air bladder compressed to engage the knee disk. To simulate STS (4), during the second extension, the locking rod was manually disengaged so that the spring beam and springs were free to return to full extension.

Once the tensile testing machine test had demonstrated device functionality, the upper KAFO upright was placed in a vice and the joint was manually flexed and extended to mimic another ten cycles of KEA STS-mode use. The ramp walking mode was then tested as

follows: the locking rod was rotated 180° to align the single, long notch in the locking rod with the straight edge of the spring beam slot. A preload spring compression force that corresponded to 20° of knee flexion was applied. The joint was then cycled through ten flexions and extensions between 45° and 0°. With each extension, the sliding lock was free to be retracted once the joint angle fell below the preload angle, and was extended into the knee disk notch with every flexion by compression of the air bladder.



Figure 4.11: Photograph of the KEA during the function tests after undergoing extension with the springs locked in a compressed state. The knee disk is automatically unlocked by the actuator return spring when extension occurs with the springs locked in a compressed state.

### 4.4.3 Results

The test revealed that the sliding lock, pneumatic actuator, actuator return spring, and air bladder functioned as designed, but the locking rod did not function properly for all cycles. During the first joint extension with the spring beam locked, part (2) of the function test procedure described above, the locking rod notch did not fully engage, and as a result, when extension commenced, the spring beam slipped off of the locking rod notch, and the springs rapidly returned to their full length. Because the notch had partially engaged before the beam slipped, the cables had briefly returned to zero tension. With the cables at zero tension, the sliding lock was retracted by the actuator return spring and thus unlocked the knee disk. As a result, when the spring beam slipped off the locking rod notch, the sudden extension of the springs to maximum length within the case caused a loud noise as the spring beam made contact with the case end, as well as a rapid rotation of the knee disk, but did not cause an unwanted joint moment because the knee disk was unlocked. The improper engagement could have been due to poor locking rod alignment, since locking rod orientation was not checked by the tester prior to commencing the first cycle. It could also have been due to insufficient stiffness in the locking rod spring that biases the locking rod to the locked position. A stiffer spring would have exerted a larger engagement force, and may have resulted in full engagement. The remainder of the trials worked properly, with loading and unloading response of the springs (Figure 4.12 and 4.13) very similar to those seen in the previous two tests. By the end of each joint flexion trial, the force leveled off at 199.2 N, a 4 % difference from the 208.1 N observed during the KEA loading response test. During joint extension, the force dropped in a similar way to the extension-assist response test results, down to 148 N, instead of 136 N. However, the KEA function test was not designed for quantitative analysis, since manual disengagement of the locking rod from the spring beam was provided during extension-assist. The direction of the manual force applied to the locking rod to prevent engagement between a notch and the spring beam was such that the manual disengagement force slightly raised the measured force during extension-assist.

The force-displacement curves from extension and flexion of the joint while the spring beam was locked in a compressed state are presented in Figure 4.14 and Figure 4.15,

respectively. Spring beam locking (Figure 4.14) was characterized by a period of proximal spring beam movement at the start of extension, from 0 to 20 mm vertical KAFO extension, during which the full extension-assist moment was provided until the face of the spring beam came into contact with the nearest proximal locking rod notch face, at 20 mm vertical KAFO extension. As a worst case, the distance traveled by the beam before coming into contact with a notch would be 3 mm, the distance between two locking rod notches, which corresponds to 6.8° of joint extension. Furthermore, full engagement of the beam was not instantaneous. There was an additional range of joint extension over which the extension-assist moment decreased to zero, from 20 to 50 mm vertical KAFO extension. As a consequence, when the braced limb was extended with the locking rod in place, the joint extended 7.2° before the spring beam was fully locked and cable tension was zero.

The possible range of joint extension before the full spring force was borne exclusively by the locking rod was determined from Figure 4.14 and the locking rod inter-notch distance. The range was between 7.2° of extension, if joint flexion were to end with the spring beam aligned with a notch face, and 14° (7.2° + 6.8°), if flexion were to end with the beam slightly proximal to the next most distal notch face.

Figure 4.15 shows the force required to flex the joint with the spring beam locked. The response is as expected, the reverse of that observed during locking, but with the final applied force, 207.8 N, higher than the initial force of 143 N in Figure 4.14. The difference was due to friction between the cables and the spring case, as explained earlier.

Because the locking mechanism did not function properly for all tensile testing machine trials, the upper KAFO upright was placed in a vice and the KEA was manually flexed and extended to determine if improper function was a regular occurrence. In ten STS-mode and ten ramp walk mode cycles, there was no occurrence of the spring beam slipping off of the locking rod notch. However, in three of the STS-mode trials, the tester was able to push the locking rod slightly laterally in the posterior direction, indicating that, though sufficiently engaged, the spring beam face was not entirely engaged with the locking rod notch face.
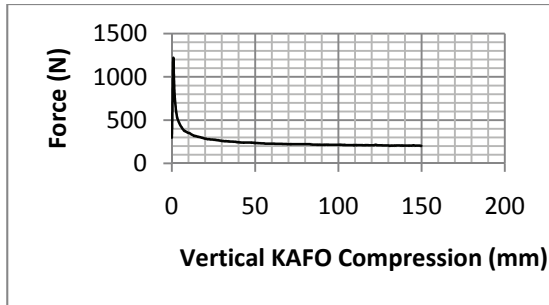
Figure 4.12: KEA loading response during joint flexion simulating stand-to-sit (1).
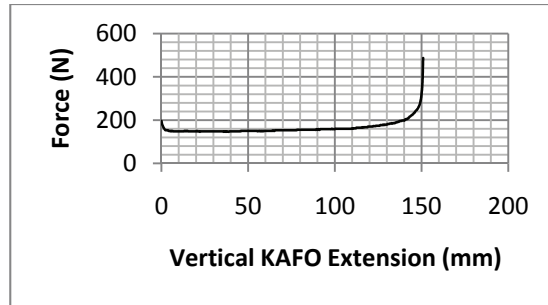


Figure 4.13: KEA extension-assist response during joint extension with the spring beam unlocked, simulating STS (4).
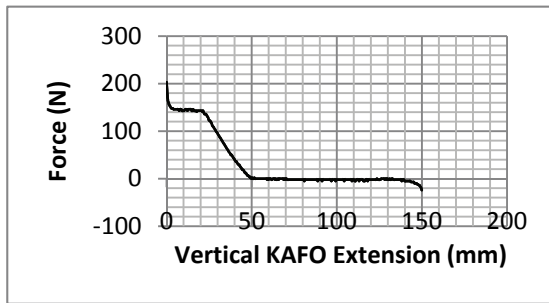


Figure 4.14: KEA extension with spring beam locked in place by the locking rod, simulating free knee extension (2).
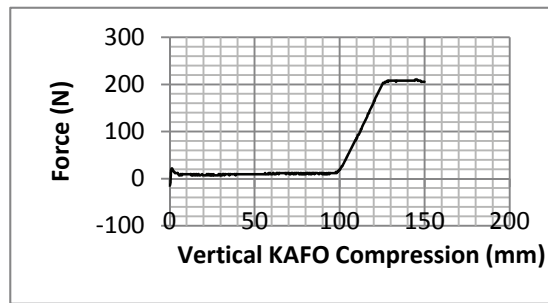


Figure 4.15: KEA flexion with spring beam locked simulating returning the knee to the flexed position (3).

# Chapter 5. Biomechanical Evaluation

To determine whether the extension-assist provided by the KEA to a user was beneficial for STS and ramp walking, an evaluation of the effects of the KEA on an individual during use was required. Tests were perfomed to determine whether the KEA effectively provided an extension moment to the knee to assist an individual during stand-to-sit, sit-to-stand, ramp ascent, and ramp descent. The tests also permitted verification of the proper functioning of the device when worn by a user and helped determine if modifications to the design for proper functioning were needed. The biomechanical evaluation was approved by The Ottawa Hospital Council of Research Ethics Board (COREB) and The University of Waterloo Office of Research Ethics (UWORE) Research Ethics Board (Appendix I).

## 5.1 KEA Preparation for Biomechanical Evaluation

The KEA prototype, KAFO uprights, and the single axis KAFO joint used in the mechanical evaluations were incorporated by a certified orthotist into an existing KAFO for use in biomechanical testing (Figure 5.1). The existing KAFO was meant for use on the right leg. The KAFO had a thermoplastic thigh cuff, shank cuff, and foot plate. The thigh and shank cuffs were connected by single-axis joints mounted on 19.0 mm x 4.8 cm x 6.3 cm (3/4 in x 3/16 in x, 1/4 in) hard 304-2B stainless steel KAFO uprights from Becker Orthotics, the same uprights used for the mechanical tests. The shank cuff and foot plate were connected by Tamarack articulating ankle joints to allow for dorsiflexion and plantarflexion, and resist ankle rotation in the transverse (inversion/eversion) and frontal (coronal) planes.

## 5.2 Purpose

The biomechanical evaluation conducted on the KEA was a proof-of-concept pilot study on able-bodied subjects. The goals of the biomechanical evaluation were to:

1. Determine the moment provided by the KEA during STS and ramp walking.

2. Determine the effect of the KEA on STS and ramp-walking kinematics.

3.  Determine whether the KEA allowed an able-bodied user to reduce quadriceps use for STS and ramp walking.

4.  Determine whether the KEA functioned properly during use for STS and ramp-walking tasks and if there were any design issues associated with the device being incorporated into a KAFO and worn by a user, and if any modifications to the design were required for proper functioning.



Figure 5.1: KEA prototype mounted on a preexisting right-leg KAFO for biomechanical trials.

## 5.3 Methods

Biomechanical evaluations on the KEA were carried out at The Gait and Motion Analysis (GAMA) Laboratory at The Ottawa Hospital Rehabilitation Centre (OHRC). Participants were requested to perform STS and stand-to-sit tasks as well as ramp walking upwards and

downwards using the KEA, and they were given time to practice the tasks with the KEA before the tests commenced. The participants were instructed to practice using quadriceps muscles as little as possible to complete the tasks. The purpose of the participant using as little quadriceps as possible was to show the difference in quadriceps muscle activation levels with and without the extension-assist. Two separate tests, each with two components, were conducted. The first test examined the effect of the KEA as participants performed the stand-to-sit and sit-to-stand tasks. The tasks were first executed while wearing the KAFO, but without assistance from the KEA. The movements were then repeated with assistance from the KEA. Ground reaction forces, body segment kinematics, and electromyographic signals from the rectus femoris, vastus medialis, biceps femoris, and gluteus maximus were recorded. The data gathered were used to determine the joint dynamics and muscle use for the above tasks performed with and without aid from the KEA. Effects of the device on stand-to-sit and sit-to-stand kinematics were also assessed. The second test examined the effect of the KEA on ramp gait. Participants performed ramp ascent and descent while wearing the KAFO, both tasks with and without assistance from the KEA. Body segment kinematics and rectus femoris, vastus medialis, biceps femoris, and gluteus maximus muscle activation levels were recorded to compare kinematics and muscle use in ramp ascent and descent between tasks performed with and without assistance from the KEA.

### 5.3.1 Participants

Participants were recruited from the students and staff of the University of Waterloo and the staff of the OHRC. A convenience sample of two able-bodied male participants (Table 5.1) was recruited for the pilot study. The two participants were selected based on leg size, length, and knee height, such that proper KAFO fit could be achieved with little to no modification.

Table 5.1: Relevant Participant Characteristics

| Participant | Sex | Weight (kg) | Height (cm) |
|-------------|-----|-------------|-------------|
| P1          | M   | 70          | 176         |
| P2          | M   | 64          | 168         |

## 5.3.2 Instrumentation, Equipment, and Measurements

Kinematic data from lower limb and trunk movement was recorded using a seven-camera, infra-red Vicon motion analysis system (MX3+). The Vicon system recorded data at 120 Hz. Thirty-nine reflective, 14 mm diameter, spherical markers were attached to the participant's feet, lower and upper legs, and torso (Figure 5.2). A six degree-of-freedom (6-DOF) marker set was used to track the participant's motion. Use of a 6-DOF marker set allowed for the tracking of each segment in three-dimensions, and thus resulted in a more accurate determination of segment kinematics and joint dynamics. Of the 39 markers, sixteen were used as calibration markers to denote the endpoints of segments. Calibration markers were only required during the standing calibration trials to determine segment lengths. The remaining markers acted as tracking markers and were worn during all trials, with sets of three or four markers used to define the position and orientation of each segment. A list of the anatomical locations of the markers can be found in Appendix J.
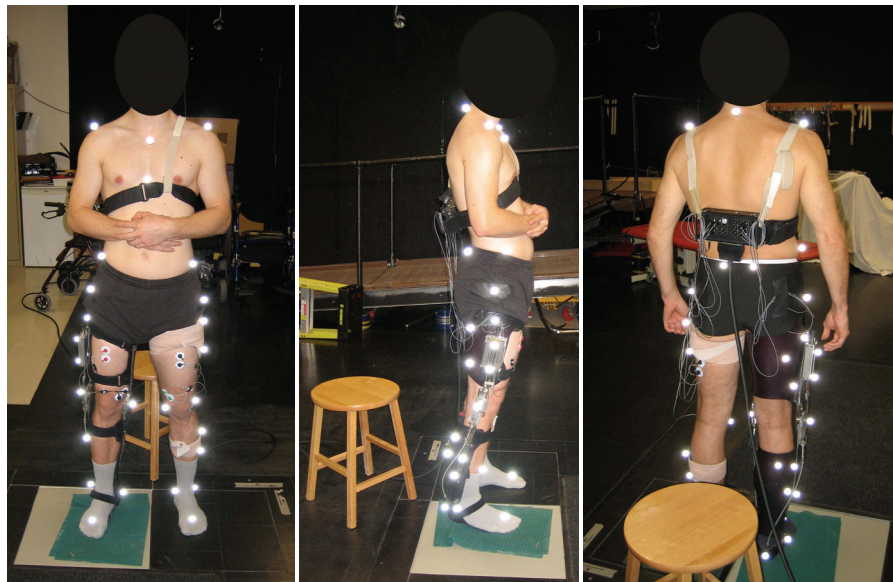


Figure 5.2: Participant equipped with motion capture markers and EMG equipment.

Two force-plate load cells (Advanced Mechanical Technologies Inc.), embedded side-by-side in the floor, were used to measure the overall force acting between each foot and the ground during the stand-to-sit and STS trials. The force plates obtained measurements with a

frequency of 120 Hz. The use of two force plates permitted ground reaction force from each foot to be measured, and therefore allowed joint moments to be calculated for each leg individually. However, the force plates were only utilized for STS trials, since the ramp was not outfitted with a recess in which to embed a force plate. For this reason, during ramp gait trials, only kinematics and muscle activation levels were examined.

Muscle activation levels were measured using surface electromyography (EMG), which measures the electrical impulses sent to the muscles. The strength of the signals recorded by the EMG electrodes relate to the level of muscle contraction. Electrodes were placed bilaterally on the quadriceps and buttocks, on the vastus medialis, rectus femoris, and gluteus maximus, three of the principal muscles involved in knee and hip extension [15], as well as on the left biceps femoris to monitor antagonistic contractions. The right biceps femoris could not be monitored, because the muscle was covered by the KAFO thigh cuff. The cuff would have contacted the EMG sensors and amplifier and cause the EMG readings to be inaccurate. The Surface Electromyography for the Non-Invasive Assessment of Muscles (SENIAM) electrode placement protocol [113] was followed. SENIAM is a European concerted action in the Biomedical Health and Research Program (BIOMED II) of the European Union. A single ground/reference electrode was placed on the fibular head to capture a base reading. All signals were recorded at a rate of 1000 Hz.

For the STS trials, a wooden stool was placed directly behind the force plates. The stool had no arms or backrest so as to not obscure the tracking markers during kinematic data collection. The seat and legs of the stool were thin to provide the least obstruction of the markers located on the heels and ankles from the rear camera views. The height of the stool, 46 cm, corresponded to a seated position with a knee angle of 90°. Figure 5.2 shows the experimental setup and a participant with motion tracking markers and EMG electrodes applied.

For the ramp walk trials, a 6 m long ramp inclined at an 8° angle was used (Figure 5.3). The top end of the ramp was connected to a 1.5 m long platform so that the ramp ascent trials could end comfortably on a level surface. Railings were provided on both sides of the ramp and platform, in case the participant were to stumble. The ramp was positioned in the

centre of the room during ramp walking tests to allow for all Vicon cameras to track the motion of the participant during the trials.


Figure 5.3: Ramp used for ramp gait trials.

### 5.3.3 Data Collection Procedure

5.3.3.1 Equipment Calibration

Before trials commenced for a given participant, there were several equipment calibration procedures that were followed. The Vicon cameras were first calibrated using a calibration tool in Vicon's Nexus software package. The program tracks the movement of a set of markers on a T-shaped wand as it is waved around the capture volume to determine the location of each camera relative to the others. The wand was then placed at the user-chosen origin of the capture volume to determine the spatial orientation of the cameras relative to the room. Finally, the force plate readings with no load applied were set to zero.

After all trials were completed (as detailed in the following subsection), EMG readings were taken for maximal voluntary contractions (MVC) of each of the four muscles involved in the trials. The MVC signals were later used to normalize the EMG signals recorded during the trials. The MVC tests consisted of an isometric contraction of a given muscle as forcefully as possible against infinite resistance. Maximal contractions were repeated three times for each muscle, and were held for three seconds each time. Patient positions during the MVC tests followed the SENIAM guidelines [113].

## 5.3.3.2 Stand-to-Sit and Sit-to-Stand

After camera calibration was completed, the stand-to-sit and sit-to-stand tests were conducted as follows:

- The participant stood in front of the stool, with arms crossed over the abdomen to minimize marker obstruction.

- Feet were positioned beside each other spaced comfortably apart in a natural standing postion, and with heels approximately in-line with each other, with each foot on a separate force plate and the stool placed at a comfortable distance behind the participant, as judged by the participant.

- The participant then sat down onto the stool. When equipped with the KAFO with the KEA deactivated, the participant was instructed to sit at a self-selected speed. When the KEA was active, the instruction was to sit with minimal quadriceps muscle usage, to allow the device to do as much work as possible while still completing the task successfully. A trial was completed when the participant was fully seated with a vertical torso, with the KEA spring beam locked in position.

- The participant could then move around and adjust their seated position, as desired. Before commencing the sit-to-stand trial, the participant was instructed to return the feet to a similar position as when stand-to-sit ended, if they had shifted, and to transfer a portion of their bodyweight onto the feet, in preparation for the sit-to-stand task.

- The participant then rose from the chair until standing upright, arms crossed over abdomen to minimize marker obstruction. Again, when rising with the KEA deactivated, the participant was instructed to perform sit-to-stand at a self-selected speed. When the KEA was active, the instruction was to unlock the spring beam by pulling on the locking rod and to rise with minimal quadriceps usage, to allow the device to provide as much of the joint extension moment as possible, while still

121

completing the task successfully. A trial was completed when the participant was standing fully erect.

- This process was repeated until a total of 20 successful trials were recorded for the STS test. Five successful trials were recorded for each case: with and without the device active, for stand-to-sit and sit-to-stand. Subjects rested as needed between trials. A successful trial was one in which the individual was able to transition from standing to seated or seated to standing in one motion, without assistance from the examiner, with both feet remaining in constant contact with the force plate, without the feet moving or slipping.

### 5.3.3.3 Ramp Ascent and Descent

For the ramp ascent and descent tests, the ramp was moved into the middle of the testing area, after completion of the stand-to-sit and sit-to-stand tests. The cameras were re-oriented and re-calibrated to provide a taller capture volume so that the system could track the markers when the participant was on the higher portion of the ramp. The participant was then asked to apply the ramp mode preload to the KEA by rotating the locking rod into the ramp mode position and flexing the knees until the locking rod engaged with the spring beam. The ramp gait test was then conducted, according to the following protocol:

- The participant began the test standing still, at the bottom of the ramp.

- The participant ascended to the top of the ramp onto the platform and stopped, thus ending the ramp ascent trial.

- The participant then completed a ramp descent trial by descending the ramp and stopping when the foot of the ramp was reached.

- For trials with the KEA deactivated, participants were instructed to ascend or descend the ramp at a self-selected pace. For trials with the KEA active, the participant was instructed to ascend the ramp with minimal quadriceps usage, to allow the device to provide as much of the required moment as possible, while still completing the task

122

successfully. The participant was also instructed to use a hand-bladder to actuate the pneumatic actuator to engage and disengage the knee disk during gait.

- Trials were continued until five successful trials were recorded for each condition: ascent and descent, with and without assistance from the device. Subjects were allowed to rest as needed. A successful trial was one in which the individual was able to ascend to the top platform or descend to the foot of the ramp without stopping and without assistance from the examiner.

## 5.3.4 Data Processing

The marker position, ground-reaction force, and EMG data captured during testing were first post-processed using the Vicon Nexus software package. A model of the participants was created and the markers positions captured in the trial video sequences were mapped to the model. Timing events were manually labelled to indicate when STS, stand-to-sit, or ramp gait stance phase for the braced right leg began and ended. The processed data from the five successful trials for each test condition (STS, stand-to-sit, ramp ascent, and ramp descent, each performed with and without the KEA activated) were then exported to Visual3D, a modeling software program for kinematic and dynamic analysis of human movement. Visual3D was used to calculate joint angles, joint angular velocities, and joint moments from the marker position and ground-reaction force data. The data were then normalized to 100 % of the STS, stand-to-sit, or ramp stance-phase time to allow for comparison between trials and subjects of parameters as a function of percent gait cycle. Data from Visual3D were then exported to Microsoft (MS) Excel for analysis.

Raw EMG signal data from the trials and the MVC tests were exported to MS Excel, where the signals were rectified, then smoothed using a moving average with a 50 ms window size.

## 5.3.5 Data Analysis

In MS Excel, the normalized data were ensemble averaged across the five trials for each test condition of each subject. Average ankle angle, knee angle, hip angle, ankle angular velocity,

knee angular velocity, and hip angular velocity were plotted for each test condition, as was ankle moment, knee moment, and hip moment for the STS and stand-to-sit test conditions. Critical points along these curves were subsequently determined. Critical points were points at which a relevant event occurred or an important piece of information could be extracted. For example, initial and final angles, maximum flexion or extension angular velocities, and maximum moments were often chosen as critical points. The critical points chosen for each test condition are listed and described in Table 5.2. Figure 5.4a and Figure 5.4b contains representative averaged curves for STS and stand-to-sit, and ramp gait, respectively, in order to show the locations of the critical points. Critical point values were extracted from the individual trials and subsequently averaged across the trials from the same test condition for each participant (P1 and P2).

The extension-assist moment provided by the KEA was interpolated from the moment versus angle data derived from the mechanical testing, using the knee angle curves calculated in Visual3D for trials that used the extension-assist. When the knee underwent flexion, the loading response test results were used (Section 4.2.3), while the extension-assist response test results (Section 4.3.3) were used when the knee underwent extension. Thus, extension-assist moment vs. normalized task time data were created for all trials that involved KEA use (Appendix L). The important values from the device moment curves are presented with the kinematic and dynamic critical points in the following section. For stand-to-sit and STS, device moment at the start and end of the motion are reported as SDM1 and SDM2, respectively. For ramp gait, the initial moment when the preload knee angle is reached is presented as RDM1, the maximum resistive moment during knee flexion as RDM2, the maximum assistive moment during knee extension as RDM3, and the final moment as RDM4.

For evaluation of the EMG data, the maximum single peak, the mean value, and the integral (the area under the EMG curve, which takes task duration into account) were calculated in MS Excel from the smoothed EMG signals.

124

Table 5.2: Critical points for STS and stand-to-sit, and ramp ascent and descent test curves

| STS and Stand-to-Sit Test Critical Points | |
|---|---|
| **Point** | **Description** |
| SAA1 | Initial ankle angle |
| SAA2 | Maximum dorsiflexion angle |
| SAA3 | Final ankle angle |
| SKA1 | Initial knee angle |
| SKA2 | Final knee angle |
| SHA1 | Initial hip angle |
| SHA2 | Maximum hip flexion angle |
| SHA3 | Final hip angle |
| SAAV1 | Maximum ankle dorsiflexion angular velocity (AV) |
| SAAV2 | Maximum ankle plantarflexion AV |
| SKAV1 | Maximum knee flexion AV during stand-to-sit |
| SKAV2 | Maximum knee extension AV during STS |
| SHAV1 | Maximum hip flexion AV |
| SHAV2 | Maximum hip extension AV |
| SAM1 | Maximum ankle plantarflexion moment |
| SKM1 | Maximum knee extension moment |
| SHM1 | Maximum hip extension moment |
| **Ramp Ascent and Descent Test Critical Points** | |
| **Point** | **Description** |
| RAA1 | Ankle angle at start of stance |
| RAA2 | Ankle angle at end of stance |
| RKA1 | Knee angle at start of stance (ascent only) |
| RKA2 | Knee angle after weight acceptance |
| RKA3 | Maximum knee extension angle after weight acceptance (ascent only) |
| RKA4 | Final knee angle |
| RHA1 | Hip angle at start of stance |
| RHA2 | Hip angle at end of stance |
| RAAV1 | Maximum ankle dorsiflexion AV |
| RKAV1 | Knee flexion AV during initial flexion |
| RKAV2 | Knee AV during subsequent knee extension (ascent only) |
| RKAV3 | Maximum pre-swing knee flexion AV |
| RHAV1 | Maximum hip extension AV |
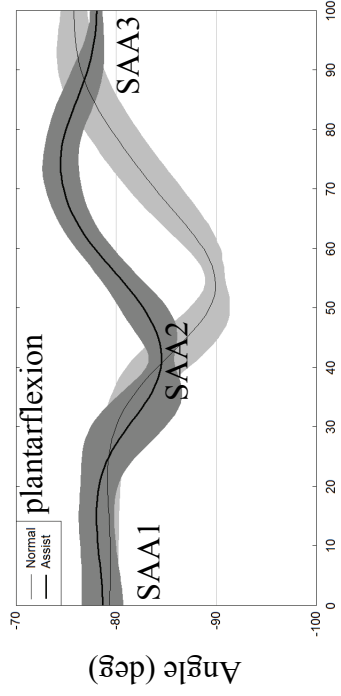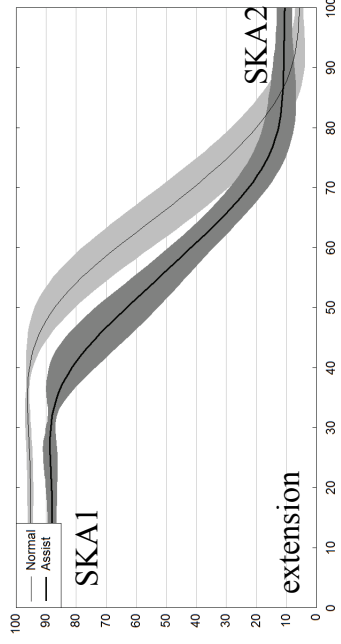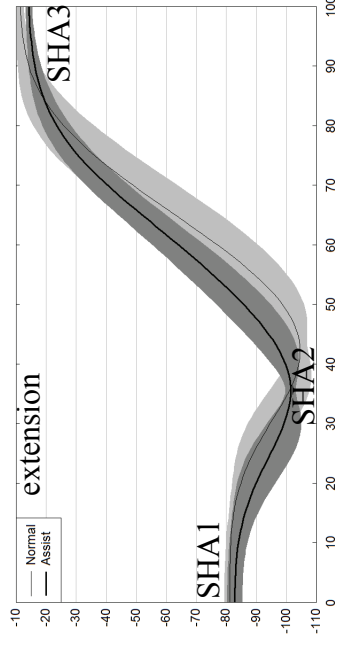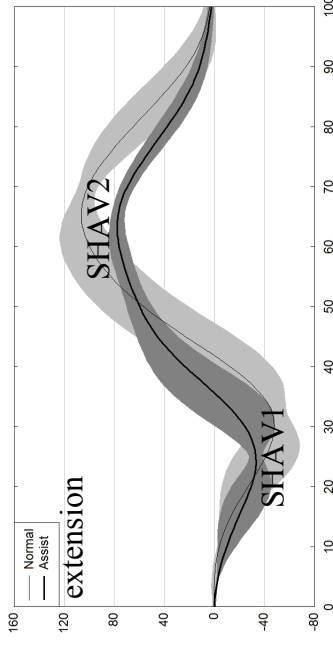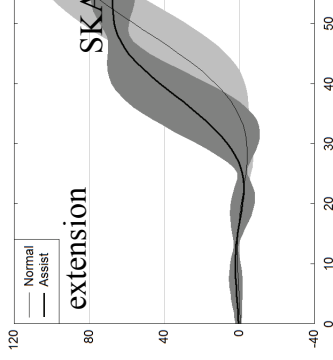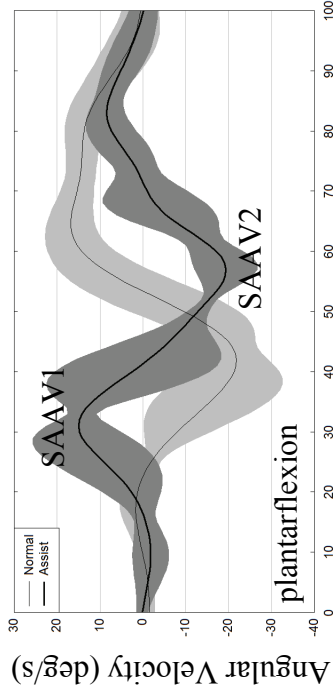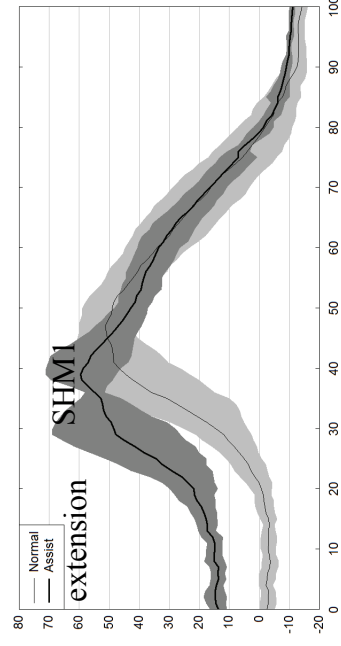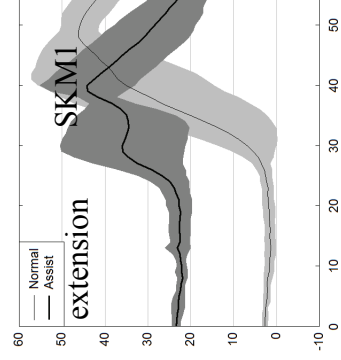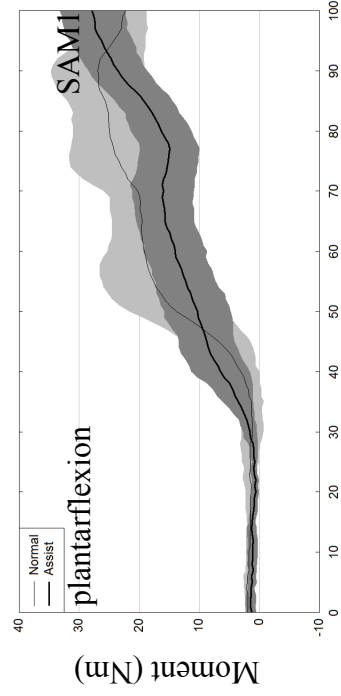
Figure 5.4a: Representative joint angle, angular velocity, and moment graphs with critical points labeled. Curves shown are from P1 STS trials.

126
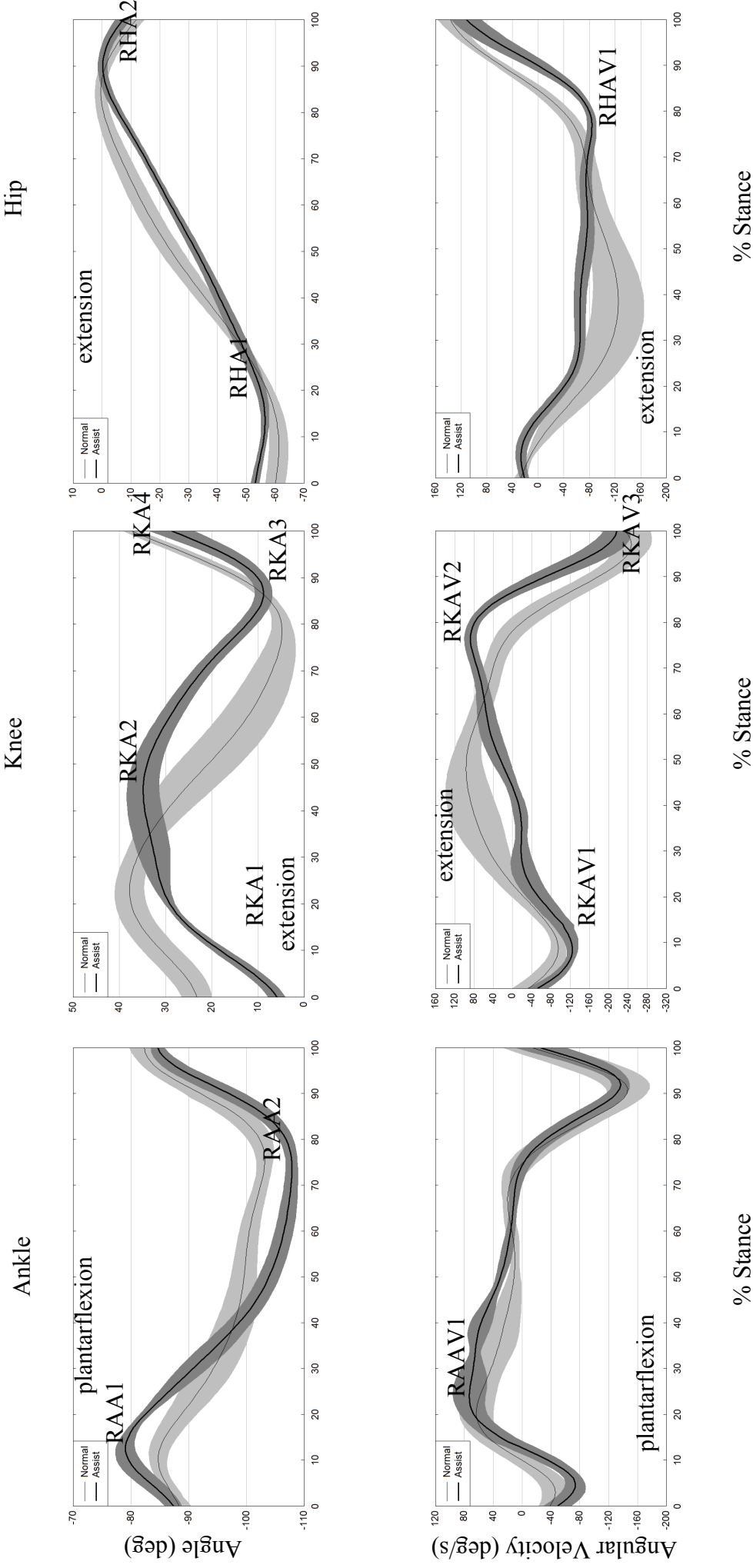
Figure 5.4b: Representative joint angle and angular velocity graphs with critical points labeled for ramp gait. Curves shown are from P1 ramp ascent trials.

127

## 5.4 Results

Biomechanical test results are presented in this section in tabular form to highlight the differences in kinematics, dynamics, and muscle activation caused by KEA use. Graphs of the kinematic and dynamic data from both participants are presented in Appendix K. Curves of the moments generated by the device can be found in Appendix L. EMG parameter values for the different test conditions expressed as a percent of maximal voluntary contraction appear in Appendix M.

### 5.4.1 Stand-to-Sit and STS

Table 5.3 presents the critical point values of both participants (P1 and P2) for stand-to-sit and STS with right-leg KEA assistance (assist) and without KEA assistance (normal), as well as the moment provided by the KEA. Table 5.4 presents the percent difference between the EMG parameter values for normal task completion and for completion with the extension-assist.

The extension-assist provided by the KEA allowed the participants to perform both stand-to-sit and STS in a slower and more controlled manner, while maintaining similar joint angles. Participant 1 (P1) was able to reduce hip and knee angular velocities by an average of 21 % as a result of the extension-assist. Maximum knee angular velocity (SKAV2 and SKAV1) for P1 was 26.2 and 10.5 deg/s slower, while maximum hip angular velocity (SHAV2 and SHAV1) was 33.3 and 27 deg/s slower, for STS and stand-to-sit, respectively, with KEA use.

Maximum knee moments (SKM1) of the right leg varied little for P1 between the normal and assisted trials, with a 7 % increase to 55 Nm for stand-to-sit and a 1 % decrease to 50.5 Nm for STS due to the extension-assist. These values were compared to the extension-assist moment values from the knee angle versus extension-assist moment curves (Appendix L) to determine the amount of assistance provided by the KEA. For stand-to-sit, the KEA provided a maximum extension moment (SDM2) of 45.5 Nm. Therefore, the KEA provided 82 % of the 55 Nm right knee moment (SKM1 Right), or 36 % of the 125.5 Nm total knee moment

(SKM1 Right + Left, 55.2 + 70.3 Nm). For STS, the KEA was able to provide a maximum assistance (SDM1) of 28.5 Nm, 56 % of the 50.5 Nm moment required by the right knee (SKM1 Right) and 22 % of the 129.4 Nm total knee moment (SKM1 Right + Left, 50.5 + 78.9 Nm).

The effect of the extension-assist on the quadriceps of P1 can be seen in the EMG parameters. The average of the maximum, mean, and integral EMG parameters of the right quadriceps (vastus medialis and rectus femoris) was calculated to determine the effect of the extension-assist on the right quadriceps. KEA use caused a decrease in quadriceps muscle activation levels of 38 % in the right leg, while the average of the left quadriceps muscle activation parameters was nearly equal with and without the assist. The average of the left quadriceps EMG parameters increased only 3 % with KEA use.

For P2, the effect of the extension-assist was more immediately visible than for P1. P2 had difficulty in successfully completing STS without the extension-assist, and was forced to generate extra momentum through a ballistic forward and upward arm movement, involving an upward swing of the arms that were folded across the chest, in order to rise successfully without the extension-assist. Even with the additional momentum from the arms, P2 still had difficulty rising, with six trials discarded due to unsuccessful STS attempts. With the KEA active, P2 was able to rise in a slow and controlled manner, without arm movement, and with no unsuccessful attempts.

Table 5.3: Critical point values for stand-to-sit and STS tests. Note: angles are presented in (deg), angular velocities in (deg/s), and moments in (Nm).

**P1**

| | RIGHT (with KAFO) | | | | | | | | LEFT (without KAFO) | | | | | | | |
|---|---|---|---|---|---|---|---|---|---|---|---|---|---|---|---|---|
| | Stand-to-sit assist | | Stand-to-sit normal | | STS assist | | STS normal | | Stand-to-sit assist | | Stand-to-sit normal | | STS assist | | STS normal | |
| P1 | avg | SD | avg | SD | avg | SD | avg | SD | avg | SD | avg | SD | avg | SD | avg | SD |
| SAA1 | -76.0 | 1.3 | -75.9 | 1.7 | -78.7 | 2.1 | -79.3 | 0.8 | -76.6 | 0.5 | -76.1 | 1.9 | -86.1 | 2.7 | -80.7 | 1.6 |
| SAA2 | -85.6 | 1.5 | -86.1 | 1.5 | -85.7 | 0.6 | -90.6 | 0.7 | -92.5 | 0.6 | -90.9 | 1.1 | -92.8 | 0.7 | -92.2 | 0.5 |
| SAA3 | -78.5 | 1.4 | -79.3 | 1.1 | -78.0 | 0.6 | -75.8 | 1.3 | -85.0 | 2.0 | -81.2 | 2.1 | -79.5 | 0.7 | -76.3 | 1.7 |
| SKA1 | 11.4 | 4.2 | 5.7 | 0.6 | 88.6 | 2.1 | 95.4 | 0.8 | 12.6 | 0.8 | 6.9 | 1.8 | 87.8 | 1.1 | 84.9 | 1.5 |
| SKA2 | 89.1 | 1.1 | 95.3 | 0.9 | 10.6 | 2.5 | 5.7 | 1.3 | 85.4 | 1.7 | 83.3 | 1.6 | 11.6 | 0.9 | 6.6 | 2.1 |
| SHA1 | -18.6 | 3.5 | -12.8 | 1.9 | -82.8 | 2.6 | -81.2 | 1.9 | -19.7 | 1.0 | -13.5 | 1.5 | -74.8 | 3.2 | -68.8 | 1.9 |
| SHA2 | -102.9 | 2.4 | -105.6 | 0.9 | -103.7 | 2.2 | -107.1 | 1.2 | -87.0 | 1.2 | -87.6 | 0.5 | -89.8 | 1.1 | -89.2 | 0.9 |
| SHA3 | -80.8 | 3.6 | -80.1 | 2.3 | -14.2 | 1.1 | -11.4 | 1.1 | -70.8 | 2.0 | -66.1 | 1.7 | -14.4 | 0.4 | -12.2 | 1.3 |
| SAAV1 | 21.8 | 3.3 | 16.5 | 6.4 | 21.5 | 6.8 | 28.2 | 3.1 | 26.2 | 7.0 | 23.8 | 7.4 | 9.3 | 4.9 | 18.3 | 1.0 |
| SAAV2 | -16.1 | 5.5 | -12.7 | 3.3 | -20.9 | 5.7 | -20.6 | 3.4 | -12.6 | 8.2 | -19.6 | 4.7 | -16.6 | 3.6 | -16.5 | 2.8 |
| SKAV1 | -81.2 | 7.2 | -91.7 | 10.4 | -- | -- | -- | -- | -65.6 | 5.1 | -78.7 | 11.9 | -- | -- | -- | -- |
| SKAV2 | -- | -- | -- | -- | 73.5 | 7.4 | 99.7 | 6.2 | -- | -- | -- | -- | 62.9 | 6.8 | 89.0 | 5.0 |
| SHAV1 | 92.4 | 12.8 | 119.4 | 12.0 | 45.3 | 5.4 | 60.7 | 6.5 | 75.6 | 10.2 | 98.1 | 8.2 | 28.8 | 3.6 | 38.4 | 5.9 |
| SHAV2 | -46.3 | 4.8 | -52.0 | 7.7 | -78.9 | 5.3 | -112.2 | 7.1 | -32.7 | 4.8 | -49.1 | 3.4 | -69.6 | 4.8 | -102.0 | 6.0 |
| SAM1 | 14.5 | 4.5 | 27.3 | 8.8 | 28.0 | 5.4 | 31.1 | 7.3 | 23.2 | 7.4 | 30.9 | 6.2 | 34.1 | 5.9 | 29.8 | 4.0 |
| SKM1 | 55.2 | 2.9 | 51.5 | 3.1 | 50.5 | 5.7 | 51.1 | 3.6 | 70.3 | 4.9 | 69.5 | 2.1 | 78.9 | 3.4 | 85.4 | 4.8 |
| SHM1 | 65.9 | 6.1 | 53.5 | 3.3 | 67.6 | 5.3 | 60.4 | 5.5 | 45.5 | 4.9 | 62.5 | 4.0 | 49.4 | 3.8 | 64.8 | 3.6 |
| SDM1 | 26.4 | 3.7 | -- | -- | 28.5 | 0.6 | -- | -- | -- | -- | -- | -- | -- | -- | -- | -- |
| SDM2 | 45.5 | 1.3 | -- | -- | 7.9 | 0.7 | -- | -- | -- | -- | -- | -- | -- | -- | -- | -- |

**P2**

| | RIGHT (with KAFO) | | | | | | | | LEFT (without KAFO) | | | | | | | |
|---|---|---|---|---|---|---|---|---|---|---|---|---|---|---|---|---|
| | Stand-to-sit assist | | Stand-to-sit normal | | STS assist | | STS normal | | Stand-to-sit assist | | Stand-to-sit normal | | STS assist | | STS normal | |
| P2 | avg | SD | avg | SD | avg | SD | avg | SD | avg | SD | avg | SD | avg | SD | avg | SD |
| SAA1 | -75.8 | 1.3 | -73.9 | 0.9 | -76.3 | 2.1 | -73.6 | 2.5 | -71.4 | 2.1 | -70.8 | 1.9 | -75.7 | 1.5 | -68.1 | 1.8 |
| SAA2 | -87.5 | 1.2 | -92.3 | 1.7 | -89.6 | 1.0 | -89.1 | 3.0 | -89.5 | 1.8 | -89.8 | 2.0 | -96.1 | 0.6 | -93.1 | 1.7 |
| SAA3 | -77.0 | 1.9 | -77.1 | 1.1 | -74.9 | 1.4 | -74.3 | 2.2 | -76.0 | 1.8 | -69.7 | 2.1 | -71.0 | 0.5 | -70.1 | 1.5 |
| SKA1 | 9.2 | 1.5 | 5.2 | 3.2 | 87.8 | 1.7 | 92.7 | 2.4 | 5.8 | 4.1 | 4.4 | 3.3 | 86.5 | 1.4 | 79.7 | 1.9 |
| SKA2 | 88.3 | 2.5 | 95.0 | 1.3 | 7.3 | 2.2 | 4.1 | 1.1 | 86.5 | 1.6 | 81.9 | 2.1 | 3.3 | 1.0 | 2.4 | 1.1 |
| SHA1 | -11.2 | 2.3 | -8.4 | 2.5 | -77.9 | 1.2 | -80.9 | 2.0 | -12.0 | 1.8 | -10.1 | 1.8 | -76.9 | 1.2 | -73.1 | 1.4 |
| SHA2 | -100.7 | 2.1 | -107.0 | 1.8 | -97.1 | 2.1 | -105.3 | 2.1 | -94.0 | 1.5 | -98.2 | 1.8 | -89.8 | 1.6 | -95.7 | 2.2 |
| SHA3 | -79.6 | 2.1 | -76.7 | 4.3 | -8.2 | 2.6 | -6.7 | 2.7 | -78.4 | 1.8 | -70.8 | 3.4 | -7.4 | 2.0 | -7.6 | 1.9 |
| SAAV1 | 15.6 | 2.9 | 21.6 | 2.2 | 19.9 | 5.3 | 32.6 | 5.1 | 13.3 | 2.7 | 12.2 | 2.4 | 17.0 | 4.7 | 25.5 | 2.0 |
| SAAV2 | -16.1 | 2.4 | -20.5 | 5.1 | -14.4 | 8.4 | -23.0 | 7.6 | -16.6 | 3.2 | -19.5 | 5.1 | -12.1 | 8.6 | -12.2 | 3.1 |
| SKAV1 | -66.4 | 6.2 | -71.8 | 10.4 | -- | -- | -- | -- | -52.5 | 4.1 | -60.2 | 8.1 | -- | -- | -- | -- |
| SKAV2 | -- | -- | -- | -- | 44.0 | 15.5 | 77.9 | 14.2 | -- | -- | -- | -- | 38.2 | 8.6 | 68.6 | 13.0 |
| SHAV1 | 77.4 | 7.7 | 81.1 | 12.1 | 40.4 | 5.9 | 47.1 | 4.3 | 68.0 | 6.6 | 75.3 | 11.9 | 24.0 | 1.8 | 41.8 | 2.7 |
| SHAV2 | -40.2 | 6.5 | -39.3 | 5.3 | -49.2 | 20.9 | -82.6 | 12.3 | -27.5 | 6.8 | -34.6 | 5.8 | -42.1 | 17.4 | -78.0 | 12.0 |
| SAM1 | 23.1 | 2.7 | 20.2 | 6.1 | 17.9 | 1.1 | 23.4 | 2.8 | 10.0 | 2.5 | 10.8 | 4.7 | 14.0 | 6.7 | 18.8 | 4.6 |
| SKM1 | 60.0 | 5.8 | 68.3 | 7.8 | 57.1 | 4.0 | 63.5 | 13.2 | 52.1 | 5.9 | 52.0 | 5.0 | 76.2 | 8.1 | 74.1 | 9.6 |
| SHM1 | 78.4 | 10.8 | 67.5 | 6.6 | 75.5 | 4.2 | 59.0 | 6.1 | 37.1 | 4.6 | 42.7 | 8.5 | 32.1 | 3.3 | 51.4 | 6.1 |
| SDM1 | 21.5 | 8.2 | -- | -- | 28.3 | 0.4 | -- | -- | -- | -- | -- | -- | -- | -- | -- | -- |
| SDM2 | 44.9 | 2.2 | -- | -- | 7.0 | 0.6 | -- | -- | -- | -- | -- | -- | -- | -- | -- | -- |

Table 5.4: Percent difference between normal task completion and completion with extension-assist for STS and stand-to-sit tasks . Negative values indicate a reduction in muscle activation with KEA use.

| | RIGHT (with KAFO) | | | LEFT (without KAFO) | | | |
|---|---|---|---|---|---|---|---|
| | Vastus medialis | Rectus femoris | Gluteus maximus | Vastus medialis | Rectus femoris | Gluteus maximus | Biceps femoris |
| **P1 STS** | | | | | | | |
| Maximum | -27.6 | -24.0 | 36.1 | -12.5 | -11.3 | -8.6 | -15.8 |
| Mean | -49.3 | -42.9 | 37.7 | 1.3 | -6.2 | 8.0 | 13.6 |
| Integral | -41.0 | -34.0 | 59.4 | 17.5 | 8.4 | 25.6 | 32.9 |
| **P2 STS** | | | | | | | |
| Maximum | 29.8 | 27.9 | 27.4 | 30.2 | 66.2 | -34.5 | 31.1 |
| Mean | 19.1 | 22.4 | -5.5 | 45.5 | 48.3 | -7.2 | 0.0 |
| Integral | 92.0 | 93.1 | 50.4 | 134.8 | 138.7 | 49.5 | 60.1 |
| **P1 Stand-to-sit** | | | | | | | |
| Maximum | -3.7 | -55.6 | 49.3 | 1.6 | -7.7 | -28.5 | -9.3 |
| Mean | -41.0 | -45.8 | 13.0 | 11.6 | 13.7 | -6.5 | 6.2 |
| Integral | -40.9 | -45.6 | 13.1 | 11.1 | 12.4 | -6.2 | 6.5 |
| **P2 Stand-to-sit** | | | | | | | |
| Maximum | -32.0 | -41.9 | -35.2 | 19.7 | 6.4 | -8.9 | 10.6 |
| Mean | -12.1 | -25.3 | 47.3 | 69.6 | 48.0 | 162.0 | 81.8 |
| Integral | -16.7 | -29.7 | 39.9 | 60.3 | 40.2 | 146.6 | 71.3 |

As was the case with P1, P2 had similar joint angles for stand-to-sit and STS with and without KEA use. Angular velocities also decreased with KEA use for P2, as they had for P1. Stand-to-sit was only slightly slower with the assist than without, but STS knee and hip angular velocities (SKAV2 and SHAV2) were 44 and 40 % slower, respectively. The large reduction of angular velocities was expected because of the change in STS strategy.

The knee moments (SKM1) for P2 with the device were reduced by 12 % to 60.0 Nm for stand-to-sit and 10 % to 57.1 Nm for STS. The KEA provided 44.9 Nm of the knee extension moment (resistance to knee flexion) during stand-to-sit (SDM2), corresponding to 75 % of the 60.0 Nm right knee moment (SKM1 Right) and 40 % of 112.1 Nm total knee moment (SKM1 Right + Left, 60.0 + 72.1 Nm). A maximum extension-assist (SDM1) by the KEA of 28.3 Nm was supplied for STS, providing 50 % of the required 57.1 Nm extension moment for the right knee (SKM1 Right), and 21 % of the 133.3 Nm total knee moment (SKM1 Right + Left, 57.1 + 76.2 Nm).

EMG results for P2 did not show the same reductions as for P1. KEA use only caused a reduction in the average of the maximum, mean and integral EMG parameters of the right

quadriceps (rectus femoris and vastus medialis) for stand-to-sit, by 26 %. Nearly all other parameters were seen to increase, including an increase of the average of the maximum, mean, and integral EMG parameters during stand-to-sit of 41 % for the left quadriceps and 100 % for the left gluteus maximus. The increase in activation levels were likely caused by the change in sit-to-stand task completion strategy, slower task completion with the extension-assist, and the participant not being completely at ease with device use. Causes for the increases seen are presented more fully in Chapter 6.

### 5.4.2 Ramp Ascent and Descent

Table 5.5 presents the critical point values for participants P1 and P2 for the ramp ascent and ramp descent tests with the KEA (assist) and without the KEA (normal), as well as the moments supplied by the KEA to the right knee at key instances. Table 5.6 presents the percent difference between EMG parameter values for normal and assisted task completion for ramp walking.

Ankle and hip angles and velocities were found to be similar for trials with and without the device for both ramp ascent and descent. However, KEA use considerably altered knee joint kinematics. At the initiation of ramp ascent stance, P1 and P2 both adopted nearly fully extended knee angles (RKA1), 5.9° and 6.8°, respectively, to ensure engagement of the sliding lock with the knee disk. During the trials without the extension-assist, P1 and P2 initiated stance with 23.2° and 41° knee angles. However, it should be noted that the 41° knee angle for P2 is abnormally high, recalling from Figure 3.3 regarding ramp ascent kinematics that the average starting knee angle for 8° ramp ascent is approximately 20°. Though the starting knee angles were much lower with the extension-assist, the maximum flexion angles (RKA2) during ramp ascent with and without the assist were similar; 35.1° and 38.2°, and 45.8° and 50.2° for P1 and P2, respectively. Therefore, the KEA required the leg to rotate through a much larger knee flexion range while weight-bearing during ramp ascent than occurred without the extension-assist. Accompanying the increased range of knee flexion caused by KEA use was an increase in knee flexion angular velocity due to KEA use of 29 % for P1 and 92 % for P2 as the knee flexed rapidly until the preload angle was passed

and the springs provided resistance to further flexion. There was also a slight change in the shape of the knee angle curve for both participants as a result of the extension-assist, as can

Table 5.5: Critical point values for ramp gait tests. Note: angles are presented in (deg), angular velocities in (deg/s), and moments in (Nm).

| P1 | Ascent assist | | Ascent normal | | Descent assist | | Descent normal | |
|---|---|---|---|---|---|---|---|---|
| | avg | SD | avg | SD | avg | SD | avg | SD |
| RAA1 | -78.8 | 1.8 | -84.5 | 1.5 | -72.8 | 2.2 | -72.3 | 1.5 |
| RAA2 | -108.1 | 1.1 | -103.4 | 1.4 | -106.5 | 1.6 | -103.5 | 0.7 |
| RKA1 | 5.9 | 1.9 | 23.2 | 6.6 | -- | -- | -- | -- |
| RKA2 | 35.1 | 3.4 | 38.2 | 5.4 | 32.5 | 2.2 | 29.8 | 3.7 |
| RKA3 | 8.5 | 1.9 | 4.4 | 2.6 | -- | -- | -- | -- |
| RKA4 | 28.7 | 4.9 | 37.4 | 1.7 | 33.5 | 2.9 | 63.2 | 3.2 |
| RHA1 | -56.6 | 1.3 | -61.3 | 3.4 | -33.0 | 1.6 | -31.6 | 2.0 |
| RHA2 | 0.0 | 1.6 | 0.5 | 2.0 | 0.8 | 1.8 | -5.8 | 2.1 |
| RAAV1 | -84.6 | 15.0 | -72.9 | 16.5 | -78.5 | 12.4 | -84.4 | 8.4 |
| RKAV1 | -127.7 | 11.6 | -98.8 | 15.9 | -156.8 | -20.0 | -153.7 | 22.3 |
| RKAV2 | 89.6 | 11.2 | 104.4 | 37.4 | -- | -- | -- | -- |
| RKAV3 | -217.9 | 28.1 | -248.9 | 41.9 | -23.2 | -15.3 | -235.6 | 26.4 |
| RHAV1 | 86.9 | 8.3 | 126.4 | 40.2 | 70.1 | 8.8 | 66.2 | 5.1 |
| RDM1 | 20.5 | 0.5 | -- | -- | 20.3 | 0.8 | -- | -- |
| RDM2 | 24.3 | 1.2 | -- | -- | -- | -- | -- | -- |
| RDM3 | 14.3 | 0.9 | -- | -- | -- | -- | -- | -- |
| RDM4 | 11.1 | 0.6 | -- | -- | 23.9 | 1.0 | -- | -- |
| **P2** | | | | | | | | |
| RAA1 | -80.4 | 2.9 | -90.7 | 1.8 | -70.4 | 1.3 | -76.4 | 0.8 |
| RAA2 | -119.5 | 2.3 | -104.8 | 1.5 | -106.9 | 4.5 | -106.9 | 1.9 |
| RKA1 | 6.8 | 3.6 | 41.0 | 4.2 | -- | -- | -- | -- |
| RKA2 | 45.8 | 2.6 | 50.2 | 2.7 | 40.5 | 4.0 | 34.0 | 2.2 |
| RKA3 | 23.6 | 4.6 | 8.2 | 2.2 | -- | -- | -- | -- |
| RKA4 | 26.6 | 1.8 | 36.4 | 4.5 | 45.5 | 2.1 | 55.7 | 4.4 |
| RHA1 | -60.9 | 2.9 | -63.0 | 1.5 | -34.0 | 2.4 | -29.1 | 4.5 |
| RHA2 | -3.0 | 2.4 | 5.0 | 1.5 | -2.1 | 2.5 | 7.9 | 3.7 |
| RAAV1 | -95.6 | 11.8 | -98.5 | 12.8 | -97.0 | 14.3 | -108.9 | 19.9 |
| RKAV1 | -153.6 | 18.0 | -80.0 | 14.8 | -162.4 | -18.3 | -185.9 | -33.3 |
| RKAV2 | 134.7 | 19.3 | 116.6 | 7.8 | -- | -- | -- | -- |
| RKAV3 | -52.3 | 29.8 | -258.6 | 23.0 | -73.0 | -34.1 | -211.9 | -34.6 |
| RHAV1 | 107.7 | 11.9 | 134.6 | 9.1 | 78.9 | 20.2 | 96.4 | 16.4 |
| RDM1 | 23.5 | 0.8 | -- | -- | 20.4 | 0.7 | -- | -- |
| RDM2 | 26.6 | 1.5 | -- | -- | -- | -- | -- | -- |
| RDM3 | 16.2 | 1.1 | -- | -- | -- | -- | -- | -- |
| RDM4 | 12.8 | 1.8 | -- | -- | 27.9 | 0.9 | -- | -- |

be seen in Figure 5.5. Instead of knee flexion occurring for the first quarter of stance, as it did in the normal trials, it occurred for the first half of stance for P1, and the first three-quarters for P2. This was, in part, a result of the larger knee flexion range as explained above. It was also due to the reduction of the rate of knee flexion caused by the springs as the preload angle was passed and the springs began to compress further. The rate change was seen as a change of slope in the knee angle graphs at approximately 20 % stance time. P2 maintained a flexed knee through to the end of stance while using the KEA, with RKA3 and RKA4 values of 23.6° and 26.6°, approximately the angle at which the springs begin to provide an extension moment. In normal trials, P2 extended the knee to 8.2° by the end of stance (RKA3) before flexing again in preparation for swing.
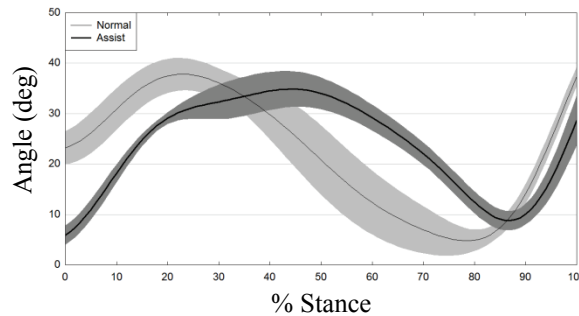


Figure 5.5: Ramp ascent knee angle with and without assistance for P1.

During ramp ascent, the device was able to provide a maximum extension moment (RDM2) of 24.3 Nm for P1 and 26.6 Nm for P2. The KEA provided a maximum extension-assist moment (RDM3) of 14.3 Nm for P1 and 16.2 Nm for P2, which corresponds to 32 % and 36 % of the required extension moment as expressed in the literature [37]. These levels fall short of the 47 % ramp ascent assistance that the KEA was designed to supply.

Because of the low extension moments provided by the KEA, and the larger knee angle flexion range and increased angular velocity associated with KEA use, as described above, most EMG parameters for ramp ascent increased greatly with KEA use. However, the KEA did allow P1 to slightly decrease the mean quadriceps activation levels, and P2 to slightly reduce gluteus maximus activation.

Table 5.6: Percent difference between normal task completion and task completion with extension-assist for ramp walking. Negative values indicate a reduction in muscle activation with KEA use.

|  | Vastus medialis | Rectus femoris | Gluteus maximus |
|---|---|---|---|
| **P1 Ascent** | | | |
| abs max | 58.2 | 68.2 | 106.5 |
| abs mean | -4.9 | -0.8 | 11.5 |
| abs int | 112.1 | 124.4 | 154.6 |
| **P2 Ascent** | | | |
| abs max | 23.1 | 215.6 | -15.1 |
| abs mean | 58.0 | 123.4 | -10.3 |
| abs int | 39.6 | 97.7 | -20.5 |
| **P1 Descent** | | | |
| abs max | 65.4 | 34.7 | 40.0 |
| abs mean | -7.9 | 1.3 | -2.6 |
| abs int | 25.0 | 38.4 | 32.8 |
| **P2 Descent** | | | |
| abs max | 166.6 | 205.4 | 78.1 |
| abs mean | 113.4 | 101.3 | 25.3 |
| abs int | 199.1 | 184.2 | 75.8 |

The effect of the KEA on ramp descent was similar to that of ascent. Ankle and hip angles and velocities varied only slightly between trial conditions, but knee angles were greatly affected by the extension moment provided by the device (Figure 5.6). During normal ramp descent, knee angle was characterized by an initial knee flexion at the beginning of stance, followed by a plateau where knee angle remained constant from approximately 25 % to 75 % of stance, and a second period of knee flexion at the end of stance to lower the body and allow for easy transference of weight to the contralateral leg. The KEA resisted knee flexion and only permitted the first period of knee flexion. The extension moment stopped the second flexion period from occurring or greatly reduced its magnitude, and resulted in a much more extended knee joint at the end of stance than was desired, thus forcing the participant to lift their body up and over the braced leg. During normal ramp descent, P1 flexed the right knee 29.7° further than during assisted ramp descent, while P2 flexed the right knee 10.2° further during normal descent trials than during assisted descent trials (RKA4). The device provided 23.9 Nm and 27.9 Nm for P1 and P2, respectively (RDM4). The moments provided by the KEA corresponded to 39 % and 45 % of the required knee moment in early to mid-stance, but 95 and 110 % of the required moment in late stance [37].

The high moments provided by the KEA in late stance inhibited knee flexion angles from reaching the knee angles observed at the end of ramp descent stance without the extension-assist (Figure 5.6). The changes in kinematics from KEA use generally caused an increase in EMG muscle activation parameters. For P1, the mean EMG activation level for vastus medialis and gluteus maximus decreased slightly with KEA extension assist compared to no assist, but all other EMG values rose considerably. For P2, the increases in EMG activation levels were much greater, with increases of upwards of 205 % for the quadriceps.
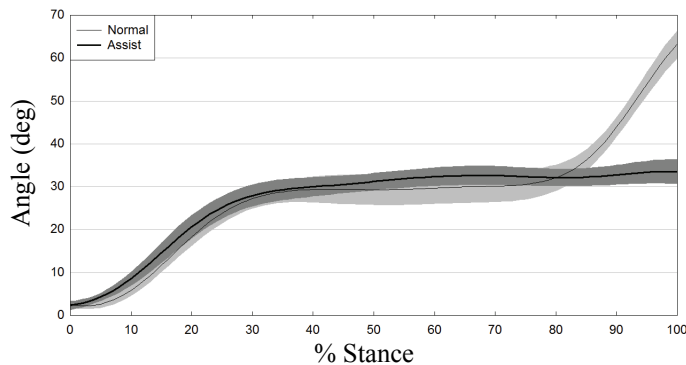


Figure 5.6: Ramp descent knee angle with and without assistance for P1.

## 5.4.3 KEA Performance

During KEA use, the pneumatic actuation system for engaging the knee disk was found to leak due to the high pressure exerted on it by the participant's bodyweight. The leak quickly left the air bladder deflated. As a result, the air bladder underfoot was removed, and a manually operated air bladder was connected to the pneumatic actuator. The hand-held air bladder was used to manually activate the pneumatic actuator to lock the knee disk. Participants were given time to adjust to manual actuation, but even with time to adjust, correct manual activation timing was challenging, and participants occasionally failed to engage the knee disk before a given stride was commenced. The rate of failure lessened as the participant became more accustomed to using the device, but missed engagements still occurred sporadically. Disengaging the knee disk prior to swing did not seem to pose a problem; failure to disengage before swing rarely occurred. Any trial in which failure to engage or disengage occurred was considered unsuccessful and discarded.

136

Both participants initially found the KEA intimidating, and used the device cautiously as they began to learn how to use it to assist STS. However, both participants quickly learned how to use the KEA effectively for stand-to-sit and STS, and soon felt fairly comfortable with its use. For ramp walking, though, the two participants initially found the KEA difficult to use. With practice, both participants improved, but P2 never looked entirely comfortable using the device, and as stated above, both participants occasionally had to catch their bodyweight when engagement of the knee disk didn't occur due to improper manual activation of the air bladder. As stated previously, trials in which this occurred were considered unsuccessful and were discarded.

Device failure occurred once during testing. Towards the end of the ramp gait test for P2, the knee disk pin came out of the hole in the knee disk support into which it was press-fit. The failure caused a loud noise as the knee disk came loose and the springs were permitted to rapidly extended back to full length within the spring case and caused the spring beam to impact the proximal end of the spring case. The participant had to quickly react to the loss of the extension moment by providing the knee extension moment himself, but there were no major consequences. The knee disk pin was re-pressed into the hole, and testing was finished. There was no damage caused by the failure, nor was there a change in function of the device after the pin was reinserted.

# Chapter 6. Discussion

## 6.1 Comparison of the KEA with Existing Devices

The KEA was designed as a modular component that could be incorporated into any KAFO to provide an assistive knee-extension moment for aiding sit-to-stand and ramp ascent. It was also designed to allow for normal function of the KAFO when the extension-assist provided by the KEA is not required. Through an extensive search of the literature, no other purely-mechanical knee extension-assist device for high-quadriceps-strength tasks was found, and only several portable devices capable of providing active knee extension moments during stance were found. Most portable devices found were powered exoskeletons, which tend to be bulky and heavy and require large amounts of energy to operate. As a result, exoskeletons have a battery life per charge of less than a few hours. This is an undesirable trait for a daily use orthosis, since it is inconvenient for a user to only be able to use an assistive device for a portion of the day before the power supply must be recharged. Only one of the portable devices in the literature was a unilateral extension-assist KAFO. That unilateral device also suffered from a very short battery life, and had a design that prevented the user from sitting. The KEA described in this thesis, on the other hand, can be used for, at minimum, its 10 year lifespan with only yearly spring replacement required, since the final design was powered by springs instead of electro-mechanically. The use of springs avoids the issue of power supply life, since only yearly spring replacement is required. However, a spring-powered design is only able to provide an extension-assist if there is an initial knee flexion under bodyweight. Therefore, the KEA is unable to provide a moment for tasks that commence with the knee flexed and that undergo no further flexion before extension begins, such as stair ascent.

The KEA was relatively small and light when compared to other devices that provide an assistive knee-extension moment. The Honda Bodyweight Support system, which provides bilateral assistance but does not provide 100 % of the required joint moment, weighs 6.5 kg. However, bilateral devices can support their own weight during use. The unilateral powered orthosis Roboknee, which can provide 100 % of the required moment for stair ascent, but only for 30-60 min per charge, weighs 5.13 kg. The KEA prototype weighed only 0.67 kg, 13

% of the Roboknee weight, and does not require recharging. The maximum medio-lateral thickness of the prototype was 27 mm and the maximum width was 70 mm, both occurring at the spring case. Total prototype length proximo-distally was 423 mm, where this length was only composed of an upper assembly 158 mm long and a lower assembly 167 mm long, with the space between assemblies spanned by the proximal and distal cables. Though information about dimensions of other existing devices is not readily available, the dimensions of the KEA in this research appear to be smaller than the existing powered devices, based on photographs provided in the literature and videos available on the internet.

High cost was an issue with the prototype, at approximately $3114. However, the majority of this cost was due to the skilled labour involved in machining a one-off prototype. Cost would be greatly reduced if a high-volume production run were to be carried out, since the materials themselves were inexpensive. Materials valuing $114 sufficed for all parts. An estimate of 2 days/unit was given for a run of 100 units carried out by The Ottawa Hospital Rehabilitation Centre machinist on the equipment available at the hospital, resulting in a fabrication cost of $1200 per unit and a total device cost of $1314, without taking into account reduced material costs associated with higher quantity purchases. From the rates provided by local machine shops, the KEA fabrication cost could be as low as $639. Cost could be reduced further by fabrication in a facility specialized for high-volume production.

The KEA cost would be in addition to that of the orthosis. According to the orthotists at The Ottawa Hospital Rehabilitation Centre, a traditional KAFO can cost approximately $2000, while a SCKAFO can cost upwards of $4500. However, since the KEA is modular, it would be purchased separately from the KAFO or SCKAFO, and therefore a potential user would not be required to buy a new orthosis in order to use a KEA. Price comparison is difficult, since there are currently no extension-assist devices for high quadriceps-strength demand tasks on the market, and research groups developing powered orthoses and exoskeletons do not make information regarding cost widely known, but at $639 plus the cost of the orthosis, the KEA would be approximately 5 % to 10 % of the cost of the HAL 5 exoskeleton [114]. Though the KEA doesn't have the same strength as the powered exoskeletons, the cost alone could make it an attractive option.

## 6.2 Mechanical Evaluation

### 6.2.1 Implications of Results

Mechanical testing of the KEA was performed to quantify the assistance the device could provide, as well as test the device function to ensure its safety before trials with human participants began. The major finding of the mechanical tests was the actual moment provided by the KEA for extension-assist was 24 % less than the moment the KEA was designed to generate. The spring response tests showed that one factor in the lower device moment was a lower spring extension force than what was specified by the manufacturer. The springs did not achieve the return force expected for a given compression, since they only reached 89 % of the 1500 N predicted spring force at 40 mm of compression, the compression that occurs due to 90° of knee flexion.

In addition to a reduced extension-assist moment due to lower spring extension forces than expected for a given compression, there was also slightly less compression occurring for a given flexion angle than was designed. The loading response test showed that an initial angle of 5° was necessary before spring compression began. This was due to knee disk notch location, slight stretch in the wire cables, and loose tolerances in the assembly of the sliding lock and sliding lock supports. Loss of 5° of knee flexion with which to compress the springs results in 2.2 mm less spring compression, a loss of approximately 40 N of spring force. The tolerance in the angles at which the sliding lock can engage, however, was essential for ease of device use. Without the 5° tolerance, the user would be required to extend the knee to, or slightly beyond, full extension in order to lock the knee disk. The result would be a greater number of missed knee disk engagements because of insufficient knee extension. Therefore, the angle tolerance was an important feature to keep.

The problems of the lower-than-theoretical spring extension force for a given compression observed in the direct pull tests and the 2.2 mm reduction in spring compression observed in the KEA loading response test caused approximately half of the reduction in extension-assist moment from the expected value. If the spring case length were reduced by 6.2 mm, 90° of knee flexion would correspond to the desired spring force of 1500N.

However, the springs would bottom out at an angle just beyond 90°, meaning further flexion would not be able to occur. If a user were to sit in a low seat, knee flexion on the braced leg would be halted by the device when 90° was reached. If the seated knee angle were much beyond 90°, the user could potentially have difficulty using the KEA to aid STS, since it would likely be difficult to place the braced leg properly on the floor in front of the chair.

The other half of the reduction in extension-assist moment was due to friction within the system. The major source of friction was rubbing between the cables and the distal end of the spring case, as described in Section 4.2.3. The friction was caused by misalignment between the direction of pull of the cables and the centerline of the spring case. However, the method of device attachment to the uprights causes the misalignment, and so complete elimination of the misalignment would not be possible in the current design. However, a reduction in the severity of the friction could be achieved by adding brass guides or small rollers to the device on the distal side of the distal spring case end.

The KEA function tests revealed some shortcomings with the locking mechanism of the device. The locking mechanism did not function properly for all trials. Though it was likely due to user error in not ensuring proper locking rod orientation, the device should be robust enough to function properly even when mistakes are made by the user. When attention was paid to the locking of the device, it locked without fail, indicating that the device was sufficiently safe for initial biomechanical testing on healthy individuals. The locking mechanism also has the innate characteristic of allowing the spring beam to be locked in only certain discrete positions. Ideally, the locking mechanism would lock at any knee flexion angle, so that the user is not forced to adopt a certain knee angle, most likely one that is slightly extended from the greatest flexion angle reached during stand-to-sit. Having the spring beam lock at the maximum knee angle that occurred during stand-to-sit would facilitate STS by allowing a more natural placement of the braced leg on the ground. This would, in turn, bring the base of support nearer to the centre of mass for the start of STS, and thus make STS easier to perform. The slight increase in knee flexion angle would also give a slightly higher extension-assist during STS.

141

## 6.2.2 Sources of Error

The tensile testing machine (Instron 4482 Universal Tester) had an intrinsic error that caused it to miss four consecutive data points for approximately every 10 s of testing carried out. As a result, all trials had gaps in the data collected. However, the gaps were small and did not always occur at the same time in each trial. As a result, across the trials for each test performed, there was data collected for all positions reached. Since each test exhibited such small variance across the trials and, with the exception of the force spike seen during device flexion, the curves obtained were smooth and changed slowly, it was deemed that the data from the other trials would accurately represent the information missed by the Tensile testing machine.

The Tensile testing machine had a maximum sampling rate of 20 Hz. The testing speed used was 300 mm/min. The Tensile testing machine therefore obtained one load measurement every 0.25 mm of vertical crosshead displacement. The accuracy of the measurements was thus limited by the sampling accuracy. The accuracy of the peak value of the spike seen during the loading test was limited by the device resolution, since the actual peak may have occurred between sampling points and the high rate of change of force may have resulted in a significant error. However, the actual value of the peak was not a critical result of the test, and thus the sampling rate error was not deemed important.

The protractor used to determine initial and final knee angles had an uncertainty of $\pm$ 0.5°. The uncertainty resulted in a maximum possible moment error of $\pm$ 0.4 Nm at maximum knee flexion.

## 6.3 Biomechanical Evaluation

### 6.3.1 Implications of Results

Biomechanical evaluation was performed to determine the performance of the KEA and the effect it has on a user. The biomechanical evaluation showed that the KEA was beneficial for STS and stand-to-sit, but did not provide a beneficial extension moment for ramp walking.

142

For STS and stand-to-sit, the benefits of the extension-assist were fairly clear. The KEA permitted these motions to be performed in a slower and more controlled manner. P1 was able to decrease quadriceps muscle usage in the right leg, with little change in muscle activation levels in the left leg, while reducing the angular velocities at the knee and hip. KEA use did cause a slight increase the right gluteus maximus activation levels for P1. This is thought to have provided stability to the leg that the quadriceps normally provide.

For P2, the expected reduction in EMG levels due to KEA assistance compared to no assistance of the right quadriceps was only seen for the stand-to-sit trials. The increase in quadriceps activation during STS does not indicate poor device performance. P2 performed STS differently as a result of KEA use. Without the aid provided by the KEA, P2 was only able to rise from seated using a tactic that relied on ballistic arm movements and fast joint rotations to generate enough momentum to reach a stable position over the base of support. Such a tactic could be difficult and/or dangerous for individuals with disabilities. With the extension-assist, P2 was able to rise using a slow and controlled STS motion that was not possible without the extension-assist. It is important to note that with the extension assist, P2 did not have to use the folded arm swing that was required when no KEA assist was used. The task completed with the KEA assist was therefore a much harder task to complete: standing up from sitting without use of arm swing, compared to the easier task without the KEA assist: standing up from sitting with use of arm swing. Since the tests were not controlled for arm swing for participant P2, a fair comparison to determine benefit of the KEA cannot be made based on muscle activation levels. It must be emphasized that P2 was not able to stand from sitting without arm swing without the KEA assist, but was able to stand from sitting without arm swing, with the KEA assist.

During STS, the KEA was able to provide 56 % and 50 % of the required knee moment for P1 and P2, respectively. This was less than the theoretical 61 % for a 70 kg individual that the device was designed to provide. Reduction of friction in the system, as described in Section 6.2, may raise the percent-assist values to or above the theoretical values. However, the friction did help the KEA achieve very high percent-assist values for stand-to-sit; 82 % and 75 % of the moment acting on the right knee of P1 and P2, respectively.

For ramp gait, results of the biomechanical evaluation were not able to indicate that the device provided useful assistance. For both ascent and descent, quadriceps muscles were not able to appreciably reduce activation levels when the KEA was used, with increases in the EMG parameters common for both ascent and descent. During ascent with KEA assist, the knee was nearly fully extended prior to the initiation of stance to ensure knee disk engagement. The extra knee extension resulted in a large increase in the range of knee flexion undergone during stance over normal ramp ascent. The extra extension also resulted in an increase in maximum knee flexion velocity, since the KEA provided no assistance before reaching the preload angle, and thus the knee essentially buckled until resistance from the device was met. The increased joint velocity may have been the cause of the higher muscle activation levels, forcing the quadriceps to work harder, even with the assistance from the device, to stop the faster knee flexion and commence extension, since the assistance during ramp ascent was only 34 % of the normal moment requirement. The results lend evidence to this hypothesis, since the increase in knee joint velocity was greater for P2 than for P1, by 63 %, as was the increase in EMG parameters, by 33 %. P1 did manage to produce very slight reductions in the mean quadriceps EMG signals. Since P1 appeared to be more comfortable with device use than P2, this may suggest that with more practice, a user may be able to learn how to use the extension moment provided for ramp walking in a beneficial way, and thus learn how to reduce quadriceps activation levels. Since angular velocity was not controlled for, the participants were able to choose between using less muscle activation for the same angular velocity in their ramp gait with and without KEA assist, or using similar muscle activation and achieving a faster higher angular-velocity ramp ascent. It seems that P1 and P2 may have been unable to "turn off" their muscle activity when using the KEA, and instead selected the "more energetic" gait at higher angular velocity with the KEA assist rather than reducing their muscle activity. Clinical testing with participants that have weak quadriceps may demonstrate the advantages of the KEA in ramp walking.

For ramp descent, the device limited knee flexion to a lower maximum value than was observed during normal ramp descent. As a result, the participants moved their trunks up and over the braced leg, instead of allowing the knee to flex further to lower the body down to a

desirable level for initiation of contralateral stance. Because the device prohibited the knee from flexing during descent by providing the full extension moment required during descent, participants should theoretically have been able to completely relax the right quadriceps while descending. However, muscle activation levels increased. Therefore, issues not related to the extension moment provided must have caused the muscle activation level increases observed. One likely explanation is that there was not a sufficient level of comfort with device use. Ideally, the participants would have had a practice period spanning several days or weeks to become completely comfortable with device use. However, the participants only took 20 to 40 minutes to practice device use for ramp gait. Therefore, the participants were not entirely comfortable with KEA use, and muscles were likely being tensed out of caution and for added stability during ramp walking. This is likely especially true for ramp ascent. During ramp ascent, missed knee disk engagement occurred sporadically. The fear of a missed engagement would likely have caused the leg muscles to tense as a precautionary measure in order to be prepared to support body weight in the event of a failed knee disk engagement.

### 6.3.2 Limitations and Sources of Error

A major limitation of the biomechanical evaluation was the short time each participant had to learn how to use the device. As described above, the participants would have ideally had several days or weeks of practice with the KEA to become completely comfortable using the device, and therefore be able to use it to its fullest potential. Instead, the participants took between forty minutes and one hour to practice stand-to-sit, STS, ramp ascent, and ramp descent. It is unlikely that the participants were completely at ease during KEA use, and as a result, the muscles would have been instinctively tensed to provide stability during use and reassurance to the participants that they would not collapse if the device were to not work as expected. This would have been especially true for ramp walking, since it was a more difficult and complex task.

Another limitation was the low number of participants. Because the biomechanical evaluation was for proof-of-concept, two participants were deemed sufficient to provide an

145

initial evaluation of the KEA. However, with two subjects, it is difficult to determine whether the results are representative of a larger population.

The comparison of the different tasks performed with and without the device was made using able-bodied individuals capable of completing all tasks without assistance. Therefore, the effects of KEA use on the participant and the results of the tests may not be consistent with what would be observed using participants with quadriceps weakness. As mentioned earlier, able-bodies subjects may not have been able to "turn-off" their muscle activity when using the KEA assist, as they were instructed to attempt.

Marker movement artifact, movement of the tracking markers relative to the body the marker is attached to, creates an inaccurate measurement of body motionand thus errors in joint kinematics and dynamics. Markers placed on clothes are especially prone to movement artifact. Both participants agreed to perform the tests in small shorts and no shirt, such that the majority of markers were placed on skin or rigid KAFO surfaces to reduce movement error. However, skin still moves relative to bone and a KAFO shifts during use, and error caused by movement artifact was not completely eliminated.

In addition to marker movement, the Vicon motion analysis system used did not have a sufficient number of cameras to track every marker for the entirety of every trial, and markers would disappear from the motion capture recording when obstructed from the view of at least two cameras. The path of the hidden marker would have to be estimated by the Nexus software package during post-processing, potentially creating small discrepancies between actual and recorded marker paths. However, marker path estimation was likely only a very small source of error.

Model accuracy was also a source of error. The model used to calculate joint dynamics relied on anthropometrics to determine body segment sizes and shapes, and used only subject weight to determine body segment parameters. Since it is highly unlikely that the subject perfectly matched the model generated, the use anthropometric data for model creation would have generated some error in the dynamic analysis results for STS and stand-to-sit.

**6.4 Future Work**

**6.4.1 Recommended Design Improvements**

Several modifications are recommended for the KEA design in order to improve the function and increase the safety and reliability of the device.

6.4.1.1 Spring Case Length Reduction

As was explained in Section 6.2.1, the device produced a lower extension moment compared to the expected extension-assist due to reduced spring force and compression. A reduction in the length of the spring case by 6.2 mm would result in a 1500 N force from the springs at 90° of knee flexion, as designed. This change, however, would cause the springs to reach their compressed length at 90° of knee flexion, and prevent the KAFO or SCKAFO joint from flexing beyond 90°, in the event that the user sits in a low seat. Further biomechanical assessment would have to be carried out to determine if a knee angle limitation to 90° was deemed acceptable by users with quadriceps weakness.

6.4.1.2 Addition of Rollers or Guides

Friction within the system accounted for half of the moment loss observed during mechanical evaluation. A set of rollers or brass sleeves on the distal spring case end to act as guides would reduce rubbing of the cables on the case end and would greatly reduce frictional losses. With rollers, the cables could be guided to the knee disk with almost no frictional losses. The guides could be attached to the spring case end or directly to the KAFO upright. Because the distal spring case end was made of aluminum, guides would also reduce or eliminate wear that would eventually occur as a result of rubbing from the stainless steel wire cables. The friction did aid stand-to-sit and the flexion phases of ramp gait by adding to the extension moment during knee flexion. However, device assistance is more desirable for knee extension than for flexion, and the loss in resistance to flexion would be more than offset by the gains in the extension-assist moment.

### 6.4.1.3 Knee Disk Pin

During the biomechanical evaluation, device failure occurred when the knee disk pin came loose from the knee disk support. The knee disk pin was simply press-fit into a hole in the knee disk support and the loading and unloading of the pin caused it to work its way out of the hole. To avoid this in the future, the pin will need to be secured to the knee disk support. Since both components are steel, welding or brazing could be a simple option for fixation.

### 6.4.1.4 Pneumatic Actuation System

The pneumatic actuation system that was supposed to be used to engage the sliding lock with the knee disk was unable to handle the high pressures caused by body weight on the air bladder underfoot, and the bladder was quickly left deflated. The system leaked at the quick-connect input of the pneumatic actuator. For biomechanical trials, a hand-held air bladder was used to control the pneumatic actuator manually. In future iterations, the pneumatic system should be replaced by a micro-servomotor and a foot switch. Since very little power is required to move the sliding lock into place, a very small motor and battery would suffice, and would not add much to device size and weight. An electro-mechanical actuator with foot switches would also allow for better knee-disk engagement control.

### 6.4.1.5 Knee Disk Return Mechanism

During the ramp ascent trials, participants felt it necessary to fully extend the knee before the initiation of stance, to ensure that the sliding lock engaged with the knee disk. The additional knee extension resulted in a large knee angle range and knee angle velocity increase during flexion from normal ramp ascent, and may have led to the difficulty in using the KEA for ramp walking. The KEA does not provide a moment for ramp walking until the preset angle is reached. Therefore, there is no reason that the knee should have to fully extend for knee disk engagement to occur. The issue that arose was that the knee disk was not sufficiently rotated for the notch to be in the proper position for engagement when the knee was at the preload angle. This occurred because the knee disk relied on the resistance to bending of the cables to return it to its original position. Although the cables were stiff, they still bent

slightly while rotating the knee disk. The knee disk was thus not at a lockable position at the preload angle, and the participants were forced to further extend the knee.

To avoid this problem, future KEA designs should include a small, light coil spring, attached to the knee disk and knee disk pin, to ensure that the knee disk returns to its original position as the knee extends during swing. The coil spring would properly align the knee disk and would allow users to initiate stance at the ramp gait preload angle.

## 6.4.1.6 Locking Mechanism Redesign

The locking mechanism used in the prototype fulfilled the major design requirements effectively; the locking rod prevented the spring beam from moving proximally, maintained the ramp ascent preload, and allowed for easy manual release of the springs for delivery of the STS extension-assist. However, it did not permit locking at any knee angle. Instead, a potential 14° difference could develop between the maximum angle reached during stand-to-sit and the angle at which the springs became fully locked. In addition, the slight offset of the notch from the case centreline caused the beam to rotate when locked, as described in Section 3.7.1, and necessitated the addition of the brass linear bearing. The locking mechanism was not ideal, and a new method of locking the spring beam should be developed. A mechanism that clamps the cables at the distal spring case end may be a solution to this problem, but could cause problems of cable wear and reduce the service life of the device. Cable clamps could also cause sticking of the clamping mechanism to the cable due to the large loads placed on the cable. The large loads would tighten the clamp grip force and increase the force required for clamp disengagement, and could cause difficulties when trying to unlock the device at the commencement of knee extension.

An electro-mechanical locking mechanism could also be a possible solution that would allow the springs to be locked at any knee angle. The function of an electro-mechanical locking mechanism would be to lock the springs in place, and not to provide the extension moment. As a result, the power requirement could be kept quite low, and would only require a small motor and battery. A non-backdriveable lead screw actuator that follows the movement of the spring beam and holds it in place when required may be a good candidate

for the new locking mechanism. Such an actuator would be able to prevent spring extension and allow for further spring compression, as desired for the KEA locking mechanism.

### 6.4.1.7 Cable Material

Stainless steel aircraft cables were used to transfer the force from the springs at the thigh to the knee disk. Other materials should be examined for use, since there is potential for reduced friction, reduced weight, and more reliable fixation methods through the use of other materials. Composite belts have been used in other orthotic devices designed at The Ottawa Hospital, and may be of use in the KEA. The aramid fibres used in the composite belts may also be potential candidates for use, since they are very light, very strong in tension, and sufficiently flexible to accommodate bending around the knee disk.

### 6.4.1.8 Size and Weight Optimization

Size and weight are of utmost concern in the design of any orthotic device, and are two of the most important factors in the decision of whether or not to use a given device. Even though the KEA was small and light relative to other powered devices that provide an extension-assist, it may still be difficult to fit the KEA under clothing. The KEA also added noticeable weight to the orthosis. Future efforts should be made to reduce the size and weight of the KEA, since neither was fully optimized during the design phase. The stress analysis carried out in the design phase was very conservative, and all components may have been over-engineered to ensure device safety. For future design iterations, more sophisticated analysis tools such as finite element analysis could be used to determine the smallest and lightest components that would withstand the applied forces, as well as determine where low stresses occur, so that weight saving techniques, like introducing holes or slots into unstressed areas, could be utilized. Furthermore, when the prototype was built, certain components were changed to facilitate fabrication. These changes increased the size and weight of the device. As an example, spring case length could be reduced by using a thinner proximal spring case end, as there is very little stress on that component. The spring beam could also be replaced by the original U-beam design. These two modifications alone would reduce the spring case length by over 20 mm. The knee disk support, made from heavy 17-4 PH stainless steel, was

¼ in. wider than necessary. Due to the design changes for the prototype, there were many small size and weight increases that could be eliminated for the creation of a second prototype.

## 6.4.2 Cyclic Testing

Once the design modifications are carried out, cyclic tests should be performed to determine the fatigue life of the KEA. A setup similar to that used in the loading response test could be used, with cycles from full extension to 90° joint flexion carried out until failure. However, the tensile testing machine available is not meant for cyclic testing, and cyclic tests would have to be carried out using other equipment. To satisfy the design requirements, the device would have to withstand at least $3 \times 10^6$ cycles, the estimated life of the KEA.

## 6.4.3 Further Biomechanical Testing

The biomechanical evaluation of the KEA was an initial proof-of-concept pilot test that involved a small sample of able-bodied participants. Before the device can eventually be brought to market, further rounds of biomechanical trials are necessary. After the next design iteration of the KEA, biomechanical trials involving a larger number of participants, first able-bodied and then those with weakened quadriceps, should be carried out to determine the changes resulting from the design revision, as well as the effects of the device when used by the target market. Individuals with varying levels of quadriceps weakness and causes of weakness should be recruited for the trials in order to determine the groups that would benefit most from KEA use. Following the second round of biomechanical evaluations and another design iteration, if necessary, a longer-term biomechanical evaluation should be carried out to determine if the benefits provided by the extension-assist are great enough to outweigh the increase in size and weight caused by the attachment of the device to the previously used orthosis. If either size or weight were too great, the participants would find the device more of a hindrance than a help, and device rejection would likely occur. This is an important issue to study before attempting to market the device.

# Chapter 7. Conclusions

A new knee-extension-assist device for individuals with quadriceps muscle weakness was designed and developed. The device, called the KEA, was designed as a modular component for integration into existing knee-ankle-foot orthoses, and was smaller, lighter, and less expensive than existing powered extension-assist devices. The KEA was passively powered by springs, and did not require large, heavy, and expensive components such as motors and power supplies. The KEA successfully provided a knee extension moment during the sit-to-stand and ramp ascent tasks, and also provided the secondary benefit of an extension moment to knee flexion during stand-to-sit and ramp descent.

Mechanical evaluation of the KEA showed that the device supplied 76 % of the extension moment than it was designed to provide. The loss of moment was due in part to reduced spring extension forces from the manufacturer specifications and reduced spring compression due to loose tolerances and play in the system. More importantly, though, the loss was due to friction. In addition to a drop in extension moment, the friction would also cause wear on the device. Wear would shorten the lifespan of the KEA. The major cause of the friction was rubbing between the proximal cables and the spring case. A simple design change that would provide a low-friction surface to guide the cables, such as small rollers, would greatly reduce system friction.

The locking rod mechanism used to hold the springs in a compressed state permitted the springs to be locked in discrete positions for sit-to-stand. Mechanical evaluation showed the discrete locking positions to be separated by upwards of 14° of joint rotation due to cable stretch and shifting of components within the KEA, as opposed to the theoretical 7° based on the inter-notch spacing. Instead of a locking system with discrete locking positions, further design iterations should look into mechanisms with continuous locking position capabilities.

Biomechanical evaluation of the KEA showed promising results for STS and stand-to-sit. The device supplied over 50 % of the required knee moment for STS. KEA assistance allowed one participant to reduce quadriceps muscle activation levels from those seen during

STS without the extension-assist, while it allowed the other participant to rise in a slow and controlled manner that was not possible without the KEA assistance. The level of assistance was slightly lower than the predicted 61% assistance from the design calculations, but elimination of the system friction may increase the value to the theoretical levels. For stand-to-sit, very high assistance values were attained, with assistance reaching 82 % for one participant. The high values were due in part to the system friction, and would decrease upon the addition of low-friction guides. The gain in extension assistance would offset the loss of flexion resistance.

Ramp gait results were not able to show benefits of KEA use as did those of STS and stand-to-sit. The knee angle range increased with the assist compared to without, the device provided a lower percent-assist for ascent than it did for STS and stand-to-sit, and knee flexion angle decreased with the assist than without due to high percent assist values for descent. These factors may have contributed to the difficulty in reducing muscle activity levels when using the device for ramp walking. The KEA was able to provide 34 % assistance to ramp ascent, instead of the theoretical 47 % assistance. It is possible that this level of assistance was too low for either participant to gain useful assistance for ramp ascent under current conditions. During KEA use for ramp ascent, the participants fully extended the knee before the initiation of stance. Full knee extension seemed to be an important factor in the difficulty of using the device for ramp ascent. The biomechanical study participants did not have sufficient time to fully acquaint themselves with device use, and as a result, were not fully comfortable with its use, especially in the case of ramp walking. Consequently, participants were likely unable to relax their muscles during device use because of discomfort and muscle tension that resulted from the use of a device that the participants did not fully trust. Had a longer practice period of days or weeks been given, the participants would likely have been more at ease and skilled with the device, and thus able to gain greater benefit from the KEA.

Biomechanical evaluation uncovered several minor shortcomings of the design. The pneumatic actuation system was found to be insufficient for knee disk engagement because the high pressures generated by applying body weight to the air bladder created leaks in the

system. An electro-mechanical solution may be more suitable for the application, since high power is not required and therefore electro-mechanical components could be kept small and light. Electro-mechanical actuators also have increased control capabilities that could improve the function of the knee disk locking mechanism. Another minor shortcoming found was that a simple press-fit of the knee disk pin into the knee disk support was not adequate, and a method of fixation or joining must be used to prevent pin movement.

Once the design recommendations outlined in the previous section are addressed in the next design iteration, cyclic load testing will need to be carried out to determine the lifespan of the device to ensure safety for long-term use. Following the cyclic testing, a second round of biomechanical trials should be conducted involving individuals with weakened quadriceps, to determine the effects of the device on the KEA end-users.

Several changes will need to be made to the KEA for future design iterations in order to create a reliable and commercially viable extension-assist device for individuals with weakened quadriceps. Most important are those described in this section, along with reduction of overall size and weight, two of the major deciding factors for a potential user as to whether or not a given assistive device will be used. Providing simple and innovative solutions to the design issues that arose during testing will eventually lead to an extension-assist device with the potential to provide greater mobility and independence to individuals afflicted by weakened quadriceps, thus improving their quality of life.

References

[1] National Center for Health Statistics, "National Health Interview Survey on Disability (NHIS-D)," vol. 2010, March 15, 2010.

[2] A. Cullell, J. C. Moreno, E. Rocon, A. Forner-Cordero and J. L. Pons, "Biologically based design of an actuator system for a knee-ankle-foot orthosis," *Mech. Mach. Theory,* vol. 44, pp. 860-872, APR, 2009.

[3] Applied Biomechanics Custom Orthotic Services Inc., "Lower Extremity Orthotics," 1998 (2010). http://www.appliedbiomechanics.com/Home/Home/legs.html

[4] A. G. McMillan, K. Kendrick, J. Michael, J. Aronson and G. Horton., "Preliminary evidence for effectiveness of a stance control orthosis" *Journal of Prosthetics & Orthotics 16(1),* 2004, pp. 6-6-13.

[5] T. Yakimovich, J. Kofman and E. D. Lemaire, "Design and evaluation of a stance-control knee-ankle-foot orthosis knee joint," *IEEE Trans. Neural Syst. Rehabil. Eng.,* vol. 14, pp. 361-369, SEP, 2006.

[6] J. C. Moreno, F. Brunetti, E. Rocon and J. L. Pons, "Immediate effects of a controllable knee ankle foot orthosis for functional compensation of gait in patients with proximal leg weakness," *Med. Biol. Eng. Comput.,* vol. 46, pp. 43-53, JAN, 2008.

[7] J. Andrysek, S. Redekop and S. Naumann, "Preliminary evaluation of an automatically stance-phase controlled pediatric prosthetic knee joint using quantitative gait analysis," *Arch. Phys. Med. Rehabil.,* vol. 88, pp. 464-470, APR, 2007.

[8] S. Hwang, S. Kang, K. Cho and Y. Kim, "Biomechanical effect of electromechanical knee-ankle-foot-orthosis on knee joint control in patients with poliomyelitis," *Med. Biol. Eng. Comput.,* vol. 46, pp. 541-549, JUN, 2008.

[9] S. E. Irby, K. A. Bernhardt and K. R. Kaufman, "Gait of stance control orthosis users: The Dynamic Knee Brace System," *Prosthet. Orthot. Int.,* vol. 29, pp. 269-282, DEC, 2005.

[10] T. Suga, O. Kameyama, R. Ogawa, M. Matsuura and H. Oka, "Newly designed computer controlled knee-ankle-foot orthosis (Intelligent Orthosis)," *Prosthet. Orthot. Int.,* vol. 22, pp. 230-239, DEC, 1998.

[11] R. B. Shepherd and A. M. Gentile, "Sit-To-Stand - Functional-Relationship between Upper-Body and Lower-Limb Segments," *Hum. Mov. Sci.,* vol. 13, pp. 817-840, DEC, 1994.

[12] A. B. Schultz, N. B. Alexander and J. A. Ashtonmiller, "Biomechanical Analyses of Rising from a Chair," *J. Biomech.,* vol. 25, pp. 1383-1391, DEC, 1992.

[13] F. Bahrami, R. Riener, P. Jabedar-Maralani and G. Schmidt, "Biomechanical analysis of sit-to-stand transfer in healthy and paraplegic subjects," *Clin. Biomech.,* vol. 15, pp. 123-133, FEB, 2000.

[14] M. W. Rodosky, T. P. Andriacchi and G. B. J. Andersson, "The Influence of Chair Height on Lower-Limb Mechanics during Rising," *J. Orthop. Res.,* vol. 7, pp. 266-271, MAR, 1989.

[15] M. E. Roebroeck, C. A. M. Doorenbosch, J. Harlaar, R. Jacobs and G. J. Lankhorst, "Biomechanics and Muscular-Activity during Sit-To-Stand Transfer," *Clin. Biomech.,* vol. 9, pp. 235-244, JUL, 1994.

[16] F. Sibella, M. Galli, M. Romei, A. Montesano and M. Crivellini, "Biomechanical analysis of sit-to-stand movement in normal and obese subjects," *Clin. Biomech.,* vol. 18, pp. 745-750, OCT, 2003.

[17] M. Anan, K. Okumupa, N. Kito and K. Shinkoda, "Effects of variation in cushion thickness on the sit-to-stand motion of elderly people," *J. Phys. Ther. Sci.,* vol. 20, pp. 51-57, FEB, 2008.

[18] M. A. Hughes, B. S. Myers and M. L. Schenkman, "The role of strength in rising from a chair in the functionally impaired elderly," *J. Biomech.,* vol. 29, pp. 1509-1513, DEC, 1996.

[19] S. Yoshioka, A. Nagano, R. Himeno and S. Fukashiro, "Computation of the kinematics and the minimum peak joint moments of sit-to-stand movements," *Biomed. Eng. Online,* vol. 6, pp. 26, JUL 3, 2007.

[20] E. Papa and A. Cappozzo, "Sit-to-stand motor strategies investigated in able-bodied young and elderly subjects," *J. Biomech.,* vol. 33, pp. 1113-1122, SEP, 2000.

[21] G. Roy, S. Nadeau, D. Gravel, F. Piotte, F. Malouin and B. J. McFadyen, "Side difference in the hip and knee joint moments during sit-to-stand and stand-to-sit tasks in individuals with hemiparesis," *Clin. Biomech.,* vol. 22, pp. 795-804, AUG, 2007.

[22] T. P. Andriacchi, G. B. J. Andersson, R. W. Fermier, D. Stern and J. O. Galante, "A Study of Lower-Limb Mechanics during Stair-Climbing," *J. Bone Joint Surg. -Am. Vol.,* vol. 62, pp. 749-757, 1980.

[23] B. J. Mcfadyen and D. A. Winter, "An Integrated Biomechanical Analysis of Normal Stair Ascent and Descent," *J. Biomech.,* vol. 21, pp. 733-744, 1988.

[24] S. M. Reid, S. K. Lynn, R. P. Musselman and P. A. Costigan, "Knee biomechanics of alternate stair ambulation patterns," *Med. Sci. Sports Exerc.,* vol. 39, pp. 2005-2011, NOV, 2007.

[25] J. E. Zachazewski, P. O. Riley and D. E. Krebs, "Biomechanical Analysis of Body-Mass Transfer during Stair Ascent and Descent of Healthy-Subjects," *J. Rehabil. Res. Dev.,* vol. 30, pp. 412-422, 1993.

[26] R. Riener, M. Rabuffetti and C. Frigo, "Stair ascent and descent at different inclinations," *Gait Posture,* vol. 15, pp. 32-44, FEB, 2002.

[27] A. Protopapadaki, W. I. Drechsler, M. C. Cramp, F. J. Coutts and O. M. Scott, "Hip, knee, ankle kinematics and kinetics during stair ascent and descent in healthy young individuals," *Clin. Biomech.,* vol. 22, pp. 203-210, FEB, 2007.

[28] A. Stacoff, C. Diezi, G. Luder, E. Stussi and I. A. Kramers-De Quervain, "Ground reaction forces on stairs: effects of stair inclination and age," *Gait Posture,* vol. 21, pp. 24-38, JAN, 2005.

[29] P. A. Costigan, K. J. Deluzio and U. P. Wyss, "Knee and hip kinetics during normal stair climbing," *Gait Posture,* vol. 16, pp. 31-37, AUG, 2002.

[30] M. Spanjaard, N. D. Reeves, J. H. Van Dieeen, V. Baltzopoulos and C. N. Maganaris, "Influence of step-height and body mass on gastrocnemius muscle fascicle behavior during stair ascent," *J. Biomech.,* vol. 41, pp. 937-944, 2008.

[31] G. B. Salsich, J. H. Brechter and C. M. Powers, "Lower extremity kinetics during stair ambulation in patients with and without patellofemoral pain," *Clin. Biomech.,* vol. 16, pp. 906-912, DEC, 2001.

[32] E. Lindeman, P. Leffers, J. Reulen, F. Spaans and J. Drukker, "Quadriceps strength and timed motor performances in myotonic dystrophy, Charcot-Marie-Tooth disease, and healthy subjects," *Clin. Rehabil.,* vol. 12, pp. 127-135, APR, 1998.

[33] J. H. Brechter and C. M. Powers, "Patellofemoral joint stress during stair ascent and descent in persons with and without patellofemoral pain," *Gait Posture,* vol. 16, pp. 115-123, OCT, 2002.

[34] N. D. Reeves, M. Spanjaard, A. A. Mohagheghi, V. Baltzopoulos and C. N. Maganaris, "Influence of light handrail use on the biomechanics of stair negotiation in old age," *Gait Posture,* vol. 28, pp. 327-336, AUG, 2008.

[35] T. Schmalz, S. Blumentritt and B. Marx, "Biomechanical analysis of stair ambulation in lower limb amputees," *Gait Posture,* vol. 25, pp. 267-278, FEB, 2007.

[36] S. Nadeau, B. J. McFadyen and F. Malouin, "Frontal and sagittal plane analyses of the stair climbing task in healthy adults aged over 40 years: what are the challenges compared to level walking?" *Clin. Biomech.,* vol. 18, pp. 950-959, DEC, 2003.

[37] A. N. Lay, C. J. Hass and R. J. Gregor, "The effects of sloped surfaces on locomotion: A kinematic and kinetic analysis," *J. Biomech.,* vol. 39, pp. 1621-1628, 2006.

[38] V. Bundhoo, E. Haslam, B. Birch and E. J. Park, "A shape memory alloy-based tendon-driven actuation system for biomimetic artificial fingers, part I: design and evaluation," *Robotica,* vol. 27, pp. 131-146, JAN, 2009.

[39] C. Mavroidis, J. Nikitczuk, B. Weinberg, G. Danaher, K. Jensen, P. Pelletier, J. Prugnarola, R. Stuart, R. Arango, M. Leahey, R. Pavone, A. Provo and D. Yasevac, "Smart portable rehabilitation devices," *Journal of NeuroEngineering and Rehabilitation,* vol. 2, pp. 18, 2005.

[40] J. L. Pons, H. Rodriguez, I. Luyckx, D. Reynaerts, R. Ceres and H. Van Brussel, "High torque ultrasonic motors for hand prosthetics: current status and trends." *Technol. Health Care,* vol. 10, pp. 121-33, 2002.

[41] E. Biddiss and T. Chau, "Dielectric elastomers as actuators for upper limb prosthetics: Challenges and opportunities," *Med. Eng. Phys.,* vol. 30, pp. 403-418, MAY, 2008.

[42] F. El Feninat, G. Laroche, M. Fiset and D. Mantovani, "Shape memory materials for biomedical applications," *Adv. Eng. Mater.,* vol. 4, pp. 91-104, MAR, 2002.

[43] V. O. D. Cura, F. L. Cunha, M. L. Aguiar and A. Cliquet, "Study of the different types of actuators and mechanisms for upper limb prostheses," *Artif. Organs,* vol. 27, pp. 507-516, JUN, 2003.

[44] A. E. Fitzgerald, C. J. Kingsley and S. D. Umans, *Electric Machinery.* New York: McGraw-Hill Book Co., 1983.

[45] H. Kazerooni, A. Chu and R. Steger, "That which does not stabilize, will only make us stronger," *Int. J. Robotics Res.,* vol. 26, pp. 75-89, JAN, 2007.

[46] The Lynch Motor Company ltd., "Technical Details - 130 Table," (2009), http://www.lmcltd.net/uploads/files/130_table.pdf.

[47] Faulhaber, "DC-Micromotors - Series 0615 ... S," (2009), http://www.faulhaber-group.com/uploadpk/EN_0615_S_MIN.pdf.

[48] K. W. Hollander and T. G. Sugar, "Design of lightweight lead screw actuators for wearable robotic applications," *J. Mech. Des.,* vol. 128, pp. 644-648, MAY, 2006.

[49] H. Kazerooni, "Human augmentation and exoskeleton systems in Berkeley," *Int. J. Humanoid Robot.,* vol. 4, pp. 575-605, SEP, 2007.

[50] A. M. Dollar and H. Herr, "Lower extremity exoskeletons and active orthoses: Challenges and state-of-the-art," *IEEE Trans. Robot.,* vol. 24, pp. 144-158, FEB, 2008.

[51] Y. Saito, K. Kikuchi, H. Negoto, T. Oshima and T. Haneyoshi, "Development of externally powered lower limb orthosis with bilateral-servo actuator," *Rehabilitation Robotics, 2005. ICORR 2005. 9th International Conference on,* pp. 394-399, 2005.

[52] G. Belforte, L. Gastaldi and M. Sorli, "Pneumatic active gait orthosis," *Mechatronics,* vol. 11, pp. 301-323, APR, 2001.

[53] J. E. Pratt, B. T. Krupp, C. J. Morse and S. H. Collins, "The RoboKnee: an exoskeleton for enhancing strength and endurance during walking," *Proceedings of the 2004 IEEE International Conference on Robotics and Automation,* vol. 3; 3, pp. 2430-2435 Vol.3, 2004.

[54] D. P. Ferris, K. E. Gordon, G. S. Sawicki and A. Peethambaran, "An improved powered ankle-foot orthosis using proportional myoelectric control," *Gait Posture,* vol. 23, pp. 425-428, JUN, 2006.

[55] H. Kobayashi, A. Uchimura, Y. Isihida, T. Shiiba, K. Hiramatsu, M. Konami, T. Matsushita and Y. Sato, "Development of a muscle suit for the upper body - realization of abduction motion," *Adv. Rob.,* vol. 18, pp. 497-513, 2004.

[56] G. S. Sawicki, K. E. Gordon and D. P. Ferris, "Powered lower limb orthoses: applications in motor adaptation and rehabilitation," *Proceedings of the 9th International Conference on Rehabilitation Robotics,* pp. 206-211, 2005.

[57] D. Aoyagi, W. E. Ichinose, S. J. Harkema, D. J. Reinkensmeyer and J. E. Bobrow, "An assistive robotic device that can synchronize to the pelvic motion during human gait training," *Proceedings of the 9th International Conference on Rehabilitation Robotics,* pp. 565-568, 2005.

[58] N. Costa and D. G. Caldwell, "Control of a Biomimetic "Soft-actuated" 10DoF Lower Body Exoskeleton," *Proceedings of the First IEEE/RAS-EMBS International Conference on Biomedical Robotics and Biomechatronics,* pp. 495-501, 2006.

[59] K. Yamamoto, K. Hyodo, M. Ishii and T. Matsuo, "Development of power assisting suit for assisting nurse labor," *JSME Int. J. Ser. C-Mech. Syst. Mach. Elem. Manuf.,* vol. 45, pp. 703-711, SEP, 2002.

[60] K. E. Gordon, G. S. Sawicki and D. P. Ferris, "Mechanical performance of artificial pneumatic muscles to power an ankle-foot orthosis," *J. Biomech.,* vol. 39, pp. 1832-1841, 2006.

[61] A. M. Bertetto and M. Ruggiu, "Characterization and modeling of air muscles," *Mech. Res. Commun.,* vol. 31, pp. 185-194, MAR-APR, 2004.

[62] N. Saga and T. Saikawa, "Development of a pneumatic artificial muscle based on biomechanical characteristics," *Adv. Rob.,* vol. 22, pp. 761-770, 2008.

[63] D. W. Repperger, C. A. Phillips, A. Neidhard-Doll, D. B. Reynolds and J. Berlin, "Actuator design using biomimicry methods and a pneumatic muscle system," *Control Eng. Pract.,* vol. 14, pp. 999-1009, SEP, 2006.

[64] D. W. Repperger and C. A. Phillips, "Developing intelligent control from a biological perspective to examine paradigms for activation utilizing pneumatic muscle actuators," *Proceedings of the 2000 IEEE International Symposium on Intelligent Control,* pp. 205-210, 2000.

[65] M. J. Gerschutz, C. A. Phillips, D. B. Reynolds and D. W. Repperger, "A computational simulated control system for a high-force pneumatic muscle actuator: system definition and application as an augmented orthosis," *Comput. Methods Biomech. Biomed. Engin.,* vol. 12, pp. 173-183, 2009.

[66] TiNi Alloy Co., "Introduction to Shape Memory Alloys," 2003 (2010). http://www.tinialloy.com/pdf/introductiontosma.pdf.

[67] Miga Motor Co., "MigaOne Data Sheet," 2009 (2010). http://www.faulhaber-group.com/uploadpk/EN_0615_S_MIN.pdf.

[68] G. Kovacs, P. Lochmatter and M. Wissler, "An arm wrestling robot driven by dielectric elastomer actuators," *Smart Mater Struct,* vol. 16, pp. S306-S317, APR, 2007.

[69] K. Choe, K. J. Kim, D. Kim, C. Manford, S. Heo and M. Shahinpoor, "Performance characteristics of electro-chemically driven polyacrylonitrile fiber bundle actuators," *J Intell Mater Syst Struct,* vol. 17, pp. 563-576, JUL, 2006.

[70] D. L. Brock, "Massachusetts Institute of Technology Artificial Intelligence Laboratory - Review of Artificial Muscle based on Contractile Polymers," vol. 2009, November, 1991.

[71] B. J. Ruthenberg, N. A. Wasylewski and J. E. Beard, "An experimental device for investigating the force and power requirements of a powered gait orthosis," *J. Rehabil. Res. Dev.,* vol. 34, pp. 203-213, APR, 1997.

[72] S. Patel, B. L. Patritti, J. Nikitczuk, B. Weinberg, U. D. Croce, C. Mavroidis and P. Bonato, "Effects on Normal Gait of a New Active Knee Orthosis for Hemiparetic Gait Retraining," *Proceedings of the 28th Annual IEEE International Conference on Engineering in Medicine and Biology Society,* pp. 1232-1235, 2006.

[73] H. Kazerooni and R. Steger, "The Berkeley Lower Extremity Exoskeleton," *J. Dyn. Syst. Meas. Control-Trans. ASME,* vol. 128, pp. 14-25, MAR, 2006.

[74] Victhom Human Bionics Inc. "Power knee", (2009). http://www.victhom.com/en/bionic-prosthesis-orthosis/power-knee.php.

[75] H. Kawamoto and Y. Sankai, "Comfortable power assist control method for walking aid by HAL-3," *Proceedings of the IEEE International Conference on Systems, Man and Cybernetics,* vol. 4; 4, pp. 6 pp. vol.4, 2002.

[76] H. Kawamoto, S. Kanbe, Y. Sankai, IEEE and IEEE, "Power assist method for HAL-3 estimating operator's intention based on motion information," *Proceedings of Ro-Man 2003: the 12th IEEE International Workshop on Robot and Human Interactive Communication,* pp. 67-72, 2003.

[77] American Honda Motor Co. Inc. "Walking assist device with bodyweight support system". (2009)*,* http://corporate.honda.com/innovation/walk-assist/.

[78] J. A. Blaya and H. Herr, "Adaptive control of a variable-impedance ankle-foot orthosis to assist drop-foot gait," *IEEE Trans. Neural Syst. Rehabil. Eng.,* vol. 12, pp. 24-31, MAR, 2004.

[79] Otto Bock Healthcare LP, "C-Leg FAQ," 2009 (2010). http://www.clegstories.com/index.php/faq

[80] Freedom Innovations LLC, "Plié Knee," 2010, 2008. http://www.freedom-innovations.com/knees/index.html

[81] Össur, "Rheo Knee," 2010 (2010). http://www.ossur.com/pages/12702

[82] Freedom Innovations LLC, "Plié MPC Knee Instructions for Use," 2008 (2010). http://www.freedom-innovations.com/knees/PlieMPCKneeInstructionsForUse.pdf

[83] Daw Industries, "True Variable Cadence," (2010), http://www.daw-usa.com/Pages/TrueVariable1.html.

[84] Össur, "Technical Manual - Rheo Knee," 2009 (2010). http://www.ossur.com/lisalib/getfile.aspx?itemid=7000.

[85] Össur, "Instructions for use: Power Knee," (2009), http://www.ossur.com/lisalib/getfile.aspx?itemid=9683.

[86] Össur, "THE POWER KNEE," 2008 (2009). http://bionics.ossur.com/pages/306.

[87] K. Suzuki, G. Mito, H. Kawamoto, Y. Hasegawa and Y. Sankai, "Intention-based walking support for paraplegia patients with Robot Suit HAL," *Adv. Rob.,* vol. 21, pp. 1441-1469, DEC, 2007.

[88] A. B. Zoss, H. Kazerooni and A. Chu, "Biomechanical design of the Berkeley lower extremity exoskeleton (BLEEX)," *IEEE-ASME Trans. Mechatron.,* vol. 11, pp. 128-138, APR, 2006.

[89] E. Yeates, "Robotic System Giving Soldiers Superhuman Strength," vol. 2010, November 19, 2007.

[90] E. Guizzo and H. Goldstein, "The rise of the body bots," *IEEE Spectrum,* vol. 42, pp. 50-56, OCT, 2005.

[91] H. Kawamoto and Y. Sankai, "Power assist method based on Phase Sequence and muscle force condition for HAL," *Adv. Rob.,* vol. 19, pp. 717-734, 2005.

[92] Honda Motor Co., "Honda to Showcase Experimental Walking Assist Device at BARRIER FREE 2008," April 22, 2008 (2010). http://world.honda.com/news/2008/c080422Experimental-Walking-Assist-Device/

[93] Honda Motor Co., "Honda Unveils Experimental Walking Assist Device With Bodyweight Support System," November 7, 2008 (2010). http://world.honda.com/news/2008/c081107Walking-Assist-Device/

[94] K. Yamamoto, M. Ishii, K. Hyodo, T. Yoshimitsu and T. Matsuo, "Development of power assisting suit - (Miniaturization of supply system to realize wearable suit)," *JSME Int. J. Ser. C-Mech. Syst. Mach. Elem. Manuf.,* vol. 46, pp. 923-930, SEP, 2003.

[95] A. M. Oymagil, J. K. Hitt, T. Sugar and J. Fleeger, "Control of a Regenerative Braking Powered Ankle Foot Orthosis," *Proceedings of the 10th IEEE International Conference on Rehabilitation Robotics,* pp. 28-34, 2007.

[96] S. K. Banala, S. K. Agrawal and J. P. Scholz, "Active Leg Exoskeleton (ALEX) for Gait Rehabilitation of Motor-Impaired Patients," *Proceedings of the 10th IEEE International Conference on Rehabilitation Robotics,* pp. 401-407, 2007.

[97] Y. Ohta, H. Yano, R. Suzuki, M. Yoshida, N. Kawashima and K. Nakazawa, "A two-degree-of-freedom motor-powered gait orthosis for spinal cord injury patients," *Proc. Inst. Mech. Eng. Part H-J. Eng. Med.,* vol. 221, pp. 629-639, AUG, 2007.

[98] K. W. Hollander, R. Ilg, T. G. Sugar and D. Herring, "An efficient robotic tendon for gait assistance," *J. Biomech. Eng. -Trans. ASME,* vol. 128, pp. 788-791, OCT, 2006.

[99] S. K. Banala, S. H. Kim, S. K. Agrawal and J. P. Scholz, "Robot Assisted Gait Training With Active Leg Exoskeleton (ALEX)," *IEEE Trans. Neural Syst. Rehabil. Eng.,* vol. 17, pp. 2-8, FEB, 2009.

[100] S. Jezernik, G. Colombo, T. Keller, H. Frueh and M. Morari, "Robotic orthosis Lokomat: A rehabilitation and research tool," *Neuromodulation,* vol. 6, pp. 108-115, APR, 2003.

[101] I. Yobotics, "RoboWalker," 2009 (2010).
http://yobotics.com/robowalker/robowalker.html

[102] Y. Mori, J. Okada and K. Takayama, "Development of a standing style transfer system "ABLE" for disabled lower limbs," *IEEE-ASME Trans. Mechatron.,* vol. 11, pp. 372-380, AUG, 2006.

[103] K. Kong and D. Jeon, "Design and control of an exoskeleton for the elderly and patients," *IEEE-ASME Trans. Mechatron.,* vol. 11, pp. 428-432, AUG, 2006.

[104] J. F. Veneman, R. Ekkelenkamp, R. Kruidhof, F. C. T. van der Helm and H. van der Kooij, "A series elastic- and Bowden-cable-based actuation system for use as torque actuator in exoskeleton-type robots," *Int. J. Robotics Res.,* vol. 25, pp. 261-281, MAR, 2006.

[105] W. K. Durfee and A. Rivard, "Design and simulation of a pneumatic, stored-energy, hybrid orthosis for gait restoration," *J. Biomech. Eng. -Trans. ASME,* vol. 127, pp. 1014-1019, NOV, 2005.

[106] S. Gharooni, B. Heller and M. O. Tokhi, "A new hybrid spring brake orthosis for controlling hip and knee flexion in the swing phase," *IEEE Trans. Rehabil. Eng.,* vol. 9, pp. 106-107, MAR, 2001.

[107] D. G. Ullman, *The Mechanical Design Process*. New York: McGraw-Hill, 1997.

[108] D. Popovic and L. Schwirtlich, "Design and evaluation of the self-fitting modular orthosis (SFMO)," *Rehabilitation Engineering, IEEE Transactions on,* vol. 1, pp. 165-174, 1993.

[109] M. A. Brehm, A. Beelen, C. A. M. Doorenbosch, J. Harlaar and F. Nollet, "Effect of carbon-composite knee-ankle-foot orthoses on walking efficiency and gait in former polio patients," *J. Rehabil. Med.,* vol. 39, pp. 651-657, 2007.

[110] J. E. Shigley, C. R. Mischke and R. G. Budynas, *Mechanical Engineering Design. 7ed.* Toronto: McGraw Hill, 2004.

[111] M. F. Spotts, T. E. Shoup and L. E. Hornberger, *Design of Machine Elements. 8 ed.* Toronto: Pearson Prentice Hall, 2004.

[112] R. C. Hibbeler, *Mechanics of Materials. 6 ed.* Upper Saddle River, NJ: Pearson Prentice Hall, 2005.

[113] SENIAM, "The SENIAM Project," (2010), http://www.seniam.org/.

[114] D. H. Wilson, "Top 5 Robots You Can Buy Right Now," January 2, 2007 (2010). http://www.popularmechanics.com/technology/engineering/robots/4208628

# Appendix A: Decision Matrix

|  |  | Concepts | | | | | | | |
|---|---|---|---|---|---|---|---|---|---|
| Criterion | Weight | 1 | 2 | 3 | 4 | 5 | 6 | 7 | 8 |
| lightweight | 10 | - | + | + | - | s | - | + | D |
| small size | 10 | - | + | + | - | - | - | s | A |
| concealment of device under clothes | 5 | s | + | - | + | s | - | - | T |
| moving parts | 4 | - | + | + | + | + | + | s | U |
| cost | 3 | s | s | + | + | + | - | + | M |
| force/torque/power transmission losses | 8 | s | - | - | - | - | - | - | |
| energy storage | 8 | - | - | - | - | - | - | s | |
| safety upon failure | 10 | - | - | - | s | - | s | - | |
| fatigue life | 8 | + | - | s | s | + | + | s | |
| simplicity | 5 | - | + | + | + | + | - | s | |
| ease of repair | 1 | s | + | + | + | + | - | + | |
| ease of incorporation to a KAFO | 5 | + | - | - | + | + | - | + | |
| ease of incorporation to Yakimovich KAFO | 6 | + | + | + | + | + | - | + | |
| tolerances of components | 5 | + | - | + | + | + | s | + | |
| noise | 7 | s | s | s | s | - | s | s | |
| amount of power assist | 8 | - | - | - | - | - | - | s | |
| added inertia to leg | 8 | - | - | + | - | - | s | + | |
| impedance during swing | 8 | s | - | - | - | - | s | - | |
| impedance during level walk | 8 | s | - | - | - | - | s | - | |
| functions at any angle | 7 | + | s | - | s | - | + | - | |
| good for different bodyweights | 6 | + | + | + | s | + | + | s | |
| assembly | 4 | s | + | + | + | + | - | + | |
| overall total | | -2 | -1 | 2 | 1 | 0 | -8 | 2 | 0 |
| weighted total | | -26 | -25 | -5 | -30 | -35 | -48 | -4 | 0 |

**Design Concepts**

1. Differential drive: using a mechanism similar to a car differential, torque from the motor could be delivered to the knee joint by attaching one side of the differential gear train to the knee, while keeping the opposite side locked via a clutch. During swing, or when the device is inactive, the motor would shut off and the clutch would be released, and thus the previously locked gear would spin freely during knee flexion or extension,
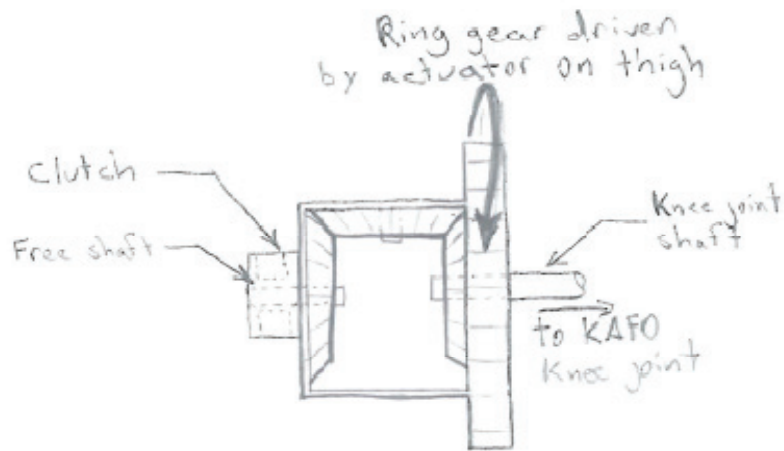
removing impedance from the knee joint.

Figure A.1: Differential drive mechanism concept sketch.

2. Timing belt replacement in Yakimovic design: For a device that would function exclusively with the Ottawalk orthosis [5], a timing belt would replace the smooth belt of the current design. A motor would be placed below the locking mechanism, attached to a gear which fit the timing belt. Torque from the motor would pull on the timing belt, attached to the upper SCKAFO support, thus providing a knee extension moment.

Figure A.2: Timing belt Ottawalk orthosis concept sketch.

3.  Cable pull from thigh: A cable attached to the lower SCKAFO upright and passing over a sheave at the knee would be directly wound by a motor attached to the upper upright.
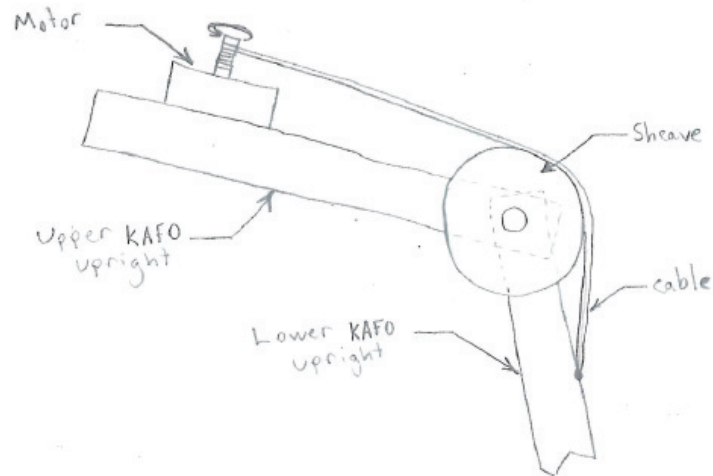


Figure A.3: Cable pull from thigh concept sketch.

4.  Varying thickness flat spring: A flat spring of increasing thickness would be forced through guides below and above the knee joint. While the thin portion of the spring was between the guides, very little restorative force, and therefore extension moment, would be present. As a linear motor forced the flat spring through the guides, the thickness of the spring would increase, thus increasing spring stiffness of the segment between the guides, and therefore increasing the knee extension moment.
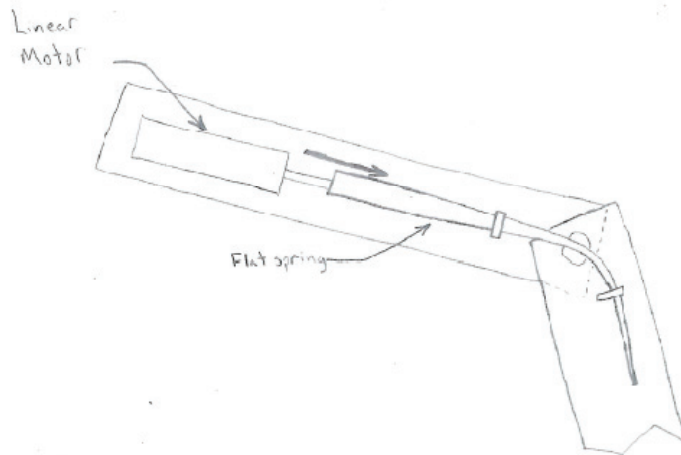
Figure A.4: Varying thickness flat spring concept sketch.

5. Dual cable pull: A cable passing over a sheave at the knee would be attached at either end to a motor; one on the upper leg, one on the lower leg. This is similar to the Cable pull from thigh design, but using two motors to increase the moment provided, without greatly increasing bulkiness in one specific location.
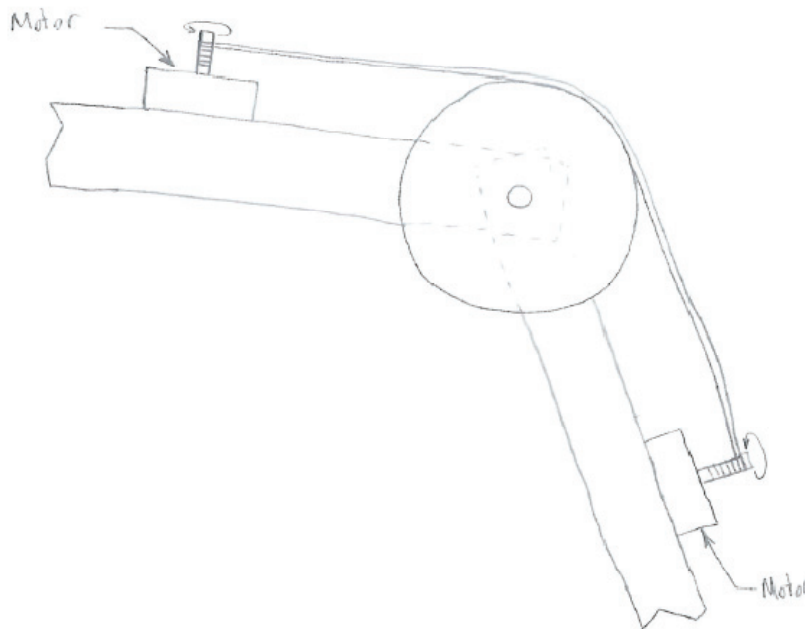

Figure A.5: Dual cable pull concept sketch.

6. Continuously varying transmission pulleys: This design would use two sheaves that could change their groove width. Connected by a V-belt, with one sheave on the thigh

driven by a motor, the other at the knee connected to the knee joint, the sheaves would change their groove width in a coordinated manner to either increase speed of rotation, or increase moment provided to the knee. When the device was inactive, or during swing, the sheave at the knee would widen its groove to a point where there was no tension in the belt, and thus the knee would be able to rotate freely.
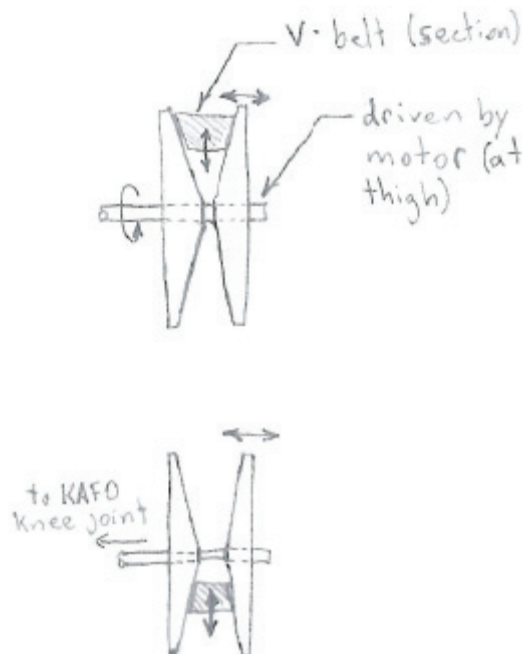


Figure A.6: Continuously varying transmission pulleys concept sketch.

7. Spring energy storage direct cable pull: In a similar setup as the Cable pull, a motor at the thigh would wind a cable attached to the lower KAFO support upright. On the other side of the motor would be an extension spring, which would be loaded by driving the motor in the opposite direction as for cable retraction. In other words, the spring would be extended when the cable was unwound during knee flexion. Thus, when the device was providing a knee extension moment, the force from the spring would assist the winding by returning its stored energy as the motor wound the cable.
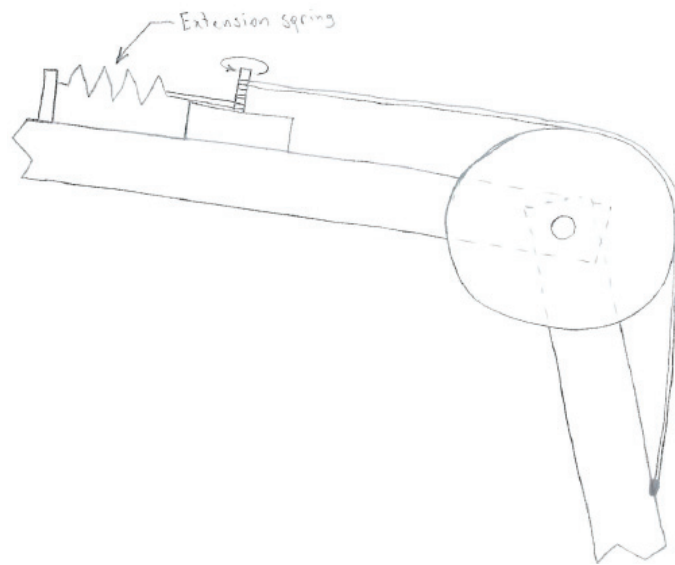
Figure A.7: Spring energy storage direct cable pull concept sketch.

7. Spring energy storage and bevel gear direct drive: In this design, a motor on the thigh would drive a set of bevel gears, the larger of which being attached to the knee joint of the KAFO. A spring would be attached to the gear at the knee, which would wind when driven the direction opposite that of rotation for knee extension. Thus, when the gear was driven for knee extension, the spring would unwind and return the energy stored in the form of added knee extension moment. In order to allow the gear to be driven in the opposite direction, and to remove impedance during swing and device inactivity, the gear at the knee would be coupled to the KAFO joint using a clutch which could be engaged and disengaged at appropriate times.
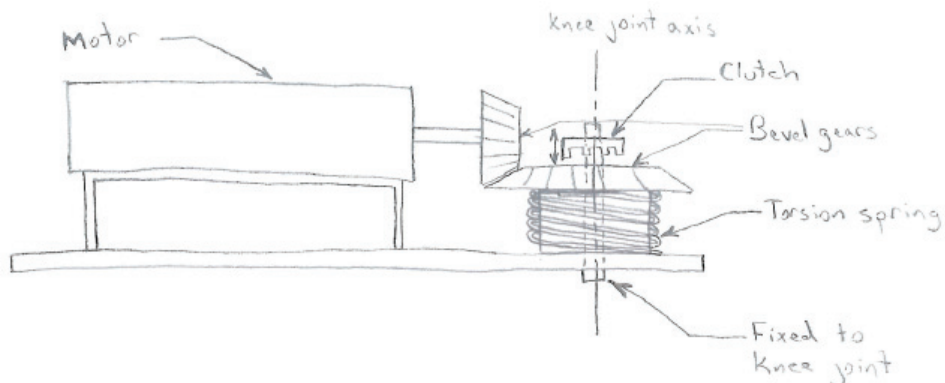


Figure A.8: Spring energy storage and bevel gear direct drive concept sketch.

# Appendix B: Torsion Spring Specification Sheet

## Mid-West Spring & Stamping

105 Etna St. Mentone, IN 46539
Phone (800)-424-0244

**SMI** Spring Manufacturers Institute

| | | | | | | | |
|---|---|---|---|---|---|---|---|
| Part Number | .262 x 3.3OD | Revision | NO B/P | Date | 09/04/2009 | Material | Chrome Silicon |
| Designer | DEFORD | Customer | ALEX SPRING | | | | |

| | | | | | Next Sm. Available | Next Lg. | Tensile |
|---|---|---|---|---|---|---|---|
| Wire Dia. | 6.655 | Max Rotation | 90.000 | Shaft Dia | 6.0 | No | 6.5 | 1722 |

Total Coils 3.000 — Max B Length — Units Metric — Stress: Off

Diameter 83.820 +- — D Type OD — Arm Length 1

Arm Length 2

| G Mod | E Mod | Density |
|---|---|---|
| 79290 | 205940 | 0.000008 |

Add. Feed

Hand Right — Spec. ASTM A 401 — APT 70

- ■ Excessive Stress

| | | | |
|---|---|---|---|
| SpringRate | 448.813 | Index | 11.595 |
| Stress | 1396 | Torque | 40393 |
| Min. ID | 70.510 | Body Length | 28.284 |
| Max. OD | 83.820 | Wire Length | 727.813 |
| Min. Rot. ID | 64.574 | Weight | 0.20253 |

| | Free | Torque 1 | Torque 2 | NPS |
|---|---|---|---|---|
| Coils | 3.00 | N/A | 3.25 | 3.23 |
| Arm angle | 0 | N/A | 90 | 83 |

### Spring Diagnostics
-- May not be suitable for cyclic service --
\* Note: Torsion angle convention
\* NPS exceeded by Rot. 2

Graph axis labels: 42K, 40K, 34K, 25K, 17K, 8.5K, 0 (Load)
Deflection: 0, 16.65, 33.31, 49.96, 66.61, 83.27
1.5K 85%, 1.4K 81%, 1.2K 68%, 879 51%, 586 34%, 293 17% (Stress % of Tensile)

6.655

83.820

28.284

Drawing Notes

Torsion -Dimensional

171

# Appendix C: Spring Force Requirement Spreadsheets

Table E.1: Spring Force Requirements for STS for a Given Knee Disk Radius and User Weight

**Linear force required for STS knee extension**

| bodyweight (kg) | 90 |
|---|---|

| | | | knee disk radius (m) | | | | | | | | | | |
|---|---|---|---|---|---|---|---|---|---|---|---|---|---|
| assist (%) | moment (Nm/kg) | moment (Nm) | 0.01 | 0.015 | 0.02 | 0.025 | 0.03 | 0.035 | 0.04 | 0.045 | 0.05 | 0.055 | 0.06 |
| 1 | 0.88 | 79.2 | 7920 | 5280 | 3960 | 3168 | 2640 | 2262.857 | 1980 | 1760 | 1584 | 1440 | 1320 |
| 0.95 | 0.836 | 75.24 | 7524 | 5016 | 3762 | 3009.6 | 2508 | 2149.714 | 1881 | 1672 | 1504.8 | 1368 | 1254 |
| 0.9 | 0.792 | 71.28 | 7128 | 4752 | 3564 | 2851.2 | 2376 | 2036.571 | 1782 | 1584 | 1425.6 | 1296 | 1188 |
| 0.85 | 0.748 | 67.32 | 6732 | 4488 | 3366 | 2692.8 | 2244 | 1923.429 | 1683 | 1496 | 1346.4 | 1224 | 1122 |
| 0.8 | 0.704 | 63.36 | 6336 | 4224 | 3168 | 2534.4 | 2112 | 1810.286 | 1584 | 1408 | 1267.2 | 1152 | 1056 |
| 0.75 | 0.66 | 59.4 | 5940 | 3960 | 2970 | 2376 | 1980 | 1697.143 | 1485 | 1320 | 1188 | 1080 | 990 |
| 0.7 | 0.616 | 55.44 | 5544 | 3696 | 2772 | 2217.6 | 1848 | 1584 | 1386 | 1232 | 1108.8 | 1008 | 924 |
| 0.65 | 0.572 | 51.48 | 5148 | 3432 | 2574 | 2059.2 | 1716 | 1470.857 | 1287 | 1144 | 1029.6 | 936 | 858 |
| 0.6 | 0.528 | 47.52 | 4752 | 3168 | 2376 | 1900.8 | 1584 | 1357.714 | 1188 | 1056 | 950.4 | 864 | 792 |
| 0.55 | 0.484 | 43.56 | 4356 | 2904 | 2178 | 1742.4 | 1452 | 1244.571 | 1089 | 968 | 871.2 | 792 | 726 |
| 0.5 | 0.44 | 39.6 | 3960 | 2640 | 1980 | 1584 | 1320 | 1131.429 | 990 | 880 | 792 | 720 | 660 |
| 0.45 | 0.396 | 35.64 | 3564 | 2376 | 1782 | 1425.6 | 1188 | 1018.286 | 891 | 792 | 712.8 | 648 | 594 |
| 0.4 | 0.352 | 31.68 | 3168 | 2112 | 1584 | 1267.2 | 1056 | 905.1429 | 792 | 704 | 633.6 | 576 | 528 |
| 0.35 | 0.308 | 27.72 | 2772 | 1848 | 1386 | 1108.8 | 924 | 792 | 693 | 616 | 554.4 | 504 | 462 |
| 0.3 | 0.264 | 23.76 | 26.4 | 1584 | 1188 | 950.4 | 792 | 678.8571 | 594 | 528 | 475.2 | 432 | 396 |

*table values in (N)

Table E.2: Spring Compression for Varied Knee Disk Radii

**Amount of spring compression for 90° flexion**

| disk rad (m) | 1/4 perimeter (m) |
|---|---|
| 0.01 | 0.016 |
| 0.015 | 0.024 |
| 0.02 | 0.031 |
| 0.025 | 0.039 |
| 0.03 | 0.047 |
| 0.035 | 0.055 |
| 0.04 | 0.063 |
| 0.045 | 0.071 |
| 0.05 | 0.079 |
| 0.055 | 0.086 |
| 0.06 | 0.094 |

Table E.3: Spring Force Requirements for Ramp Ascent for a Given Knee Disk Radius and a 90 kg individual

| | | Linear force required for 100% ramp walk knee extension | | | | | | | | | | |
|---|---|---|---|---|---|---|---|---|---|---|---|---|
| | | | | | | knee disk radius | | | | | | |
| | | 0.01 | 0.015 | 0.02 | 0.025 | 0.03 | 0.035 | 0.04 | 0.045 | 0.05 | 0.055 | 0.06 |
| angle | moment (Nm) | | | | | | | | | | | |
| 26.66667 | 12.85714 | 1285.714 | 857.1429 | 642.8571 | 514.2857 | 428.5714 | 367.3469 | 321.4286 | 285.7143 | 257.1429 | 233.7662 | 214.2857 |
| 30 | 45 | 4500 | 3000 | 2250 | 1800 | 1500 | 1285.714 | 1125 | 1000 | 900 | 818.1818 | 750 |
| 30 | 57.6 | 5760 | 3840 | 2880 | 2304 | 1920 | 1645.714 | 1440 | 1280 | 1152 | 1047.273 | 960 |
| 28.33333 | 48.21429 | 4821.429 | 3214.286 | 2410.714 | 1928.571 | 1607.143 | 1377.551 | 1205.357 | 1071.429 | 964.2857 | 876.6234 | 803.5714 |
| 25.83333 | 30.53571 | 3053.571 | 2035.714 | 1526.786 | 1221.429 | 1017.857 | 872.449 | 763.3929 | 678.5714 | 610.7143 | 555.1948 | 508.9286 |
| 21.66667 | 12.85714 | 1285.714 | 857.1429 | 642.8571 | 514.2857 | 428.5714 | 367.3469 | 321.4286 | 285.7143 | 257.1429 | 233.7662 | 214.2857 |

*table values in (N)

Table E.4: Percent Assist Provided for Ramp Walking

| | | | |
|---|---|---|---|
| so, max force for 100% ramp as | | 2304 | N |
| at a knee angle of | | 30 | deg |
| with a knee disc radius of | | 2.5 | cm |
| meaning, with a linear ext'n of | | 1.3 | cm |
| | | | |
| but max for STS springs | | 840 | N |
| at knee angle of | | 30 | deg |
| with disk radius | | 2.5 | cm |
| ie extension of | | 1.3 | cm |
| giving STS assist of | | 36.45833 | % |
| | 80kg | 41.01563 | % |
| | 70kg | 46.875 | % |
| | 60kg | 54.6875 | % |
| | 50kg | 65.625 | % |

# Appendix D: Compression Spring Specification Sheet

**Report**          *Advanced Spring Design*

**Developed for:**

My Customer
My Customer Addess 1, Address 2
Customer City, Illinois, 61101, United States
Phone: 1-800-800-8000

**Developed by:**

Advanced Spring Design
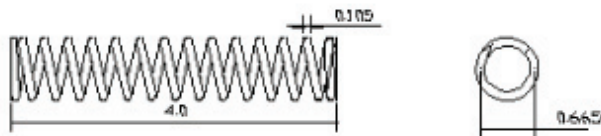Advanced, Spring
Design, Alabama, 12345, United States
Phone:

**Cylindrical Compression Spring, Round Wire**    **Material:**    Music Wire

**End Type:** Closed/Ground      **Condition:** Preset/Not Peened

**Grade:**    Commercial      **Buckling Constaints:** End fixation not known

| | | | | | |
|---|---|---|---|---|---|
| Wire Dia. [in] | 0.105 | Coil Mean Dia [in] | 0.665 | Active Coils | 12.865 |
| Wire Tolerance [in] | +/- 0.0008 | Coil ID [in] | 0.56 | Total Coils | 14.865 |
| Rate [lbf/in] | 46.1856 | Coil OD [in] | 0.77 | Dead Coils | 0 |
| Spring Index | 6.3333 | Diameter Tol. [in] | +/- 0.028 | Pitch [in] | 0.2946 |
| Nat. Frequency [Hz] | 259.737 | Shaft OD [in] | | Pitch Angle [deg] | 8.0268 |
| Wire Length [in] | 31.3109 | Min. ID [in] | 0.532 | Free Len. Tol. [in] | +/- 0.1168 |
| Wire Weight [lb] | 0.077 | Hole ID [in] | | Allowable Solid Ht. [in] | |
| | | Expanded OD [in] | 0.8037 | | |

| | Free | Point 1 | Point 2 | Solid | Buckle |
|---|---|---|---|---|---|
| Load [lbf] | 0 | 25 | 112 | 112.657 | |
| Load Tolerance [lbf] | 0 | +/- 5.9946 | +/- 8.0826 | | |
| Length [in] | 4 | 3.4587 | 1.575 | 1.5608 | |
| Deflection [in] | 0 | 0.541295 | 2.425 | 2.4392 | |
| % of Max. Deflection | 0 | 22.2 | 99.4 | 100 | |
| Corrected Stress [psi] | 0 | 45265 | 202786 | 203975 | |
| % of Tensile Stress | 0 | 16.9 | 75.5 | 75.9 | |

**Design Status:**      **Direction of Coiling:** Optional      **Estimated Cycle Life:**      <1E5

Stress > 60% Safety Limit



0.105

4.0

0.665

174

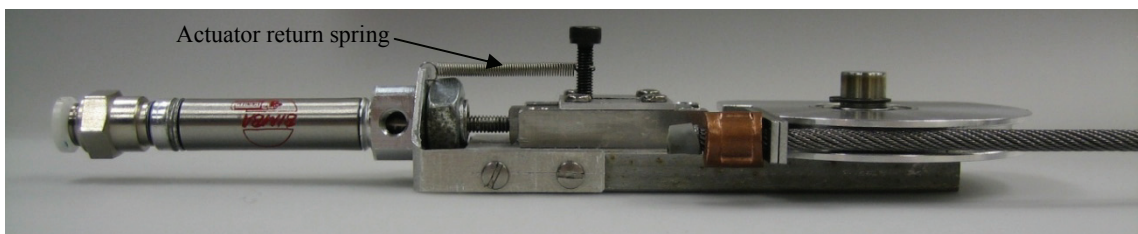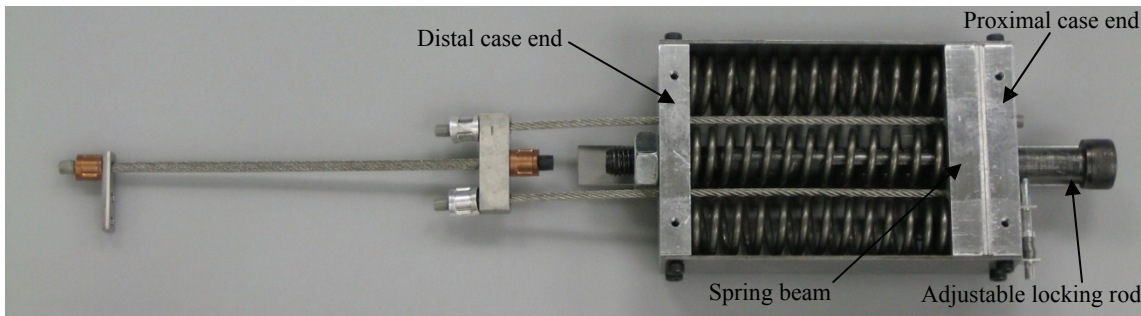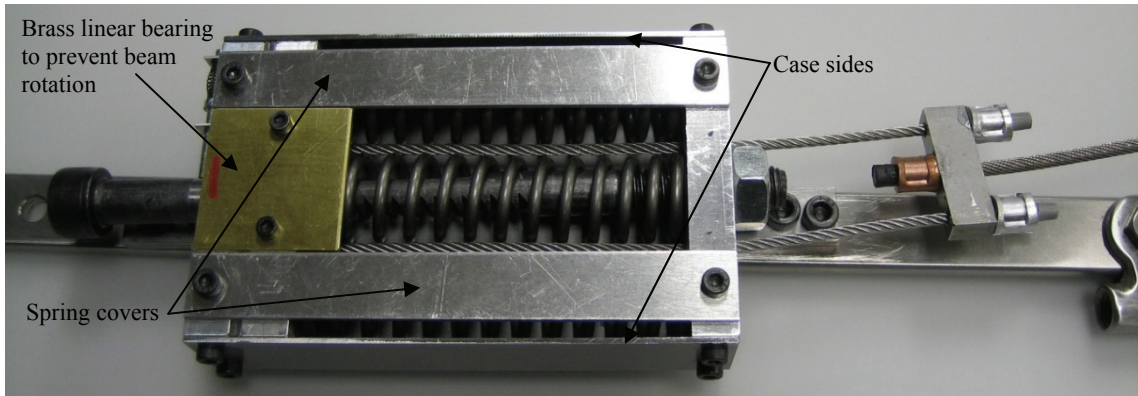# Appendix E: Partial Exploded View of the KEA

Springs

Locking rod

Locking rod spring pin support

Locking rod spring

Locking rod spring pin

U-beam

Long notch

Ratchet notches

Spring case

Locking rod nut

Proximal cables

Cable connector

Distal cable

KAFO attachment base

Knee disk

Knee disk pin

Knee disk cable support

Sliding lock bracket

Knee disk support

Sliding lock

Sliding lock supports

Actuator support bracket

Pneumatic actuator

Note: Air bladder and knee disk bearing are not shown

175

# Appendix F: Failure Mode Analysis

| Event | Result | Consequence |
|-------|--------|-------------|
| Cables pull out from end stops | No resistance to spring extension or knee flexion. Springs extend to full length rapidly | Possibility of user collapse. Loud noise as spring beam makes contact with proximal case end |
| Improper notch engagement | Spring beam may slip off notch. Springs extend rapidly, either caught by next notch, or full spring extension | *(1) Knee disk disengaged*: loud noise as spring beam makes contact with proximal case end or next notch. Knee disk spins about knee-disk pin rapidly.<br>*(2) Knee disk engaged*: little weight borne on leg: quick, unexpected knee extension |
| Locking rod notch yields | Same as above | Same as (1) and (2) above |
| U-beam notch engagement area fails | Springs extend to full length rapidly | Same as (1) and (2) above |
| Spring case or knee disk support fasteners fail | Spring case or support comes loose from KAFO, moves violently as springs extend | Case or support may contact the user skin as it moves, injuring the user |
| KAFO attachment base fails | Spring case comes loose from KAFO, moves violently as springs extend | Case may contact user as it moves, injuring the user |
| Springs fail from fatigue | Springs fracture but are contained within the case | No extension moment is provided, user may stumble |
| Knee disk pin fails under load | Knee disk comes free from the KEA | Cables do not provide tension to keep springs compressed. Springs extend rapidly and cause loud noise as spring beam makes contact with proximal case end or locking rod notch. Possibility of user collapse. |
| Knee disk notch yields | Knee disk rotates as far as yielding occurs, springs extend slightly | Extension-assist moment decreases |
| Sliding lock yields | Same as above | Same as above |
| Pneumatic actuator fails | Sliding lock will not engage with knee disk notch | *Springs elongated*: springs will not compress because no tension created in distal cable<br>*Springs compressed*: user must manually slide lock into knee disk notch so that springs can be safely released and extended |

# Appendix G: Additional Prototype Photographs

Modified sliding lock bracket



Knee disk free to rotate around knee disk pin

KAFO uprights



Springs compress with knee flexion, extend with knee extension (when locking rod disengaged)

Knee disk locked, coupled to lower KAFO upright
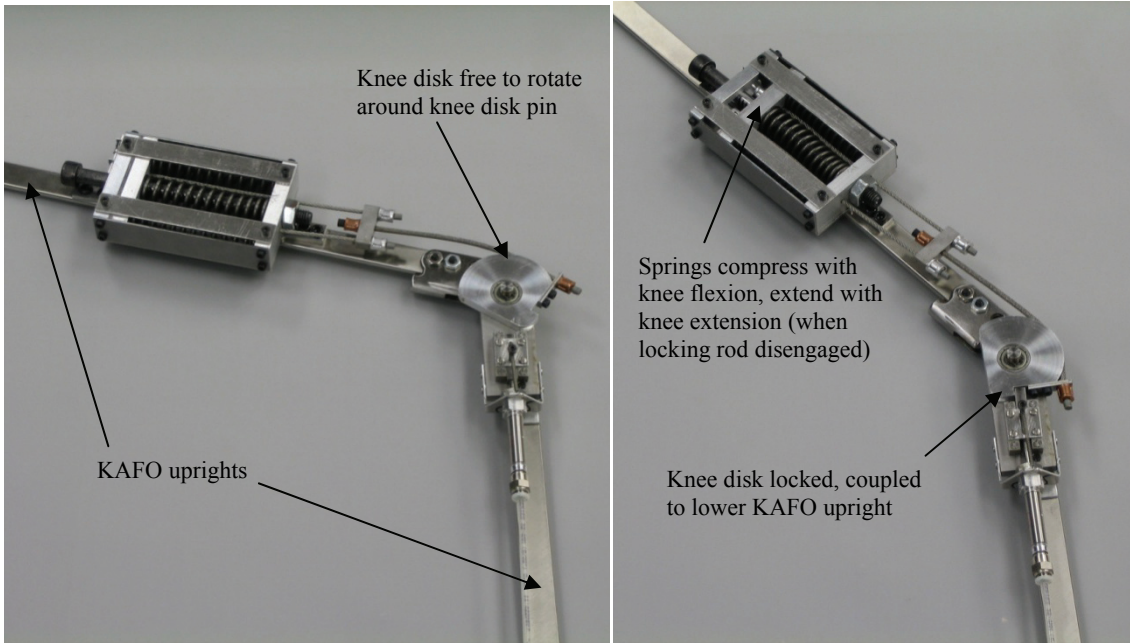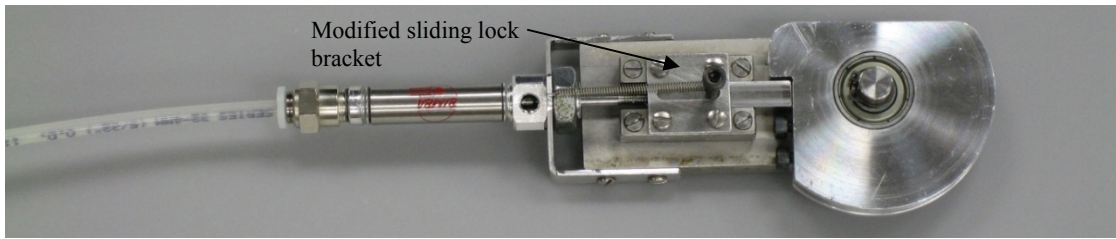
# Appendix H: Bill of Materials

**Bill of Materials**

| Component | Material | Shape | Dimensions (inches) | Dimensions (mm) | Qty (/device) | provider | cost ($) |
|---|---|---|---|---|---|---|---|
| Spring beam backing | 17-4 PH stainless | sheet 18 Ga. / 0.050" | 0.886 x 2.6 | 22.5 x 66 | 2 | MC | 22.03 |
| Knee disk cable support | 17-4 PH stainless | sheet 18 Ga. / 0.050" | 1 x 1/4 | 25.4 x 6.35 | 1 | MC | \| |
| Case - sides | 17-4 PH stainless | sheet 18 Ga. / 0.050" | 4.375 x 1.125 | 111.125 x 28.575 | 2 | MC | \| |
| Case - bottom | 17-4 PH stainless | sheet 18 Ga. / 0.050" | 4.375 x 2.638 | 111.125 x 67 | 3 | MC | V |
| Knee disk support bar | 17-4 PH stainless | rectangular bar | 1/4 x 1+1/4 x 3 | -- | 1 | MC | 8.69 |
| Cable connector piece | 17-4 PH stainless | rectangular bar | 1/4 x 3/8 x 1+1/4 | 6.35 x 9.525 x 31.7 | 1 | MC | \| |
| Knee disk lock piece | 17-4 PH stainless | rectangular bar | 1/4 x 1/4 x 1+1/4 | 6.35 x 6.35 x 25.4 | 1 | MC | \| |
| Knee disk lock piece supports | 17-4 PH stainless | rectangular bar | 1/4 x 1/4 x 1+1/5 | 6.35 x 6.35 x 25.5 | 2 | MC | V |
| Knee disk pin | 17-4 PH stainless | round bar | $\Phi$5/16 x 3/4 | 8 x 19 | 1 | MC | 0.95 |
| Lock rod | Class 12.9 bolt steel | metric socket cap bolt | -- | M10 x 1.5 - 150 | 1 | MC | 2.06 |
| Lock rod nut | Class 8.8 bolt steel | metric hex nut | -- | M10 x 1.5 nut | 1 | OF | 0.22 |
| Compression springs | custom from Trakar | -- | -- | -- | 3 | Trakar | 12.84 |
| Case - proximal end | 7075-T651 Al | rectangular bar | 3/8 x 1 x 2.638 | 9.5 x 25.4 x 67 | 1 | RC | 11.713 |
| Case - distal end | 7075-T651 Al | rectangular bar | 3/8 x 1 x 2.638 | 9.5 x 25.4 x 67 | 1 | RC/MC | \| |
| Spring beam | 7075-T651 Al | rectangular bar | 3/8 x 1 x 2.638 | 9.5 x 25.4 x 67 | 1 | RC | V |
| Knee disk | 7075-T651 Al | round bar | $\Phi$2+1/4 x 1/4 | -- | 1 | RC/MC | 8.525 |
| Knee disk bearing | steel ball bearing | dble shielded | ID 5/16 OD 3/4 W 1/4 | 8x19x6 | 1 | GBS | 5.58 |
| Proximal (thin) cable | 7x19 stainless aircraft | -- | $\Phi$3/32 x 7 | -- | 2 | MC | 11.80 |
| Distal (thick) cable | 19x7 stainless aircraft | -- | $\Phi$1/8 x 5+1/2 | -- | 1 | MC | 4.55 |
| Proximal stop sleeves | Aluminum | -- | ID 3/32 OD 11/32 W 5/16 | -- | 4 | OF | 1.32 |
| Distal stop sleeves | Copper | -- | ID 1/8 OD 11/32 W 5/17 | -- | 2 | OF | 1.10 |
| Actuator support bracket | 6061 Al | sheet 18 Ga. | | | 1 | RC | |
| Lock rod spring pin support | 6061 Al | sheet 22 Ga. | 1.2 x 0.24 | | 1 | RC | |
| Lock rod spring pin | 6061 Al | round bar | $\Phi$3/16 x 1.142 | $\Phi$5 x 29 | 1 | RC | |
| Spring cover strips | 6061 Aluminum | sheet 18 Ga. | | 111 x 14 | 2 | RC | |
| Linear bearing | Brass | sheet 18 Ga. | | 30 x 32 | 1 | RC | |
| Lock rod spring | from 'click' pen | -- | -- | -- | 1 | -- | |
| Pneumatic actuator | | | $\Phi$3/8 | | 1 | Bimba | 16.7 |
| Socket head cap screws | class 12.9 | | | M3 x 12 | 20 | OF | 4.00 |
| Socket head cap screws | grade 8 | | 4-40 x 1/2 | | 4 | | 0.80 |
| Socket head cap screws | grade 8 | | 10-32 x 3/8 | | 2 | | 0.40 |
| Button head cap screws | grade 8 | | 10-32 x 3/8 | | 2 | | 0.40 |
| Flat head cap screws | grade 8 | | 10-32 x 5/8 | | 3 | | 0.60 |
| Retaining ring for knee disk | stainless steel | -- | ID 0.281 W 0.025 | -- | 1 | RC | |
| Air bladder | | | | | 1 | | |
| Air bladder tubing | nylon | 32-4mm | | $\Phi$4 x 30 | 1 | | 0.50 |

MC = McMaster-Carr
GBS = General Bearing Service
RC = Rehab Centre machine shop
OF = Ottawa Fasteners

Total
114.28

# Appendix I: Ethics Approval Documentation

September 22, 2010

Dr. Edward Lemaire
The Ottawa Hospital Rehabilitation Centre
Institute for Rehabilitation Research and Development
Room 1402
505 Smyth Road
Ottawa, ON   K1H 8M2

Dear Dr. Lemaire:

**Re: Protocol #   2010496-01H     Pilot Test of a Knee-Extension-Assist Device for Knee-Ankle-Foot Orthoses**

**Protocol approval valid until -     September 21, 2011**

Thank you for the letter from Alex Spring dated September 10, 2010. I am pleased to inform you that this protocol underwent expedited review by the Ottawa Hospital Research Ethics Board (OHREB) and is approved. No changes, amendments or addenda may be made to the protocol or the consent form without the OHREB's review and approval.

Approval is for the following:
- COREB Application
- English Recruitment Notice received August 30, 2010
- English Information Sheet and Consent Form dated April 21, 2010
- French Recruitment Notice received September 10, 2010
- French Information Sheet and Consent Form dated April 21, 2010

The validation date should be indicated on the bottom of all consent forms and information sheets (see copy attached). If the study is to continue beyond the expiry date noted above, a Renewal Form should be submitted to the OHREB approximately six weeks prior to the current expiry date. If the study has been completed by this date, a Termination Report should be submitted.

The Ottawa Hospital Research Ethics Board is constituted in accordance with, and operates in compliance with the requirements of the Tri-Council Policy Statement: Ethical Conduct for Research Involving Humans; Health Canada Good Clinical Practice: Consolidated Guideline; Part C Division 5 of the Food and Drug Regulations of Health Canada; and the provisions of the Ontario Health Information Protection Act 2004 and its applicable Regulations.

Yours sincerely,

Raphael Saginur, M.D.
Chairman
Ottawa Hospital Research Ethics Board

Encl.

RS/ll

# University of Waterloo – Research Ethics Board Approval

Dear Researcher:

The recommended revisions/additional information requested in the ethics review of your ORE application:

Title: Pilot Test of a Knee-Extension-Assist Device for Knee-Ankle-Foot Orthoses
ORE #: 16700
Faculty Supervisor: Dr. Jonathan Kofman (jkofman@engmail.uwaterloo.ca)
Faculty Supervisor: Dr. Edward Lemaire (elemaire@ottawahospital.on.ca)
Student Investigator: Alexander Spring (anspring@engmail.uwaterloo.ca)

have been reviewed and are considered acceptable. As a result, your application now has received full ethics clearance.

A signed copy of the Notification of Full Ethics Clearance will be sent to the Principal Investigator or Faculty Supervisor in the case of student research.

*********************************************
Note 1: This clearance is valid for four years from the date shown on the certificate and a new application must be submitted for on-going projects continuing beyond four years.

Note 2: This project must be conducted according to the application description and revised materials for which ethics clearance have been granted. All subsequent modifications to the protocol must receive prior ethics clearance through our office and must not begin until notification has been received.

Note 3: Researchers must submit a Progress Report on Continuing Human Research Projects (ORE Form 105) annually for all ongoing research projects. In addition, researchers must submit a Form 105 at the conclusion of the project if it continues for less than a year.

Note 4: Any events related to the procedures used that adversely affect participants must be reported immediately to the ORE using ORE Form 106.

Best wishes for success with this study.

--------------------------------
Susanne Santi, M. Math.,
Senior Manager
Office of Research Ethics
NH 1027
519.888.4567 x 37163
ssanti@uwaterloo.ca

# Appendix J: Marker Placement

| Code | Segment/joint | Location | Type |
|---|---|---|---|
| RTOE | right foot | 2nd metatarsal | tracking |
| RHEEL | right foot | calcaneus | tracking |
| RMA | right foot/ankle | medial malleolus | calibration |
| RLA | right foot/ankle | lateral malleolus | tracking/calibration |
| RSK1-4 | right shank | lateral side of shank cuff | tracking |
| RMK | right knee | medial epicondyle | calibration |
| RLK | right knee | lateral epicondyle | calibration |
| RTH1-4 | right thigh | lateral side of thigh cuff | tracking |
| RGT | right hip | greater trochanter | calibration |
| LTOE | left foot | 2nd metatarsal | tracking |
| LHEEL | left foot | calcaneus | tracking |
| LMA | left foot/ankle | medial malleolus | calibration |
| LLA | left foot/ankle | lateral malleolus | tracking/calibration |
| LSK1-4 | left shank | rigid plate bound to lateral side of shank | tracking |
| LMK | left knee | medial epicondyle | calibration |
| LLK | left knee | lateral epicondyle | calibration |
| LTH1-4 | left thigh | rigid plate bound to lateral side of thigh | tracking |
| LGT | left hip | greater trochanter | calibration |
| RPSI | pelvis | posterior superior iliac spine | tracking/calibration |
| RIC | pelvis | iliac crest | tracking/calibration |
| LPSI | pelvis | posterior superior iliac spine | tracking/calibration |
| LIC | pelvis | iliac crest | tracking/calibration |
| XSTRN | trunk | xiphoid process | tracking |
| MSTRN | trunk | manubrium | tracking |
| RAC | trunk | acromion process | tracking/calibration |
| LAC | trunk | acromion process | tracking/calibration |
| C7 | trunk | 7th cervical vertebra | tracking |

# Appendix K: Graphs of Kinematic and Dynamic Data
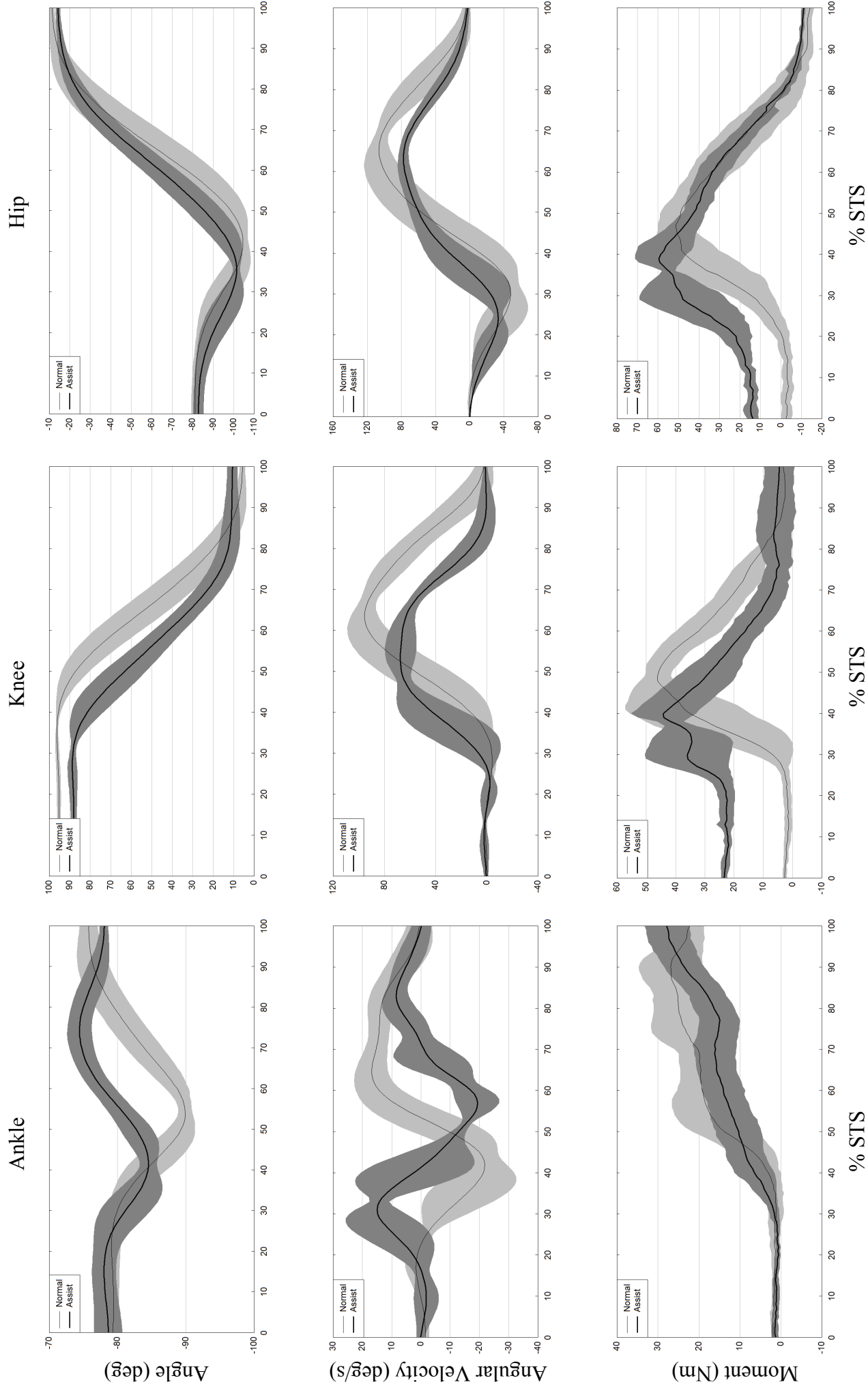


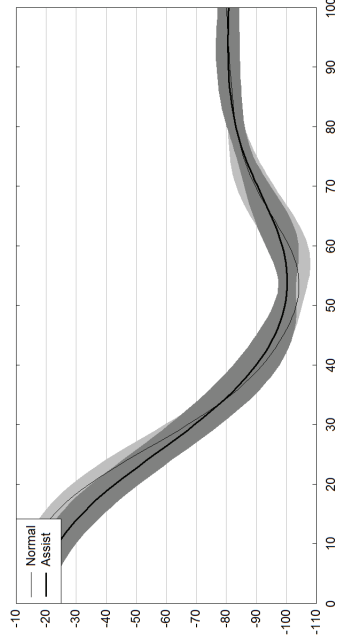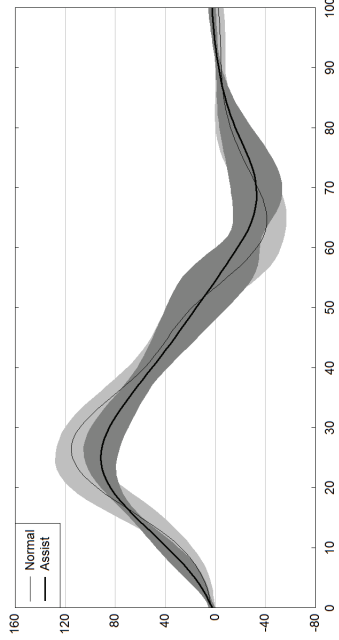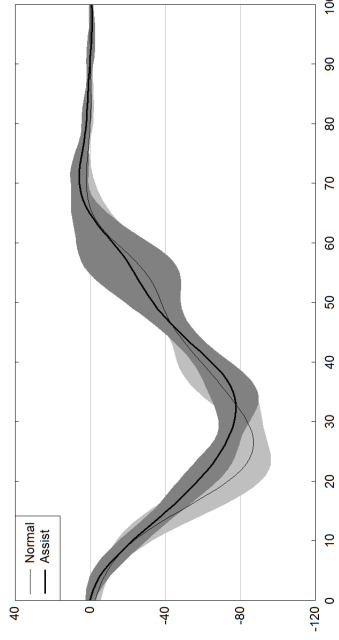Figure K.1: P1 STS joint kinematics and dynamics ensemble averages

183
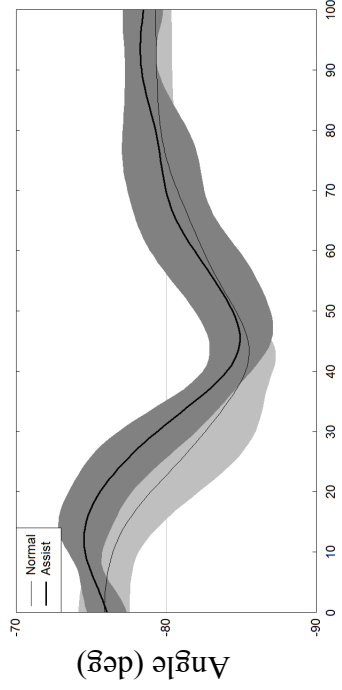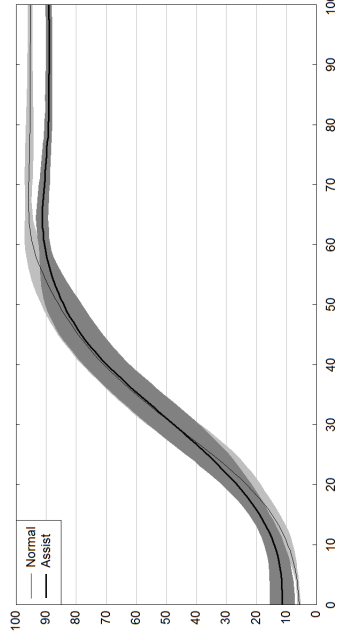
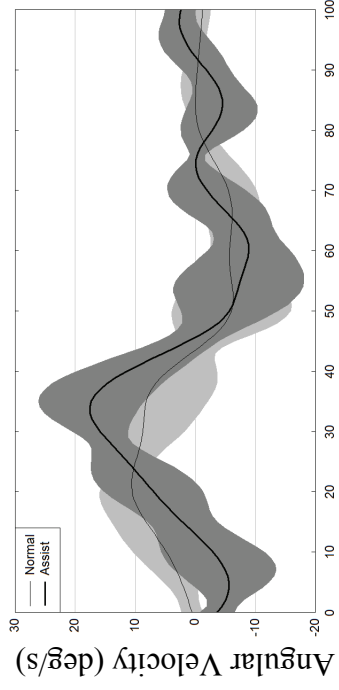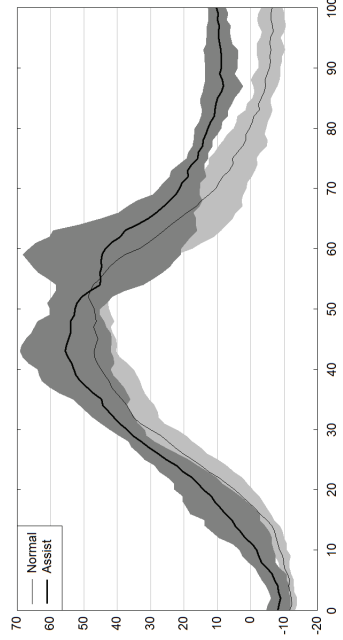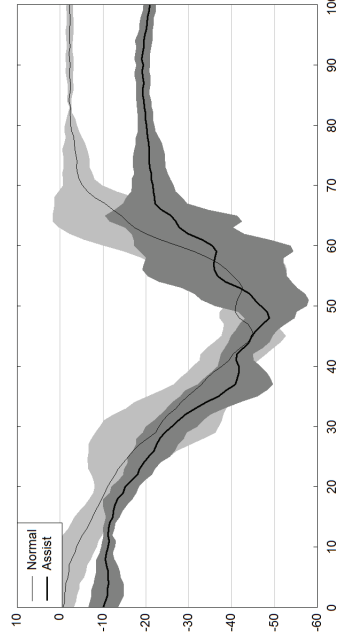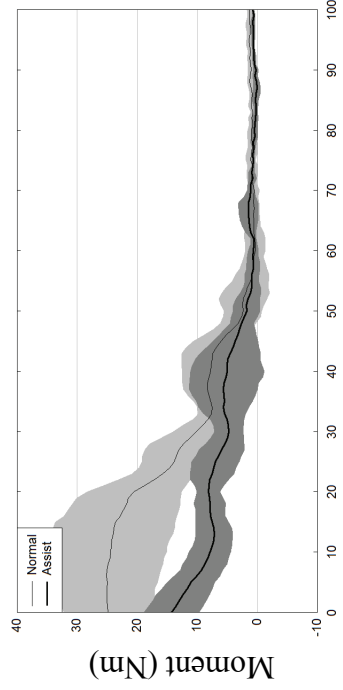Figure K.2: P1 stand-to-sit joint kinematics and dynamics ensemble averages
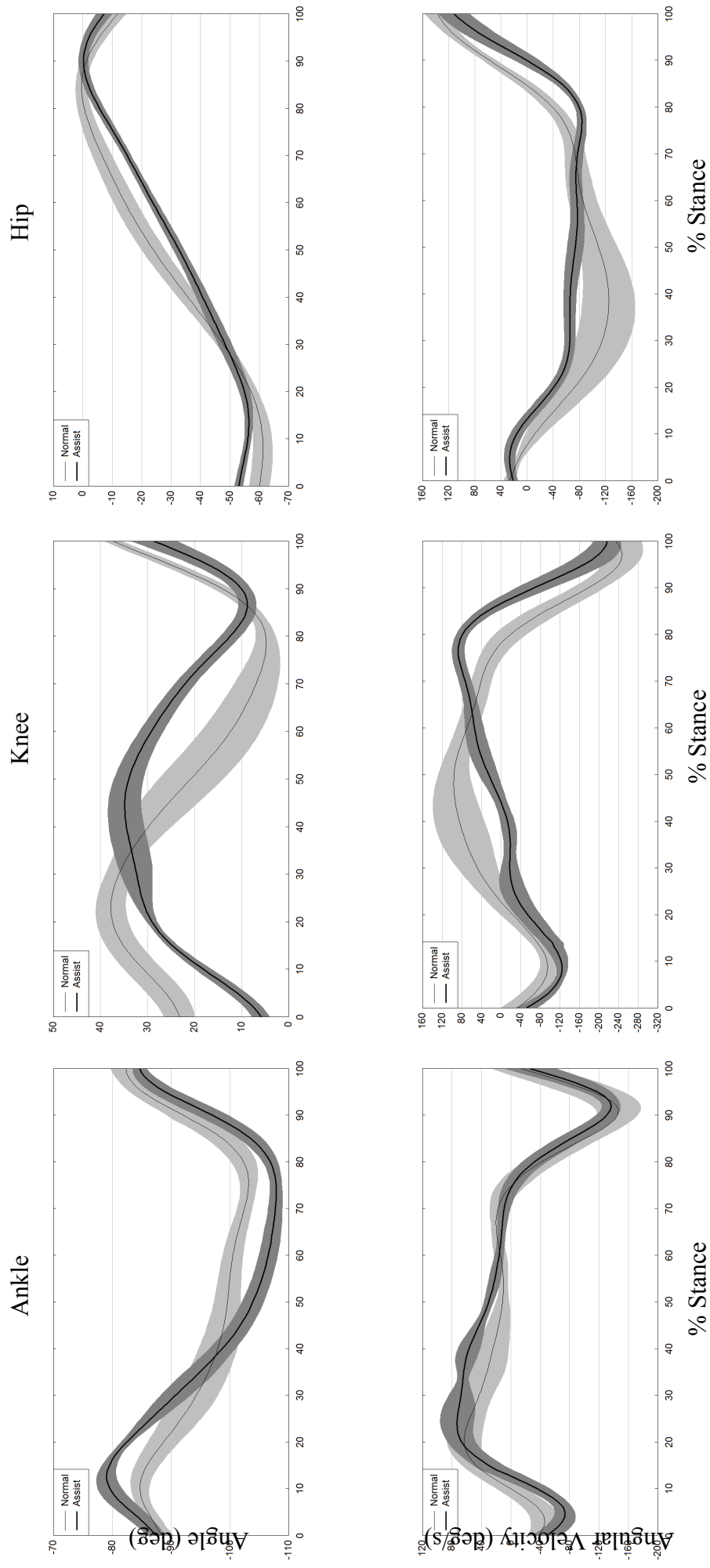
184

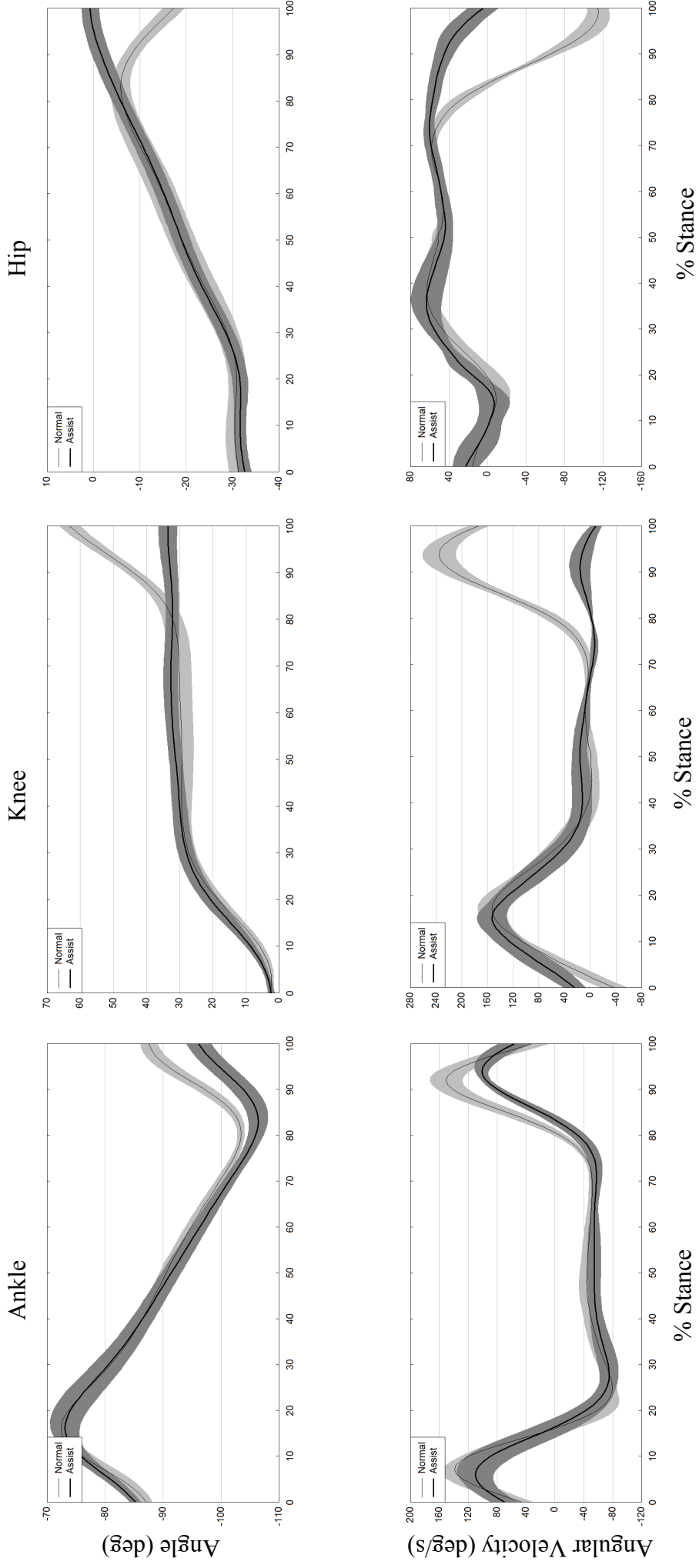Figure K.3: P1 ramp ascent joint kinematics ensemble averages

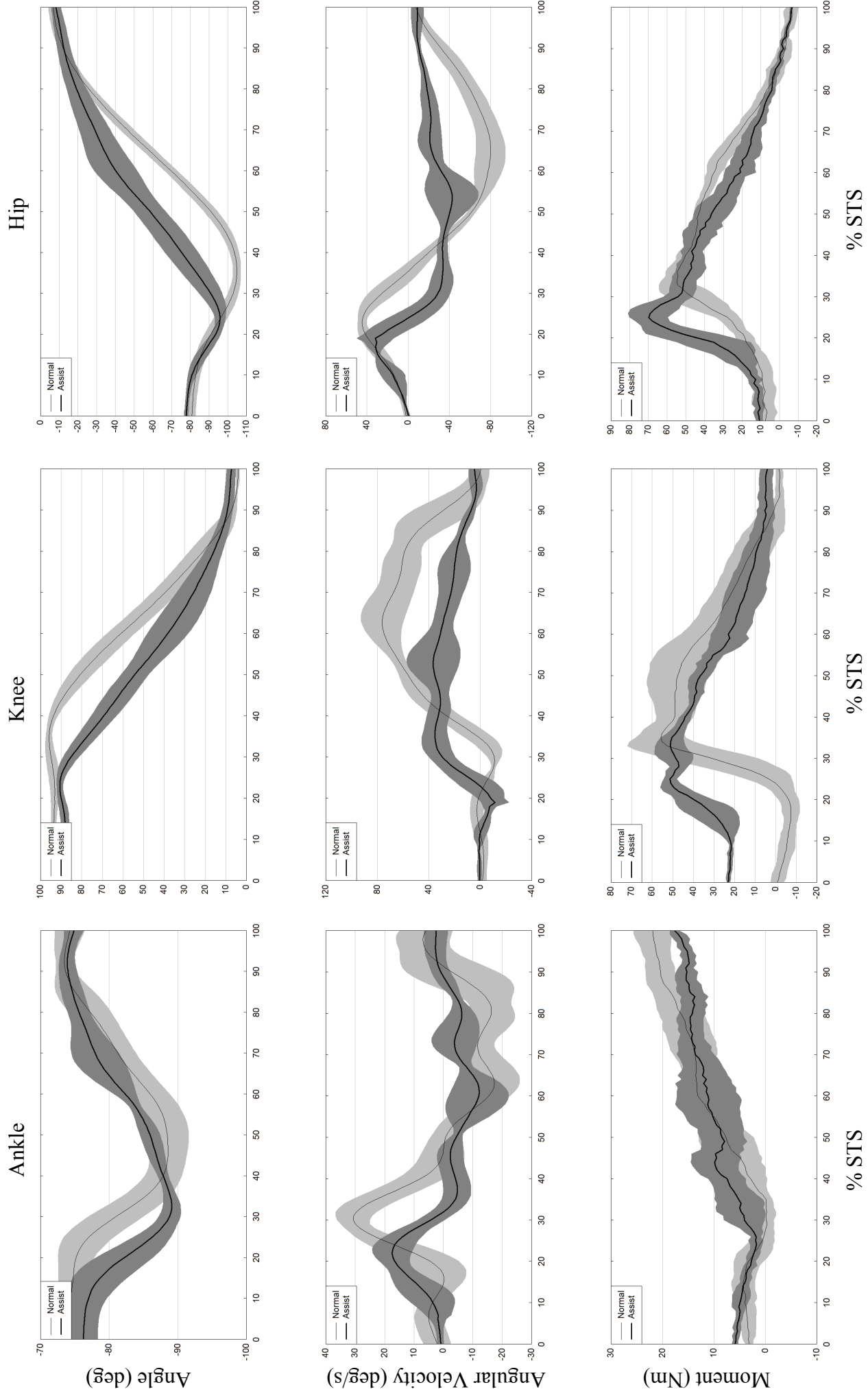Figure K.4: P1 ramp descent joint kinematics ensemble averages

186

Figure K.5: P2 STS of joint kinematics and dynamics ensemble averages
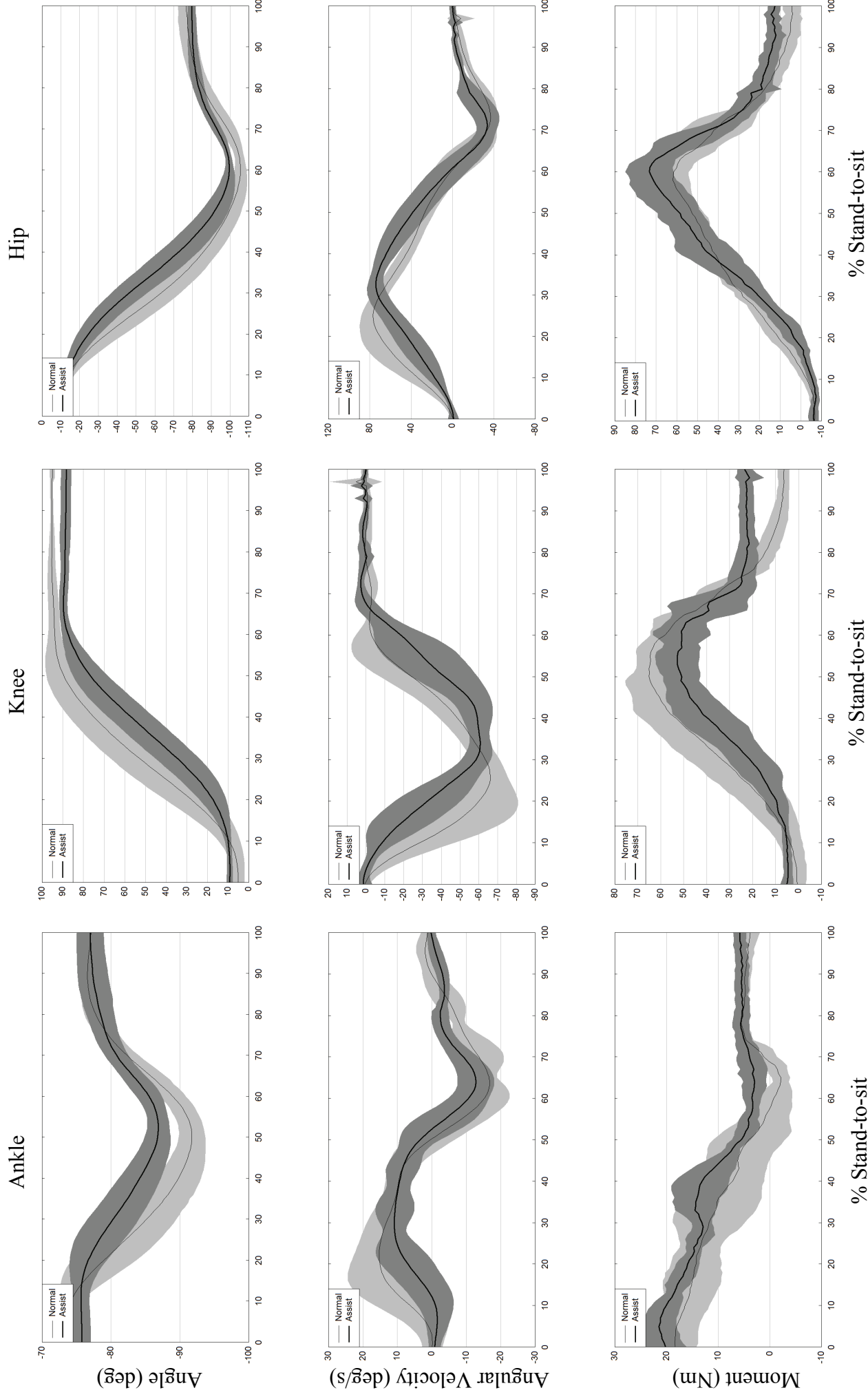
187

Figure K.6: P2 stand-to-sit joint kinematics and dynamics ensemble averages
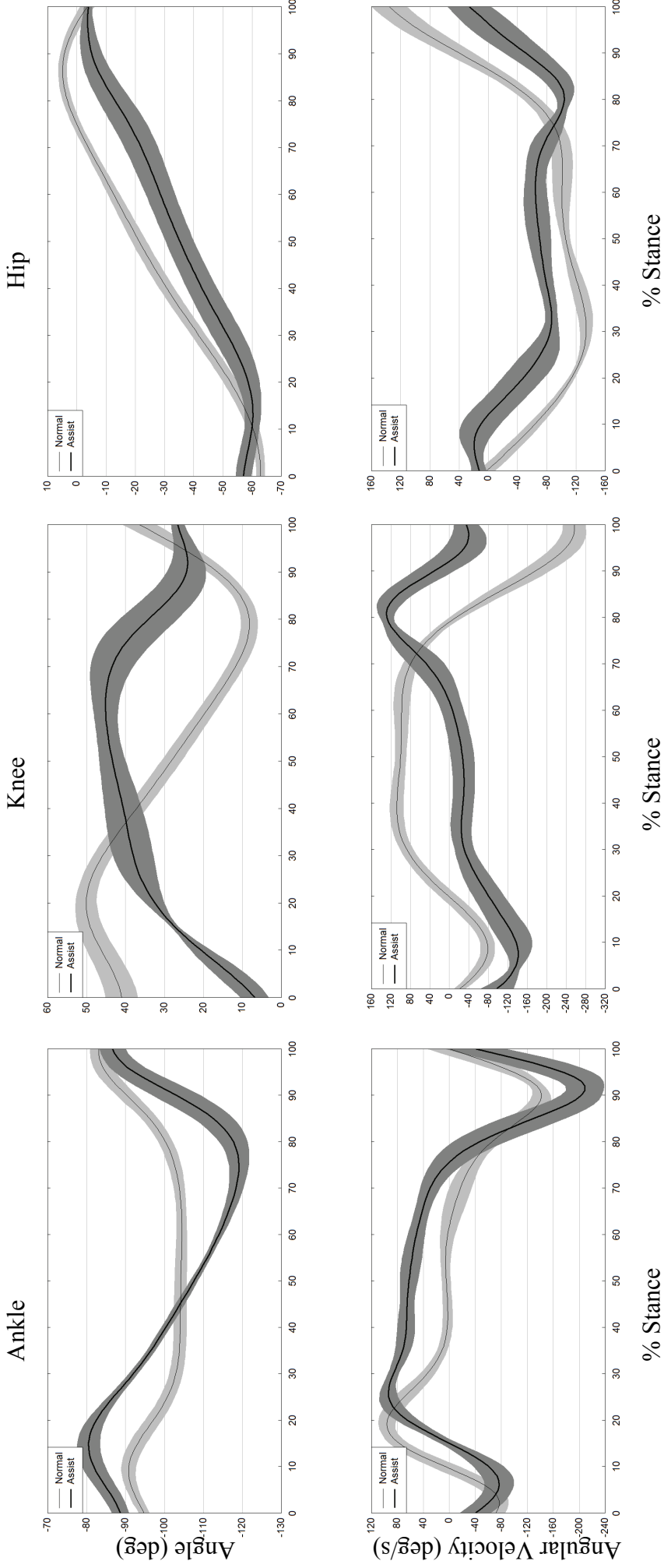
188

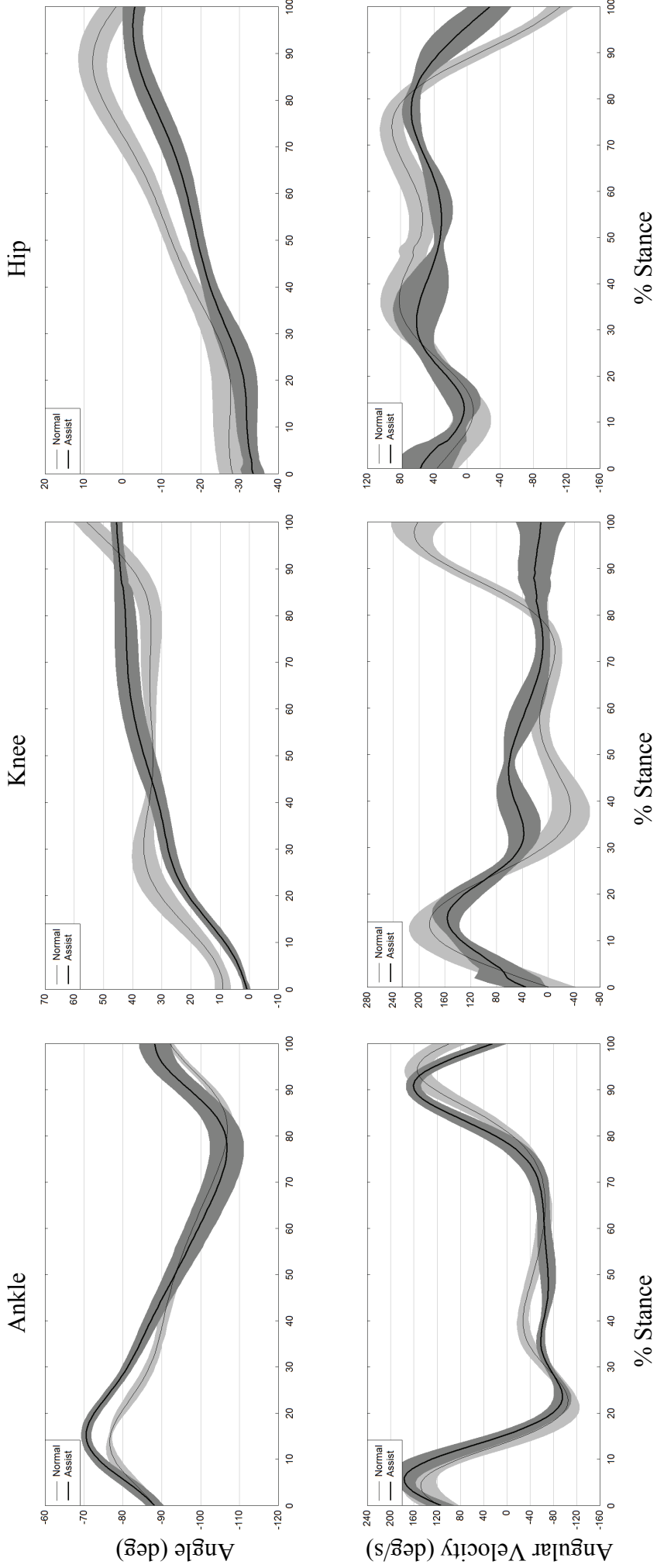Figure K.7: P2 ramp ascent joint kinematics ensemble averages

189

Figure K.8: P2 ramp descent joint kinematics ensemble averages
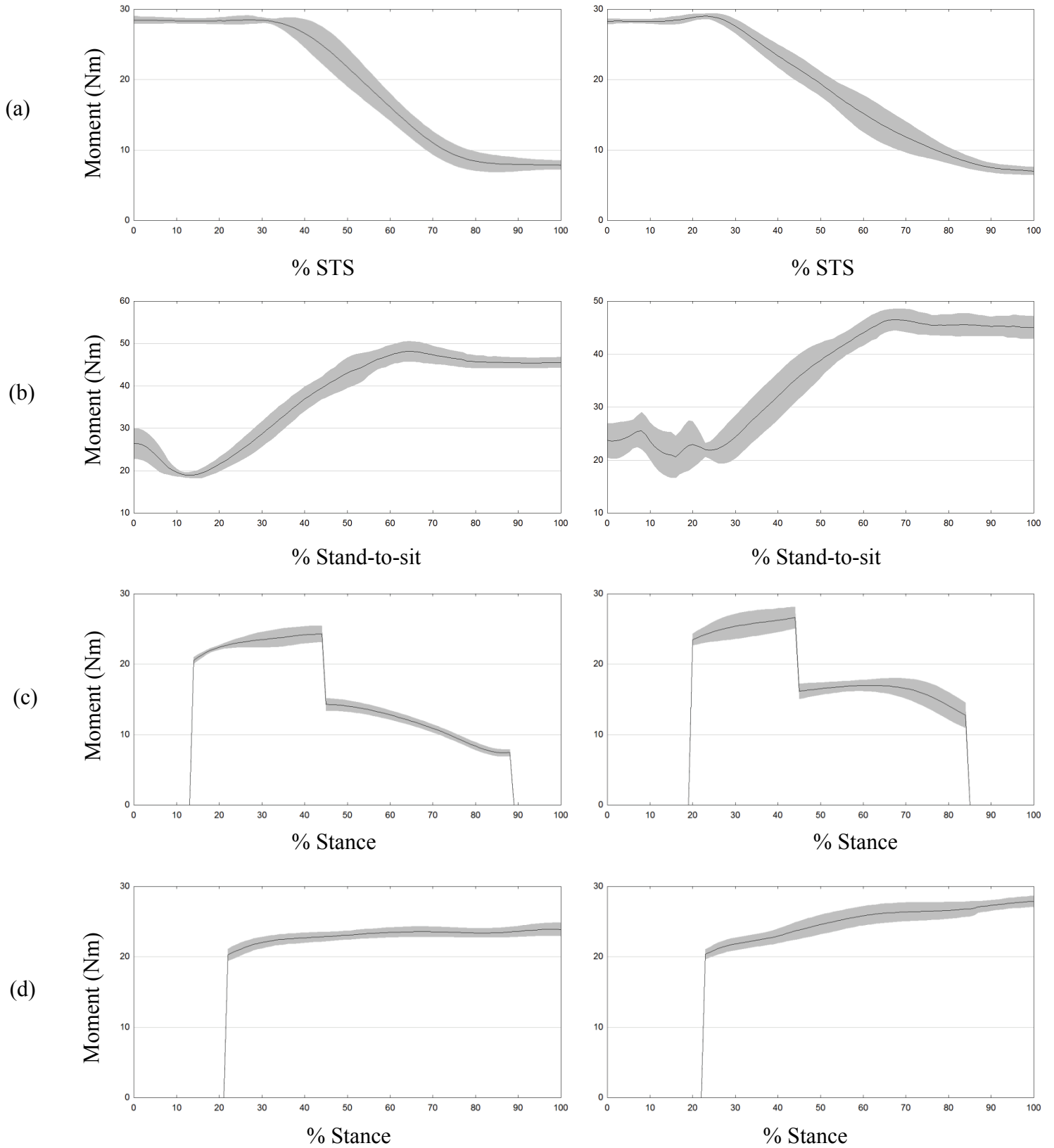
190

# Appendix L: Device Moment Graphs



Figure L.1: Device moment curves for (a) STS, (b) stand-to-sit, (c) ramp ascent, and (d) ramp descent

# Appendix M: EMG % MVC Values

Table M.1: EMG parameter values for STS and Stand-to-sit as a percent of maximum voluntary contraction

| | RIGHT | | | LEFT | | | |
|---|---|---|---|---|---|---|---|
| | Vastus medialis | Rectus femoris | Gluteus maximus | Vastus medialis | Rectus femoris | Gluteus maximus | Biceps femoris |
| **P1 STS Normal** | | | | | | | |
| abs max | 30.7 | 6.1 | 13.4 | 58.9 | 20.5 | 17.3 | 9.1 |
| abs mean | 8.3 | 2.5 | 4.9 | 9.8 | 3.8 | 5.2 | 2.3 |
| abs int | 21.7 | 6.7 | 13.0 | 25.4 | 9.9 | 13.6 | 6.0 |
| **P1 STS With Assist** | | | | | | | |
| abs max | 22.2 | 4.6 | 18.2 | 51.5 | 18.2 | 15.8 | 7.6 |
| abs mean | 4.2 | 1.4 | 6.8 | 9.9 | 3.6 | 5.6 | 2.7 |
| abs int | 12.8 | 4.4 | 20.7 | 29.9 | 10.7 | 17.1 | 8.0 |
| **P1 Stand to Sit Normal** | | | | | | | |
| abs max | 24.4 | 7.5 | 11.0 | 45.0 | 20.0 | 12.3 | 10.4 |
| abs mean | 5.5 | 1.9 | 3.4 | 7.9 | 3.5 | 3.2 | 2.3 |
| abs int | 16.0 | 5.6 | 10.0 | 22.7 | 10.3 | 9.4 | 6.8 |
| **P1 Stand to Sit With Assist** | | | | | | | |
| abs max | 23.5 | 3.3 | 16.5 | 45.7 | 18.4 | 8.8 | 9.4 |
| abs mean | 3.3 | 1.1 | 3.9 | 8.8 | 4.0 | 3.0 | 2.5 |
| abs int | 9.5 | 3.1 | 11.3 | 25.3 | 11.5 | 8.8 | 7.2 |
| **P2 STS Normal** | | | | | | | |
| abs max | 23.0 | 25.6 | 15.3 | 74.6 | 40.9 | 20.9 | 9.8 |
| abs mean | 7.1 | 5.6 | 4.9 | 15.9 | 8.2 | 7.7 | 3.4 |
| abs int | 20.7 | 16.5 | 14.5 | 46.6 | 24.2 | 22.9 | 10.1 |
| **P2 STS With Assist** | | | | | | | |
| abs max | 29.8 | 32.8 | 19.5 | 97.1 | 68.0 | 13.7 | 12.9 |
| abs mean | 8.5 | 6.9 | 4.6 | 23.1 | 12.2 | 7.2 | 3.4 |
| abs int | 39.8 | 31.9 | 21.7 | 109.4 | 57.7 | 34.2 | 16.2 |
| **P2 Stand to Sit Normal** | | | | | | | |
| abs max | 22.8 | 29.8 | 11.9 | 50.7 | 35.9 | 8.5 | 5.6 |
| abs mean | 6.1 | 4.6 | 1.8 | 11.0 | 7.2 | 2.1 | 1.4 |
| abs int | 23.8 | 17.9 | 7.0 | 42.5 | 27.9 | 8.1 | 5.5 |
| **P2 Stand to Sit With Assist** | | | | | | | |
| abs max | 15.5 | 17.3 | 7.7 | 60.7 | 38.2 | 7.7 | 6.1 |
| abs mean | 5.4 | 3.4 | 2.7 | 18.6 | 10.6 | 5.4 | 2.6 |
| abs int | 19.8 | 12.6 | 9.8 | 68.2 | 39.1 | 19.9 | 9.5 |

Table M.2: EMG parameter values for ramp gait as a percent of maximum voluntary contraction

| | Right | | |
| --- | --- | --- | --- |
| | Vastus Medialis | Rectus Femoris | Gluteus Maximus |
| P1 Ramp Ascent Normal | | | |
| abs max | 9.5 | 8.0 | 7.0 |
| abs mean | 6.8 | 5.3 | 4.1 |
| abs int | 3.4 | 2.6 | 2.0 |
| P1 Ramp Ascent With Assist | | | |
| abs max | 15.0 | 13.4 | 14.4 |
| abs mean | 6.4 | 5.3 | 4.6 |
| abs int | 7.2 | 5.9 | 5.1 |
| P1 Ramp Descent Normal | | | |
| abs max | 9.9 | 7.1 | 2.3 |
| abs mean | 11.1 | 7.2 | 1.4 |
| abs int | 3.8 | 2.5 | 0.5 |
| P1 Ramp Descent With Assist | | | |
| abs max | 16.4 | 9.6 | 3.2 |
| abs mean | 10.3 | 7.3 | 1.4 |
| abs int | 4.8 | 3.4 | 0.7 |
| P2 Ramp Ascent Normal | | | |
| abs max | 14.8 | 4.3 | 10.5 |
| abs mean | 8.2 | 2.8 | 4.0 |
| abs int | 4.5 | 1.5 | 2.2 |
| P2 Ramp Ascent With Assist | | | |
| abs max | 18.2 | 13.6 | 8.9 |
| abs mean | 13.0 | 6.3 | 3.6 |
| abs int | 6.3 | 3.1 | 1.7 |
| P2 Ramp Descent Normal | | | |
| abs max | 9.7 | 4.6 | 2.0 |
| abs mean | 7.1 | 3.9 | 1.1 |
| abs int | 2.7 | 1.4 | 0.4 |
| P2 Ramp Descent With Assist | | | |
| abs max | 26.0 | 14.2 | 3.6 |
| abs mean | 15.2 | 7.8 | 1.4 |
| abs int | 8.0 | 4.1 | 0.7 |